SAND2008-1224
Unlimited Release
Printed February 2008

An Assessment of MELCOR 1.8.6: Design Basis Accident Tests of the Carolinas Virginia Tube Reactor (CVTR) Containment (Including Selected Separate Effects Tests)

Jack Tills
Jack Tills & Associates, Inc.
Sandia Park, New Mexico 87047-0549
Sandia Contract No. 176741

Allen Notafrancesco
USNRC, Office of Nuclear Regulatory Research
Rockville, Maryland 20852-2738

Pamela Longmire
Reactor Modeling and Analysis Department
Sandia National Laboratories
P.O. Box 5800
Albuquerque, New Mexico 87185-0748

Abstract

The MELCOR computer code has been developed by Sandia National Laboratories under USNRC sponsorship; to provide a capability for independently auditing analyses submitted by reactor manufacturers and utilities. MELCOR is a fully integrated code (encompassing the reactor coolant system and the containment building) that models the progression of postulated accidents in light water reactor power plants. In order to assess the adequacy of containment thermal-hydraulic modeling incorporated in the MELCOR code, a key containment test facility was analyzed. This report documents MELCOR code calculations for simulating the design basis accident tests performed in the Carolinas Virginia Tube Reactor (CVTR) containment. These tests are a series of steam blowdown experiments in a large scaled test facility; close to replicating a design basis simulation of a postulated main steam-line break inside a large dry PWR containment. The key objectives of this MELCOR assessment are to study: (1) the expansion and transport of high energy steam releases, (2) heat and mass transfer to structural passive heat sinks, and (3) containment pressure reduction due to spray actuation. Also, several relevant separate effects test (small scale) experiments are also analyzed with MELCOR assessing the fundamental heat and mass transfer modeling. Moreover, MELCOR results are compared to the CONTAIN code for the same tests.

INTENTIONALLY BLANK

Contents

Figures

Tables

INTENTIONALLY BLANK

1 Introduction

The MELCOR computer code [Gau05a, Gau05b] has been developed by Sandia National Laboratories (SNL) under USNRC sponsorship to provide a capability for independently auditing analyses submitted by reactor manufactures and utilities. MELCOR is a fully integrated code (encompassing the reactor coolant system (RCS) and the containment building) that models the progression of postulated accidents in light water reactor power plants. Characteristics of accident progression that can be treated with MELCOR include the thermal-hydraulic response in the RCS, reactor cavity, containment and confinement buildings; and a variety of severe accident related processes.

In order to assess the adequacy of containment thermal-hydraulic modeling incorporated in the MELCOR code, a key containment test facility was analyzed. This report documents MELCOR code calculations for simulating the design basis accident (DBA) tests performed in the Carolinas Virginia Tube Reactor (CVTR) containment. These tests are a series of steam blowdown experiments in a large scale test facility.

The CVTR facility is a decommissioned reactor containment building. In the late 1960's, as part of an effort to provide experimental information for use in developing and evaluating analytical methods for safety analyses of nuclear power plants, three tests were conducted and are described in Reference Sch70. These tests come close to replicating a design basis simulation of a postulated main steam-line break (MSLB) inside a large dry pressurized water reactor (PWR) containment. This facility is represented as a large scale integral experiment, in which the key objective is the study of modeling or analytical simulation of various processes occurring during a DBA event, such as 1) the expansion and transport of high energy steam releases, 2) heat and mass transfers to passive heat sinks, and 3) containment pressure reduction due to sprays.

The CVTR experiment is part of the overall traditional suite of integral containment test programs and accordingly used for any code when assessing the adequacy of containment modeling. To focus the assessment on important code modeling areas, a Phenomena Identification and Ranking Table (PIRT) type process [Wil96] is used to identify important modeling areas. Appendix A provides a description of those key phenomena investigated with the CVTR analysis. Moreover documented in Appendices B through E to this report are several key separate effects test (SET) experiments also analyzed with the MELCOR code. These SETs include phenomena associated with 1) natural and forced convective condensation in the presence of noncondensible gases, 2) transient convective condensation in superheated atmospheres, and 3) pressure reduction by sprays. Prior to studying any integral scaled test facility, these SET assessments are necessary to understand fundamental heat and mass transfer modeling and to make adjustments in the modeling where needed. The CONTAIN code [Mur97] was also assessed against the CVTR test data and selected separate effects testing, and was documented in Til02a. That report and other CONTAIN efforts were used as guideposts for the MELCOR assessments discussed in this report.

Section 2 provides a description of the CVTR facility, test procedures, and instrumentation. Section 3 presents a PIRT type review of key phenomena, associated code modeling aspects (nodalization, model inputs, etc.), and a discussion of current (MELCOR and CONTAIN) and

earlier (CONTEMPT) treatments [Har79] of key phenomena modeling (e.g., heat and mass transfers in air/steam environments). The main body of the report is the analysis of the CVTR tests using the MELCOR code. This analysis is provided in Section 4, where comparisons of measured and calculated quantities such as gas pressure and temperature profiles for each of the three CVTR tests are discussed. Additionally, comparisons between calculations performed with both the MELCOR and CONTAIN codes are also included in the analysis with causes for differences noted and discussed. Section 5 presents a summarization of the findings and conclusions, including some recommendations when using MELCOR for containment performance analysis. Listings of the various MELCOR input decks used for the SETs and CVTR calculations are provided in Appendices F and G, respectively.

2 Facility and Test Description

2.1 Facility

The CVTR test facility and the series of experiments performed in this facility are described in Reference Sch70. The CVTR containment, shown in Figure 2-1, is a reinforced concrete, right vertical cylindrical structure (diameter 17.68 m or 57.96 ft) with a flat base and hemispherical dome. Above the operating floor is the *operating region*, and below this floor are two distinct regions -- the *intermediate* and *basement regions*. The total free volume of the containment is about 6426 m^3 (226,920 ft^3); approximately 3993 m^3 (141,000 ft^3) is above the operating floor and about 2435 m^3 (86,000 ft^3) is below this floor[1]; and the flow path between these two large volumes is 30.6 m^2 (329 ft^2), which is about 12% of the floor area.

Within the containment are various steel-lined concrete, concrete, and steel (e.g., equipment) structures located by regions. A list of structures given in Reference Sch70 is also presented in Table 2-1. Some uncertainty is indicated in the test report regarding the surface area of concrete (+/- 5%) and miscellaneous steel (+/- 50%). These uncertainties are addressed through sensitivity calculations discussed in Section 4.

A containment pressure reduction water spray system is part of the CVTR test configuration. The spray header is located just above the containment *bend line*. Spray nozzles are uniformly spaced around the containment circumference to provide the maximum spray coverage. Comments in the test report suggest that the average spray droplet diameter for the spray nozzle is ~1 mm (0.001 meters).

Steam for the blowdown tests is supplied by a nearby coal-fired electric generating station. The steam was released, above the operating floor, vertically through a diffuser section, which consisted of a 3 m (10 ft) pipe with about 126 1-inch diameter holes drilled both axially and circumferentially along the side of the pipe.

2.2 Tests

The CVTR experiments principally consist of three simulated design basis tests for an MSLB event, and are identified as CVTR Tests 3, 4 and 5. For all these tests, the steam release profile (relating to mass flow rates, enthalpy and duration) is nearly identical; the profile "shape" is somewhat rectangular; that is, the release flow attains a specified level (~45 kg/s with 2780 kJ/kg specific enthalpy) and stays relatively constant for about 160 seconds. Considering the blowdown release ramp-up and ramp-down, the total blowdown transient is about 170 seconds. And consistent with any postulated design basis MSLB event, the break elevation is situated relatively high inside the containment (2 to 8 meters above the operating deck). The key difference between each test is spray flow rates. Specifically for CVTR Test 3, sprays were not activated; for CVTR Tests 4 and 5, sprays were activated at about 200 seconds with a flow rate of 0.0183 m^3/s (290 gpm) and 0.03155 m^3/s (500 gpm), respectively.

[1] Typical PWR large dry containments have about 70-80% of free volume above the operating floor (open region); whereas, the CVTR facility has approximately 62% of free volume above the operating floor.

2.3 Instrumentation

Various types of data measurement instrumentation were incorporated into the CVTR facility. However due to the nature of the devices, some data is judged to be more accurate and reliable than other measured parameters. Typically, containment pressure and temperature measurements are the main focus when comparing against code predictions. Uncertainty associated with the pressure (gauge) measurements is +/- 5% and is attributed primarily to transient temperature effects on the individual transducer. Most thermocouples have a maximum uncertainty of ~ +/- 2 K (+/- 1 °F); however, with respect to some locations (i.e., basement region), the uncertainty may be as high as +/- 10 K (+/- 5.7 °F).

Also, as part of the CVTR instrumentation array, there were "heat plug" assemblies fitted into the containment wall at two separate locations that measured local heat transfer. *Heat plug 1* was placed just above the operating floor and *heat plug 2* was placed about 6 m (20 ft) higher than the other assembly and closer to the top of the steam diffuser. Shown in Figure 2-2 are the approximate vertical locations of the heat plugs in the operating region. Thermocouples were placed in the atmosphere a few inches from the heat plug surface, and a number of thermocouples were located on the surface and within the steel liner that is backed by concrete. Inverse transient heat conduction calculations were used to recover heat flux at the surface of the heat plugs. Heat flux gauge measurements (direct) and condensate run-off were also measured at the heat plug locations although the errors associated with these measurements precluded the use of the data collected for model validation purposes.

At the approximate locations of the heat plugs, ultrasonic type anemometers were installed, as well as in the annulus region between the containment wall and operating floor. The anemometer located at heat plug 2 failed, but the remaining two devices operated throughout CVTR Test 3. These measurements however were considered somewhat uncertain with no bounds on the uncertainty range given, and only the peak velocities at the locations were reported.

Movie cameras were used to record the injection of steam into the containment building. The cameras were started just before the injection and provided visual records of the highly turbulent mixing process that occurs during a DBA blowdown event.

2.4 Scaling

When comparing the CVTR facility and tests against a typical PWR large dry containment and a representative DBA event, the following scaling aspects are highlighted:

a. The CVTR free volume is about one-tenth of a "generic" PWR large dry containment;
b. The CVTR heat sink surface (area or mass) to volume ratio is about twice that of a "generic" PWR large dry containment;
c. The CVTR blowdown releases are more representative of an intermediate size MSLB (break area) resulting in a longer steam release duration than a postulated design basis MSLB in a PWR large dry containment which are characterized by higher steam release rates in about one-half the transient time.

Therefore considering these key scaling attributes for the periods where containment sprays are not activated, the CVTR pressure responses are more sensitive to the heat and mass transfer processes (i.e., overall heat transfer to the containment structure and components is above the nominal PWR DBA event) than would be in the full-scale plant configuration. Accordingly, this distortion is recognized in the code assessment phase of this work. Moreover, since the break location is at a relatively high containment elevation, the potential for steam/gas stratification is extremely possible and needs to be investigated.

Table 2-1 Listing of CVTR structures (Reference Sch70).

Number	Title	Location*	Material	Area (m^2)	Thickness (m)	Volume (m^3)
1	Cylindrical shell	O,I,B	Steel	1437.2	0.00635	9.4
			Concrete	1437.2	0.60961	876.1
2	Dome of shell	O	Steel	498.9	0.01270	6.3
			Concrete	498.9	0.53341	266.2
3	Foundation mat	B	Concrete	245.3	1.37162	336.4
4	Operating floor	O	Concrete	230.2	0.76201	175.4
5	Header Cavity	B	Concrete	121.2	1.21921	147.8
6	Reactor Compartment	I	Concrete	154.2	1.44782	223.1
7	Fuel canal	I	Concrete	148.6	0.60961	90.6
8	Fuel canal supports	B	Concrete	26.0	0.30480	7.9
9	Floor reactor compartment	I	Concrete	13.3	0.91441	12.1
10	Concrete supports	B	Concrete	89.2	0.76201	68.0
11	Steam generator shield	O	Concrete	37.2	0.60961	22.7
12	Moderator overflow tank	B	Steel	51.3	0.01905	1.0
13	Pressurizer	I	Steel	16.4	0.11430	1.9
14	Pressurizer discharge tank	O	Steel	21.1	0.01270	0.27
15	Steam generator	O	Steel	47.7	0.07620	3.63
16	Moderator coolers	B	Steel	26.0	0.00635	0.16
17	Shutdown coolers	I	Steel	6.1	0.00305	0.02
18	Pumps, primary injection	B	Steel	23.2	0.02539	0.6
19	Fuel handling apparatus	O	Steel	46.5	0.02387	1.1
20	“I” beams	O	Steel	209.0	0.04115	8.6

*assumed location: O = operating region (above operating floor), I = intermediate region, B = basement region.

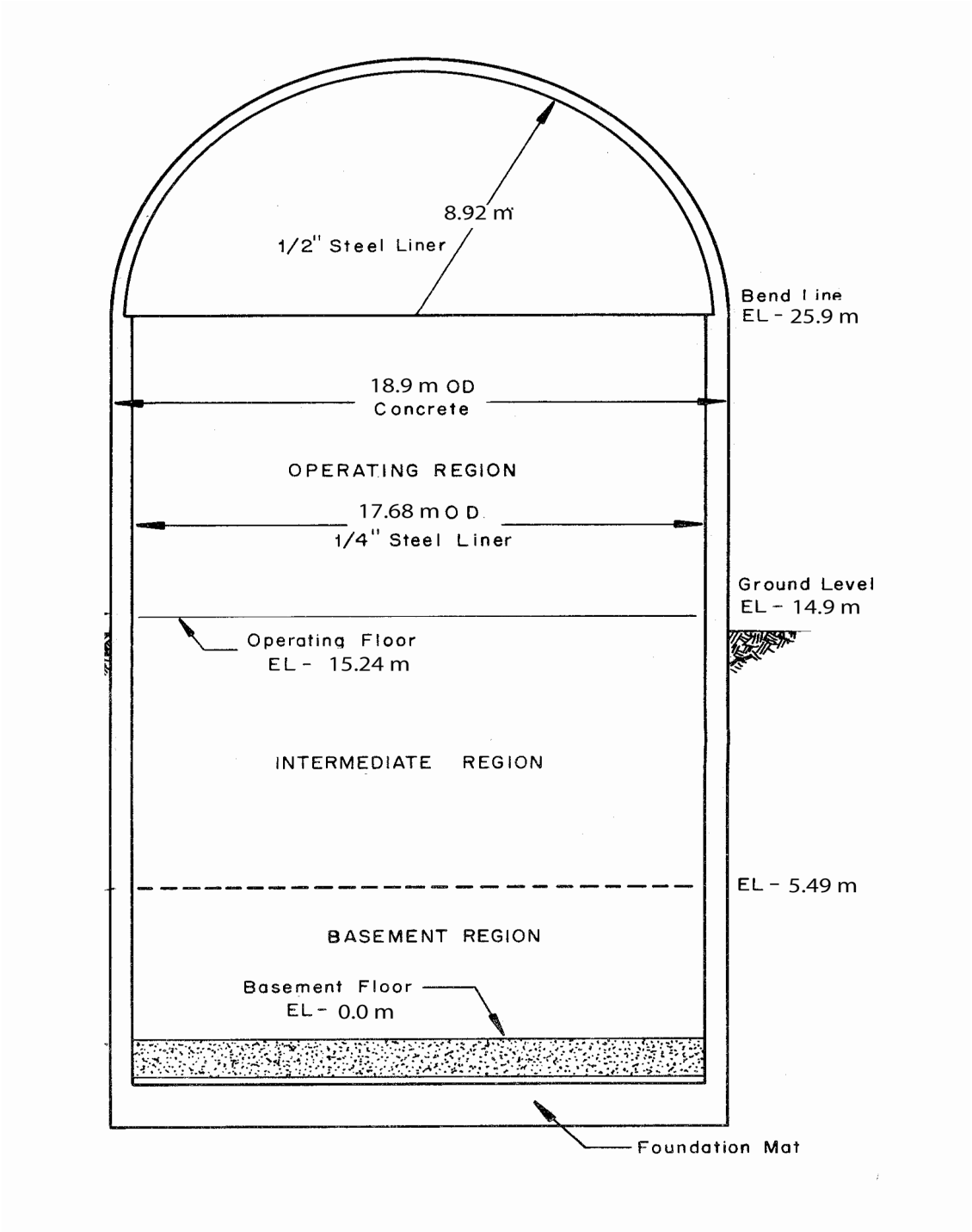

Figure 2-1 CVTR facility [Sch70].

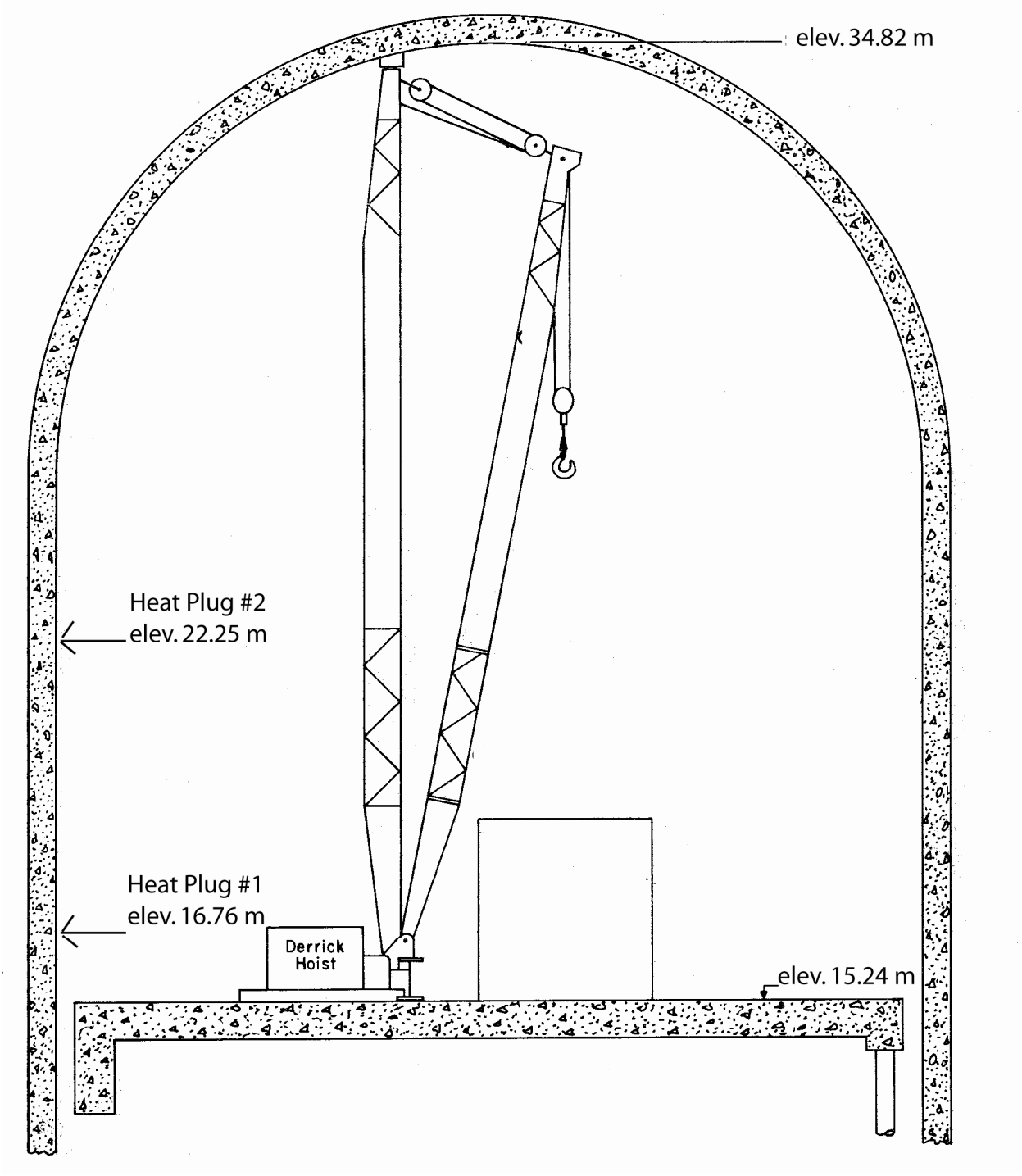

Figure 2-2 CVTR operating region showing the approximate locations of heat plugs #1 and #2 (elevation referenced to 0.0 meters at basement floor level) [Sch70].

INTENTIONALLY BLANK

3 MELCOR Model Description

3.1 Containment Phenomena Identification and Validation Focus

To establish a connection between an experimental program, code validation and containment accident analysis, it is necessary to systematically identify and assign importance to various phenomena occurring within the containment, and then establish the corresponding connection with code models. This effort has been performed in previous studies [Til96, Til02a, and Til02b]; Table 3-1 is extracted from Til02a (with minor additions) and is presented below, showing the relationship between important phenomena along with separate and integral tests used to validate models. Appendix A provides a description of the components, processes, and phenomena listed in Table 3-1. Highlighted in this table are the CVTR tests and the cross comparisons with phenomena which show that the tests are useful for assessing modeling of key processes due to the many measurements taken in the CVTR facility (e.g., pressure, gas and structure temperatures, condensation coefficients, spray water temperature and collection pans, gas circulation velocities, and photographic images of the blowdown progression).

The key figures of merit in comparing code results to test data are containment pressures and local gas temperatures, along with condensation coefficients for structural heat sinks added as a key model indicator. Typically for containment testing and design basis transient analyses, containment pressure is appropriately treated as a global parameter and therefore the use of a simpler calculation methodology may be possible. Whereas, when attempting to calculate *regional* containment gas temperatures resulting from steam transport and potential stable steam/gas stratification, a more complicated model is warranted. These aspects are pursued and key insights are discussed later in Section 4 dealing with multi-cell calculations.

With reference to the MELCOR code, it is noted that each of the important phenomenon listed in Table 3-1 has corresponding models included and discussed in the MELCOR reference manual [Gau05b], shown here in Table 3-2. The exception concerns phenomena associated with jet-plume gas interaction and entrainment processes. For these processes, neglect of momentum transport within a control-volume along with the absence of concentration front tracking precludes the ability to predict or distinguish jet-plume behavior arising from injections of high energy line breaks.[2] In most cases, however, the jet-plume importance is limited to short periods (blowdown), and neglect of the exceedingly complex phenomenon (linked to geometry, etc.) typically results in a conservative (*over*) estimate of containment pressurization. Local temperatures may be under predicted within the jet or plume; however, because the period of interest is relatively short, the error is limited to localities near the break. Consequently, neglect of jet-plume phenomenon modeling is often considered an acceptable short-coming for the control-volume approach to DBA assessment. Justification for this acceptance is, in part, the result of analysis of experiments such as for the CVTR DBA tests using a control-volume code such as MELCOR or CONTAIN. The CVTR tests therefore provide important data on both the global and regional effects of high energy steam line breaks in containments including mixing and transport processes, and those

[2] The MELCOR code does allow the user the flexibility to include (by input) volumetric flow from jets into a volume, with a control volume calculated velocity that is specified by the user through the use of an effective control volume hydraulic flow area. Usage of this type of input specification is intended mainly for sensitivity analysis, and is demonstrated in the multi-cell CVTR calculations to investigate the importance of forced convective condensation on predicted peak pressure during the blowdown period.

phenomena associated effects of operating engineered safety features (sprays). The process modeling for pressurization, mixing, transport, heat and mass transfer are all addressed in the CVTR tests to some extent, and MELCOR modeling is assessed for each of these processes in Section 4.

3.2 Nodalization Model

The MELCOR CVTR model is based on the information documented in the final facility test report [Sch70]. Accordingly, the physical aspects of the containment structure were appropriately modeled, e.g., free volumes, flow paths, etc. The heat sink input is based on "best-estimate" concrete areas as tabulated in the final report, Table 2-1 in Section 2, and on the upper bound estimate for exposed miscellaneous steel (this corresponds to 50% of the tabulated major-component steel area at 3/8" thickness). In the tests, steam is injected approximately 2 to 8 meters above the operating floor from a diffuser pipe. There are two baseline or reference MELCOR calculations of all three CVTR tests; they are distinguished by the use of a single cell (one control volume) and a multi-cell (multiple control volumes) nodalization of the containment free volume. A summary of the key model/input options selected for the calculations are presented in Table 3-3.

Early code assessments of the CVTR experiments were performed with one-cell models, and predominately, design-basis licensing calculations for large dry PWR containments are also performed in this manner. This approach is generally acceptable because the current PWR containment designs consist of largely open regions, and use sprays and/or fan coolers which are activated quickly following the onset of a postulated design basis MSLB (or LOCA) sequence, resulting in a relatively well-mixed containment free volume. Moreover, for the short-term portion of the postulated accident transient, the use of a single cell model usually results in a slightly higher peak calculated containment pressure than a multi-cell containment model. This occurs because in the single cell case, predicted are higher non-condensible gas mass fractions, resulting in a slightly lower overall heat transfer rate than in the multiple cell case, even though *all* the structural passive heat sinks are instantaneously exposed in the single cell model. The difference between single and multi-cell pressurization however is emphasized as slight. In both instances, natural convection heat and mass transfer are modeled, with no estimates of forced convection being made, and this choice is typically the source of most of the conservatism associated with DBA assessments. Also, in the single cell case the containment atmosphere temperature would be "averaged," and if needed, spatial temperature predictions would be missing. So that when analyzing the more advanced plant designs which may not utilize containment sprays or fan coolers, a multi-cell plant nodalization is warranted to recover region-to-region temperature profiles. Consequently, MELCOR assessments of the CVTR experiment were grouped based on a single cell and a multi-cell facility nodalization of the free gas space.

Shown in Figure 3-1 is the MELCOR CVTR multi-cell nodalization schematic. Note that in the pursuit of the multi-cell MELCOR assessments of the CVTR experiments, these results would be aimed at providing *best estimate* predictions for containment pressures and temperatures.[3] Moreover, regarding both types of nodal schemes, appropriate code sensitivities were performed to gain insights for analyzing full-scale plant configurations.

3.3 Heat and Mass Transfer Modeling

The process of heat and mass transfer for containment analysis is extremely important for an adequate estimate of peak pressure and temperature, and therefore for an assessment of the margin of safety for containment integrity and/or safety equipment function. Because of the importance attributed to this process, a great deal of attention has been devoted to understanding the phenomena of both free and forced convective condensation during DBA events. As a result, this process (along with some overlap to other processes) is singled out for in depth assessment in this report.

3.3.1 MELCOR Models and User Input

The MELCOR modeling for heat and mass transfer from containment atmosphere to passive structures and components is based on a heat and mass transfer analogy (HMTA), where common heat transfer correlations (free and forced circulation) are used to obtain both sensible energy and, by analogy mass transfers, through temperature and concentration boundary layers, respectively. In most containment analysis scenarios, the dominant transfer process affecting figure-of-merits is due to condensation heat (i.e., via mass transfer) transfer in the presence of noncondensible gases. In this case, the main resistance to condensation is the build-up of noncondensible gases near the surface of the structure, Figure 3-2. The build-up effectively depresses the partial pressure of vapor in the boundary layer, and therefore degrades the condensation process. As a result, condensation heat transfer coefficients are known to be sensitive to small amounts of bulk air concentrations (i.e., air/steam mass ratios), especially under free convective conditions. This behavior and MELCOR's modeling ability to simulate the process is discussed in more detail for the Dehbi free convection separate-effects tests included in Appendix B. The convective correlations that are the basis for the HMTA modeling is discussed briefly below.

A widely used heat transfer correlation for Nusselt number *Nu*, developed for turbulent, vertical wall heat transfer under natural convection conditions, is modeled in MELCOR as

$$Nu_{nat} = CRa^{m} + D,$$

where *C*, *m*, and *D* are constants set by the user (or remain as defaults); and, *Ra* is the Rayleigh number. For turbulent, forced flow the Nusselt equation is

$$Nu_{forced} = C\,\mathrm{Re}^{m}\,\mathrm{Pr}^{n} + D,$$

[3] Arguments that multi-cell calculations are conservative may also be advanced based on the neglect of forced convection or adjustment of natural convection condensation coefficients correlations. Multi-cell calculations have the potential for minimizing the conflicting aspect of too high noncondensible gas fractions (under-estimating heat transfer) and too much structure contact with blowdown steam (over-estimating heat transfer) that must be considered for single-cell calculations.

where again the constants C, m, n, and D are set by the user; Re and Pr are the Reynolds and Prandtl numbers, respectively. In order to conform to the heat transfer equations for Nusselt number used in the CONTAIN assessment report [Til02a], the value of C in the free convection equation is set (sensitivity coefficient 4110(1)) to 0.14; m remains set to the default setting of 1/3, and D is zero, by default. As with the CONTAIN equations for forced flow, the default MELCOR settings C = 0.037, m=0.8, and n=$\frac{1}{3}$ are used. Although equations for laminar flow are also included in the MELCOR modeling for convection, turbulent conditions are most often used based on the expected flow conditions inside containments and the default laminar to turbulent range settings. Transition from natural to forced convection is, as in CONTAIN, set to the maximum of either the free or forced Nusselt number,

$$Nu = \max\left[Nu_{nat}, Nu_{forced}\right].$$

In MELCOR, this setting is invoked by setting the sensitivity coefficient 4060 (1) equal to -1 (see Appendix C for experimental justification for this method of treating free to forced transition). For both single and multi-cell calculations, the calculated lumped cell flow velocity (forced) along structure surfaces is too small to force $Nu_{forced} > Nu_{nat}$, that is, unless flows within a control volume are specified by input for the blowdown period. Specification of flows in this case is not a normal feature of DBA analyses since estimation of blowdown driven air/steam flows is outside the scope of analytical modeling, whether by finite-difference or control volume methods, for the reasons mentioned above (e.g., jet/plume interaction/entrainment). However, the use of flow or velocity specification for structure condensation heat transfer is useful for other purposes, e.g., for minimum backpressure calculations, sensitivity investigations, or for indirect confirmation of measured velocities via structure heat flux measurements. In terms of the latter, calculations are discussed in Section 4 for the multi-cell nodalization that confirm velocity measurements during the CVTR Test 3 blowdown period.

For each structure (not flooded) where condensate forms, film flow is assumed based on Nusselt laminar film theory (as assumed in CONTAIN). Film heat transfer is therefore governed by conduction through the average thickness of condensate film on the structure. As an example, shown in Table 3-4 are laminar film flow parameters obtained for the MELCOR HMTA for a representative vertical structure of length 3.5 meters, immersed in a saturated steam/air atmosphere where condensation occurs for a constant bulk to wall surface temperature difference of 30 degrees. A couple of points are obvious from these results: 1) film resistance R_{film} due to the laminar film layer is a small fraction of the total resistance (i.e., film R_{film} plus steam/air boundary layer resistance R_v); and, 2) film flow is clearly in the laminar range (film Reynolds number < 1000 for laminar flow according to the MELCOR default setting). Typical minimum air/steam mass ratios for the CVTR single cell calculations are ~1.5; therefore, free convective condensation heat transfer coefficients of 300 to 400 W/m^2-K maximum may be anticipated with the MELCOR HMTA model for the CVTR tests for vertical structures of reasonable height. Film heat transfer for laminar flow may be somewhat affected by waves formed on the film surfaces, but these effects are known to be relatively minor, especially for situations where the film forms by condensation. In any case, the assumption of laminar film flow represents a conservative (higher) estimation for the condensate film resistance to total energy transfer from the atmosphere to the surrounding heat sinks.

In most "as-built" containments, major structural walls and equipment have a layer of paint which also represents a resistance to condensation heat transfer. In the CONTAIN code, for example, paint resistance is explicitly modeled with a series conductance added to the film layer and surface node resistance. For MELCOR, there is no explicit modeling of paint resistance, and therefore in essentially all containment analyses to date, paint resistance has been neglected. Two options for including paint resistance are available however. In the first option, the paint layer is modeled as a separate material layer for representing a composite structure (e.g., paint over concrete or steel). The disadvantage of this approach is that the thin paint layer with its small thermal capacitance can require small timesteps for adequate convergence of the heat conduction solution. Another approach is equivalent to the method implemented in the CONTAIN modeling where the heat capacity of the paint is neglected compared to the surface node of the structure, with only the resistance (or conductance) of the paint is accounted for in the conduction model. The CONTAIN method for treating paint layers can be simulated in MELCOR by adjusting the thermal conductivity of the surface node; that is, by modifying the effective conductivity to include the added resistance of the paint layer. This approach is used here to investigate the sensitivity to paint layer modeling applied to the single-cell calculation of CVTR Test 3: results are discussed in Section 4.

While thermal radiation heat transfer between the containment atmosphere and structures is a small contributor to the total heat transfer for DBA containment analysis, it is nevertheless, treated in the MELCOR modeling and its inclusion may be of some importance in correctly modeling conditions where the containment gas has significant superheat. Users may select thermal radiation with gray-gas or equivalent-band models. In the calculations that included thermal radiation here, the gray-gas model is selected. Emissivity of dry structures is an user input which is specified as 0.9. The radiation path or beam lengths for these CVTR calculations are also user input, and the values are generally based on an enclosure relationship [Sie81] where the beam length L for boundary volume V enclosed by total structure area $\sum A_i$ is given by

$$L = \frac{3.6V}{\sum A_i} .$$

3.3.2 Licensing Models Previously Used for CVTR Test Analysis Compared to MELCOR Modeling

One of the more often cited licensing models for treating free convective condensation in containment analyses is the Uchida correlation [Pet96]. Unlike the mechanistic MELCOR and CONTAIN HMTA methodology[4], the Uchida correlation is from a class of semi-empirical correlations, where measured condensation coefficients[5] are related to a single independent variable – in this case, air/steam mass ratios. The correlation, or a form of it, has been used in a number of early (e.g., CONTEMPT-LT) and recent proprietary codes to describe condensation in the presence of noncondensible gases. It is appropriate to compare such a well known correlation

[4] Comparisons between the MELCOR and CONTAIN implementation of the HMTA modeling are addressed in Appendix B (Dehbi Natural Convection Condensation Tests Analysis) and Appendix C (Wisconsin Flat Plate Condensation Tests Analysis).

[5] Condensation coefficients are defined by $q = h_{cond}(T_b - T_w)$, where q is the total heat flux transferred from the atmosphere at temperature T_b to the heat sink with surface temperature T_w.

with the MELCOR model since most of the early analysis of the CVTR tests were performed using the Uchida data, and most plant licensing reviews of containment response for DBA events have been supported by analyses using the Uchida data.

The Uchida correlation was developed based on a series of tests in a relatively small (few cubic meters) chamber where heat transfer to a small vertical plate was measured for various noncondensible gas types (nitrogen, air, argon) and steam amounts at saturation. The test procedure restricted the initial or starting atmosphere (e.g., dry air) to a pressure of 1 bar. As a result, the air density was fixed for all subsequent increases in vessel pressure due to the injection of saturated steam. Typical implementation of the Uchida data is through a fit of the measured condensation coefficient to bulk air/steam mass ratio. For example, Peterson [Pet96] provides a best-fit correlation as

$$h_{cond} = 335\left[\frac{W}{m^2 - K}\right]\left(\frac{m_{air}}{m_{steam}}\right)^{-0.7}$$

In other approaches, e.g. with the NRC's CONTEMPT code, the coefficient data are extracted from Uchida's experimental results. However, the choice of data extracted has generally not been performed in such a way so as to replicate the results from correlations. As a result the table of Uchida data found in the CONTEMPT code does not correspond to a best-fitting of the original Uchida data. Shown in Figure 3-3 are the comparisons of the Uchida "best-fit" correlation, the CONTEMPT table values, and the MELCOR HMTA model results for vessel conditions monitored in the Uchida tests. Differences between the various approaches are most obvious for the CONTEMPT tables, with the Uchida correlation and MELCOR HMTA calculations showing very good agreement. The Uchida semi-empirical method is a simple approach to a complicated process that involves the phenomena associated with the transfer of mass and energy from the containment atmosphere to passive structures. Some of the short-comings not treated in this simple semi-empirical correlation are:

- effect of air density change (stratification) on condensation
- effect of condensate film build-up on condensation
- changes in condensate rate for varying bulk to wall temperature difference
- amounts of sensible versus latent heat transfer occurring during condensation
- implementation for superheated atmospheres

These shortcomings are addressed in the following subsections.

Air density. Of the five short-comings listed, the most important potentially is the first dealing with the effect of air density on condensation, as was pointed out in Peterson [Pet96]. In the early assessment of the CVTR tests, analyses were typically restricted to single-cell representations of the CVTR containment vessel. For these assessments, fixing air density at the initial ~1 bar air pressure was effectively accomplished simply by its application. Consequently, a single-cell analysis of the CVTR tests, with the Uchida data for condensation modeling, represented an appropriate and consistent use of the Uchida data. However, as we will see from the CVTR measurements, air density throughout the containment is anything but constant during the test – since air density varies significantly from the region above the operating floor to the basement

region. Therefore, the possibility of applying test results to containment conditions outside the domain of the test data exists and can result in significant error.[6] Figure 3-4 is a plotting of MELCOR results for various initial air pressures showing that for initial pressures below atmospheric, the condensation coefficient is predicted to trend below the value calculated at atmospheric pressure (1 bar), and predicted to trend above for initial pressures greater than atmospheric. The insert in the figure shows that these trends can also be experimentally derived from data collected by Kataoka [Kat92]. A more pronounce variance obtained by Anderson [And98] and reported in Herranz [Her98] is shown in the insert in Figure 3-5, where the MELCOR results for low initial air pressure from 0.26 bar to 0.7 bar is plotted and compared to the Uchida correlation – again, showing the potential for significant error. As can be seen from both figures with inserts, the MELCOR HMTA model correctly accounts for air density effects on the predicted condensation coefficient, and therefore represents a suitable model for either single-cell or multi-cell calculations where air density is anticipated to change as a function of location in the containment.

Condensate film. In the experiments performed by Kataoka, condensation coefficients were measured at three locations along a 4 meter vertical wall. Film build-up along the wall was suspected in the relatively small variations noted in the measured coefficients. The effect however was in the range of about +/- 10%. MELCOR calculations of a similar geometry (wall length ~3.5 meters) show an equivalent sensitivity to film thickness effects (e.g., compare resistance percentages for diffusive boundary layer R_v with film resistance R_{film} in Table 3-4). Additionally, the calculations also indicate that for the conditions of the test (similar to the Kataoka tests), the film flow is in the laminar regime (film Reynolds number less than ~1000); therefore, the film heat transfer process is dominated by conduction through the condensate layer.

In MELCOR version 1.8.6, all structures are treated as consisting of a single network of connected surfaces for the purpose of film tracking, and with laminar film heat transfer modeled as heat conduction through the film thickness – the so called Nusselt model. A condition of fixed or maximum film thickness is not modeled by default, as is the case in the CONTAIN treatment of condensate build-up (i.e., without film tracking input). To minimize the effect of condensate build-up in MELCOR, the user can however artificially reduce the effective length of a structure, thereby reducing the condensate thickness – approaching a zero film thickness. Setting a fixed film thickness is not available with the MELCOR 1.8.6 version film model.[7] The input procedure for reducing film thickness (via structure characteristic length) is used in the CVTR single-cell calculation to investigate pressure and temperature sensitivity to condensate film modeling.

Bulk to wall temperature difference. The Uchida data was obtained with a constant wall temperature of ~322 K, according to Peterson [Pet96]. This test procedure results in an increasing bulk to wall temperature difference when the vessel saturation temperature and consequently air/steam mass ratio decreases during the test runs; for example, see Figure 3-6. For air/steam

[6] Note, even though the effect of air density change can have a significant affect on condensation, applications may show a more modest trend due to the offsetting of errors. The degree of offset is however largely dependent on the distribution of heat sinks within a specific containment design; therefore, the potential for application error cannot be discounted.

[7] An exception to the fixing of film thickness is the option in 1.8.6 version to revert back to a 1.8.5 method of specifying the maximum film thickness. This option is not used in this report since the possibility of instability with this method is suggested in the 1.8.6 user manual.

mass ratios ranging from 0.75 to 8, the bulk to wall temperature difference varies from about 80 to 15 degrees. Shown in Figure 3-7 is the MELCOR calculated condensation coefficient values for bulk to wall temperature differences of 5 to 50 degrees. For temperature differences greater than ~30 degrees, there is a noticeable reduction in the condensation coefficient for a given air/steam mass ratio. The good agreement therefore apparent in Figure 3-3 between the Uchida data and the MELCOR HMTA model results points to an appropriate treatment of condensation coefficient versus bulk to wall temperature difference that is obtained using the MELCOR HMTA model.

Sensible versus latent heat transfer. Another shortcoming of the Uchida correlation approach is that there is a lack of information on the partitioning of energy removed from the atmosphere by sensible and latent energy transfers – in this case, only total energy transfer is measured. In a closed system, if the partitioning is calculated incorrectly, the atmosphere may remain saturated when in reality superheating should occur (too little energy attributed to mass transfer), or a partitioning error may result in predicted superheating when saturation should be calculated (too much energy attributed to mass transfer). In previous licensing audits using the CONTEMPT code with the Uchida data, an assumed percentage (8%) of sensible to total energy transfer was recommended. Shown in Figure 3-8 is the MELCOR calculated partitioning of sensible to total energy transfer percentage for an initial air pressure of 1 bar (single-cell appropriate). The percentage is seen to vary with the air/steam mass ratio. At an air/steam ratio of ~1.5 (corresponding to the ratio at the end of the CVTR blowdown with a single-cell model), the percentage is ~3%, which is less than half of the licensing recommended value. Sensitivity calculations with increased sensible heat transfer are investigated with the single-cell CVTR calculation series.

Superheated atmospheres. The Uchida data applies only for condensing saturated atmospheres. For superheated atmospheres, implementation of an adequate and defendable approach to extend the saturated data into the superheated region does not appear in earlier code documentation. Most separate-effects condensation tests have been conducted for saturation conditions with the exception of the Phebus FPT0 tests [Phe94] where superheated conditions existed during periods of significant condensation. Appendix D addresses this issue of superheated condensation using the Phebus test as a benchmark for the MELCOR HMTA model. The very good results obtained with MELCOR for this test is the only experimental data supporting the MELCOR modeling usage under superheated conditions. In test analyses performed in the CVTR test report and in the open literature, the containment temperature maximum is predicted to be superheated. The justification for a predicted superheat is not clear from the CVTR data, or defendable from analyses that utilize a mass transfer correlation such as the Uchida correlation. This issue regarding superheating in the CVTR vessel is discussed further in Section 4.

(Note, for calculations where condensate drain-off from structures goes to an initially dry sump, as in the case of CVTR tests, the minimum (estimated) volume fraction of the pool below which equilibrium thermodynamics will be enforced is reduced by input from the default setting (1.0E-6) to 1.0E-10. The setting for this limit condition is via sensitivity coefficient 4411(5). Failure to satisfy the limit, that is, failure to have pool fractions above the set limit can, especially under superheated conditions, force evaporation of drain-off water and result in an artificial reduction for superheat. Since the appropriate limit condition to prevent a forced equilibrium calculation may not be known for all containment geometries and scenarios, sensitivity calculations are suggested to assure that gas temperatures are not being artificially depressed during periods of condensate drain-off.)

Table 3-1 Important containment phenomena addressed in experiments based on design and beyond design basis ranking criteria (containment pressure and temperature).

		Separate*				Integral									
		Wisc. Flat plate	MIT Dehbi	Phebus FPT0	JAERI spray	HDR V44	HDR T31.5	HDR E11.2	HDR E11.4	CVTR Test 3	CVTR Test 4&5	NUPEC M-7-1	NUPEC M-8-2	NUPEC M-8-1	NUPEC M-4-3
Component: Process	**Phenomena**														
Atmosphere:															
pressurization	multi-component gas compression/expan.			3	3	3	3	3	3	3	3	3	3	3	3
	spray mass and energy exchange				3						3	2	2		
	atmospheric cooling by fancoolers														
mixing	jet-plume gas interaction/entrainment					1	1	2	1	1	1	1	1	1	1
	buoyancy/stratification (regional)				3	3	3	3		3	3	3	3	3	3
	spray dynamics				2						2	2	2		
	fan dynamics														
transport	buoyancy					1	3	3	3	3	3	3	3	3	3
	form and friction losses					3	3	1	1	1	1	1	1	1	1
Structure Interior:															
heat transfer	1-D transient conduction					3	3	3	3	3	3	3	3	3	3
Structure Surface:															
mass transfer (cond/evap)	free convection	3	3	3	1	3	3	3	3	3	3	1	1	1	1
	forced convection	3				1	1	1	1	3	3				

[ ] not present, 1- present, 2- present and significant, 3- measured
*Discussed in report appendices (B-E)

Table 3-2 MELCOR modeling for important phenomena to DBA containment analysis.

Component: Process	Phenomena	MELCOR 1.8.6 version Reference Manual (RM)	Model Comparison to CONTAIN Code
Atmosphere:			
Pressurization	Multi-component gas compression/expansion	RM (CVH/FL; pp. 18-27, 30-37) RM (CVT; pp. 1-30) RM (NCG/H2O; pp. 1-16)	Equivalent atmospheric equilibrium approach with slight difference due to variation in gas property relationships and treatment of two-phase (atmosphere/pool) interaction via voiding/energy exchange
	Spray mass and energy exchange	UG (SPR)	Equivalent approach with MELCOR has added capability in treating droplet size distributions and control volume fall though, in addition to rainout from structures
	Atmospheric cooling by fan cooler	RM(CVH/FL; pp. 57-58)	Limited modeling capability for MELCOR; no mechanistic treatment of fan cooler condensation field
Mixing	Jet-plume gas Interaction/entrainment	RM(CVH/FL; p.24, 65)	Both codes allow similar specification of flow velocity via volume velocity calculation based on effective volume flow area (useful for sensitivity analysis only)
	Buoyancy/stratification (regional)	RM(CVH/FL; pp. 49-54)	CONTAIN uses a hybrid flow solver to prevent nonphysical circulation flows between control-volumes that is unique to code.
	Spray dynamics	UG(SPR)	Neither code allows spray induced mixing via droplet/gas drag.
	Fan dynamics	UG(FCL: p. 6)	Both codes allow intra-compartment fan flow w/o momentum transport.
Transport	Buoyancy	RM(CVH/FL; pp. 49-54)	Equivalent approach with variable static head calculated as function of elevation
	Form and friction losses	RM(CVH/FL; pp.52-56)	MELCOR pipe friction modeled separately with forward/reverse form factors
Structure Interior:			
Heat transfer	1-D transient conduction	RM(HS; pp. 3-16)	CONTAIN uses Crank-Nicholson scheme (cell-centered difference) with explicit paint conductance; MELCOR fully implicit scheme (cell boundary difference) – no explicit paint conductance
Structure Surface:			
Heat and Mass Transfer (evap/cond)	Free convection	RM(HS; pp. 16-26, 38-42, 58-62)	Heat and Mass Transfer Analogy (HMTA): Default convection correlation is a factor 0.1/0.14 lower; film tracking by default with Nusselt film theory approach (laminar flow range applicability equivalent to CONTAIN approach)
	Forced convection	UG*(CVH; p. 13) RM(HS; pp. 16-26, 38-42) RM(CVH/FL; p. 24, 65)	Equivalent HMTA approach: MELCOR velocity calculated at cell level; whereas, CONTAIN velocity calculated at structure level

*User Guide

Table 3-3 Key modeling/input options used in the CVTR MELCOR calculations.

Test	Model/Input Options
#3	• one-cell and 19 cell nodalization • specified thermal properties for steel and concrete • default convective velocities • no paint on surfaces • default film thickness (single network film tracking) • overflow condensate to sump • flooding of lower concrete structures in contact with sump • atmospheric radiation to structures • loss coefficients (CFC) set to 1 • upper bound estimate misc. steel mass - 50% measured large structure steel
#4	• one-cell and 19 cell nodalization • sprays modeled with pass through for stacking cells above operation floor • default spray droplet diameter • default convective velocities • no paint on surfaces • default film thickness (single network film tracking) • overflow condensate to sump • flooding of lower concrete structures in contact with sump • atmospheric radiation to structures • loss coefficients (CFC) set to 1 • upper bound estimate misc. steel mass - 50% measured large structure steel
#5	• same as #4, except for adjustment in the spray source rate

Table 3-4 Natural convective condensation on vertical surface* using MELCOR HMTA model (shaded → minimum air/steam ratio for single-cell CVTR Test 3 calculation).

Pressure = 1.5 bar; $T_b - T_w$ = 30 K									
Air Mass Fraction	Air/Steam Ratio	T_b	T_w	T_i	$\bar{\delta}$	Re_{film}	h_{nat}	% Resistance [boundary-layer], R_v	% Resistance [film], R_{film}
0.3	0.43	378.1	348.1	351.6	1.21E-04	153.5	649.8	88.4	11.7
0.4	0.67	374.9	344.9	347.4	1.12E-04	110.7	495.8	91.7	8.3
0.5	1.00	371.1	341.1	342.8	1.03E-04	78.4	375.7	94.2	5.8
0.6	1.50	366.3	336.3	337.5	9.52E-05	53.2	277.6	96.0	4.0
0.7	2.33	360.0	330.0	330.8	8.67E-05	33.2	195.0	97.4	2.6
0.8	4.00	351.1	321.1	321.6	7.74E-05	17.7	124.2	98.5	1.5
0.9	9.00	336.2	306.3	306.4	6.59E-05	6.2	62.7	99.3	0.7
Pressure = 3 bar; $T_b - T_w$ = 30 K									
Air Mass Fraction	Air/Steam Ratio	T_b	T_w	T_i	δ	Re_{film}	h_{nat}	% Resistance [boundary-layer], R_v	% Resistance [film], R_{film}
0.3	0.43	399.4	369.4	374.2	1.26E-04	277.8	890.8	83.8	16.2
0.4	0.67	395.8	365.8	369.3	1.16E-04	202.3	685.6	88.4	11.6
0.5	1.00	391.5	361.5	363.9	1.08E-04	144.7	523.4	91.8	8.2
0.6	1.50	386.1	356.1	357.8	9.89E-05	99.2	389.4	94.3	5.7
0.7	2.33	379.0	349.0	350.1	9.00E-05	62.7	275.6	96.3	3.7
0.8	4.00	369.1	339.1	339.7	8.01E-05	34.0	177.3	97.9	2.1
0.9	9.00	352.5	322.5	322.8	6.78E-05	12.4	91.3	99.0	1.0

* representative characteristic length = 3.5 meters

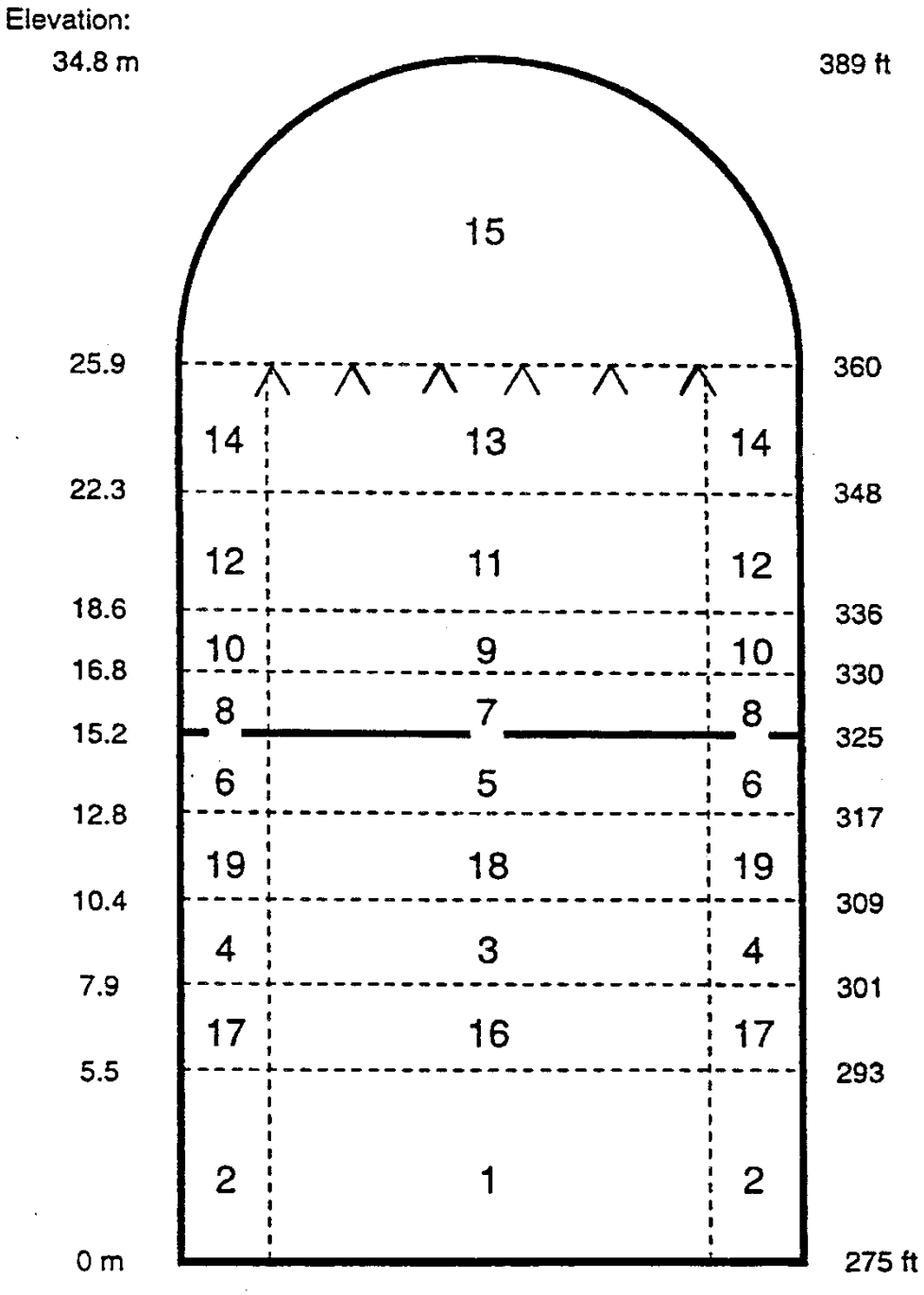

Figure 3-1 CVTR facility nodalization scheme used for the MELCOR multi-cell calculations.

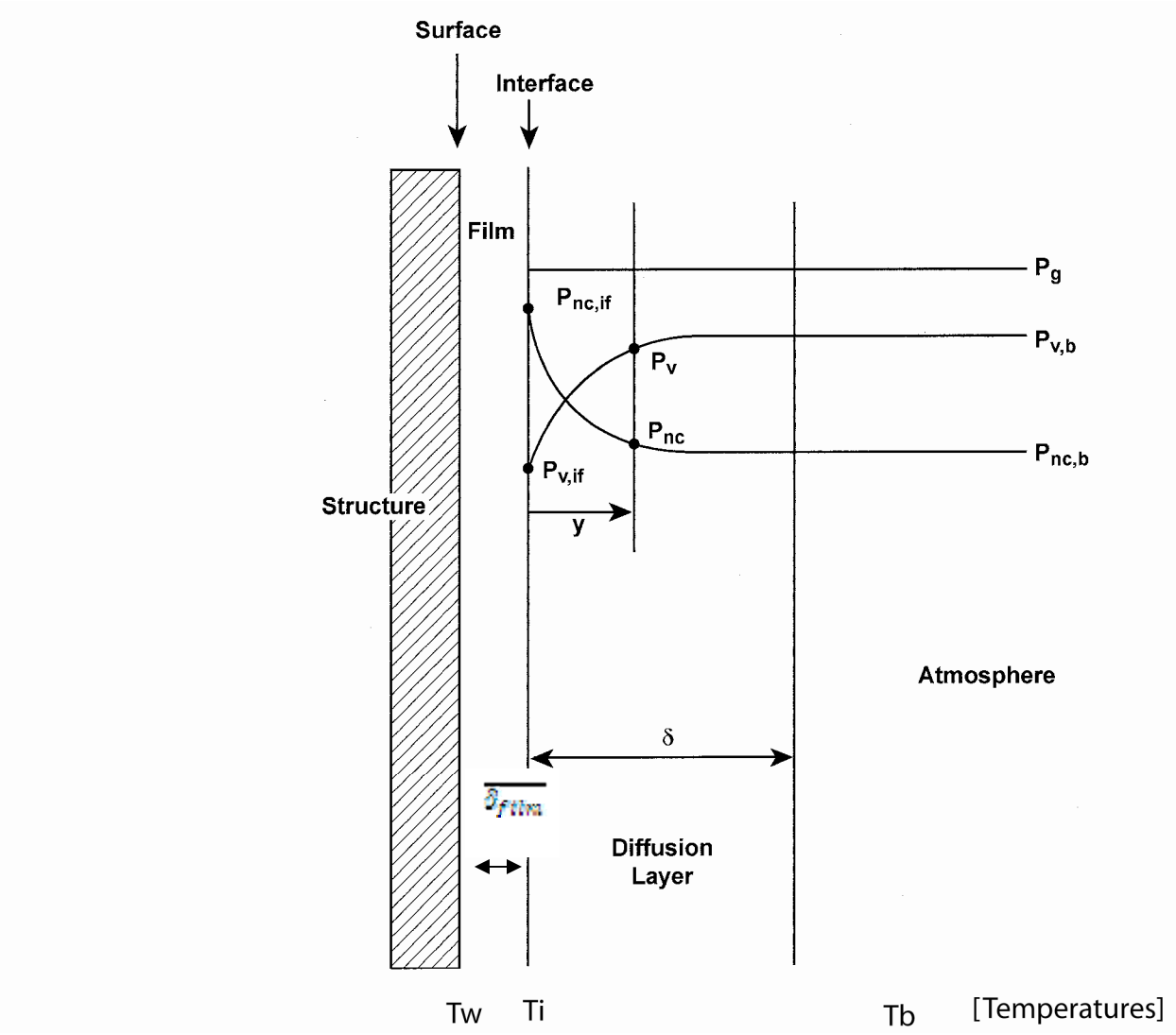

Pv = vapor partial pressure

P_{nc} = noncondensible gas pressure

Pg = total pressure

Tw = surface temperature

Ti = film interface temperature

Tb = bulk atmosphere temperature

Figure 3-2 MELCOR Heat and Mass Transfer Analogy (HMTA) model sketch.

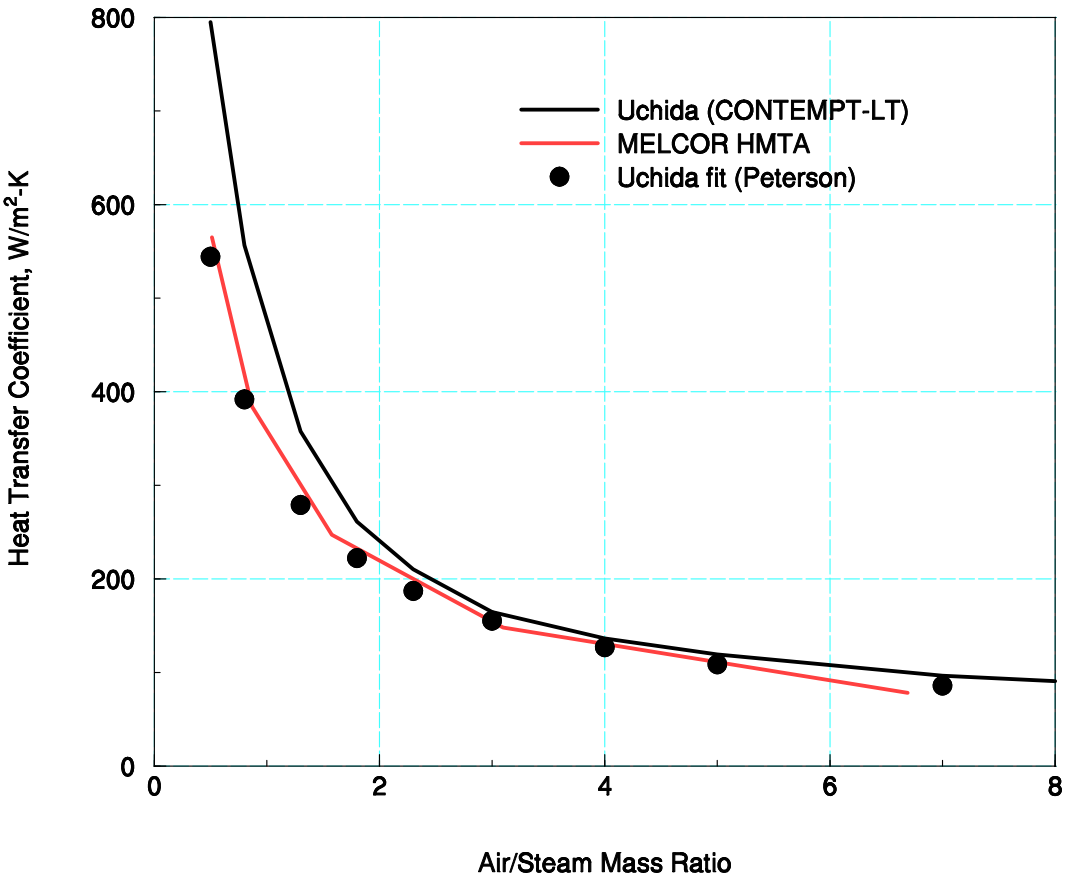

Figure 3-3 Condensation heat transfer coefficient prediction by MELCOR HMTA model for the conditions of the Uchida condensation tests (initial air pressure at 1 bar). (Minimum air/steam ratio for single-cell CVTR test calculation is ~1.5 at end of blowdown injection.)

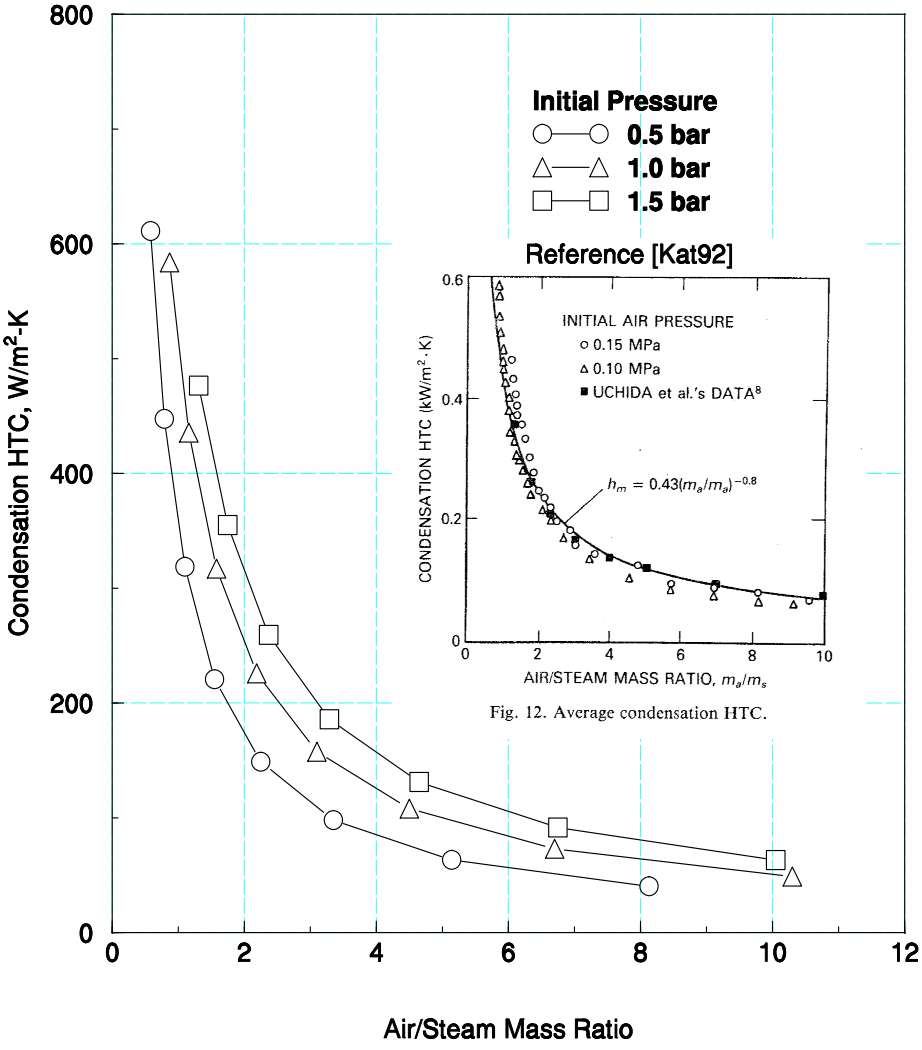

Fig. 12. Average condensation HTC.

Figure 3-4 MELCOR calculation of condensation coefficient for varying initial air pressure. Insert shows Kataoka data compared to another form of the Uchida correlation [Kat92].

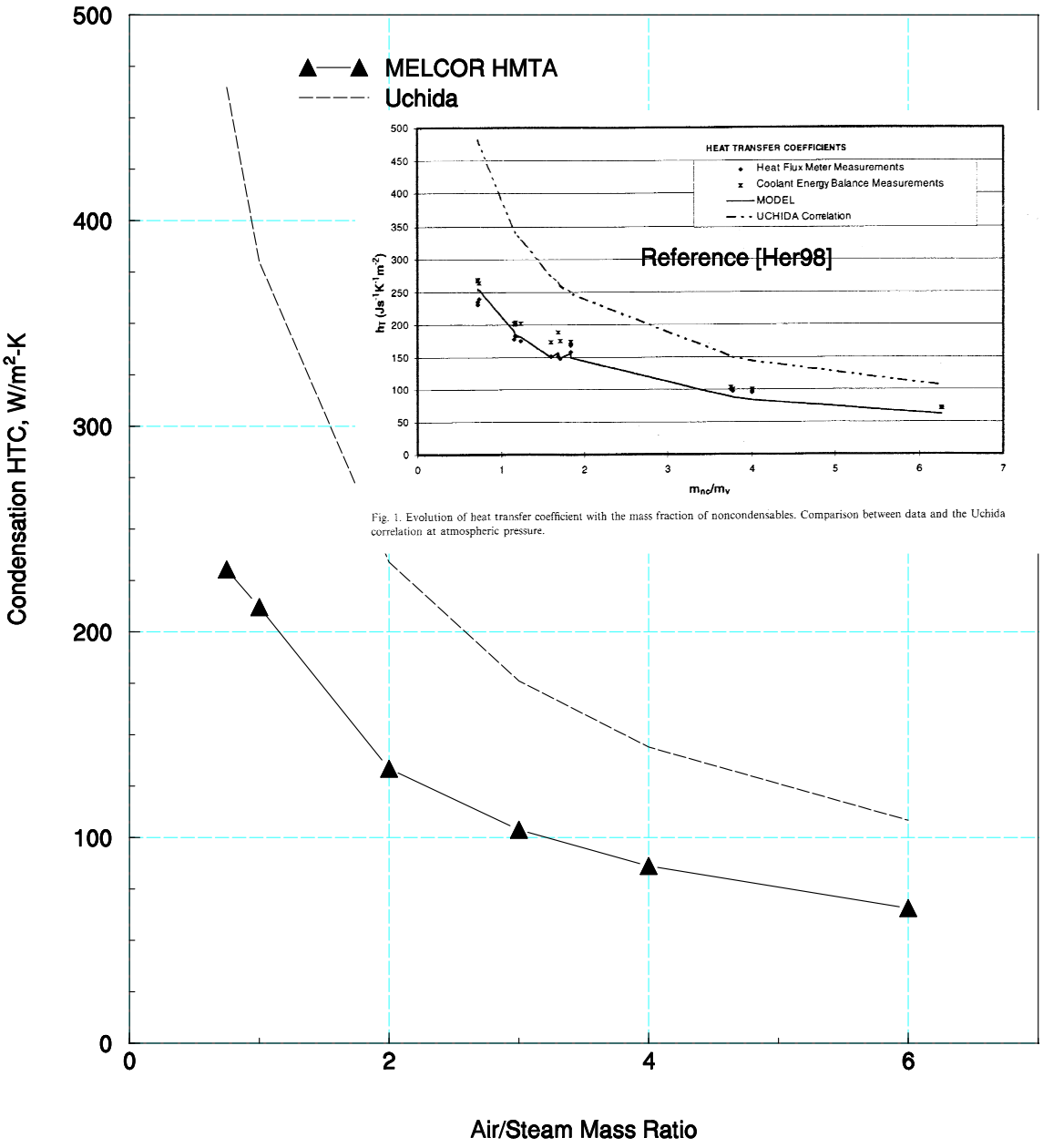

Figure 3-5 MELCOR calculation of condensation coefficient for low initial air pressure. The insert shows data collected by Herranz (Her98) in the Wisconsin test vessel and reported in Reference [And 98].

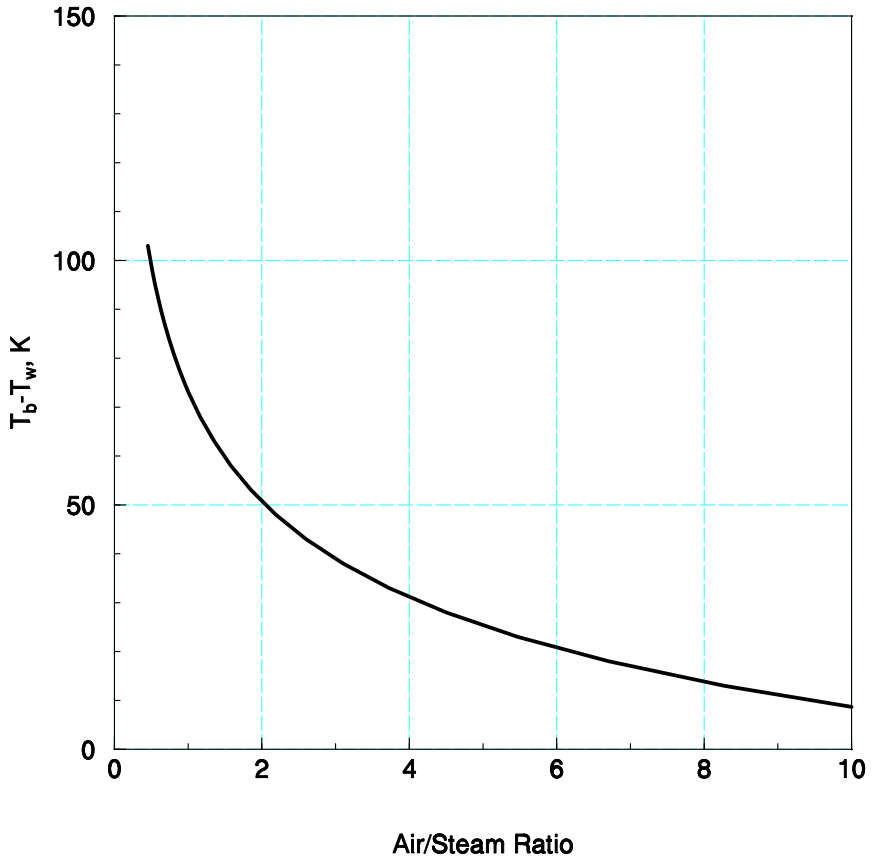

Figure 3-6 Bulk to wall temperature difference for conditions during the Uchida condensation tests (based on Peterson [Pet96] comment concerning condensing plate fixed temperature of 322 K.)

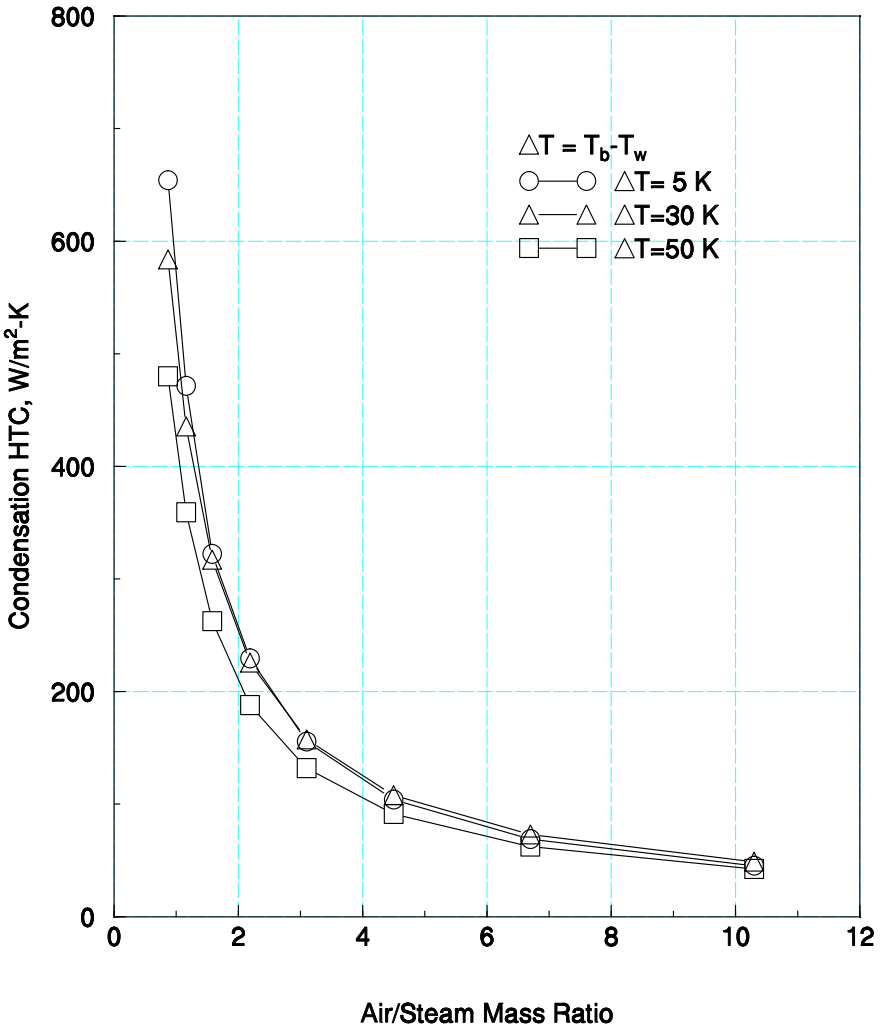

Figure 3-7 MELCOR calculated condensation coefficient for varying bulk to wall temperature difference.

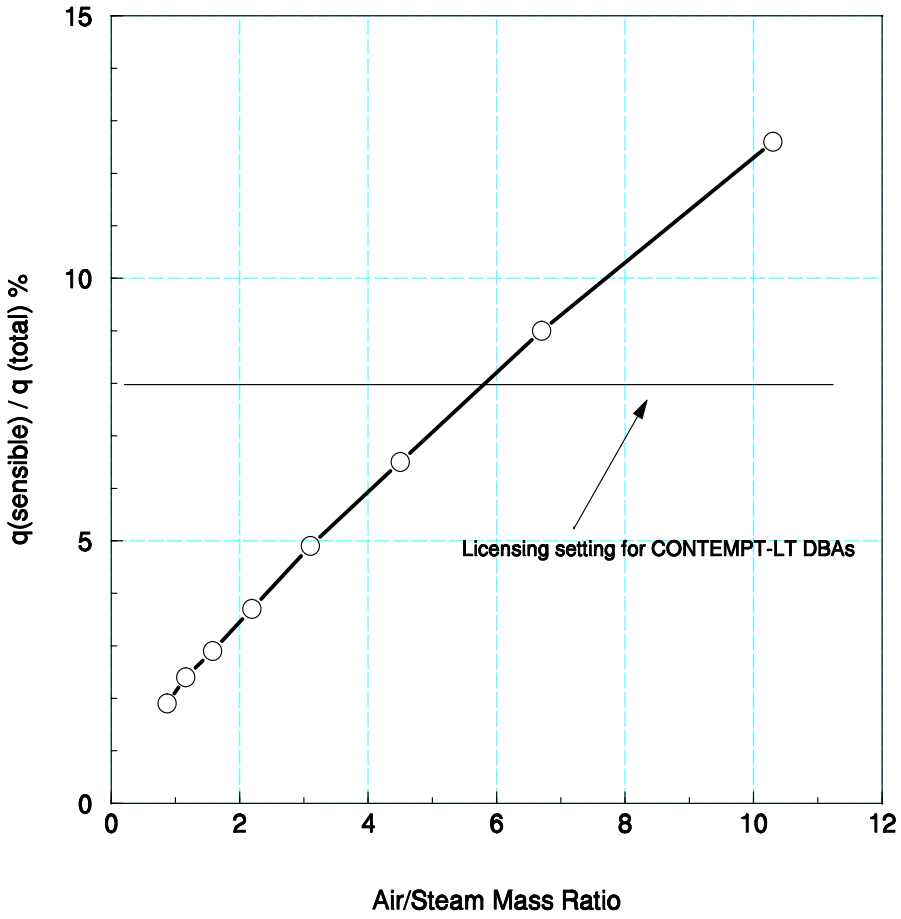

Figure 3-8 Sensible heat ratio calculated using the MELCOR HMTA (1 bar initial air pressure, bulk to wall temperature difference = 30 K, saturated bulk condition).

4 MELCOR CVTR Assessments

The CVTR report (Sch70) may not be easily obtainable for most readers; therefore, each introduction section below first discusses interpretation of measurements for a specific test including the original figures from the test report. At the time that the test report was written, measurements were taken in English units. Since current containment codes such as CONTAIN and MELCOR are written for input/output in SI units, the test report figures are translated to SI units in the subsections that discuss code-to-code or code-to-measurement comparisons. With respect to elevations referenced in the test report, Table 4-1 provides the translation from English to SI units, with the associated change in the reference elevation for the containment basement floor; i.e., the elevation of 0.0 meters corresponds to 275 ft. elevation in Sch70. In the discussion that follows, the emphasis is on the comparison of MELCOR results to measurements; however, code-to-code comparisons between MELCOR and CONTAIN are also included to show the extent of parity between these two codes for DBA-type analyses. The inputs for both codes are essentially identical (i.e., control volume(s) and heat sinks) and therefore slight variations in results are mainly due to some small differences in process or phenomena modeling.

4.1 CVTR Test 3 (without spray activation)

Shown in Figures 4-1 and 4-2 are early camera snapshots taken during the Test 3 blowdown from the side and top locations in the containment operating region (above the operating floor). The photo results show the general degree of turbulence associated with the event and the shape of an emerging and rising jet-plume as the steam front moves out from the diffuser pipe and contacts the containment wall. The blowdown is visible because the air/steam cloud is supersaturated at these times, with the image obtained from reflective light off the mist of liquid water suspended in the open space. An upward movement of the jet-plume is distinguishable in the side-on photo at ~2 seconds, indicating the significant effect that buoyant forces have on the diffuse jet. A downward snapshot, Figure 4-2, shows a dark region near the diffuser pipe that suggests a small local region of superheated steam, which quickly become supersaturated a short distance from the source.

In Figures 4-3 and 4-4, pressure and gas temperature measurements taken during the blowdown and cooldown (post-injection) periods are plotted. The cluster of gauge pressure measurements vertically throughout the containment reveal the global aspect of the pressure response, while the spread in temperature measurements indicate a regional or local response to the steam mixing and transport processes.

Results from inverse heat conduction calculations, based on the heat plug measured temperatures (bulk and liner imbedded thermocouples), were used to derive heat flux and condensation heat transfer coefficients along the containment wall in the operating region. Shown in Figure 4-5 are the derived condensation heat transfer coefficients at heat plug 1 and 2 locations. In the figure, TAEH is the name of the inverse conduction code, and the uncertainty associated with the method used to derive the condensation heat transfer coefficient at heat plug location #2 is shown in Figure 4-6. The corresponding average bulk temperature at each heat plug location is plotted in Figure 4-7; the measurements show that the bulk temperatures are nearly equal, indicating good mixing in the region surrounding the heat plug locations (see Figure 2-2 for relative location of heat plugs). Consequently, significant differences in the condensation heat transfer coefficients at each location are attributed to relative differences in observed turbulence, or forced convective

condensation as the air/steam cloud contacts the containment wall. The significantly higher heat transfer coefficient for heat plug 2 (higher elevation) appears to indicate more turbulence in this region just above the injection elevation; whereas, at the lower measurement (heat plug 1) below the injection, the turbulence appears to be less, resulting in a smaller measured coefficient. The shift in the timing of the coefficient peaks is also instructive, and seems to indicate an early reduction of the more elevated measurement as a consequence of stalling the jet-plume as the upper dome region (dead-ended region) begins to "fill." Below the injection, at heat plug 1 location, the steam flow is less due to counter-buoyant forces with the receiving volume below the operating floor "filling" at the rate less than observed for the dome region. Therefore, the increase in the heat plug 1 condensation rate proceeds at an increased rate due to the regional change in air/steam mass ratio with time versus any significant change due to turbulence.

Assuming saturated steam conditions in the containment, the temperature recordings in Figures 4-4 and 4-7 can be converted to steam partial pressures and then re-formulated as air/steam mass ratios in Figures 4-8 and 4-9, respectively. The degree of stratification indicated by both the vertical temperature profiles and derived air/steam mass ratios clearly indicate that above the operating floor mixing is nearly complete during most of the blowdown; however, below the operating floor there is significant stratification of temperature and steam concentration throughout the test.

The maximum velocities (speeds or currents) that were measured for both Test 3 and 5 (before sprays were turned on) with two functioning anemometers were 9.1 m/s (30 ft/s) and 4.6 m/s (15 ft/s) near heat plug location #2 and in the annulus between the operating floor and containment wall, respectively. Although, the uncertainty of these measurements is unknown, these velocities are found in the analysis below, subsection 4.1.2, to correspond well with wall velocities needed to predict condensation coefficients at each heat plug location based on forced convection conditions.

4.1.1 Single Cell Model

Single cell (one control volume) models have been used for design basis analyses, and almost exclusively for existing PWR plant licensing reviews. Validation of conservative features of these models has been, in part, based on code comparisons to integral tests such as the CVTR tests. The conclusions from these comparison studies were that the single cell models are conservative and therefore acceptable for licensing review purposes. Consequently, the single cell MELCOR calculations for the CVTR tests are appropriately discussed here with respect to results obtained with other qualified containment codes (e.g., CONTAIN) in code-to-code benchmarking and in code-to-measurement comparisons. The CONTAIN code is selected for the benchmark comparisons since this code has previously undergone an extensive review for DBA containment application [Til02a, Til02b].

4.1.1.1 Reference Case

Shown in Figure 4-10, is the comparison of the MELCOR and CONTAIN calculated single-cell pressure profiles plotted against the measured pressure for Test 3. Plotted in Figure 4-11 is a similar comparison of the code calculated gas or vapor temperatures with the measured maximum gas temperature in the dome region of the CVTR containment. These two figures are discussed separately in terms of the code-to-code and code to measurement comparisons.

Code-to-code benchmarking. The agreement between the MELCOR and CONTAIN calculations of CVTR pressure response is generally shown to be very good, especially during the injection period where the peak pressure calculated with MELCOR at 2.64 bar is compared to 2.63 bar for the CONTAIN code. During the relaxation or de-pressurization period starting at ~170 seconds there is a small variation in the calculated pressures between codes, with the MELCOR code showing a more rapid de-pressurization rate than CONTAIN. This behavior is due to a difference between the models for treating film condensate on structures for this reference case. For CONTAIN, the maximum film thickness is, by input, limited to a very small value (0.00005 meters) to simulate the typical single cell applications where film thickness is neglected (as with the Uchida correlation). For the MELCOR reference case, the film modeling is treated according to the default method where each structure is calculated as a single network, with film tracking applied to each vertical structure. In this approach, film thickness is determined based on a Nusselt film equation for laminar, condensate flow (film Reynolds number < 1000) along a vertical surface. Shown in Figure 4-12 is a comparison of the film thickness calculation for each method, MELCOR versus CONTAIN. During the injection period, the resistance to heat transfer from atmosphere to structure through the condensate film is very small compared to the resistance from the gaseous diffusion layer along the structure surface; therefore, film modeling tends to be unimportant during this period and, consequently, both code heat transfer calculations (and pressure response) are essentially identical.[8] When the containment begins to de-pressurize, however, the additional amount of film mass associated with thicker films, as in the case of the MELCOR calculation, provides a large effective water surface and reservoir for both sensible heat and evaporative cooling of the atmosphere. Since, by input, the CONTAIN calculation is run with a smaller film thickness (to better simulate Uchida-type analyses), a smaller amount of film mass is available either for sustained evaporation or sensible heat cooling. Therefore, the CONTAIN atmosphere cools at a slower rate in these comparisons and maintains a higher pressure relative to the MELCOR calculation.

In both the MELCOR and CONTAIN calculations, the gas temperatures are predicted to be slightly superheated during the injection period (e.g., ~10-15 degrees at the end of the injection). The different treatments for film condensate modeling between codes (through input in the case of CONTAIN) is also the source of the observed differences in gas temperatures. The energy corresponding to 10-15 degrees superheating is small (~1% of available latent and sensible energy) and therefore a few degrees difference between superheated gas temperatures between codes does not represent an important concern. Shown in Figure 4-13 is the gas and saturation temperatures plotted along with the measured maximum temperature in the dome region. The very good agreement between the two codes for calculated saturation temperature is apparent during the injection period which suggests the good agreement between the codes for pressure response. Again, the cause of the more rapid decline in saturation temperature for MELCOR is the larger amount of retained condensate on structures for this calculation compared to the CONTAIN input model.

[8] Of course, this only occurs when the free convective correlation for calculated Nusselt number is the same; i.e., when the sensitivity coefficient 4110(1) is set to 0.14 (see Section 3).

Code-to-measurement. The comparisons shown in Figures 4-10 and 4-11 are consistent with the general assumption regarding single cell DBA calculations; that is, single cell pressure calculations are generally conservative. This assumption is based mainly on the thought that free convective condensation modeling (as used in these single cell models) will significantly under-estimate heat transfer from the atmosphere to the structural heat sinks. For example, shown in Figure 4-14 is the calculated heat transfer coefficient for the containment shell compared to the measured (TAEH code derived) coefficients at heat plug locations #1 and #2 in the region above the operating floor. The significant under prediction in the operating region by the calculation is due to 1) the over-estimating of air/steam mass ratio in this region with a single cell nodalization, and 2) an inability to account for forced convection in the region of the injection. Figure 4-15 shows the MELCOR calculated air/steam mass ratio profile compared to a derived mass ratio based on local measured temperature in the operating region, assumed to be at saturated conditions.[9] This figure makes the point that over-estimating air/steam ratios in an injection region can be a significant source of conservatism for single cell models. For example, referring back to Figure 3-3, the single cell air/steam mass ratio minimum of ~1.5 results in a heat transfer coefficient of ~270 W/m^2-K; whereas, at a lower ratio of ~0.5, similar to the test measurement in the operating region, the heat transfer coefficient would double to ~600 W/m^2-K. In fact, for the lower heat plug location, just the correction for air/steam mass ratio would have produced reasonable agreement between the measured and calculated heat transfer coefficient for the shell. However, at the higher elevation where the larger air currents are also detected, the disparity between the calculated coefficient corrected for air/steam mass ratio and the measure coefficient remains large (factor of 2-3 higher for the measurement), clearly indicating that another phenomenon is responsible for the significant amount of under prediction in atmosphere to shell heat transfer. The missing phenomenon not accounted for in the single cell model is forced convective condensation on the shell in the highly turbulent region just above the injection elevation. Investigation of forced convective condensation and its impact for the CVTR test analysis is discussed below in reference to the multi-cell MELCOR calculations, subsection 4.1.2.

A few remarks concerning single cell calculations in reference to previously made remarks that these models are conservative for plant applications are warranted. As noted in Section 2, the distribution of the containment open space for the CVTR containment (at ~62% in the operating region) is approximately equivalent to the ~80% in operating regions of a large dry PWR plant; that is, the distribution is skewed to the operating regions where pipe breaks, such as a main steam line breaks, are expected to be located. Since pressure response is proportional to the total atmospheric energy, a pressure calculation for both the CVTR and the plant will be highly dependent on heat and mass transfer modeling in the operating region. In general, energy transfers for short-term events like blowdowns will also be dependent on the distribution of steel mass (shell, internal structures, and equipment) in the containment.[10] The steel mass will typically be proportional to the open space distribution, which for CVTR is about 65% steel mass above the operating floor. Because the single cell model will over-estimate air/steam ratios in the operating region, as indicated in the CVTR test, these models will tend to under-estimate heat transfer and

[9] Note, even if it is assumed that the measured gas temperature represent a degree of superheating of about 10 degrees, the error in the air/steam mass ratios obtained by using the measured temperatures as saturated temperatures would be less than 5% (i.e., air/steam mass ratio of 1.5 would be, assuming superheating, ~1.55).

[10] Elimination of concrete in the MELCOR single cell calculation, while retaining all steel mass, produces a peak containment pressure that is only ~10% higher than the reference calculation.

therefore over-estimate atmospheric energy content (i.e., pressure). Of course the degree of conservatism predicted for plants depends in part on the relationship between open space distribution and injection location. Significant variation in these two parameters (design or scenario) could affect the amount of conservation expected from a single cell model.

Where single cell models may not be shown to be a conservative approach for plant analysis is in the prediction of maximum containment temperatures during both the injection or later during the de-pressurization period. For example, shown in Figure 4-16 is the comparison between the single-cell calculated and measured gas temperatures throughout the CVTR containment. The more important saturation temperature, compared to superheating, is observed to be below the measured temperature in the operating region both during the blowdown and post-blowdown period. Furthermore, and perhaps more important to licensees, the gas temperature predicted for the single cell is significantly higher than measured temperatures in lower regions (basement) where typically safety equipment may be located.

4.1.1.2 Sensitivity Calculations

Some of the modeling and user imposed uncertainties common to past CVTR analyses include those items associated with the heat and mass transfer processes identified in Table 3-2, specifically heat sink conduction – Cases 2s to 8s (i.e., conduction processes dependent on condensate film thickness, paint resistance, liner-to-concrete gap resistance, and miscellaneous steel and concrete surface areas, etc.) and other modeling choices related to the sensible heat transfer, Case 9s and 10s and conditions for the tests, Cases 11s and 12s (steam enthalpy). The indicators for the sensitivity study are the CVTR containment loads (pressure and gas temperature maximums). A summary listing for the results of the sensitivity calculations is presented in Table 4-2, and the details associated with this summary are discussed below.

Conduction related sensitivities. Case 2s reveals the CVTR calculations are very sensitive to the amount of miscellaneous steel modeled. The reference calculation assumed the upper bound for the uncertainty range as a result of engineering judgment related to assessments made with the multi-cell calculation discussed in subsection 4.1.2. As shown in Table 4-2, a reduction in the amount of miscellaneous steel mass by 50% increases the calculated maximum pressure by about 0.3 bar – the largest impact of all the sensitivity cases considered. Additionally, Case 2s most closely represents the inputs associated with early CONTEMPT code application to the CVTR tests. CONTEMPT code calculations used heat sink data compiled in Table 2-1 that did not include the higher estimates of added miscellaneous steel referenced in the CVTR final test report. A review of past CONTEMPT calculations for the CVTR both in open literature [Car81] and the test report [Sch70] show that the MELCOR results for Case 2s are in good agreement the CONTEMPT results, given the known differences between each code's modeling. For example, in reference Car81 the maximums in pressure and temperature calculated with CONTEMPT are given as 2.86 bar and 418 K for Test 3, which can be compared with 2.99 bar and 419 K obtained with an equivalent MELCOR input deck. The slight under prediction of pressure is expected due to the over-estimation of the Uchida heat transfer correlation modeled in the CONTEMPT code, as discussed in Section 3. Case 2s, therefore, is further confirmation that continuity between the MELCOR modeling of DBA-type scenarios can be approximately established for not only the CONTAIN code (as pointed out in subsection 4.1.1.1), but also for the CONTEMPT code used in the past for many existing licensing reviews. This tie-back to previous confirmatory documentation is important.

Case 3s demonstrates that the use of the upper bound estimate of concrete surface area for CVTR does not significantly affect the predicted peak pressure. The difference in concrete area between the reference calculation and Case 3s is approximately 584 m^2, which is approximately a 30% increase in the total concrete area used for the reference calculation.

The CVTR structural steel, in Sch70, is given in terms of the structural area and thickness (fixed volume). In the reference calculation, internal steel is modeled assuming that both sides of a structural member is exposed to the atmosphere, in which case an adiabatic boundary condition is applied to the half thickness and the structural area is doubled. This is one interpretation for such a specification. However, an alternative modeling approach would be to consider that only one surface is exposed, as in the case of a pipe structure, such that the actual specified area and thickness is used with an adiabatic boundary condition applied to the back surface of the structure. Case 4s shows the effect of this modeling approach on pressure and temperature. In this case, thicker steel slabs are used to describe the heat sinks and therefore the transient energy transfers from the atmosphere to steel are reduced somewhat and pressure and temperature increase slightly.

Many containment models for DBA-type analyses were applied only to short-term (blowdown) periods and therefore neglected the variable gap or contact resistance associated with liner-to-concrete opening. During the pressurization process, the liner-to-concrete gap is expected to close somewhat due to compressive forces on the liner, and this mechanical process diminishes the amount of gap heat transfer resistance and also makes modeling this variable resistance difficult. However, a larger effect for DBA calculations relates to the fact that steel mass rather than concrete (with relatively low thermal conductivity) will represent the major component for transient energy transfers from the atmosphere, especially during the short, blowdown period. Including the estimated ~0.01 meters (3/8 inch) gap for the CVTR liner in Case 5s is shown to increase the calculated maximum pressure by 0.03 bars and superheating by 2 degrees: this amount of change in containment loads is considered minor.

In Section 3, a discussion relating to paint resistance modeling was included. For the CVTR analysis, paint resistance modeling, as described in Section 3, is addressed in Cases 6s and 7s. Case 6s includes a paint resistance on structures (steel and concrete) that simulates the default CONTAIN paint coefficient of 2000 W/m^2-K. Case 7s represents a reduced paint coefficient of 800 W/m^2-K that is perhaps a better representation of some reported properties for painted surfaces in containments. Both cases indicate a small effect with the inclusion of paint resistance in the MELCOR reference model.

Case 8s replaces the default film tracking model for structures with a “minimum” condensate film thickness calculation, obtained by applying an artificial structure length (0.1 meters) specifically to reduce an effective film thickness. Shown in Figure 4-17 is a comparison of MELCOR calculated film thickness for both the default and special input required to minimize the film thickness modeled. The two MELCOR calculations are also seen to bound the specified maximum film thickness used in the CONTAIN CVTR reference calculation. As indicated in Table 4-2, the effect on containment loads as a result of a significant variation of film thickness is minor.

Sensible heat transfer. Case 9s addresses the issue of thermal radiation modeling, where the inclusion or neglect of this model is seen to be relatively unimportant; that is, modeling in this area results in a small change in the degree of superheating. Previously, it was pointed out that for

superheating (~10 to 15 degrees), being associated with sensible heat transfers, represents a relatively minor contributor to the total energy transfers for short-term, DBA-type calculations. For this reason, thermal radiation modeling is not singled out as important phenomenon for DBA modeling, and therefore its neglect can be tolerated without much impact on predicted maximum containment loads. Case 10s is a sensitivity case that addresses the effect of convective sensible heating on the maximum calculated pressure and gas temperature. By increasing the sensible heat by 50%, the degree of superheating is shown to be slightly affected (10 K reduction), while the pressure maximum is relatively insensitive.

CVTR test specification. Cases 11s and 12s are interesting cases since they show how sensitive the predicted gas temperature is related to the injected steam enthalpy. The peak temperatures calculated in Cases 1 and 2s indicate a fair amount of superheat -- approximately 20 to 30 K. The amount of energy in the atmosphere corresponding to this amount of superheating is relatively small compared to the total atmospheric energy (including latent heat); therefore, slight variations in steam enthalpy could have a significant affect on atmospheric temperature, at least until saturation temperatures are reached after the injection. For the single cell calculation, in Case 1, the injected steam specific enthalpy is 2779.6 kJ/kg, and the uncertainty range for specific enthalpy is given in the CVTR final report [Sch70] as 2791–2735 kJ/kg. Cases 11s and 12s use a steam specific enthalpy of 2700 kJ/kg, a 2.8% reduction from that used for Case 1. As shown in Table 4-2, the predicted maximum gas temperature is reduced substantially with this change in the injected steam enthalpy; whereas, the pressure variation remains relatively minor for each case.

Table 4-1 Translations of various elevations for the CVTR report.

Location	Current report elevations* (meters)	Test report [Sch70] elevations (feet)
Containment:		
Basement floor	0.0	275
Intermediate-to basement region	5.49	293
Operating floor	15.24	325
Bend line	25.9	360
Maximum interior height	34.8	389.25
Heat plugs:		
#1	16.76	330
#2	22.25	348
Measurements		
TC-5	2.74	284
TC-7	6.71	297
TC-11	13.4	319
TC-23 (spray tests)	22.86	350
TC-28	28.96	370
Anemometer (heat plug #2)	22.25	348
Anemometer (annulus)	~15.24	~325

*elevations referenced in the MELCOR input and analysis

Table 4-2 Matrix of MELCOR Single-Cell Calculations for CVTR Test #3.

Case #	Description	Max. Pressure, bar	Max. Temperature, K
----	Measured	2.27	389
1	Single cell reference case*	2.64	394
2s	Case 1 with no additional misc. steel (used nominal steel inventory) nor is thermal radiation modeled (similar to early CONTEMPT code input for CVTR)	2.99	419
3s	Case 1 with maximum concrete area	2.59	391
4s	Case 1 with steel structure thickness doubled, mass remains the same	2.73	398
5s	Case 1 with containment shell air gap included (3/8 inch gap assumed)	2.67	396
6s	Case 1 with painted surfaces (hpaint = 2000 W/m^2-K)	2.67	396
7s	Case 1 with painted surfaces (hpaint = 800 W/m^2-K)	2.70	398
8s	Case 1 with minimum condensate film thickness	2.63	393
9s	Case 1 without thermal radiation modeled	2.69	404
10s	Case 1 with sensible heat multiplier set to 1.5	2.60	384
11s	Case 1 with steam enthalpy reduced by 2.8%	2.56	380
12s	Case 2s with steam enthalpy reduced by 2.8%	2.84	395

* The input for this case is the 19-cell reference input reduced to a single cell.

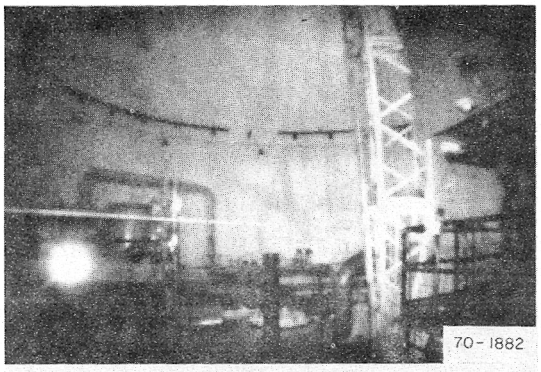

(a) t = 0 sec, Pressure = 0 psig

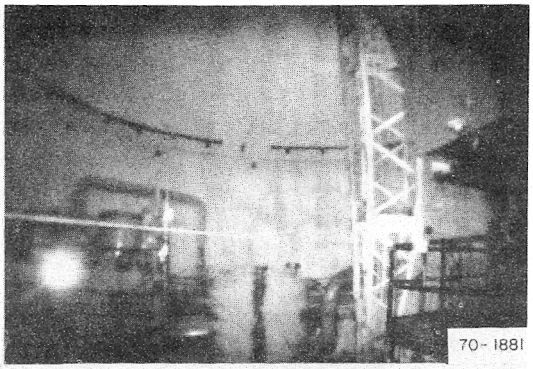

(b) t = 1.5 sec, Pressure = 0 psig

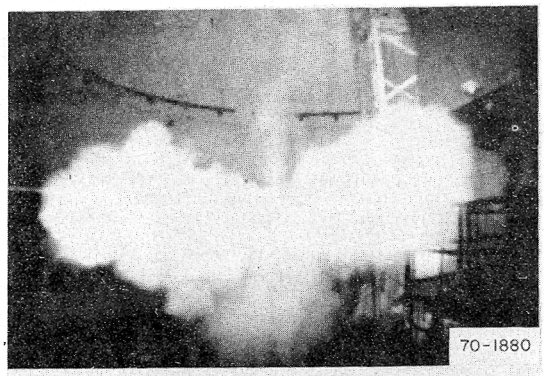

(c) t = 2 sec, Pressure = 0.1 psig

(d) t = 5 sec, Pressure = 0.9 psig

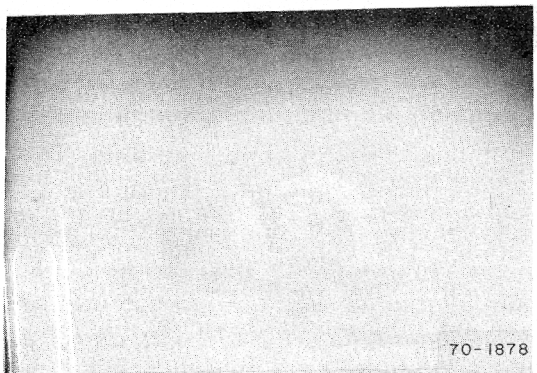

(e) t = 9 sec, Pressure = 1.4 psig

Figure 4-1 Side-on photographic sequence for CVTR Test 3 blowdown [Sch70].

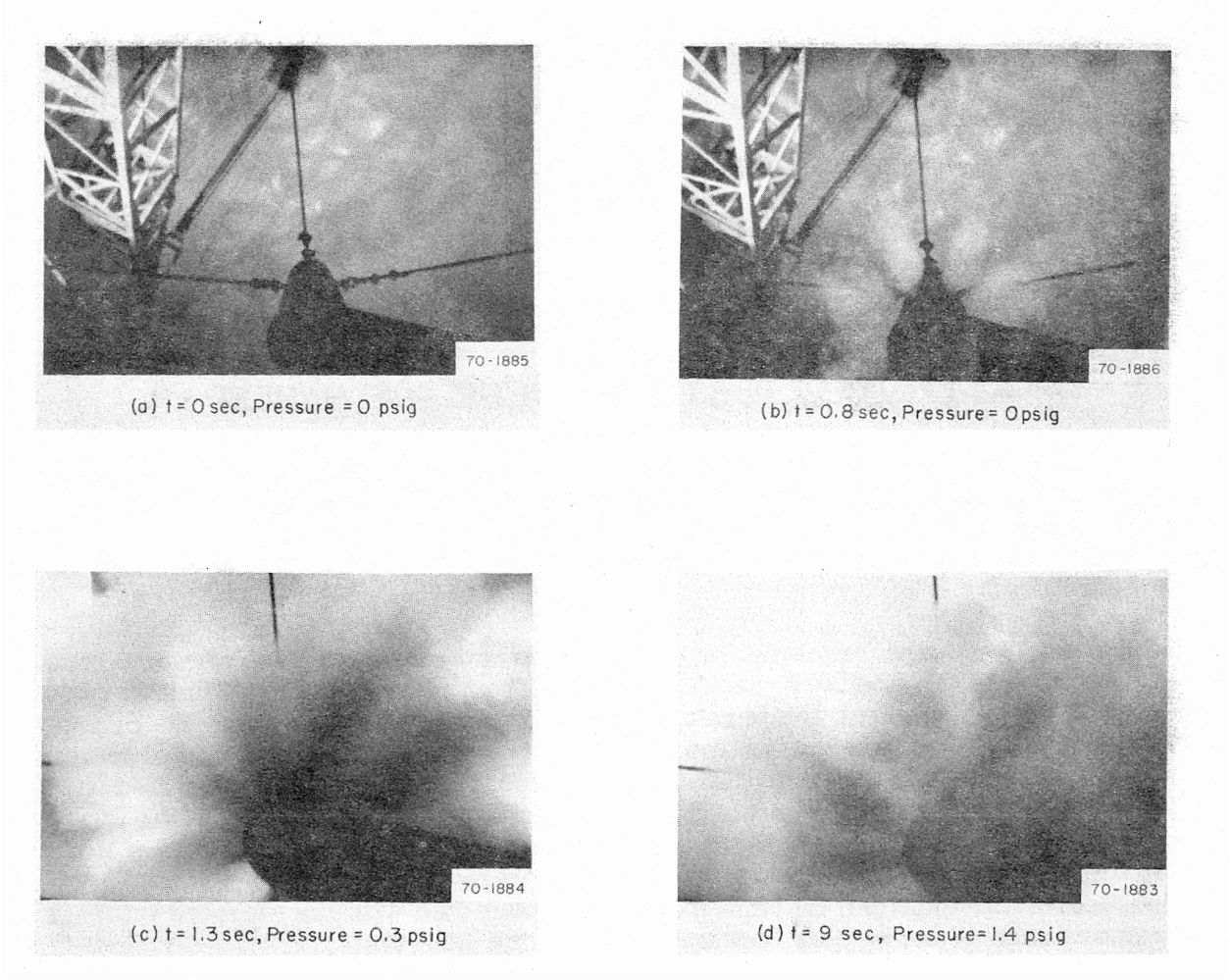

Figure 4-2 Top photographic sequence for CVTR Test 3 blowdown [Sch70].

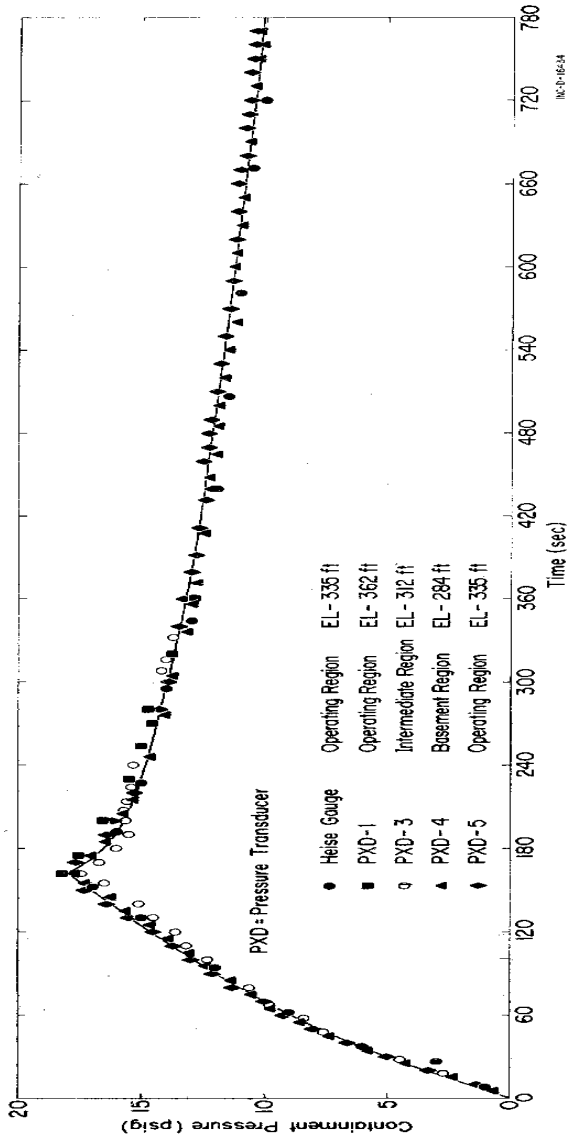

Figure 4-3 CVTR containment pressure response – pressure transducers, Test 3 [Sch70].

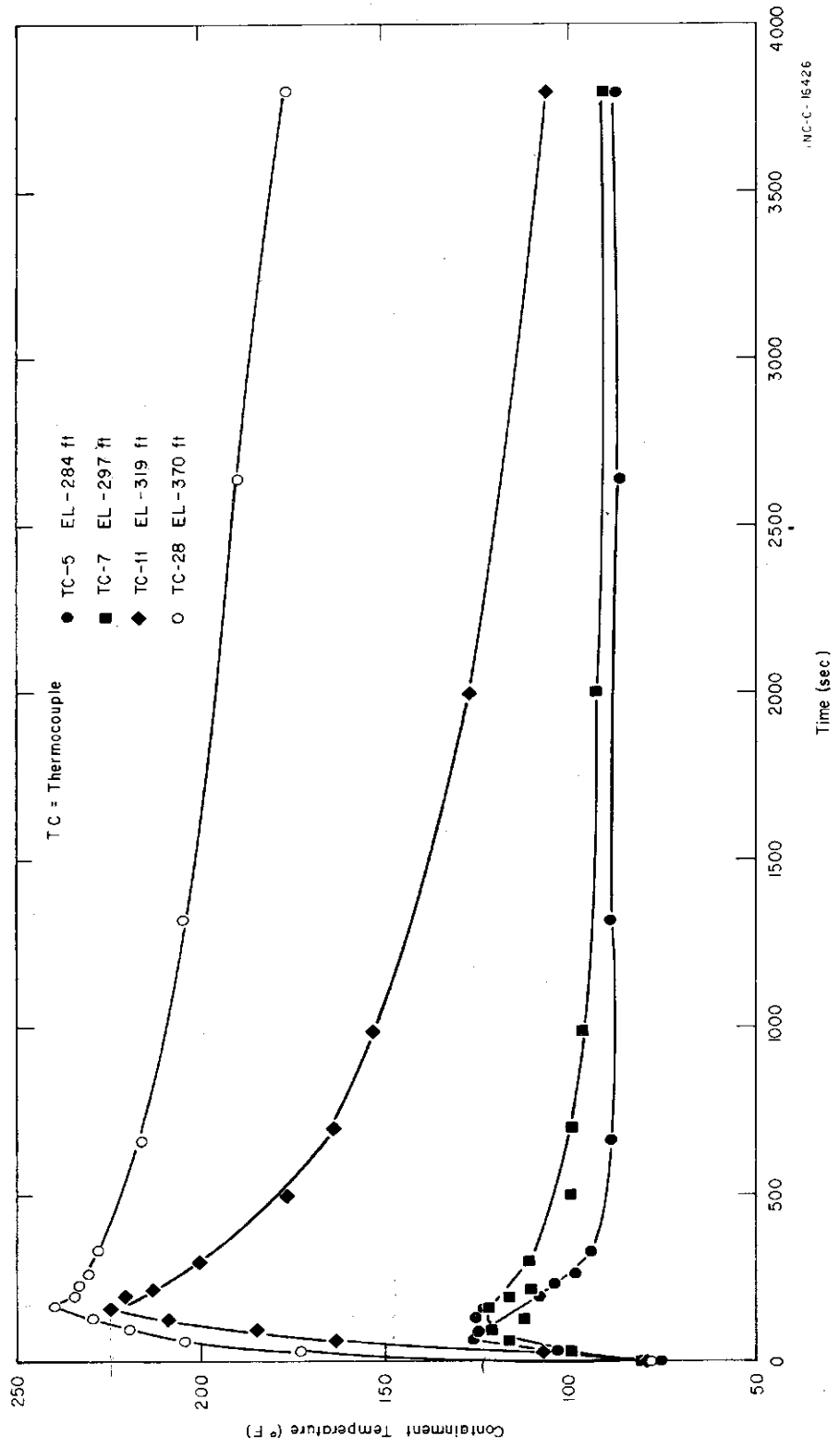

Figure 4-4 Atmosphere vertical temperature profile, Test 3 [Sch70].

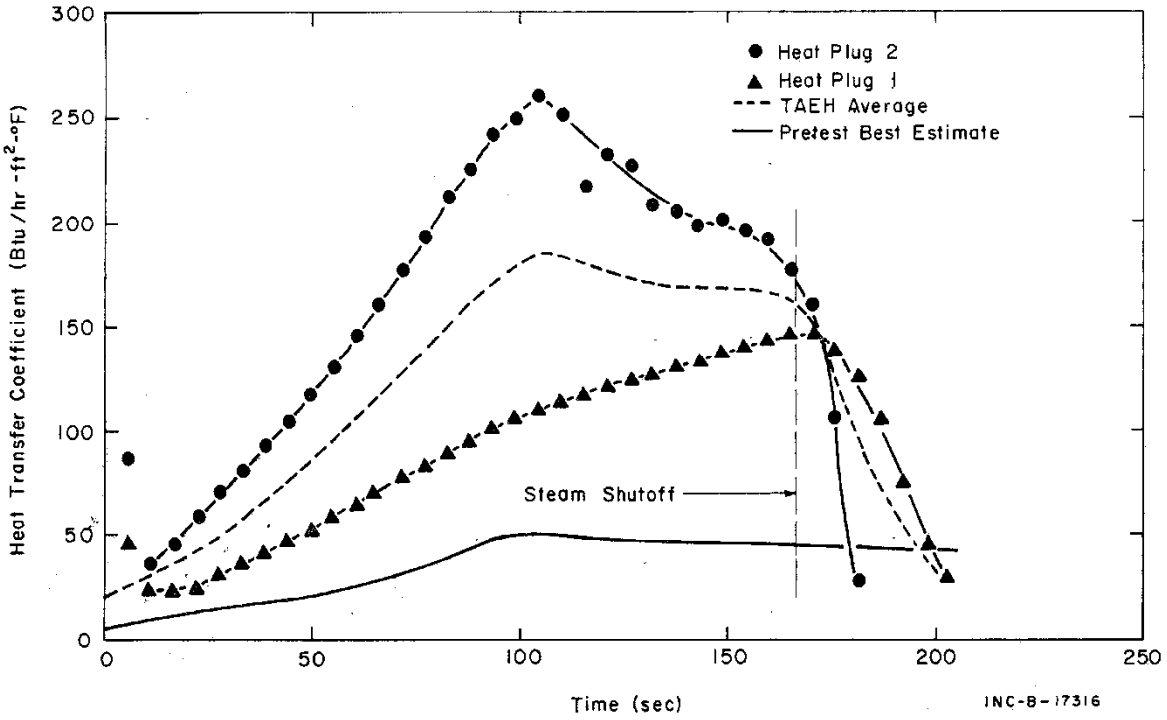

Figure 4-5 TAEH – calculated heat transfer coefficient, Test 3 [Sch70]. (Pretest best-estimate is based on single-cell CONTEMPT containment calculation with condensation modeled using Uchida correlation.)

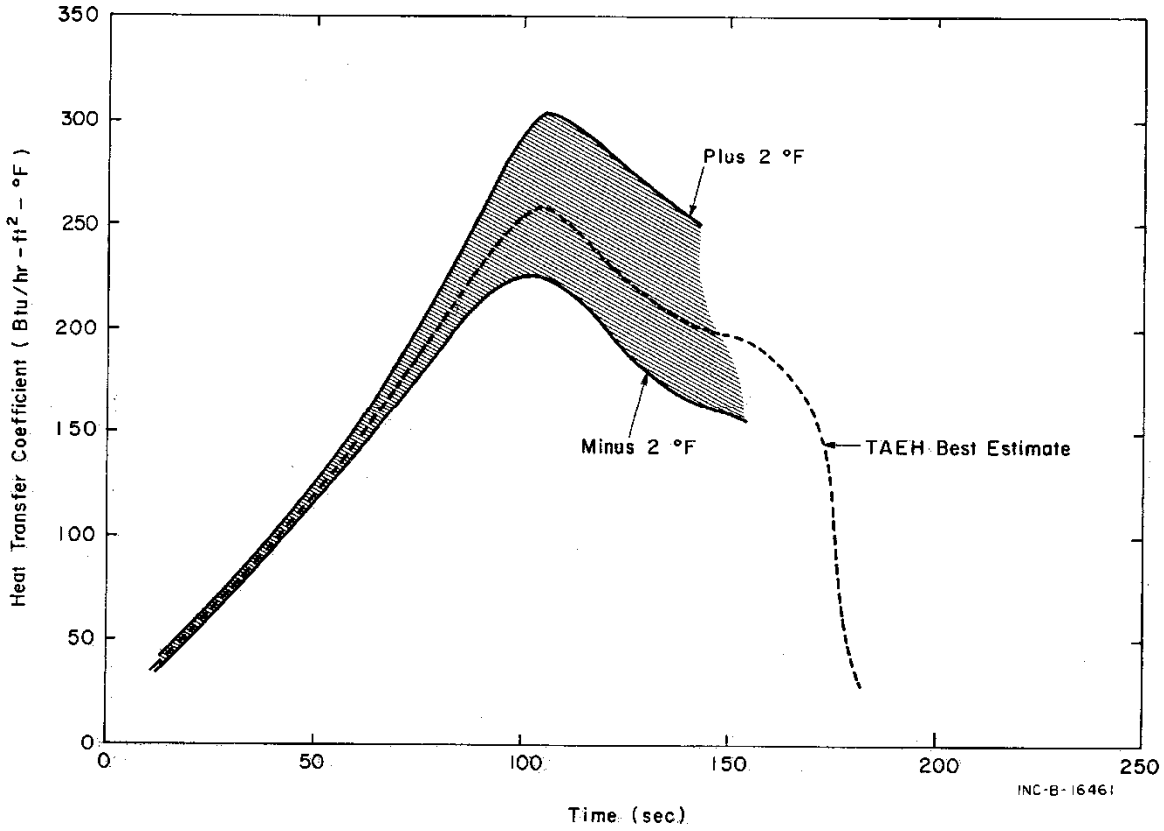

Figure 4-6 The effect of temperature uncertainties on the TAEH heat transfer coefficient – Test 3 [Sch70].

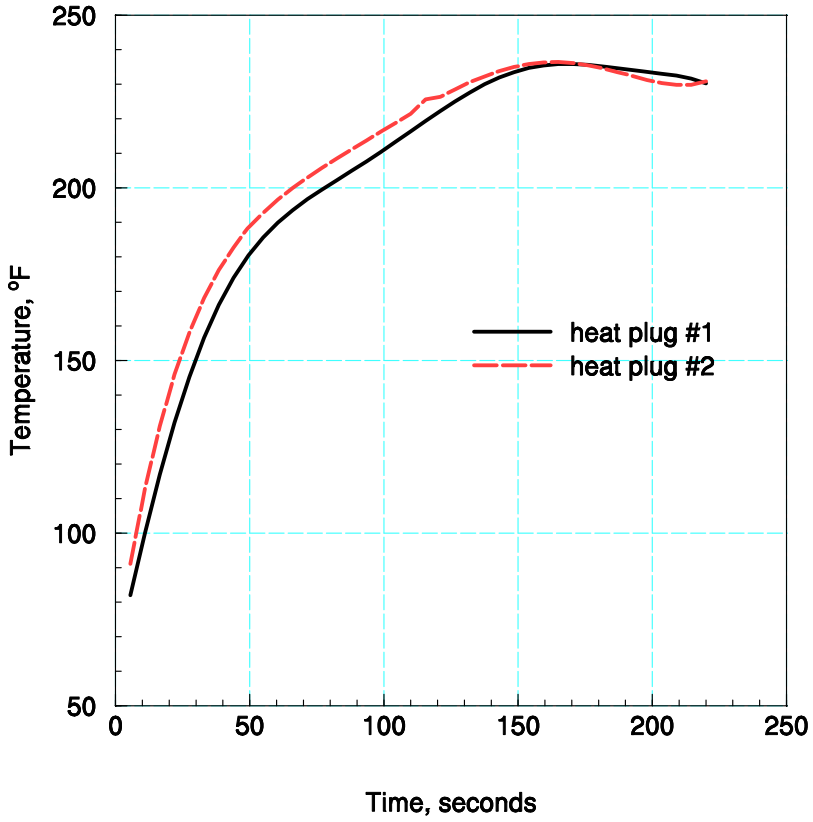

Figure 4-7 Plot of measured average bulk (gas) temperature at heat plug locations (from Tables B-VI and B-VII of CVTR test report, Appendix B) [Sch70].

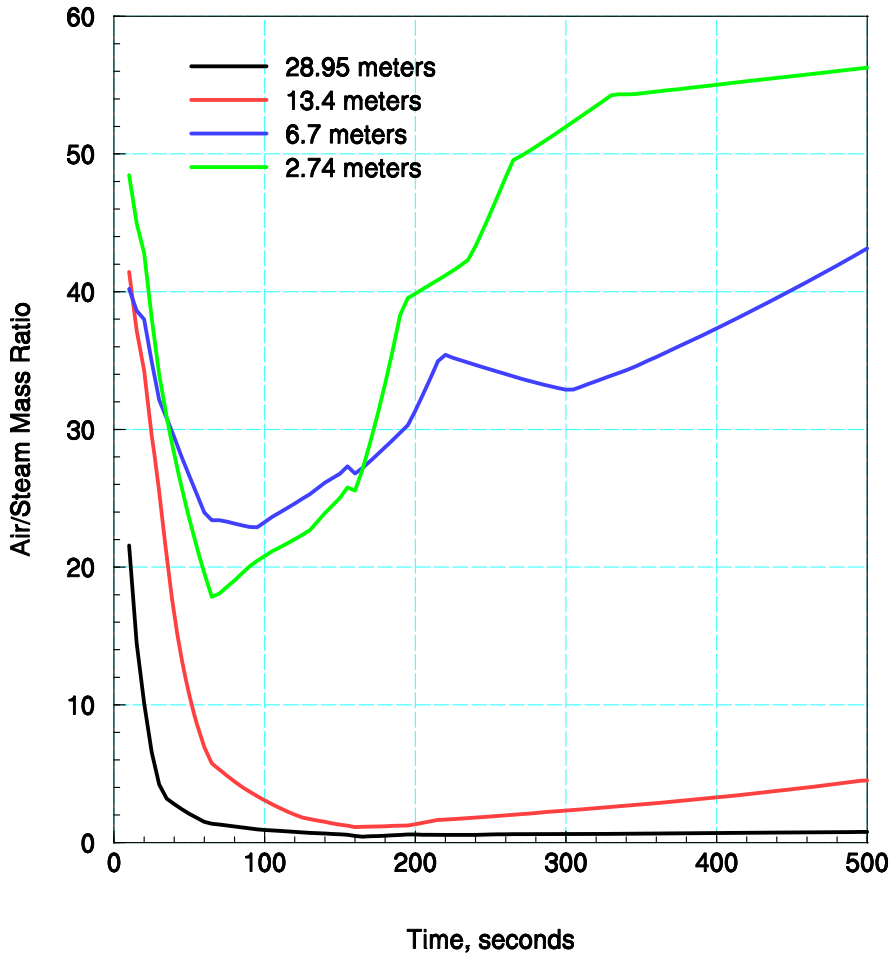

Figure 4-8 Derived air/steam mass ratios for CVTR Test 3, assuming saturation throughout the containment.

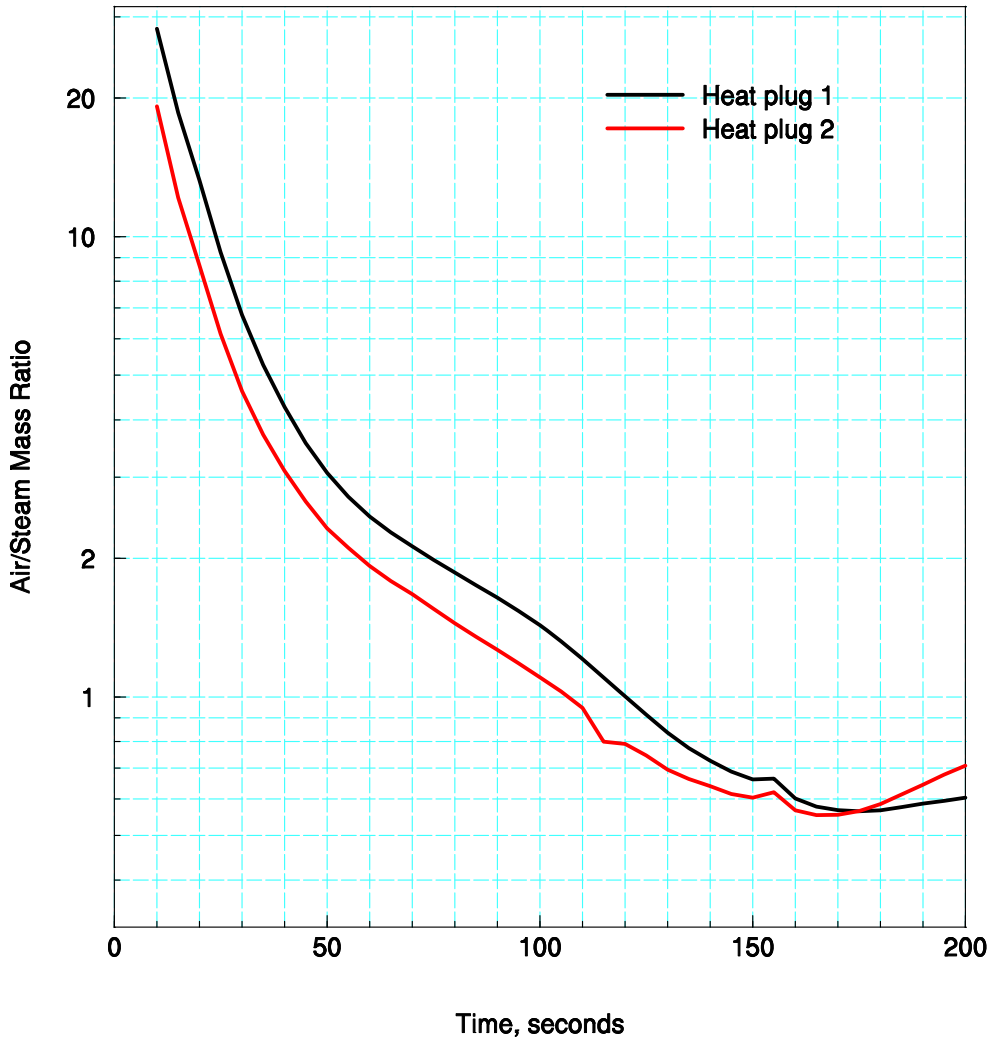

Figure 4-9 Derived air/steam mass ratios for CVTR Test 3 at heat plug locations, assuming saturation conditions.

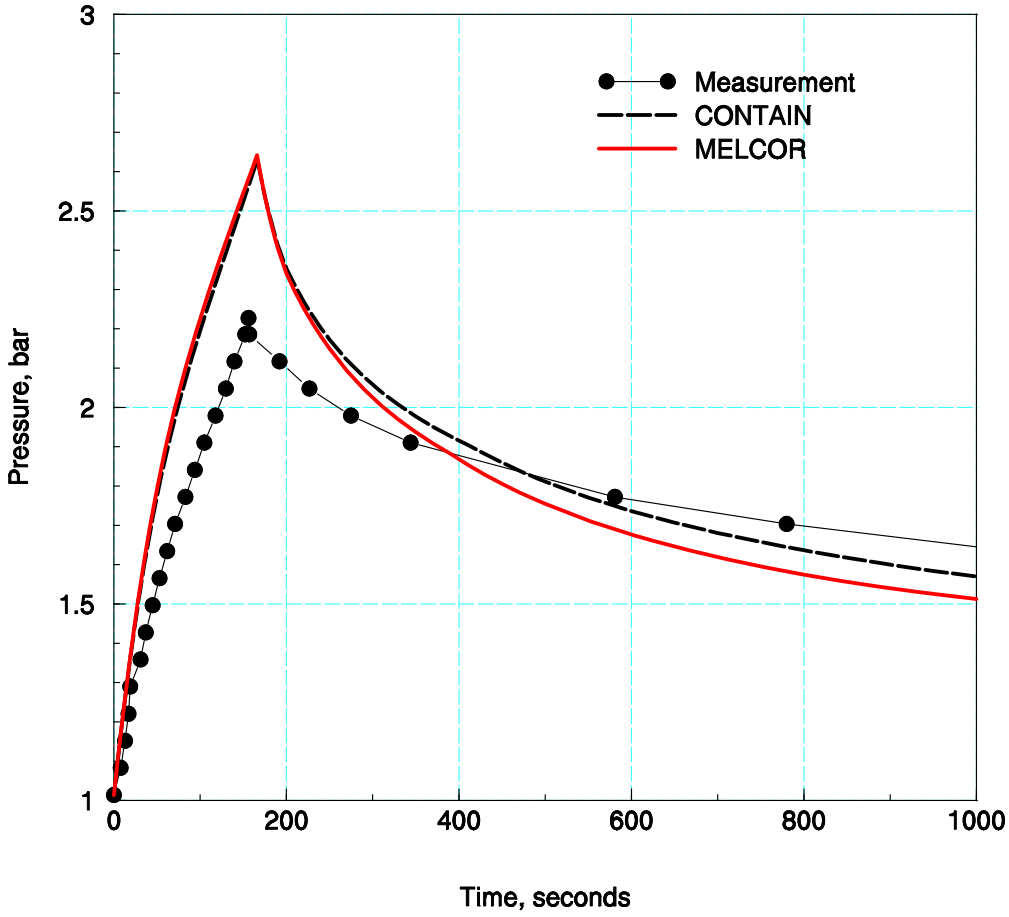

Figure 4-10 Pressure comparisons between reference code calculations (single-cell) and measurements for CVTR Test 3.

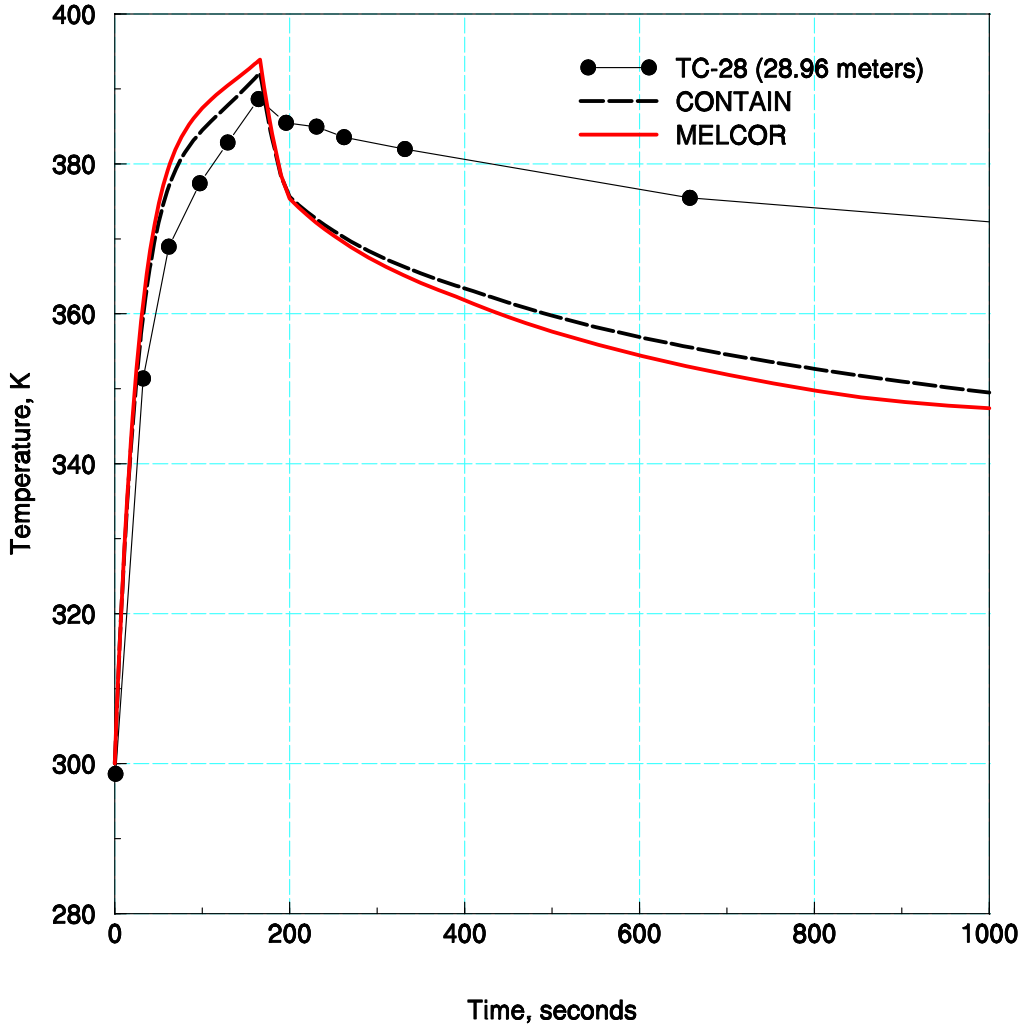

Figure 4-11 Gas temperature comparisons between reference code calculations (single-cell) and measurements for CVTR Test 3.

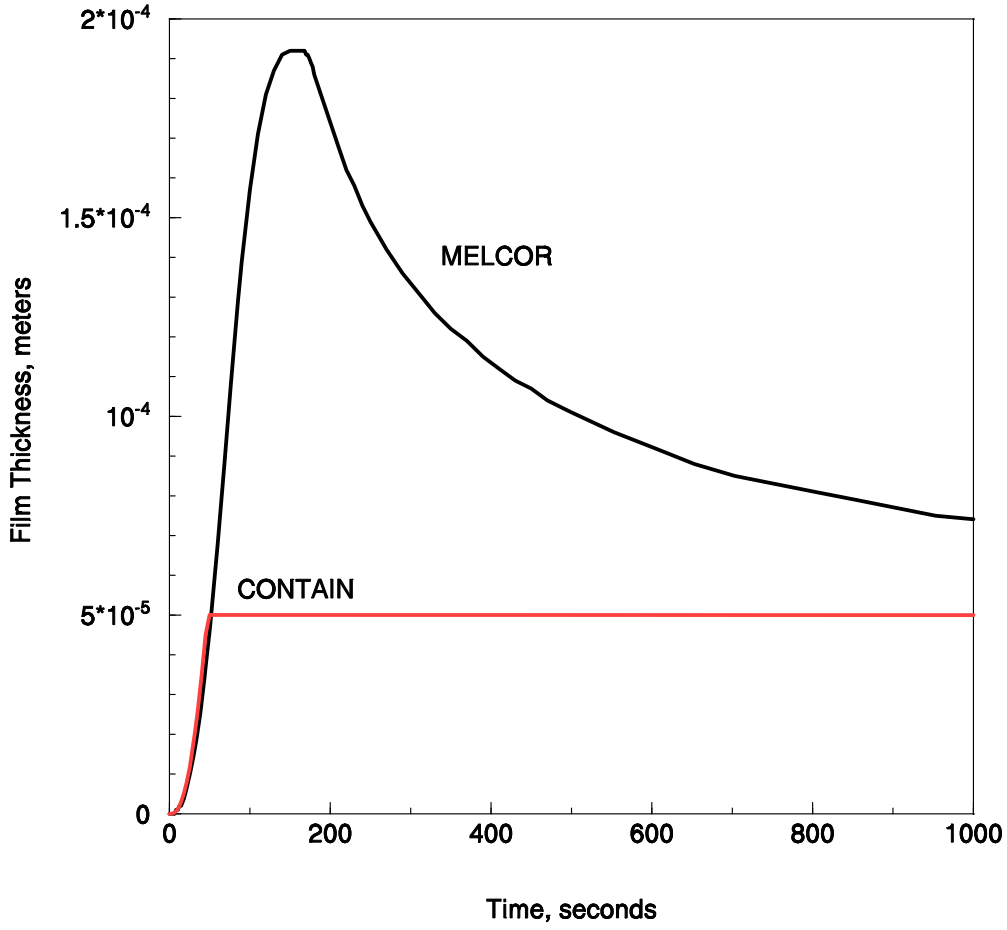

Figure 4-12 Film thickness calculated for the containment shell using the single cell MELCOR and CONTAIN reference modeling for the CVTR Test 3.

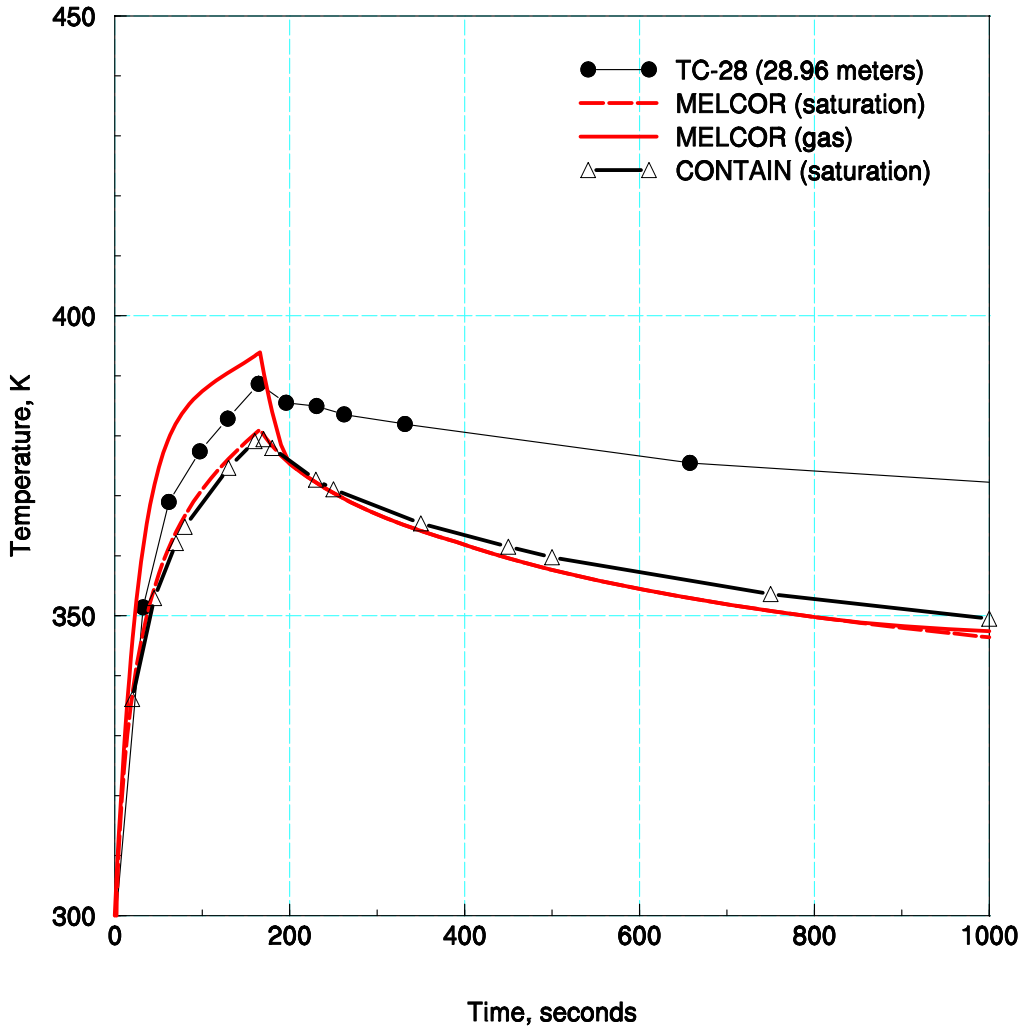

Figure 4-13 Gas temperature comparisons between reference code calculations (gas and saturation temperatures) and measurements for CVTR Test 3.

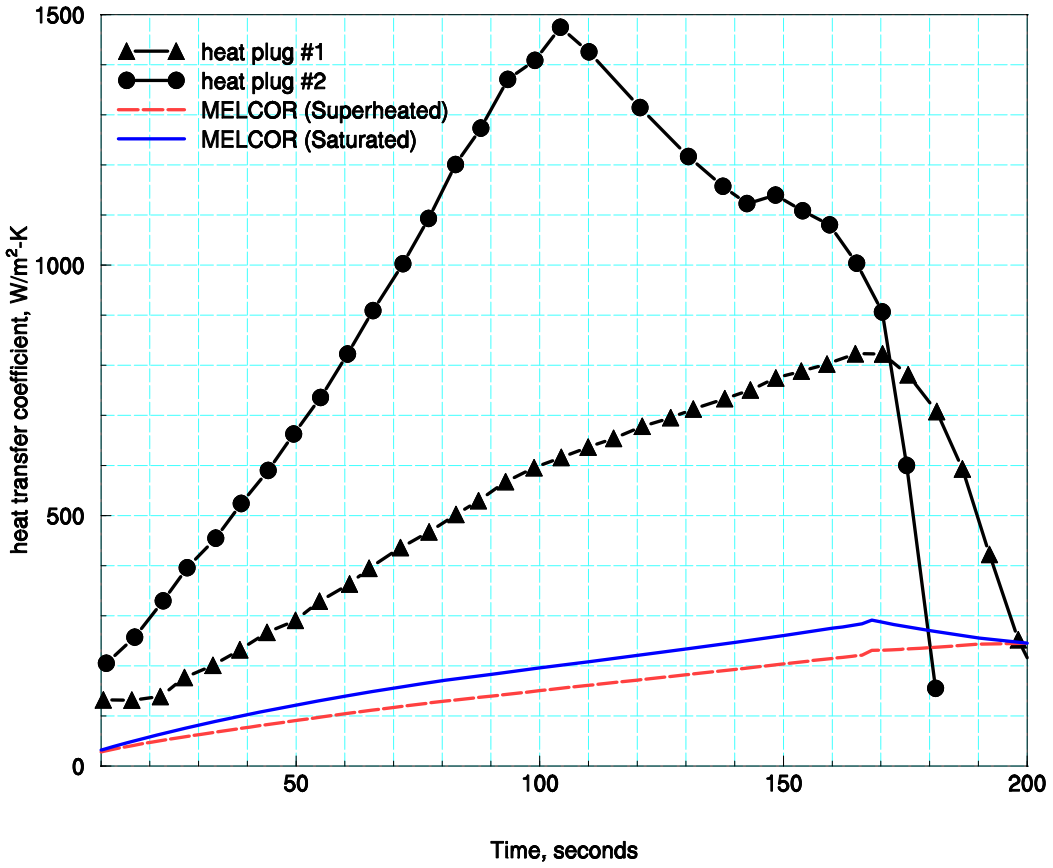

Figure 4-14 Comparison between measured and MELCOR single cell calculated shell heat transfer coefficients for CVTR Test 3.

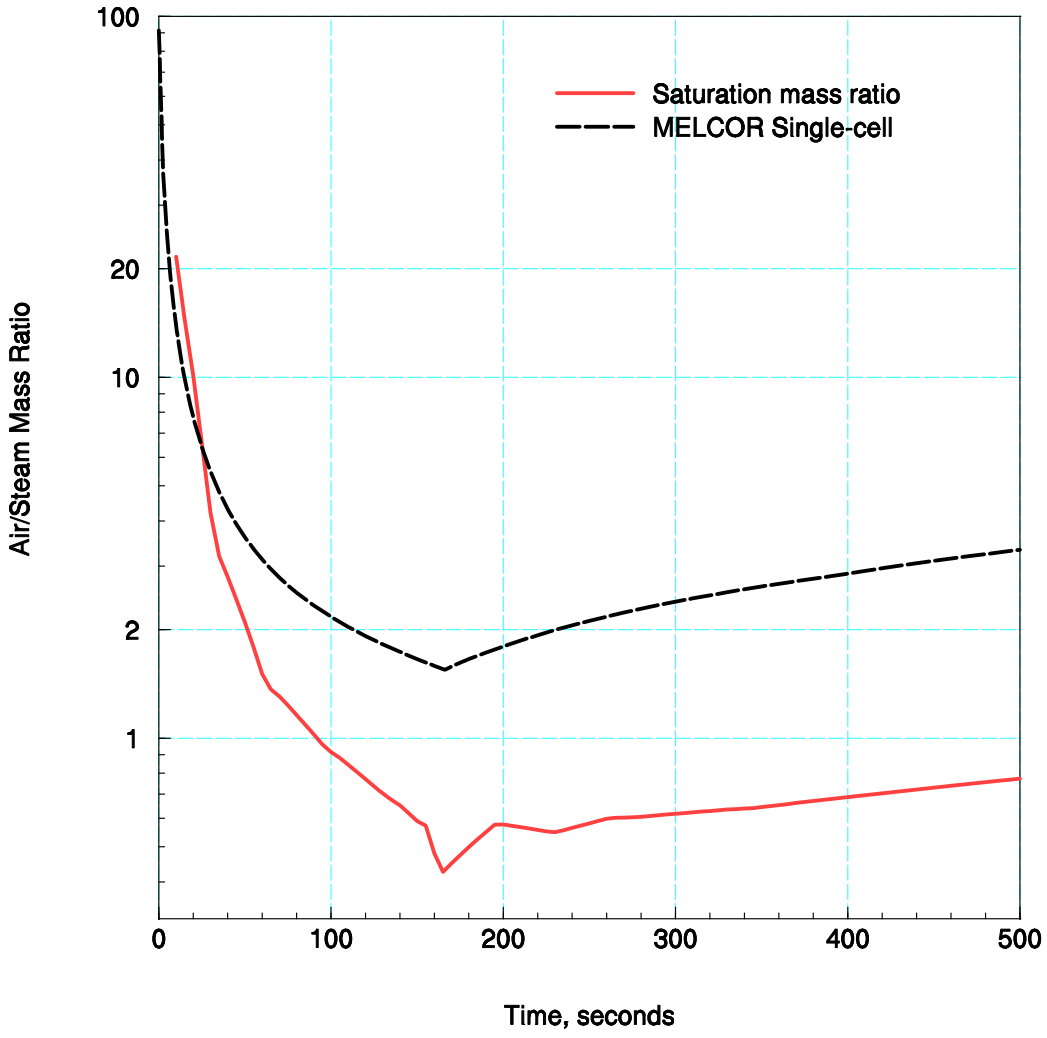

Figure 4-15 Comparison of the MELCOR calculated air/steam mass ratio for the single cell model with the measured ratio (assuming saturation) in the operating region.

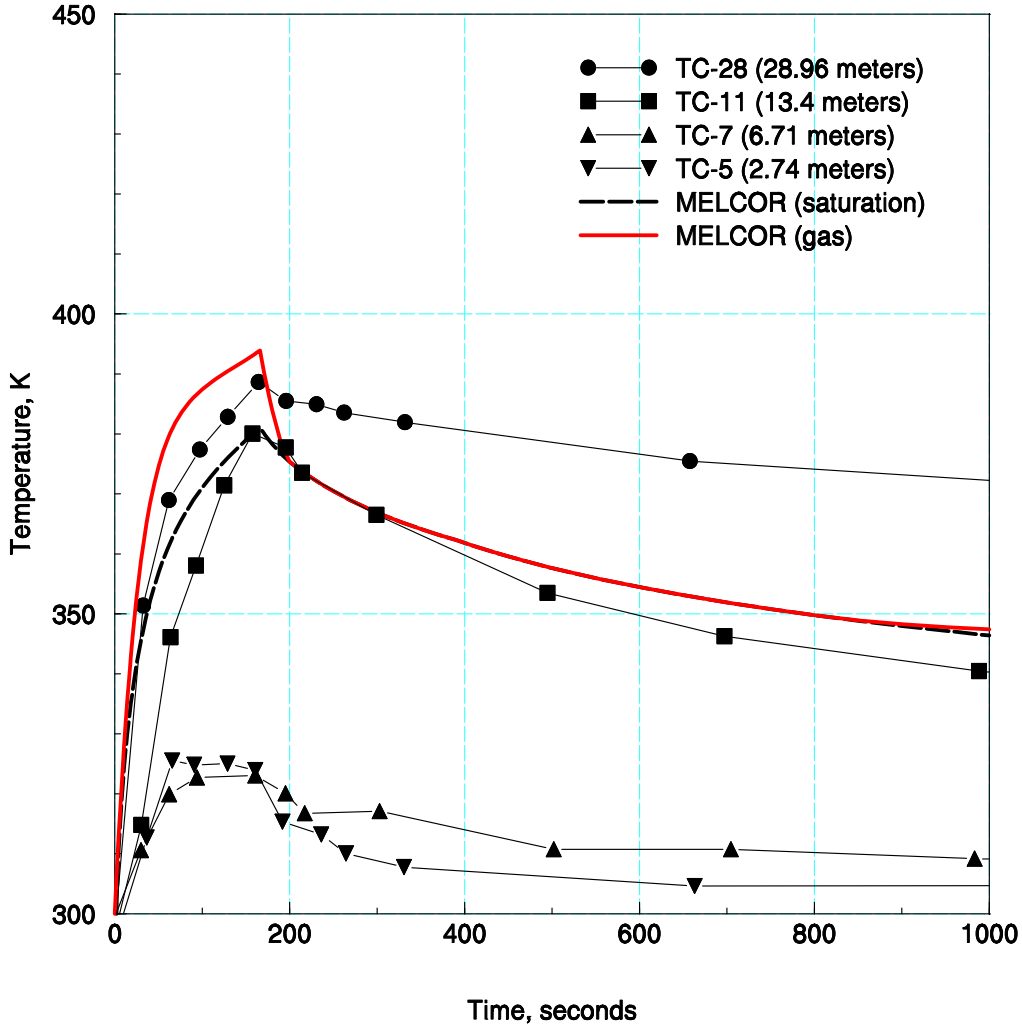

Figure 4-16 Vertical gas temperature comparisons between the MELCOR reference calculation and measurements for the CVTR Test 3.

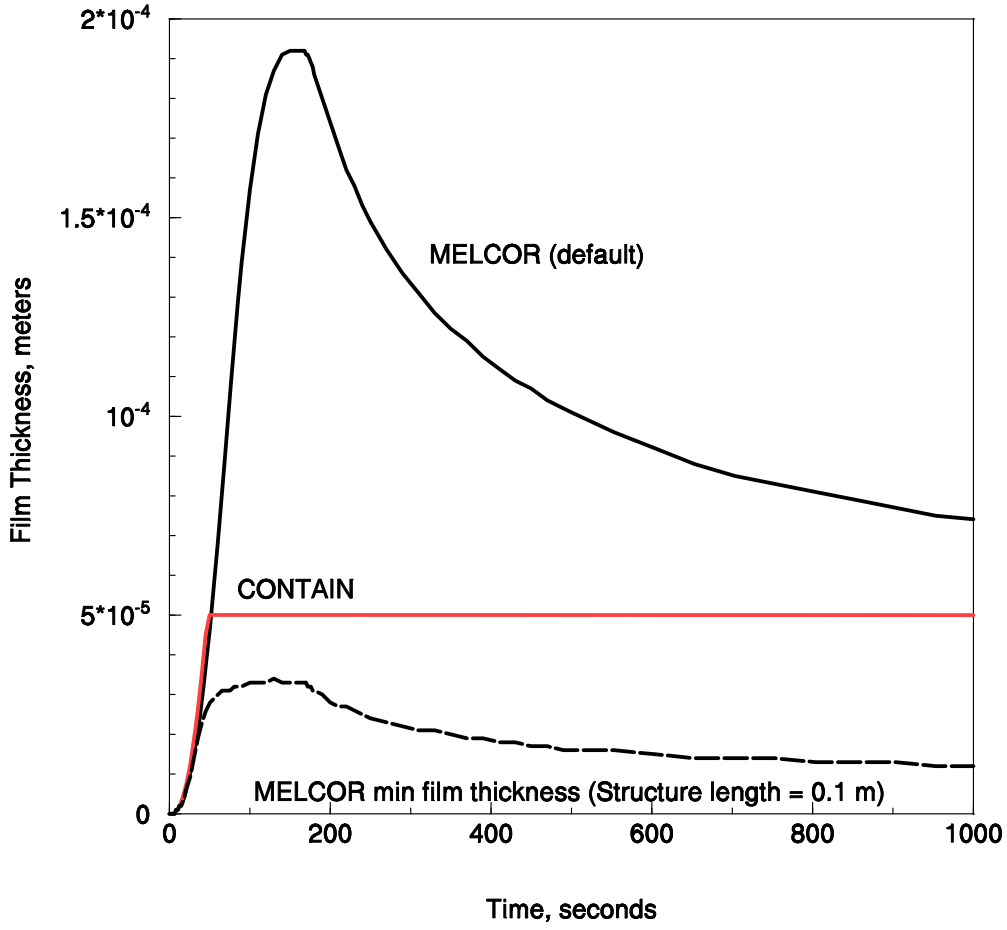

Figure 4-17 MELCOR calculated film thicknesses for the CVTR shell based on the default and fictious condensate film model input for Test 3 (single cell model).

4.1.2 Multi-Cell Model

Multi-cell containment models began to appear in the late 80's with the introduction of containments codes such as CONTAIN and MELCOR. The advantage of these codes over the single cell models represented by earlier codes (CONTEMPT, etc) was the ability to predict stratification in the containment, especially during periods where the driving forces for mixing and transport are pressure driven forces as opposed to smaller buoyancy forces. As a result, validation exercises [Kar89, Kar92] have previously shown that multi-cell models can be successful in predicting local temperature gradients within containments during a rapid pressurization event caused by a high-energy line break. In the CVTR Test 3, the steam injection into the upper, operating region produces a significant degree of stratification, as discussed above. The purpose of the multi-cell modeling effort discussed here is to show that a code such as MELCOR can calculate reasonably accurate mixing and transport within the CVTR facility, with significant stratification predicted. Because the single cell modeling tends to benefit from compensating errors, in terms of total energy transfers from the atmosphere, global responses for both the single and multi-cell are not expected to differ significantly; therefore, maximum pressures are anticipated to be similarly calculated for both models. Consequently, the following subsection emphasizes the local responses (temperatures) over the global average. A sensitivity calculation is included that focuses on a parametric method for estimating heat and mass transfer in the region near the injection (forced convection). In this sensitivity investigation, both pressure and temperature responses are discussed, comparing the changes noted between forced and free convective models.

4.1.2.1 Reference Case

The MELCOR input setup has been discussed in Section 3, where the input specification is listed in Table 3-3. Both single and multi-cell inputs, except for nodalization, are equivalent; that is, the modeling of heat sinks are treated in a similar manner (default film tracking, no paint resistance, etc.). The regional breakdown for heat sink distribution in the containment is obtained approximately from the CVTR test report where heat sinks are located in the basement, intermediate, and operating region of the facility. Miscellaneous steel (i.e., additional 50% steel mass) is distributed in relationship to the free volume vertical distribution inferred from the CVTR test report.

Code-to-code benchmarking. In the code benchmarking for the single cell modeling, the CONTAIN input was structured to simulate typical early containment calculations with minimum film thickness on structures so as to better represent the Uchida-type heat transfer coefficients. In the case of multi-cell modeling as discussed in Section 3, the Uchida-type semi-empirical approach to heat transfer is not applicable since significant stratification within the containment is expected. Consequently, the specification of minimum film thickness (0.00005 meters) is eliminated and replaced with the default setting in CONTAIN which is a factor of ten higher (0.0005 meters) than used for the single cell calculation. Although this change in film thickness for the reference CONTAIN calculation has minimal impact for the injection phase, the change does affect benchmarking of the MELCOR model during the de-pressurization phase.
Shown in Figure 4-18 are the comparisons between the measured and calculated pressure response for CVTR Test 3 using the multi-cell models in MELCOR and CONTAIN. Both codes predict essentially the same pressure maximum at the end of the injection period (~170 seconds). In

comparison to previous single cell calculations, the multi-cell peak pressure is reduced slightly, by ~0.12 bars. Unlike the single cell comparisons, where the MELCOR code predicted a somewhat faster de-pressurization rate, the multi-cell code comparisons show now that the CONTAIN code predicts the more rapid de-pressurization. This reversed response is due to the changes made in the film modeling input for the CONTAIN code, as discussed above. Figure 4-19 shows the two treatments for the film thickness modeling on the shell in the operating region, which can be compared to a similar figure for the single cell model, Figure 4-12. The CONTAIN code, now with the larger available film mass in comparison to the MELCOR default modeling, produces a slightly greater de-pressurization rate.

The gas temperatures measured in the dome region correspond to the maximum temperatures recorded for the CVTR Test 3. Shown in Figure 4-20 are the comparisons of the MELCOR and CONTAIN predicted gas temperatures in this region, along with the measurements. During the injection, both codes calculate a small amount of superheating in the dome region. The superheating calculated with the MELCOR code is somewhat smaller, as is the amount of film mass predicted for structures. The dome saturation temperatures calculated with each code are plotted in Figure 4-21. In general, both codes predict equivalent maximum saturation temperatures for the containment. For the purposes of estimating heat transfer to the surrounding equipment (i.e., equipment qualification) or wall structures, the agreement shown for calculated saturation temperatures is noteworthy since the small difference observed in terms of superheating is not significant.

Code-to-measurements. Shown in Figure 4-22 are the calculated pressure responses for the single and multi-cell MELCOR models compared to measurements. The maximum pressure calculated with the multi-cell model is slightly reduced relative to the single cell model. But the de-pressurization response is noticeably affected; with the multi-cell pressure prediction now follows more closely to the measurement trends. The more rapid de-pressurization observed for the single cell model was attributed to the smearing of the steam concentration throughout the containment with excessive condensation occurring in the lower regions. Early responses for the single and multi-cell calculation remain in good agreement due to the compensating effects, for the single cell model, having under predicted steam concentration in the operating region and over predicted steam below the operating floor. After the injection period, it is observed that the steam distribution error realized in single cell model is not fully compensated for during the entire test; that is, during the post-blowdown, the single cell model in comparison to the multi-cell model produces a non-conservative estimate for the de-pressurization rate.

A key feature for multi-cell modeling is the ability to predict local temperature (and steam concentration) variations throughout the CVTR containment. For example, plotted in Figures 4-23 and 4-24 are the calculated vertical gas and saturation temperature profiles compared to measured gas temperatures. The calculations clearly indicate a significant amount of stratification and the agreement is generally good, whether comparing gas or saturation temperatures with measurements. In most regions however superheating appears somewhat over predicted early in the transient.

It was noted in the review of gas or bulk temperature measurements (e.g., Figure 4-7) and time lapse photo images that the operating region is relatively well mixed during the test.[11] Shown in Figure 4-25 are calculated vertical temperatures in the operating region. This region is also calculated to be well mixed. With respect to wall heat transfer in the vicinity of the injection (heat plugs 1 and 2 locations), the single cell model was shown above to significantly under predicted the heat transfer coefficient due to 1) the lack of forced convection along the containment wall due to jet-plume wall interaction, and 2) an over prediction of air/steam mass ratio due to the single cell approximation of an "average" air/steam mass ratio throughout the containment. The multi-cell calculation corrects for the error in the latter, and therefore the comparison of calculated heat transfer coefficients with measurements reveals a disparity due to a lack of forced convection as the jet/plume interacts with the containment wall. Shown in Figure 4-26 are the comparisons between the reported wall heat transfer coefficients and the calculated values obtained from both the single and multi-cell MELCOR calculations. The improvement in local wall heat transfer, with the multi-cell model, is evident. Yet, there remain significant differences between both the transient trends and peak measurements. These remaining differences are attributed partly to the nature of the turbulence associated with the jet/plume wall interaction and this feature of the calculation is investigated through a sensitivity analysis in the following subsection. In general, for plant applications modeling jet/plume wall interaction is not attempted and therefore multi-cell calculations show a degree of conservatism for global, short-term response due to the neglect of these interactions. Unlike the conservatism associated with single cell models, which could be made non-conservative with a change in the containment design (distribution of heat sinks), the conservatism from neglecting jet/plume wall interactions remains regardless of design variation. Additionally, the degree of conservatism associated with this neglected interaction tends towards a "best-estimate" representation for the predicted containment loads when the blowdown injection period is shorten (less time for energy transfers) or where the relative amounts of steel in the containment is minimized.

4.1.2.2 Sensitivity Calculation (forced convection condensation)

Plotted in Figure 4-27 are condensation heat transfer coefficients calculated with the MELCOR HMTA model, showing the coefficient dependency on wall turbulence, that is, wall velocity. The calculations are performed at two representative pressures with an air/steam mass ratio of 0.67. What is apparent from the figure is that the coefficients are very much affected by the level of turbulence along the wall surface, and therefore measurements of wall heat transfer can be used, approximately, to estimate local levels of wall turbulence. For example, shown in Figure 4-28 are the coefficients calculated with the MELCOR HMTA model for atmospheric conditions *measured* in the vicinity of the heat plug locations at 100 seconds. At 100 seconds, the measured coefficient value for heat plug 2 is ~1500 W/m2-K, and the measured air current at this location is reported as ~9 m/s (30 ft/s). Lower in the containment, at heat plug 1 location, the coefficient value measured at 100 seconds is ~600 W/m2-K, and the maximum air current measured in the vicinity of that measurement is reported as ~4.6 m/s (15 ft/s), or about half of the air current measured higher up on the containment wall. It is noteworthy that the relative values measured for both coefficients

[11] Thermocouple data at locations along the centerline of the operating region from just above the operating floor to an elevation near the spring-line, and reported only for spray tests #4 and #5 prior to spray injection (i.e., during the steam injection period), showed a difference of less than ~10 K. Prior to spray injection, Tests #3, #4, and #5 are reported as essentially identical tests.

and air currents are supported by the analytical values obtained using the MELCOR HMTA model. As a result, it appears likely that these CVTR wall heat transfer measurements are a reflection of general forced convective influences on rates of wall condensation (e.g., see Appendix C) under the CVTR blowdown conditions. To investigate this finding on the multi-cell CVTR modeling, a special forced convective parametric input is formulated.

The forced convective input for CVTR test is based on a *calibration* of control volume gas velocity (by input) with the measured wall heat transfer coefficients in the operating region. It is important to point out that this type of parametric analysis is only intended to show the approximate relationship between local atmosphere/wall interaction during a blowdown and the predicted global (pressure) and local response (temperature). Shown in Figure 4-29 are the wall velocities calibrated to produce, approximately, the wall heat transfer in the region of the steam injection. The agreement with measured heat plug 1 and 2 coefficients is only approximate, Figure 4-30, since the conditions (air/steam mass ratios) calculated at the wall are not exactly those measured in the tests.[12] Nevertheless, the addition of forced convective condensation in the operating region does result in some improvement for the pressure comparisons, as indicated in Figure 4-31.[13] Shown in Figure 4-32 are the corresponding comparisons of local gas temperatures with measurements. In general, these comparisons, as with the case above without forced convection, show good agreement with measurements. A similar comparison in Figure 4-33 is shown for the calculated saturation temperatures and compared to measurements. The largest variation between gas and saturation temperature plots is observed in the lower, basement region where temperature increases are primarily the result of compression heating as air is driven down from the upper containment (operating and intermediate regions) by the steam injection. Without an account or modeling of liquid water carry-over (either as suspended droplets or globules) and/or from the entrainment of surface condensate, the predicted temperatures are shown to have significant superheating in the basement region, and this degree of superheating is not evident from measurements.

Further investigation of heat transfer in the basement region from concrete surface measurements sheds some light on what may be occurring in the basement region that increases heat transfer and reduces gas temperatures. Shown in Figure 4-34 are comparisons of calculated and measured concrete surface temperature (support columns) for both the single and multi-cell (with forced convection) calculation. The advantage of the multi-cell over the single cell model is clearly evident, where the calculation with the single control volume significantly over predicts heat transfer in the basement region. The initial under prediction for heat transfer observed for the multi-cell calculation is likely the result of neglected turbulence in the basement region. As a result, the heat transfer coefficient for structures is likely much higher in reality than calculated.

---

[12] The rapid decline of TAEH heat transfer coefficients at ~170 second is not predicted by the MELCOR modeling, and appears to indicate some abrupt change in the air/steam mass ratio at the time when the injection is terminated. It is believed that this behavior may be an artifact of the test, and therefore is not pursued.

[13] The calculations presented in this subsection include input also for the lower steam enthalpy reported in the final test report [Sch70]. Sensitivity to steam enthalpy is discussed in subsection 4.1.1. In this subsection, we are concerned with what reasonable adjustments in model input (supported by measurements) can be made to improve the comparisons between predicted and measured response for CVTR Test 3. The focus, in a relative sense, is on free versus forced convection in the vicinity of the steam injection. Both modeling cases (free and forced convective) discussed subsection have identical input for steam enthalpy.

This sensitivity study, therefore, while pointing out where some improvement is possible with the inclusion of forced convection in the vicinity of the injection, also shows that convective processes affected by turbulence may be more extensive during a high energy break event, and of course not readily accounted for even by parametric models. Figure 4-35 finally then presents an example of how the inclusion of local forced convection may improve global response calculations, especially in light of known uncertainties associated with pressure measurements (+/- 5%). While the improvement is evident, an over prediction (conservatism) is still evident due to the larger extent of turbulence not accounted for with the parametric modeling.

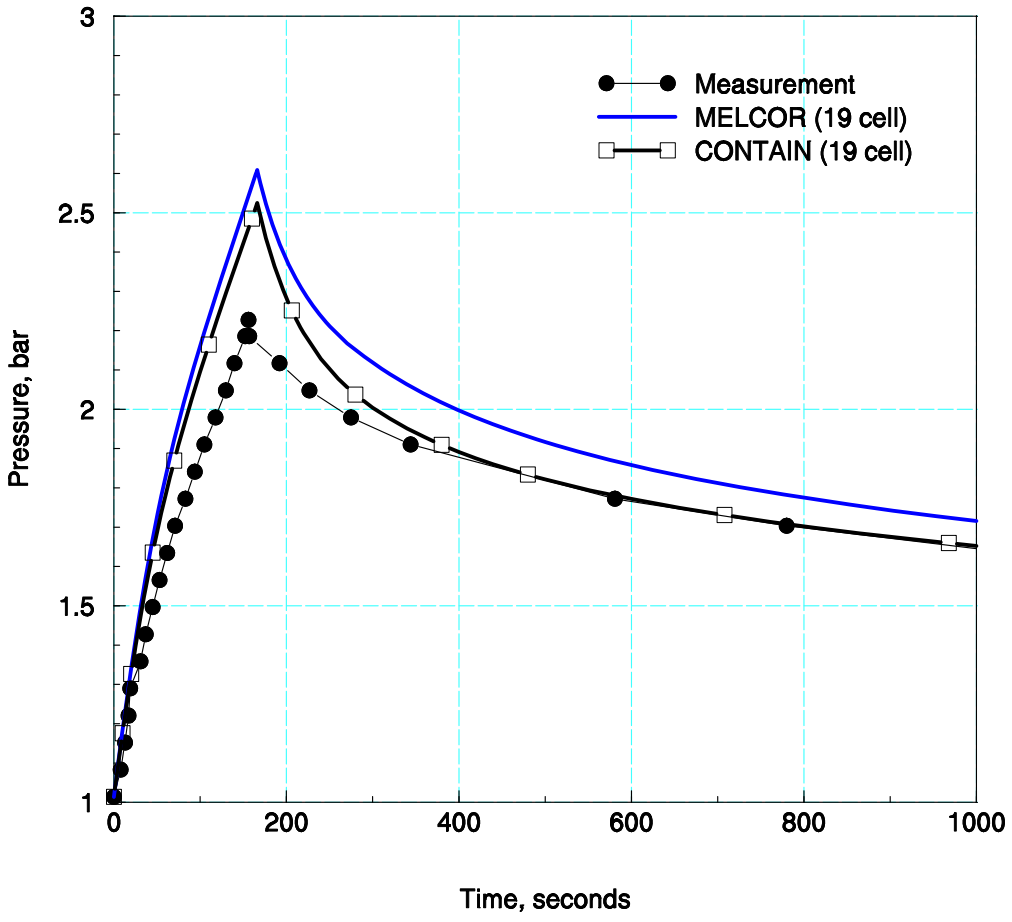

Figure 4-18 Comparison of measured [Sch70] and calculated (multi-cell) pressure for CVTR Test 3.

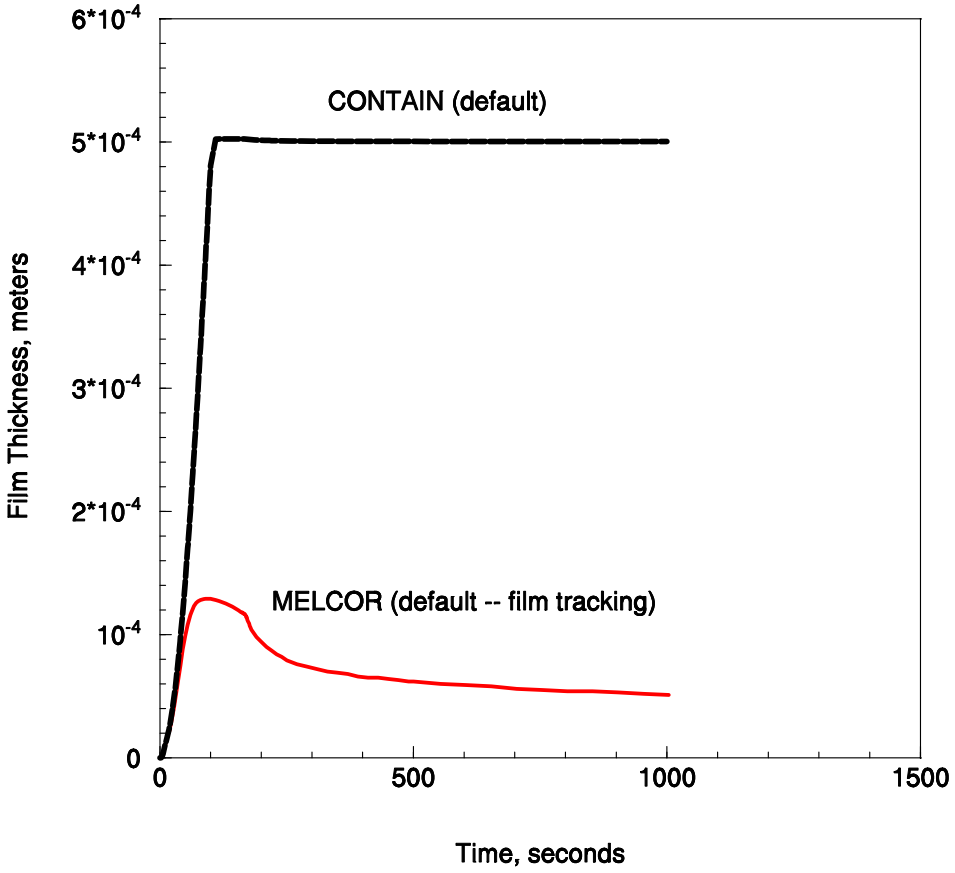

Figure 4-19 Containment shell (operating region) condensate film thickness calculated with MELCOR and CONTAIN for CVTR Test 3.

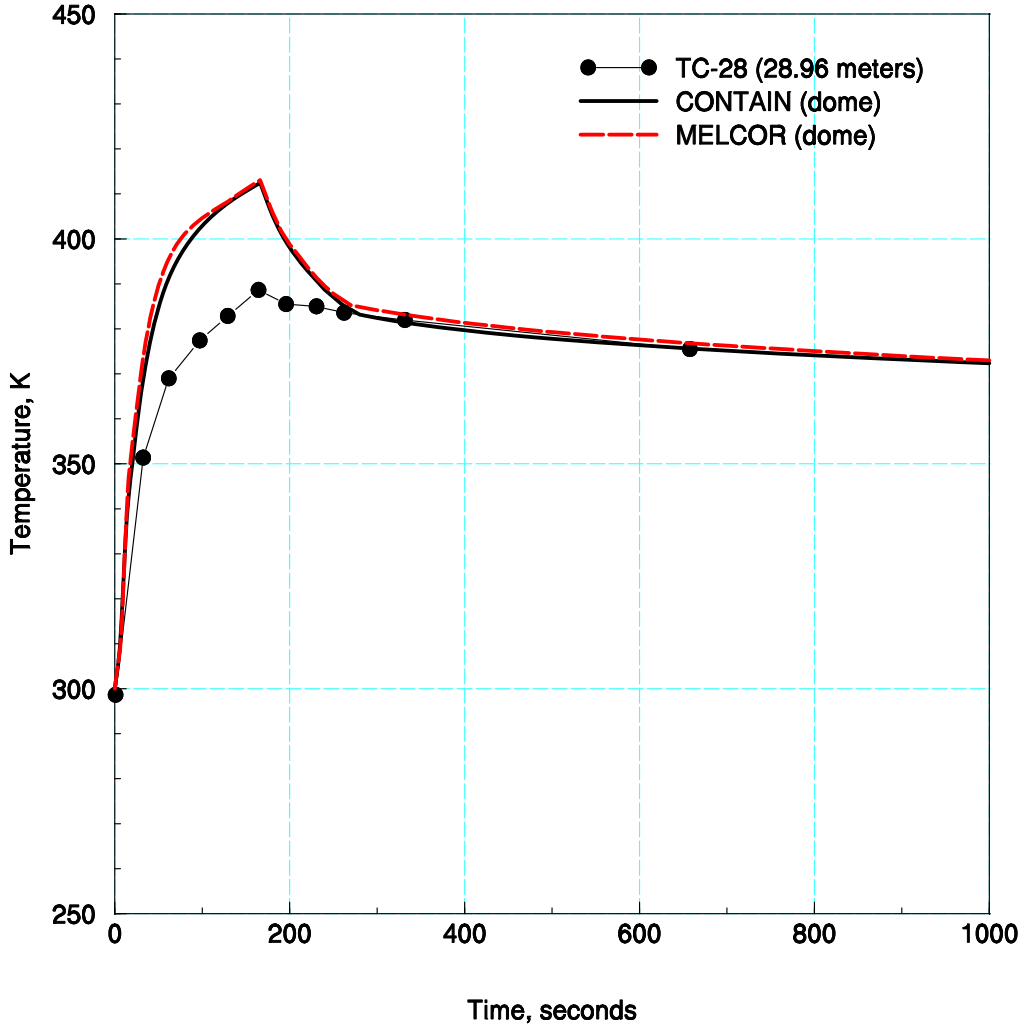

Figure 4-20 Measured and calculated dome gas temperatures for CVTR Test 3.

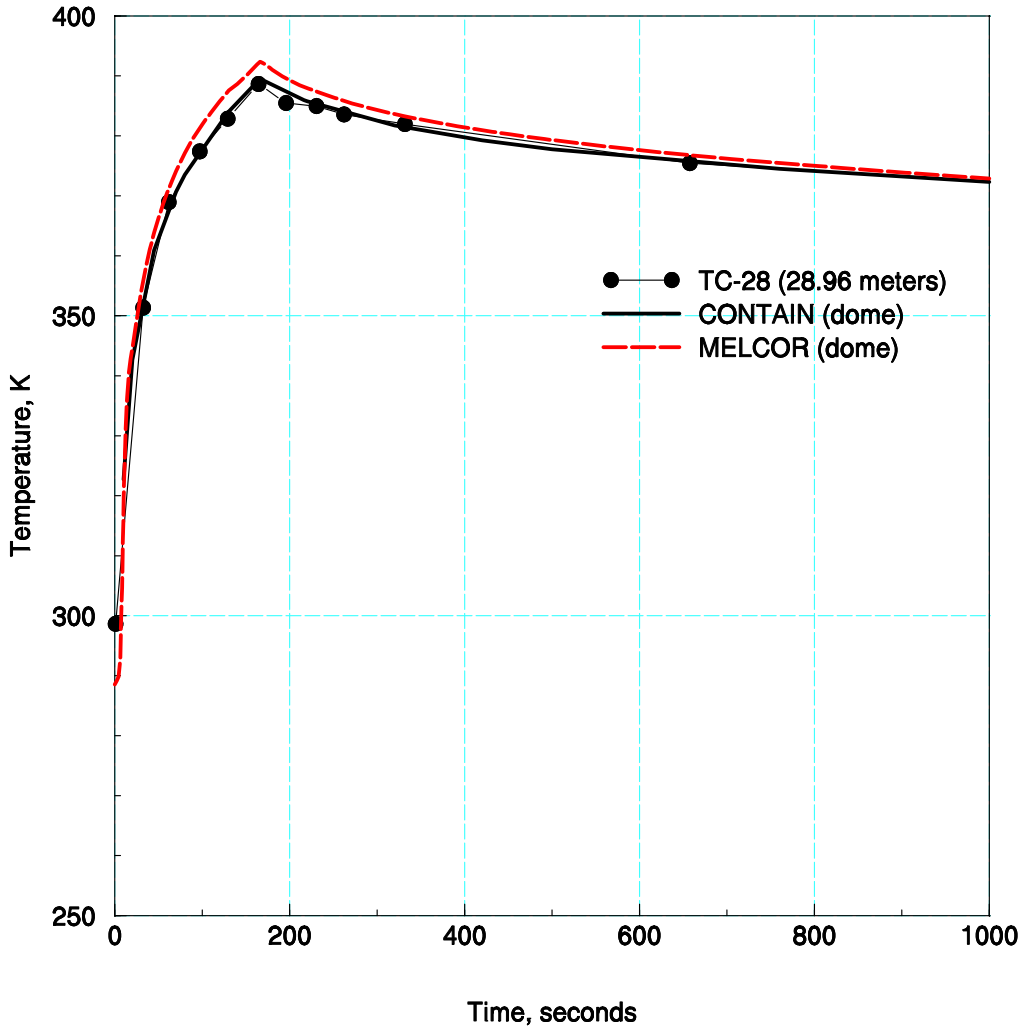

Figure 4-21 Measured and calculated (saturated) dome gas temperatures for CVTR Test 3.

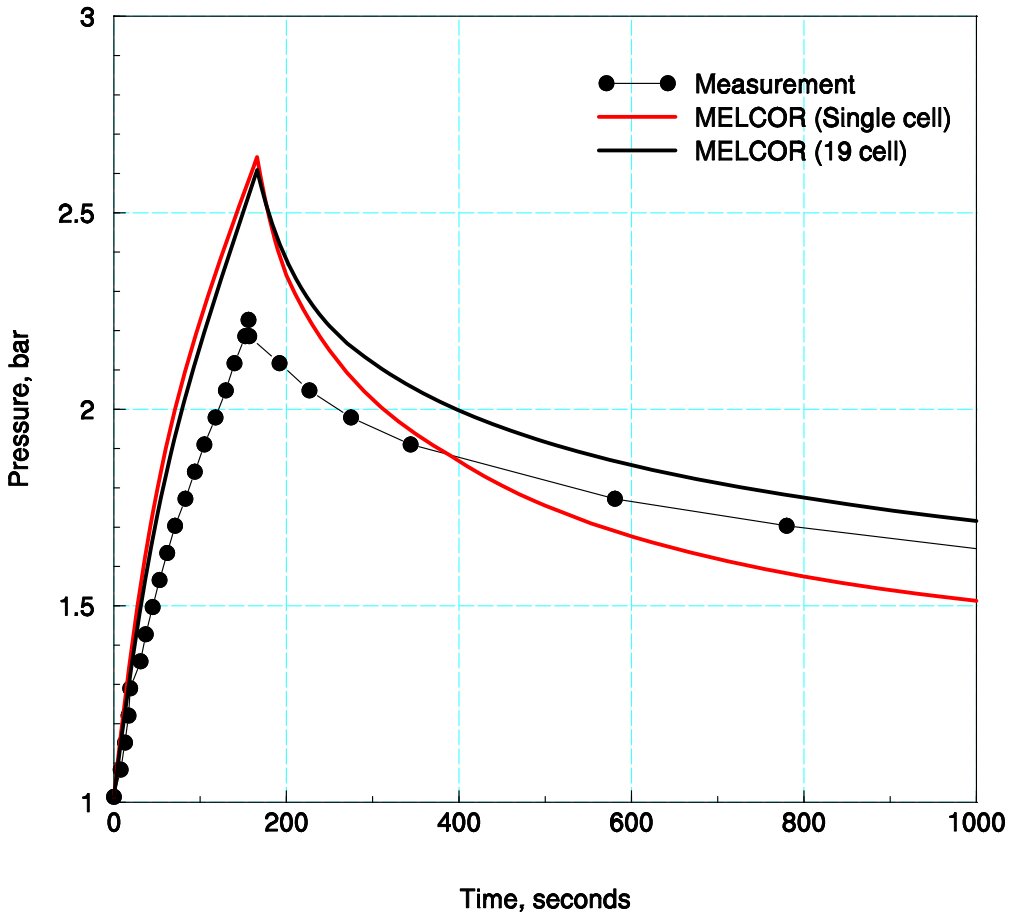

Figure 4-22 Comparison of measured and MELCOR calculated containment pressure for CVTR Test 3.

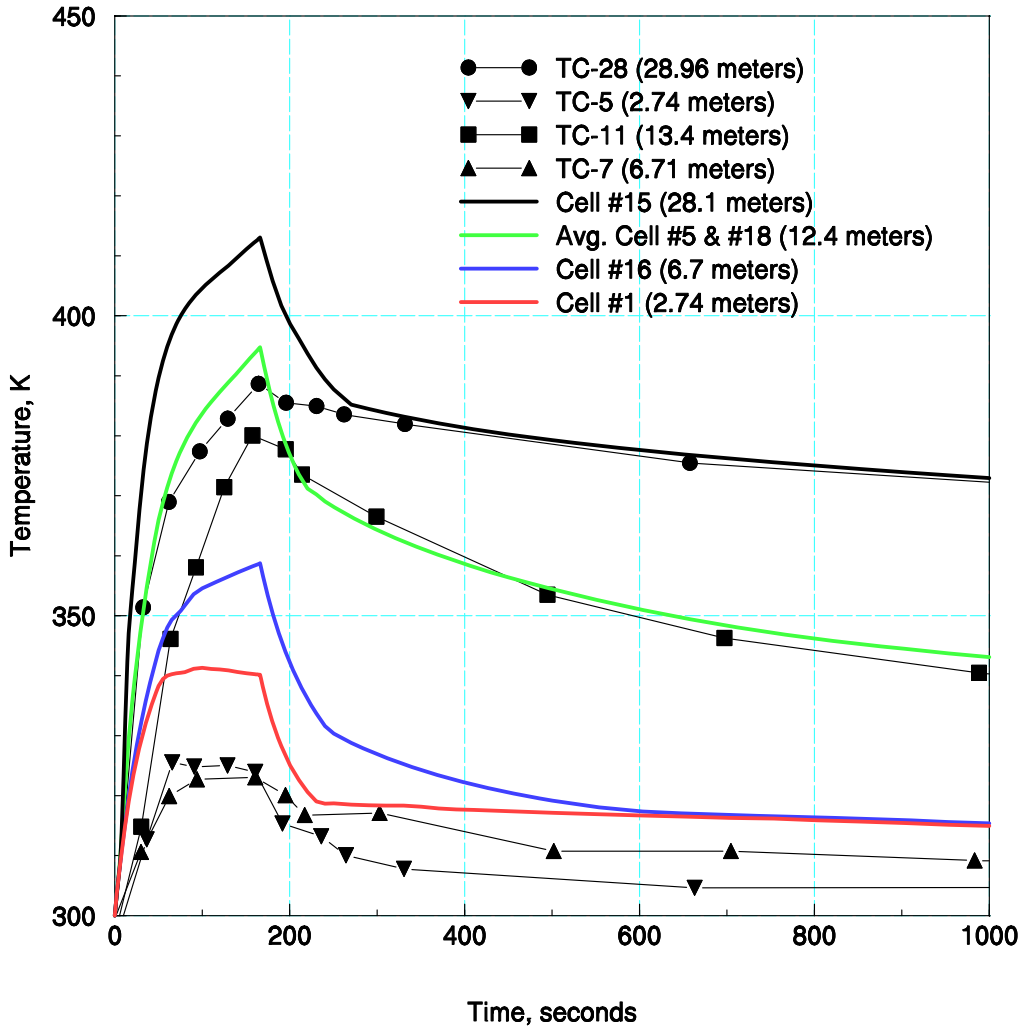

Figure 4-23 Comparison of measured and MELCOR multi-cell calculated containment gas temperatures for CVTR Test 3.

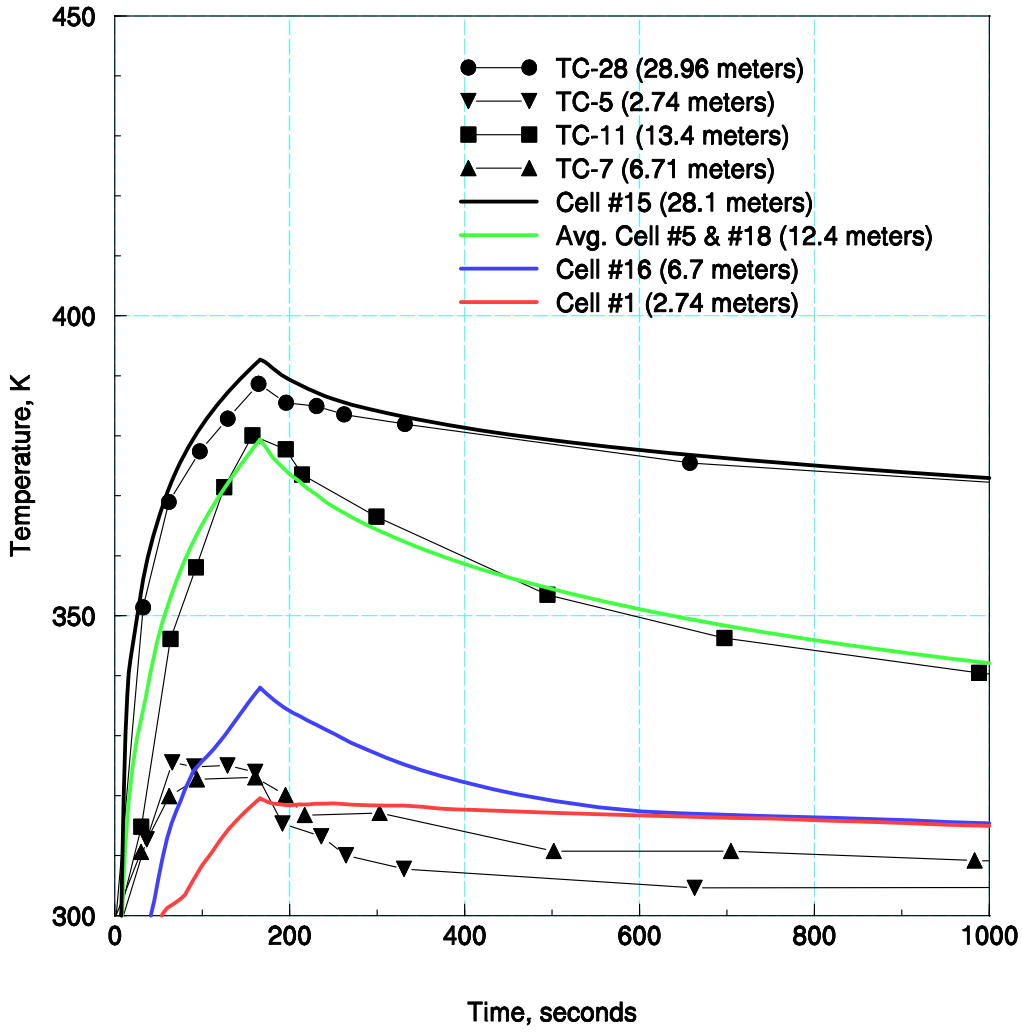

Figure 4-24 Comparison of measured gas temperatures and MELCOR multi-cell calculated saturation temperatures for CVTR Test 3.

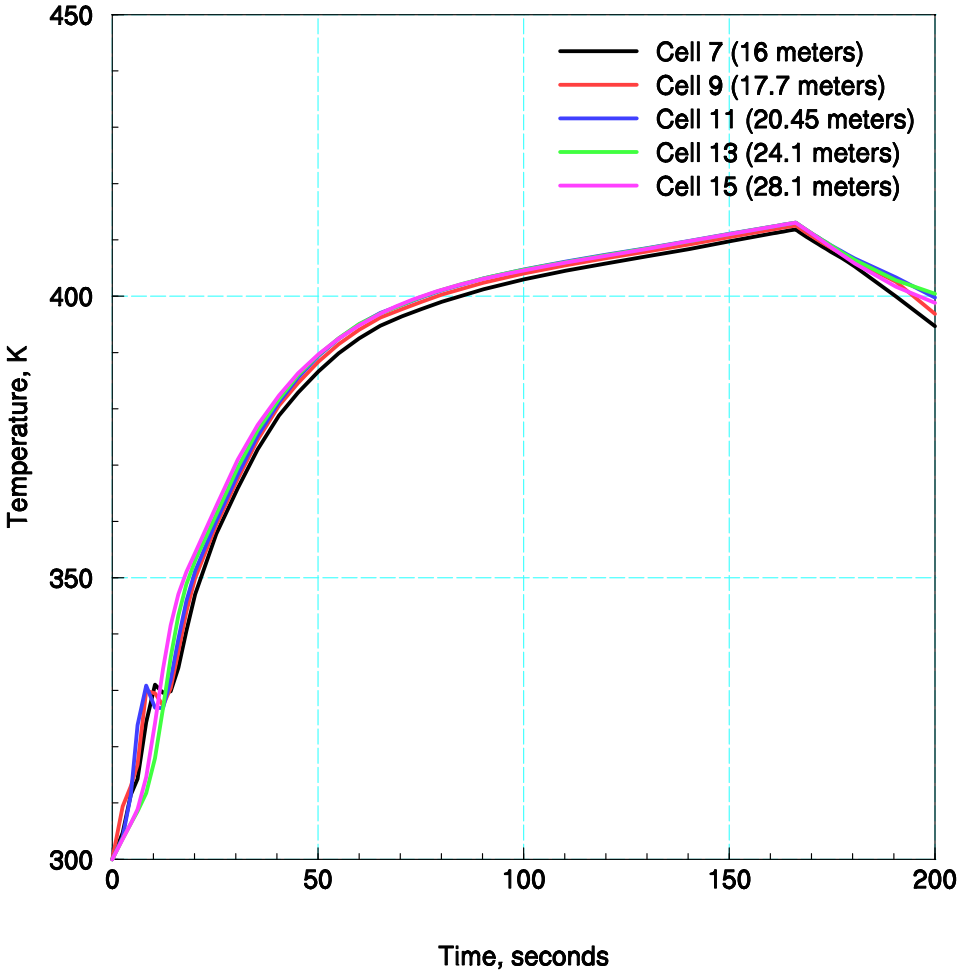

Figure 4-25 MELCOR calculated gas temperatures in the operating region of the containment for the CVTR Test 3.

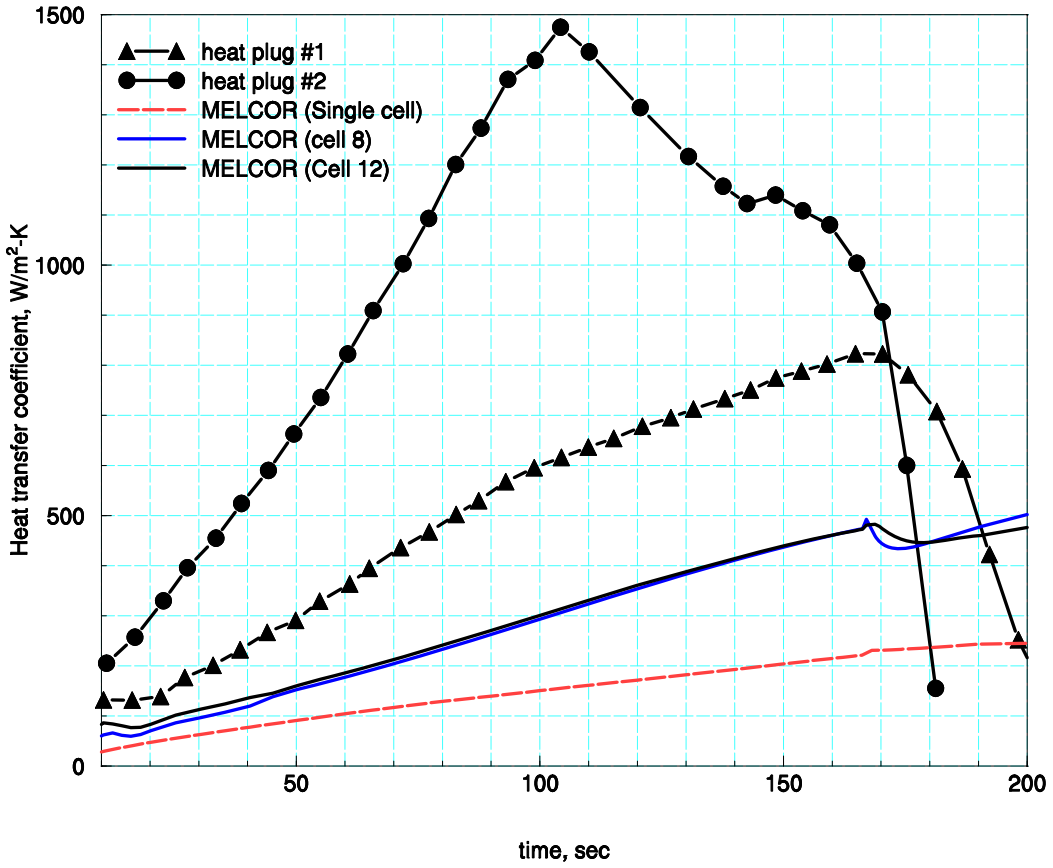

Figure 4-26 Comparison of measured and MELCOR calculated containment wall heat transfer coefficients for CVTR Test 3. Multi-cell results for cell 8 and cell 12 correspond to heat plug locations #1 and #2, respectively.

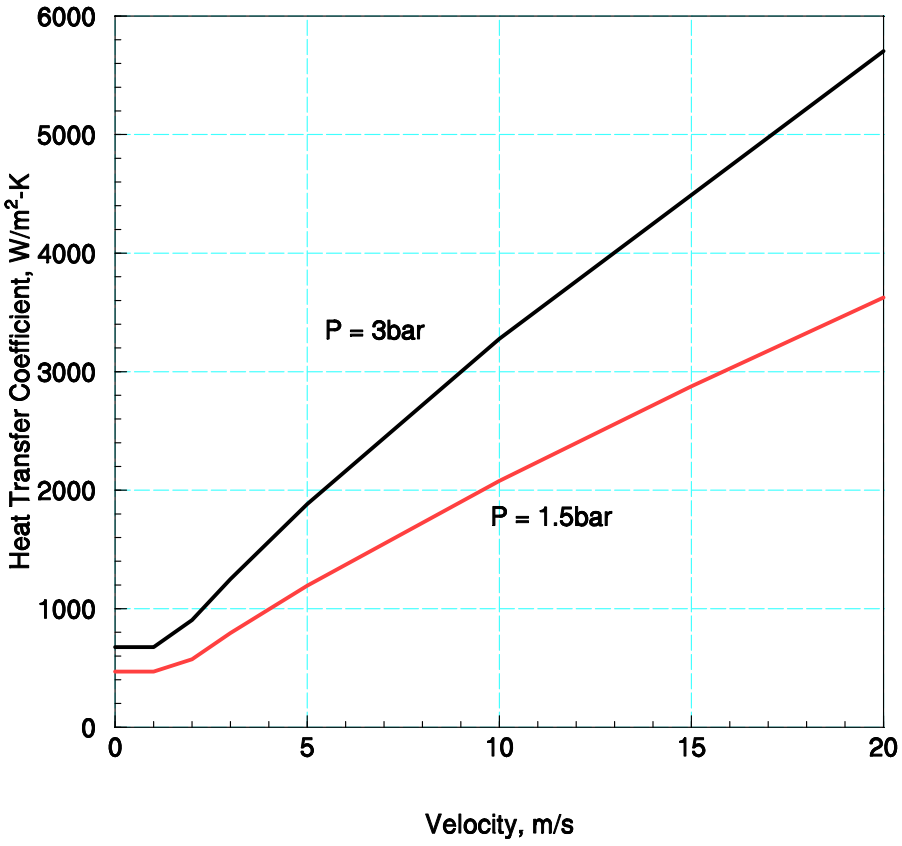

Figure 4-27 Parametric calculations of wall heat transfer coefficients based varying amount of wall turbulence (velocity) using the MELCOR HMTA model. Other settings are: 1) temperature drop from bulk to wall of 30 degrees, 2) air/steam mass ratio equal to 0.67, 3) no film thickness modeled, and 4) free to forced convection transition based on maximum calculated Nusselt number.

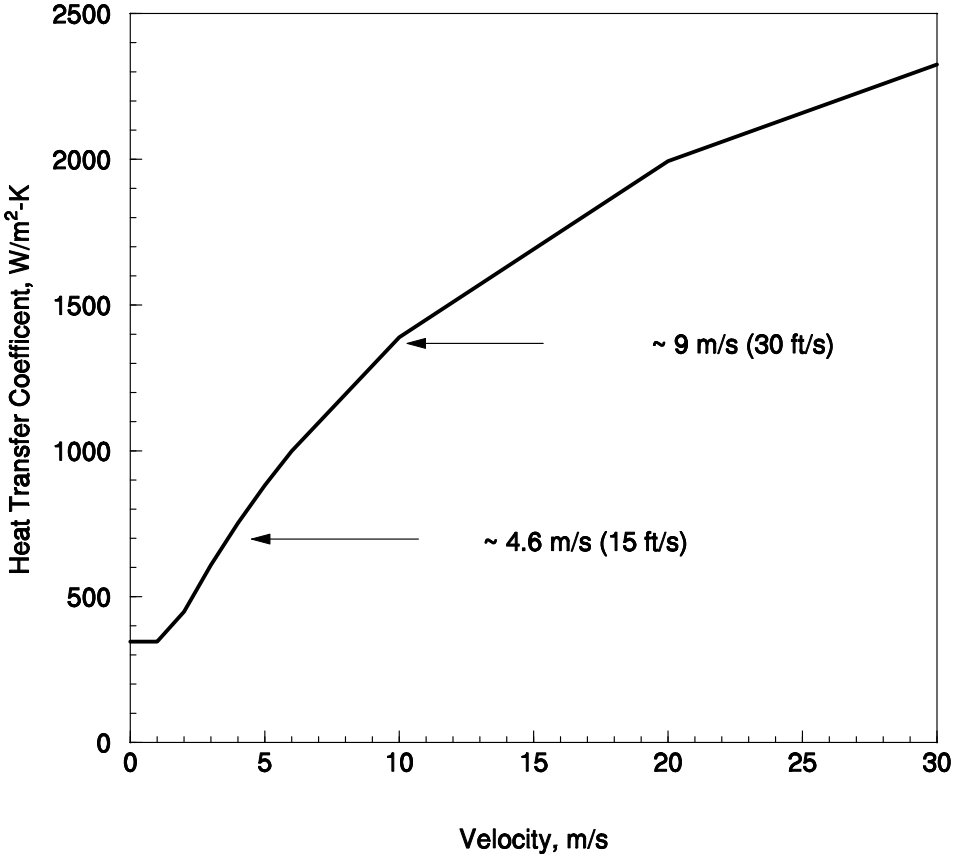

Figure 4-28 MELCOR HMTA modeling of wall condensation coefficient for the operating region using measured atmospheric conditions (pressure, air/steam mass ratio (saturated), temperatures) at 100 seconds for the CVTR Test 3.

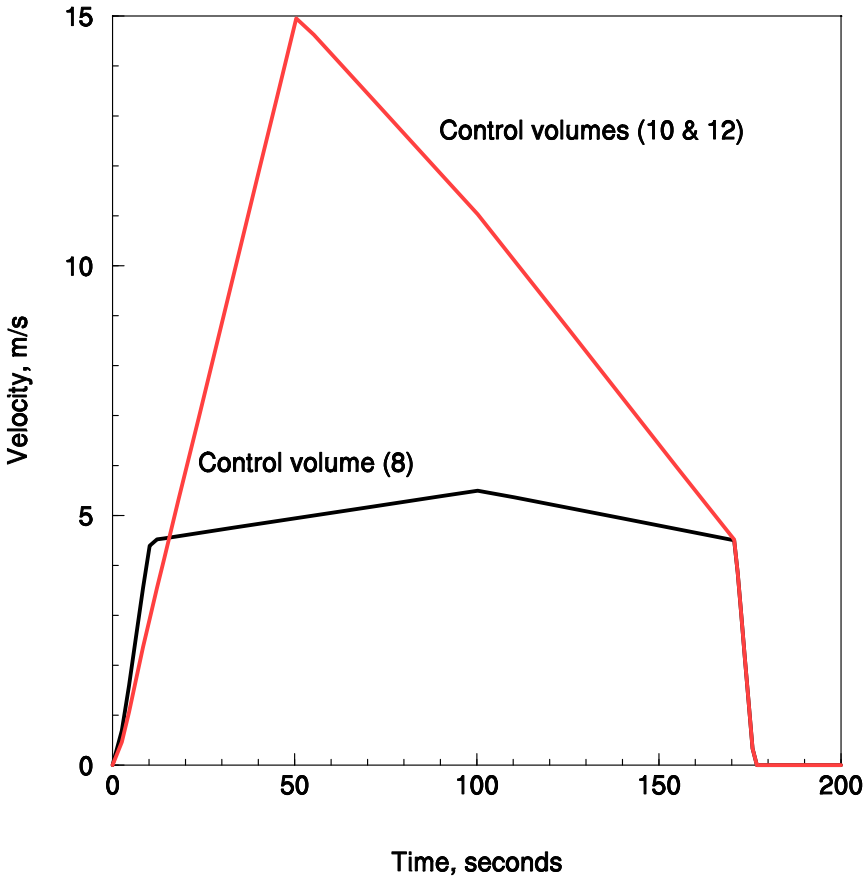

Figure 4-29 Control volume velocity input for the forced convection, multi-cell calculation of the CVTR Test 3.

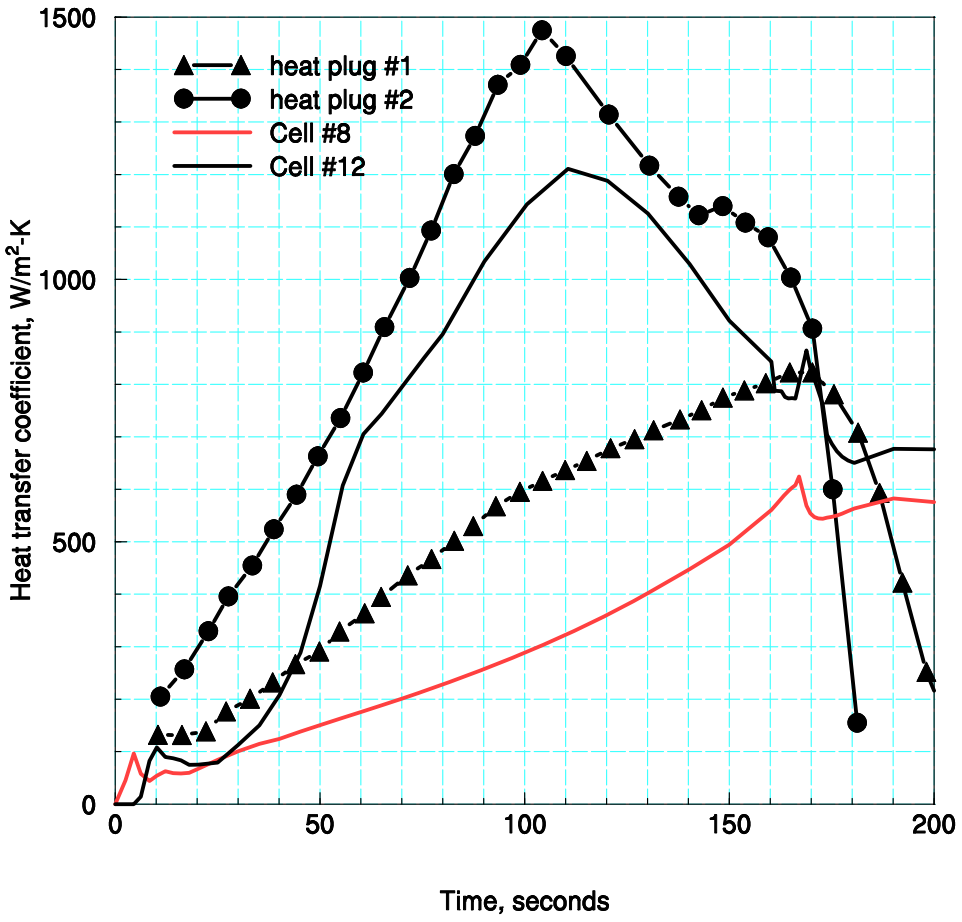

Figure 4-30 Comparison of MELCOR calculated and measured heat transfer coefficients for CVTR Test 3, based on input control volume velocities along the containment wall.

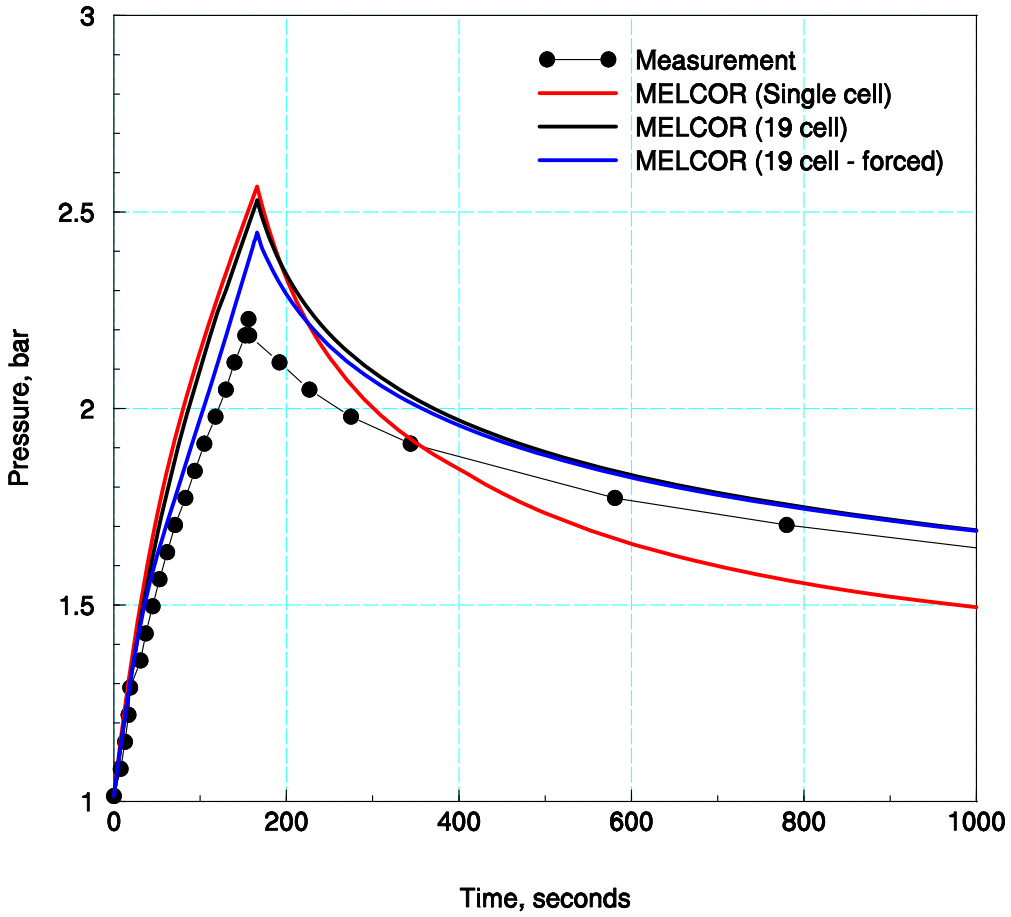

Figure 4-31 Comparison of measured and MELCOR calculated pressures for CVTR Test 3. Calculated profiles are obtained using the lower bounding limit for injected steam enthalpy (Sch70).

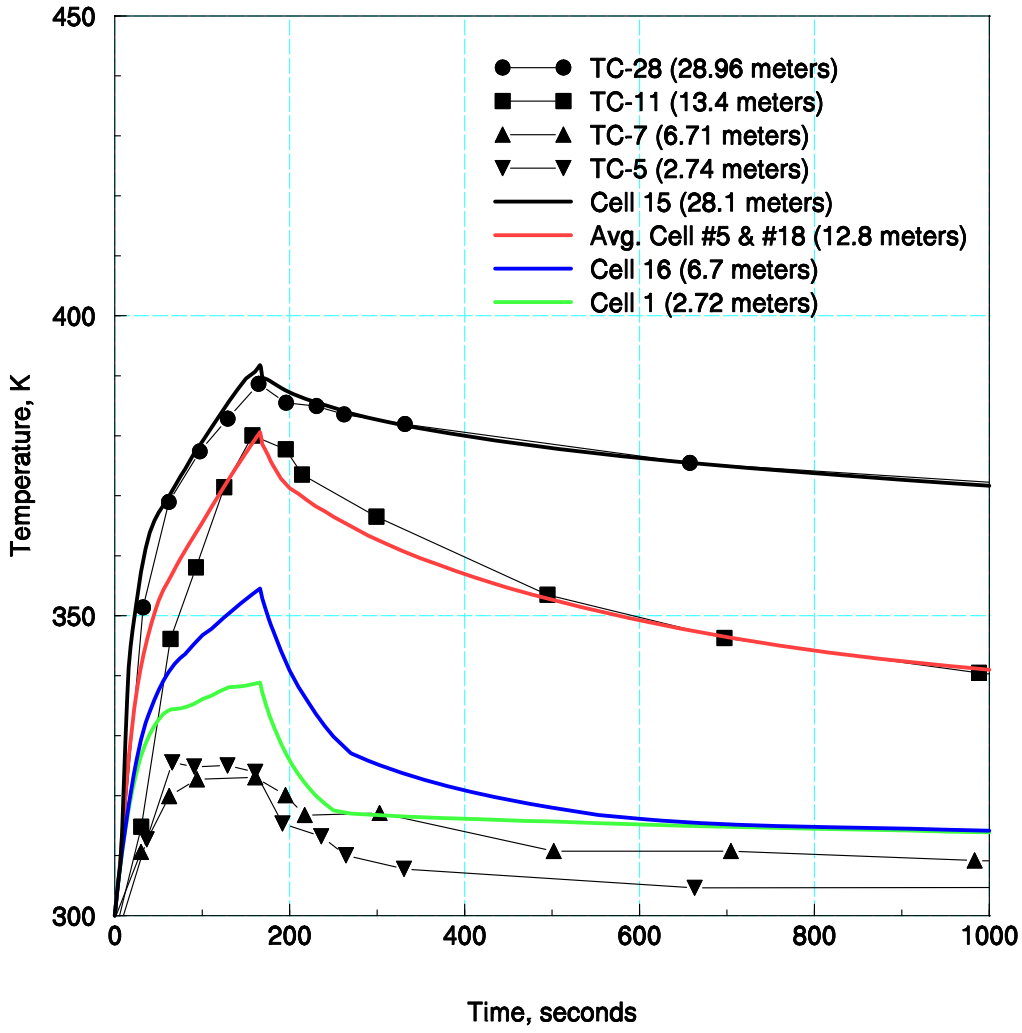

Figure 4-32 Comparison of measured and MELCOR calculated gas temperatures for CVTR Test 3. Calculated profiles are obtained with the forced convective case with input control volume velocities.

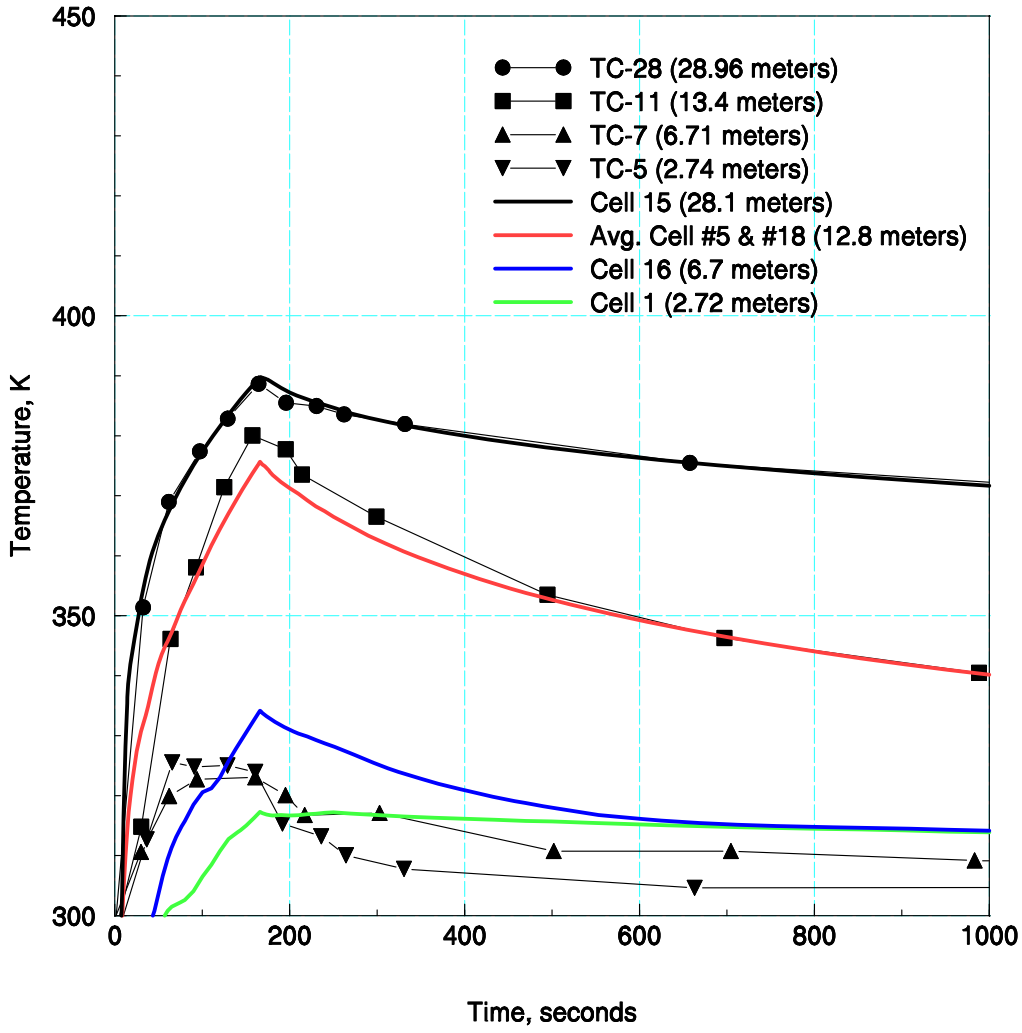

Figure 4-33 Comparison of measured and MELCOR calculated gas (saturated) temperatures for CVTR Test 3. Calculated profiles are obtained with the forced convective case with input control volume velocities.

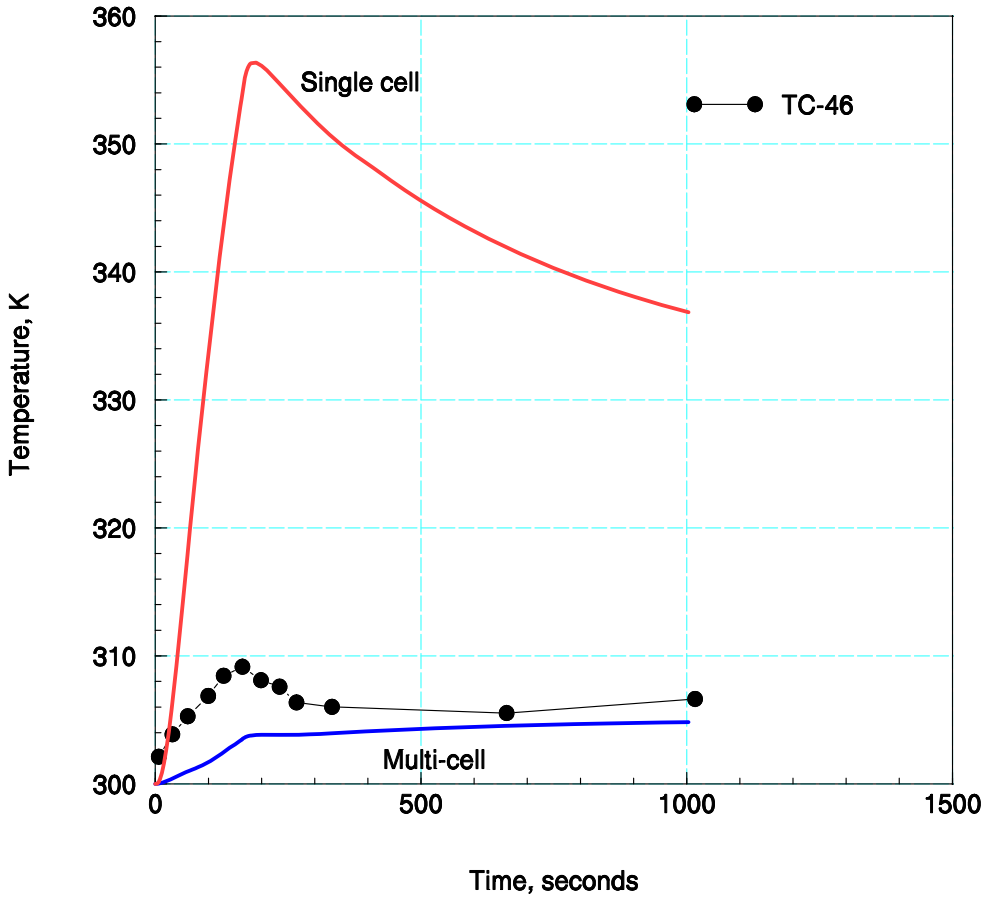

Figure 4-34 Comparison of measured and MELCOR calculated concrete surface temperature for the support columns in the basement region during the CVTR Test 3. The multi-cell calculation is obtained for the case with forced convection modeled in the operating region and is essentially identical to the same calculation using free convection throughout the containment.

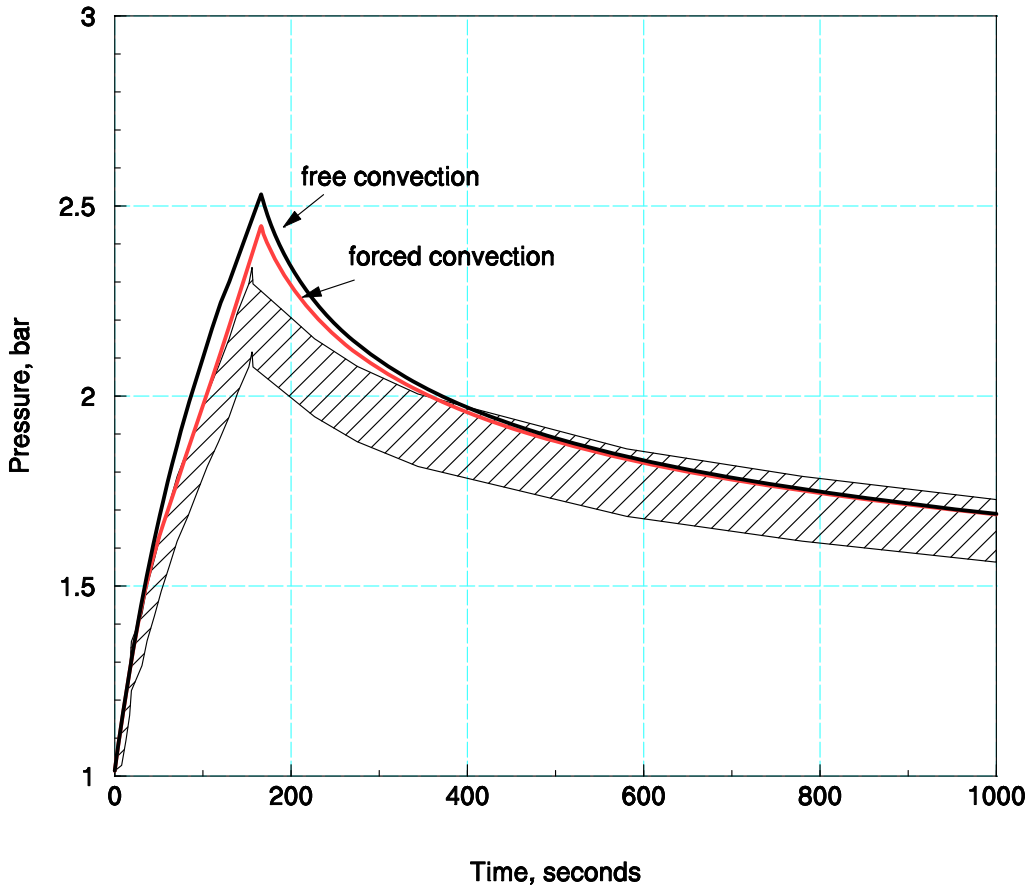

Figure 4-35 Comparison of measured (with uncertainty band) and MELCOR calculated pressure for CVTR Test 3. Calculated profiles are obtained with the lower bound limit on injected steam enthalpy as reported in final test report [Sch70].

4.2 CVTR Tests 4 and 5 (with spray activation)

Pressure reduction spray system flow rates of 0.0183 m^3/s (290 gal/min) and 0.0316 m^3/s (500 gal/min) were used during steam Tests 4 and 5, respectively. The steam injection rates and duration for each test were nearly identical to Test 3. Sprays were initiated at approximately 200 seconds, which is about 30 seconds after the steam injection termination and sprays were turned off after approximately 12 minutes of spray time. The spray nozzles were located about 15 cm (6 inches) above the bend line of the upper containment. Total spray rate was determined by the number of nozzle heads activated. Three nozzle types, positioned equally around the perimeter of the containment, produced spray droplet sizes in the range 400 to 1400 microns. Shown in Figure 4-36 is a sketch of the CVTR spray system.

Figure 4-37 shows the effect of spray activation on pressure reduction, which is at post-blowdown. Additionally, the leveling of pressure when the sprays are turned off is clearly evident in the pressure plots for Tests 4 and 5, as shown in Figure 4-38. These pressure responses to activation and de-activation of sprays are the features that good spray models are expected to reproduce. The important phenomena responsible for these trends in pressure control are the energy transfers that occur at the surface of the spray droplets. These transfers involve both sensible and latent heat transfer as the droplets thermally equalize with the surrounding atmosphere. In the CVTR tests, measurements were taken to determine the extent of thermal equilibrium between spray droplets and atmosphere. Trapping funnels were placed in various locations in the operating region, and collected water (droplet) temperatures were measured. A comparison between gas and water temperatures measured at the funnel locations provided an indicator of thermal equilibrium, and therefore spray efficiency. From these measurements it was experimentally determined that spray efficiencies of essentially 100% were obtained at distances of ~10 meters (30 feet) from the spray nozzles.

The process of attaining thermal equilibrium between gas and spray droplets means that the gas temperatures in the spray region are being cooled, as shown by temperature measurements taken in the operating region, Figure 4-39. As was seen for Test 3, relatively large vertical temperature differences exist in the containment throughout the test, Figure 4-40. The effect of sprays is to reduce the degree of stratification by decreasing the temperature in the operating region and increasing the temperature of the basement and intermediate regions. The result is that the spray actuation tends to equalize the containment temperatures. These trends are indicated by the measured vertical temperature profiles for CVTR Tests 4 and 5 shown in Figures 4-41 and 4-42, respectively. The plots also indicate that the degree of equalization increases with the spray flow rate.

4.2.1 Reference Cases

The references cases for calculating CVTR Tests 4 and 5 are derived from the MELCOR CVTR multi-cell model, where additional input for sprays is included for source cells 13 and 14. Although the spray nozzles were located at the bend line perimeter, nozzles were directed to provide coverage to the perimeter and center region of the open space below the bend line. Therefore, spray injection to cells 13 and 14 were prescribed using equal volumetric flows. The spray droplets in the operating region were allowed to cascade through the control volumes directly below the respective source volumes. Spray droplets reaching the floor of cells 7 and 8

were transported directly to the sump in the basement region (cell 1). No washdown (i.e., spray droplets contacting perimeter walls in operating region) was assumed, and the spray droplet average diameter was the default setting (0.001 meters). Sensitivity calculations are included in subsection 4.2.2 to investigate sensitivities (e.g., pressure) to variations in washdown amount and spray droplet diameter.

Code-to-code benchmarking. A sketch of the multi-cell nodalization for the spray calculations is shown in Figure 4-43. The sprays are allowed to cascade from the source volumes (cells #13 and #14) down to the operating floor. The spray system design places the spray nozzles below the dome region at the bend line. In the MELCOR code the carry-over of sprays from the overlying volumes is treated internally; however, for CONTAIN there is no internal coding to treat this behavior, so the cascading must be handled by input. The procedure used in CONTAIN is to locate a pseudo reservoir volume in each cell that transfers fall-through spray droplets. Collected spray mass in each pool volume is a source for the next lower volume. The effective emptying rate for each reservoir is set large enough so that there is no accumulation of spray water. Since spray droplets thermally equalize with the atmosphere in the first spray volume, the heat transfer in the lower cells is small; therefore, the effect on heat transfer for a cascading spray scheme is minimal, and so both code models should give similar results. Another difference in code modeling is also noted relating to the treatment of induced flows driven by unbalanced buoyancy forces. The CONTAIN code uses a hybrid flow solver to inhibit spurious convection loops as a result of the inaccuracies associated with the numerical solution of the flow equations. The MELCOR solution algorithm for the flow equations is formulated somewhat different and the need for the approach to prevent non-physical convection loops (via hybrid flow solver) is not necessary. As a result there are modeling differences associated with the flow equation solution that can be distinguished in some cases, such as in the case of the induced-buoyancy driven flows resulting from spray cooling.

The calculated pressure reduction at each spray rate is shown in Figures 4-44 and 4-45 for each code. At the higher spray rate, Test 5, the agreement is better. Shown in Figures 4-46 and 4-47 are the comparisons for calculated temperatures in the dome region, above the spray nozzles. The comparisons are not good and point out model differences in predicting induced buoyancy flows for a mixing scenario not often investigated; although, previous validation exercises for separate effects spray cooling (Appendix E) have shown that the CONTAIN code under-estimates mixing in regions above the spray source. For each test, the MELCOR calculated temperatures are significantly lower than the CONTAIN prediction; and, as seen below, these lower temperatures are in better agreement with measurement. Plotted in Figures 4-48 and 4-49 are the code comparisons for predicted average temperature (cells 10 and 11) in the region below the spray nozzles, where thermal equalization between the spray droplets and surrounding gas is noted to occur in the spray tests. In these plots, the agreement between the codes is good.

Code-to-measurement. The comparison between the measured and MELCOR calculated pressure profiles for CVTR tests with and without sprays is shown in Figure 4-50. In general, the trends during spray cooling are predicted quite well. The longer term calculations that show the leveling off of pressure when the sprays are turned off also are in good agreement with measurements, as indicated in Figure 4-51. Figure 4-52 shows that MELCOR does reasonably well in predicting dome temperatures measured above the spray nozzles which, as noted above, was not well predicted by CONTAIN. Below the spray nozzles, gas temperatures in thermal equilibrium with

spray droplets, are also shown to be well predicted with MELCOR in CVTR Tests 4 and 5. These comparisons are shown in Figures 4-53 and 4-54. Longer term vertical temperature profiles calculated for Tests 4 and 5 are plotted in Figures 4-55 and 4-56, respectively. These plots show that spray cooling tends to produce a more uniform containment temperature as the upper gas temperatures are cooled while the lower temperatures are effectively heated by enhanced gas transport (buoyancy-driven). The trending toward a more uniform temperature with time for higher spray rates is consistent with measurements. For example, the maximum vertical gas temperature difference (dome to basement) at the end of Tests 3, 4, and 5 were approximately 60, 28, and 14 degrees Kelvin; whereas, the calculated temperature differences were 60, 20, and 8 degrees Kelvin.

4.2.2 Sensitivity Calculations

Separate effects test (SET) analysis for pressure reduction due to sprays was performed for the JAERI spray vessel (Appendix E). That analysis indicated some pressure sensitivity to a washdown effect where some fraction of the spray droplets directly contacts the perimeter walls of the vessel. Additionally, the JAERI test analysis also indicated that calculated air/steam mixture temperatures below the nozzles were somewhat sensitive to input spray droplet diameter. The larger droplet diameter input resulted in higher amounts of superheating, causing an over prediction of the measured gas temperatures in the spray region. To prepare the JAERI spray vessel for a SET type analysis (with spray only effects), the vessel wall were pre-heated by a pre-conditioning steam source. As a result, the vessel walls were near the saturation temperature of the air/steam mixture when the sprays were turned on. The pre-conditioning of the JAERI spray vessel therefore became a factor to take into account when specifying both washdown and spray droplet diameter input. The CVTR spray tests, with blowdown pre-conditioning, were conducted in a manner different from the JAERI tests and therefore sensitivity cases were run to show that the variations of pressure and temperatures in the JAERI spray tests to input specifications (washdown and spray droplet size) were not similarly predicted for the CVTR tests.

A comparison between a single and multi-cell calculation for the non-spray test, Test 3, indicated the rate of depressurization calculated during the post-blowdown period is higher for the single cell case due to an overall higher rate of condensation predicted using the simpler nodalization. Also, the post-blowdown gas temperature predicted with the single cell model was shown to track well below the dome gas temperature and significantly above the gas temperature calculated in the basement region. For the tests with sprays, a similar trend is observed between single and multi-cell calculations; however, because the sprays effectively reduce containment stratification, the pressure and gas temperature differences between single and multi-cell modeling are less when sprays are activated. This behavior is shown through a series of sensitivity cases calculated using the single-cell model for the CVTR containment.

Washdown. For the washdown sensitivity case, 10% of the spray source was assumed to directly contact the perimeter walls in cells 14 and 12. The remaining 90% of the spray source was distributed equally as direct atmosphere-to-droplet contact in source cells 13 and 14. This method is identical to the procedure used in calculating JAERI spray test PHS-1. The results of this re-distribution of spray flow is shown in Figures 4-57 and 4-58 for Tests 4 and 5, where the containment pressures for the reference cases are with no washdown and the sensitivity cases with a 10% washdown. The comparisons show no significant variation in pressure as a result of washdown. The insensitivity is because the CVTR walls are not hotter than the atmosphere when

the sprays are turned on, contrary to the JAERI spray tests, and therefore the washdown spray droplets do not vaporize when contacting the walls, adding to the steam pressure in the containment. The reduction of direct contact atmospheric spray flow by 10% is not large enough to have a significant affect on the rate of pressure reduction, although a small difference in pressure is noted after a time.

Spray droplet diameter. For the spray droplet size sensitivity calculations, Tests 4 and 5 were rerun with the spray droplet diameter changed from the default (0.001 meters) to a smaller size (0.0002 meters). In these cases, because the gas temperature in the entire containment was saturated and wall surfaces wetted when the sprays were turned on, a variation in the spray droplet size had no perceivable affect on heat and mass transfer in the spray region, since the smaller spray droplet size would favor a more saturated atmosphere. As a result, the rate of pressure reduction due to the sprays or the gas temperatures calculated in the containment did not vary from the predictions in the reference cases.

Single-cell modeling. Shown in Figures 4-59 and 4-60 are comparisons of predicted containment pressure with the single and multi-cell models for Tests 4 and 5, respectively. For Test 4, with a spray rate of 0.0183 m^3/s, the differences in pressure between the single and multi-cell model are very nearly identical to what was observed without sprays. With the higher spray rate in Test 5 (0.0316 m^3/s), there is a noticeable reduction in the pressure differences predicted between the nodalization schemes. The higher spray rate produces a more uniformly mixed containment space with the result that both models predict pressures that are quite similar. An improvement in the comparison between the single and multi-cell calculations at the higher spray rate is even more pronounced for the gas temperature comparisons, as shown in Figures 4-61 and 4-62, especially during the post-spray period when the effect of spray induced mixing is clearly evident.

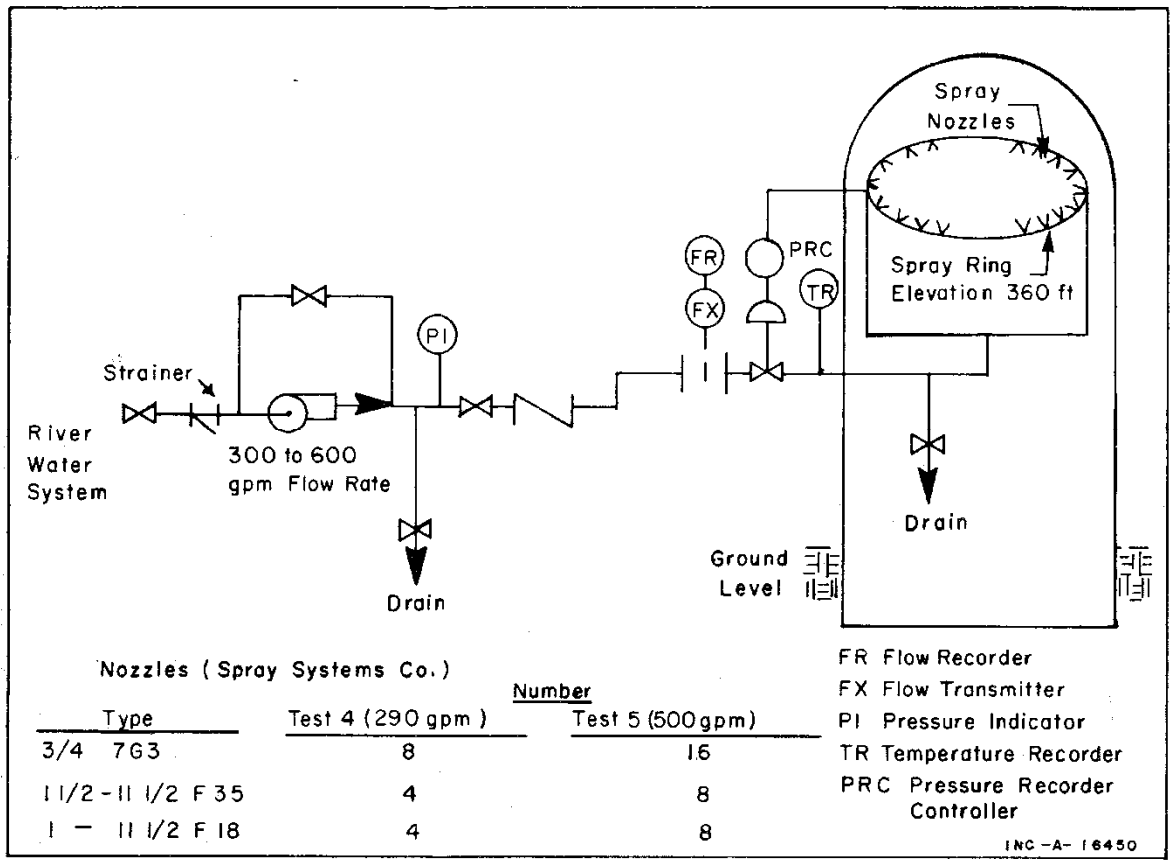

Figure 4-36 CVTR pressure reduction spray system [Sch70].

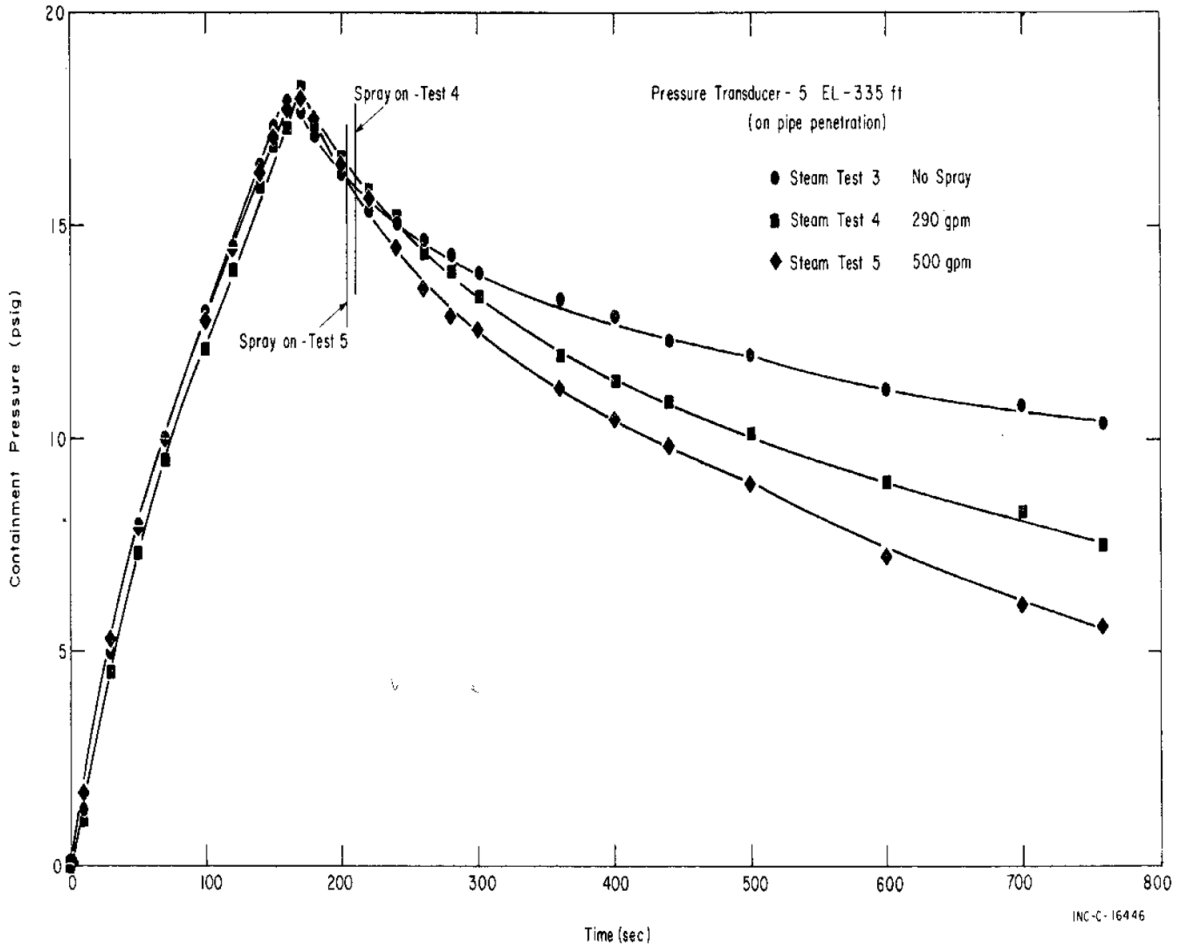

Figure 4-37 Effect of spray activation on CVTR pressure reduction [Sch70].

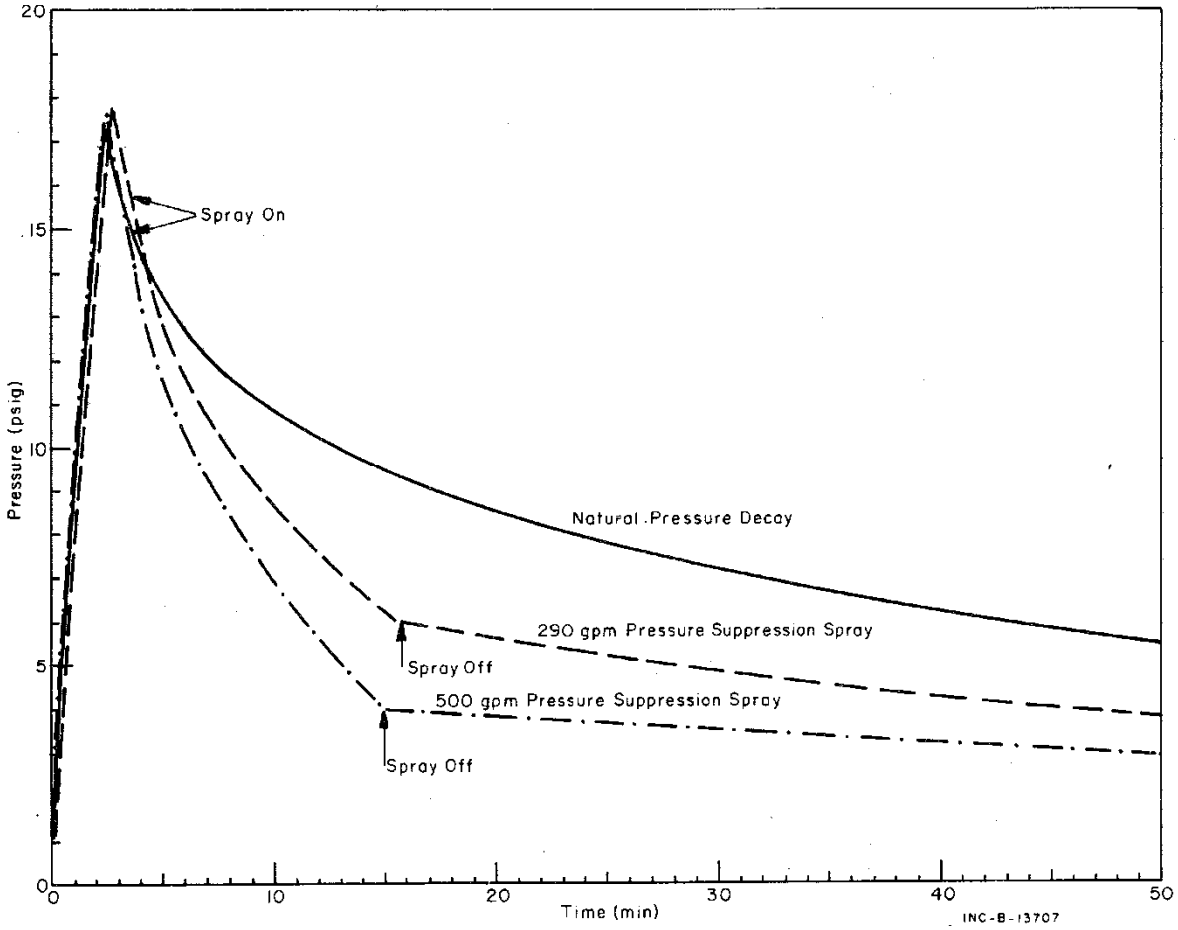

Figure 4-38 Effect of spray activation and de-activation on the CVTR pressure response [Sch70].

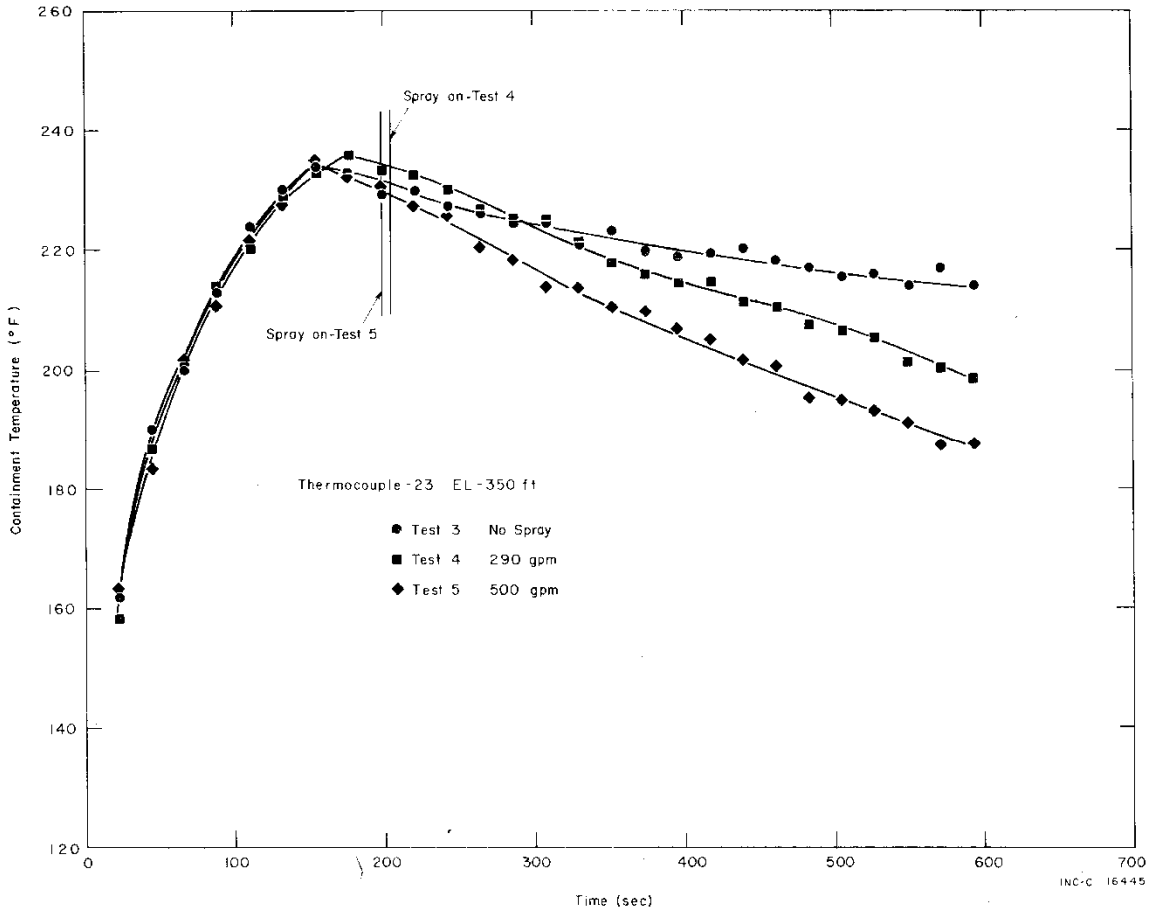

Figure 4-39 Gas temperature measurements in the operating region, below the spray nozzles, for Test 3 (no spray activation) and Tests 4 and 5 (with spray activation) [Sch70].

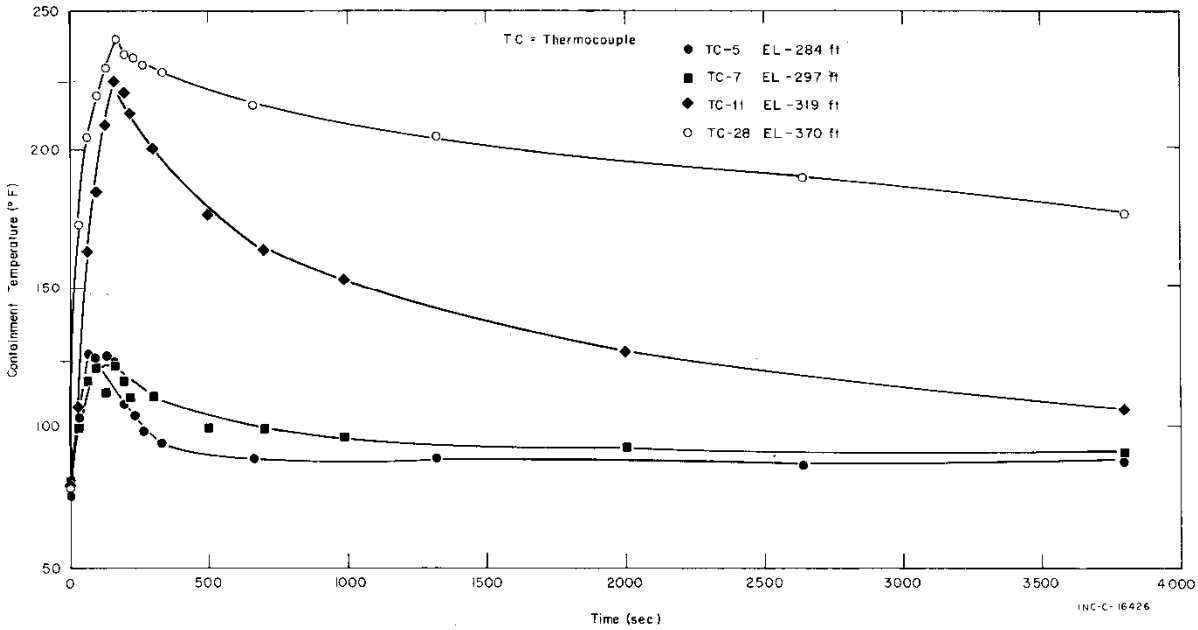

Figure 4-40 Gas temperature measurements for CVTR Test 3 [Sch70].

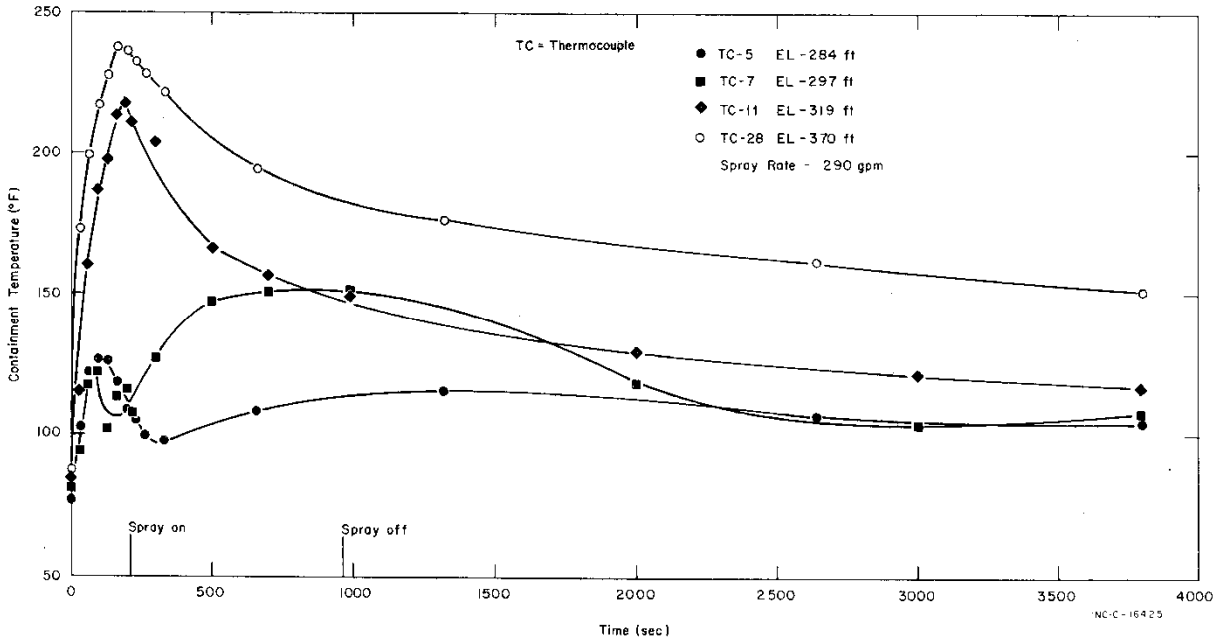

Figure 4-41 Gas temperature measurements for CVTR Test 4 [Sch70].

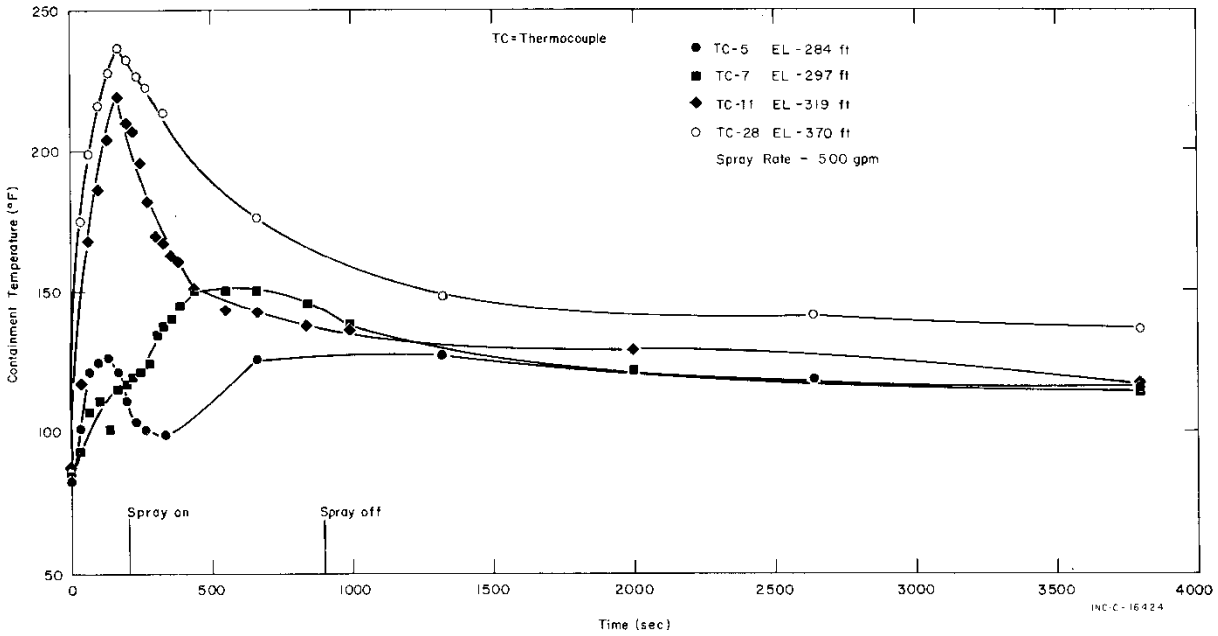

Figure 4-42 Gas temperature measurements for CVTR Test 5 [Sch70].

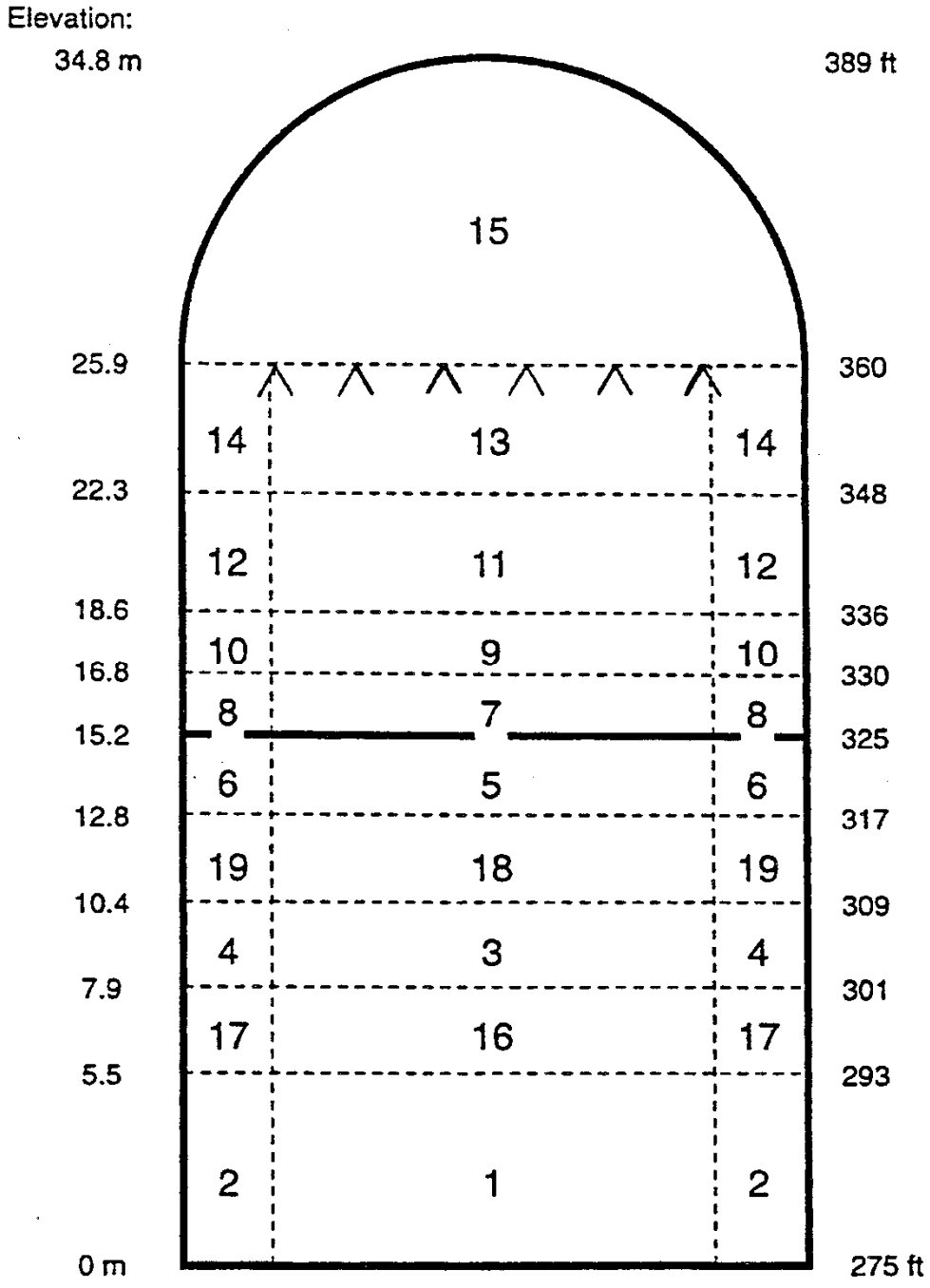

Figure 4-43 MELCOR and CONTAIN nodalization sketch for the CVTR spray tests.

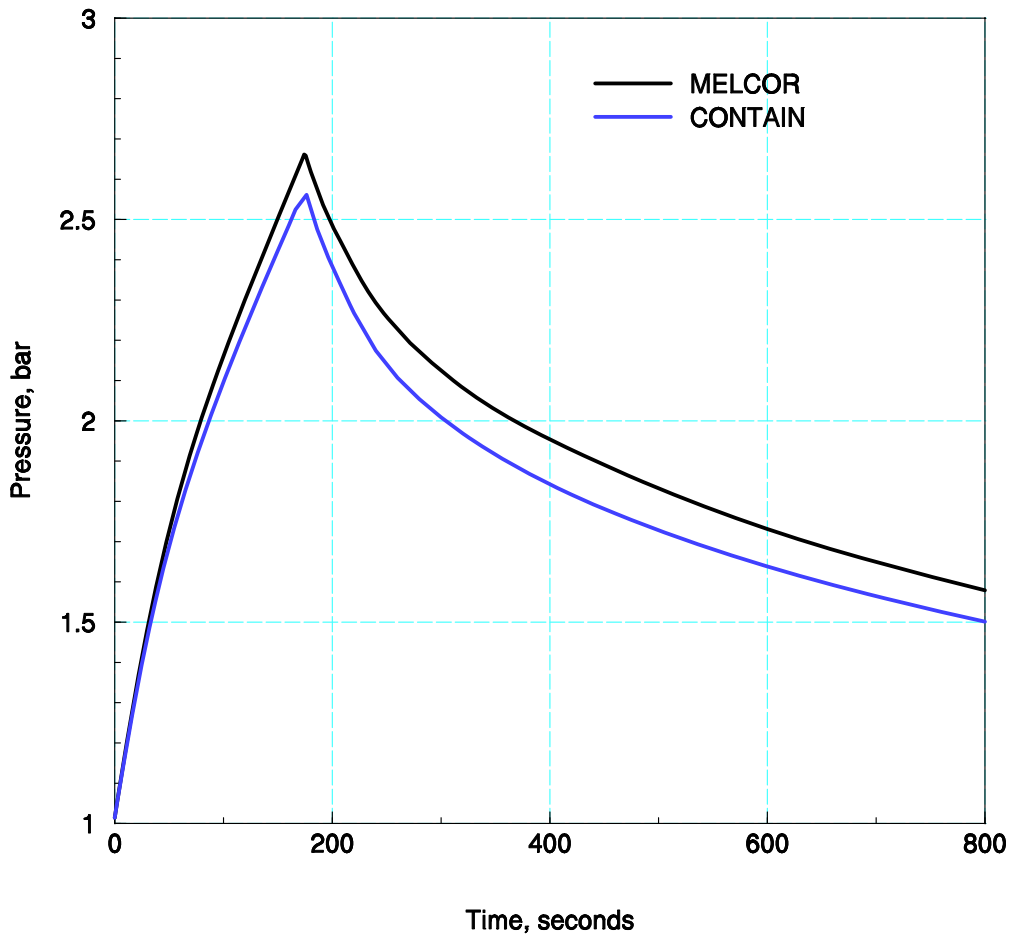

Figure 4-44 Comparison of MELCOR and CONTAIN pressure calculations for CVTR Test 4.

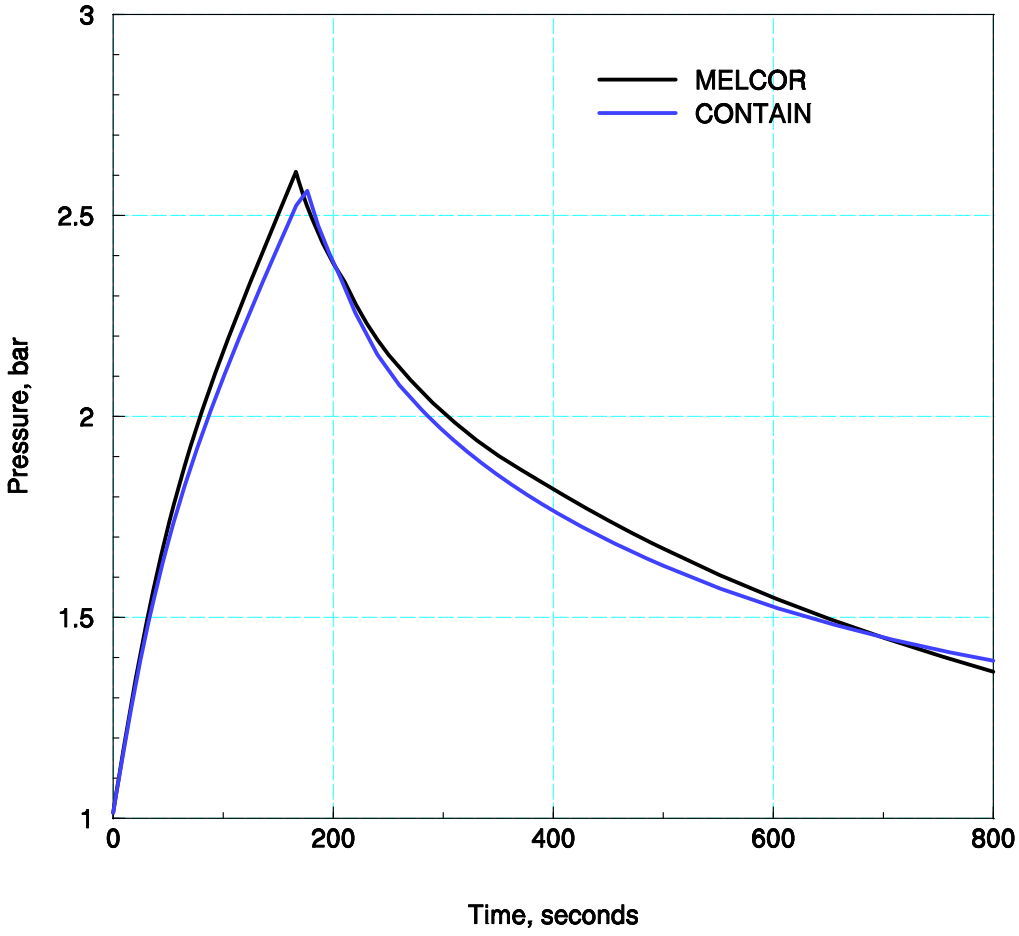

Figure 4-45 Comparison of MELCOR and CONTAIN pressure calculations for CVTR Test 5.

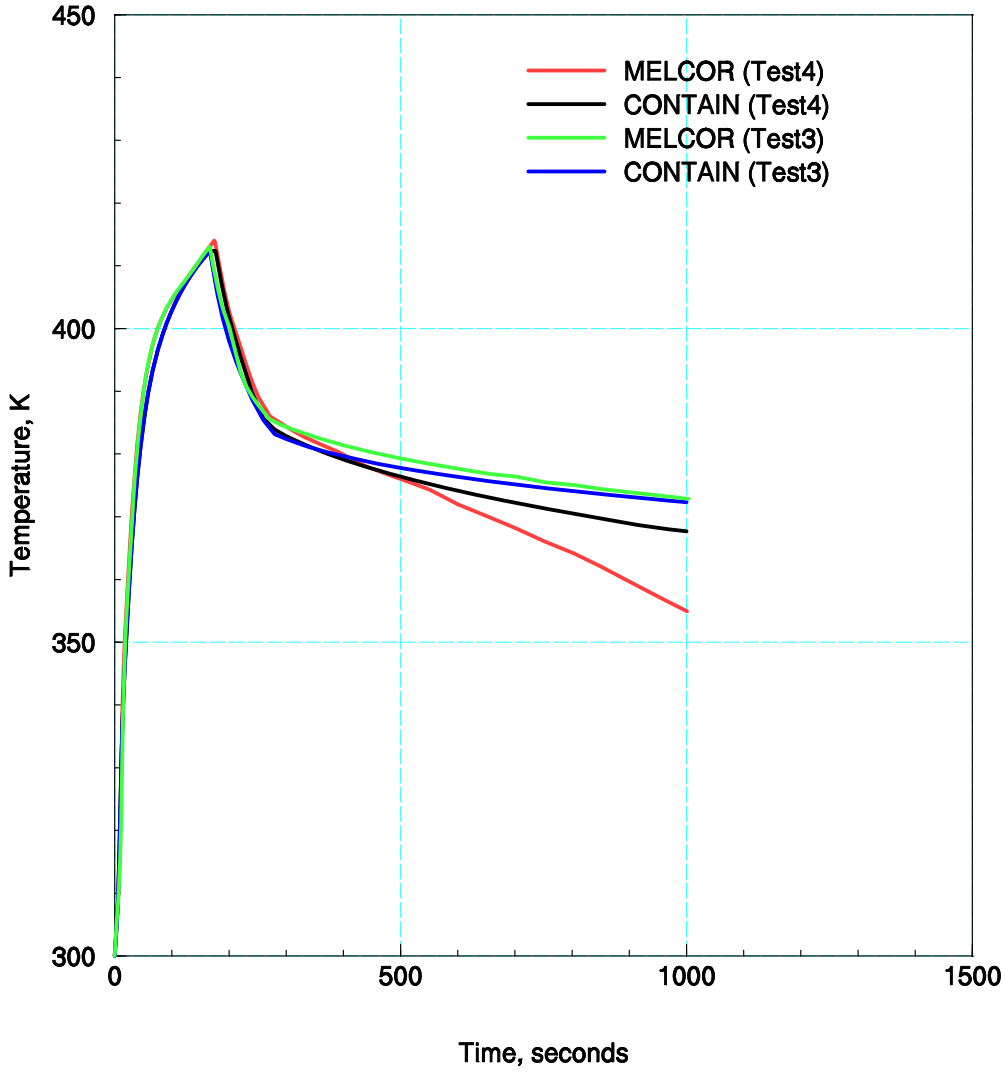

Figure 4-46 Comparison of MELCOR and CONTAIN calculated dome gas temperature for CVTR Test 4.

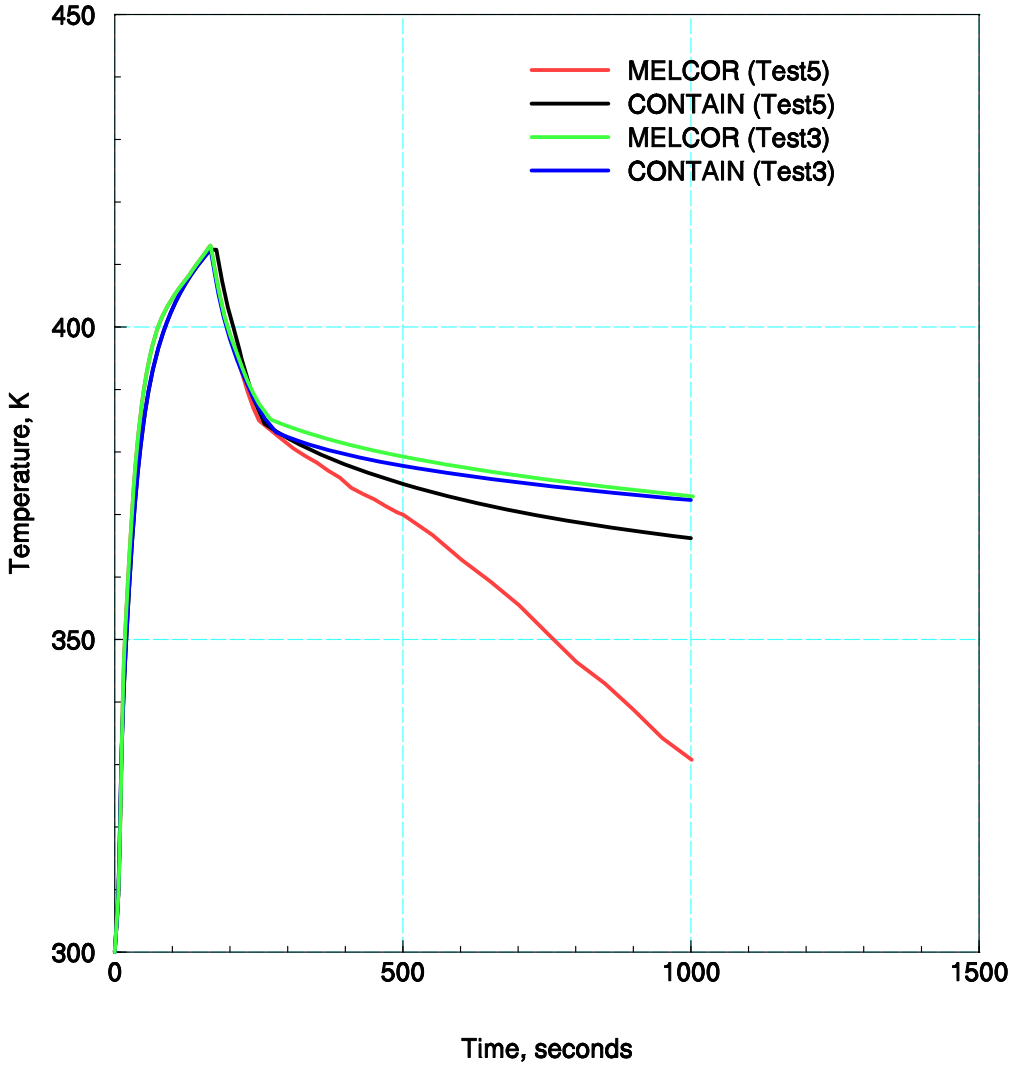

Figure 4-47 Comparison of MELCOR and CONTAIN calculated dome gas temperature for CVTR Test 5.

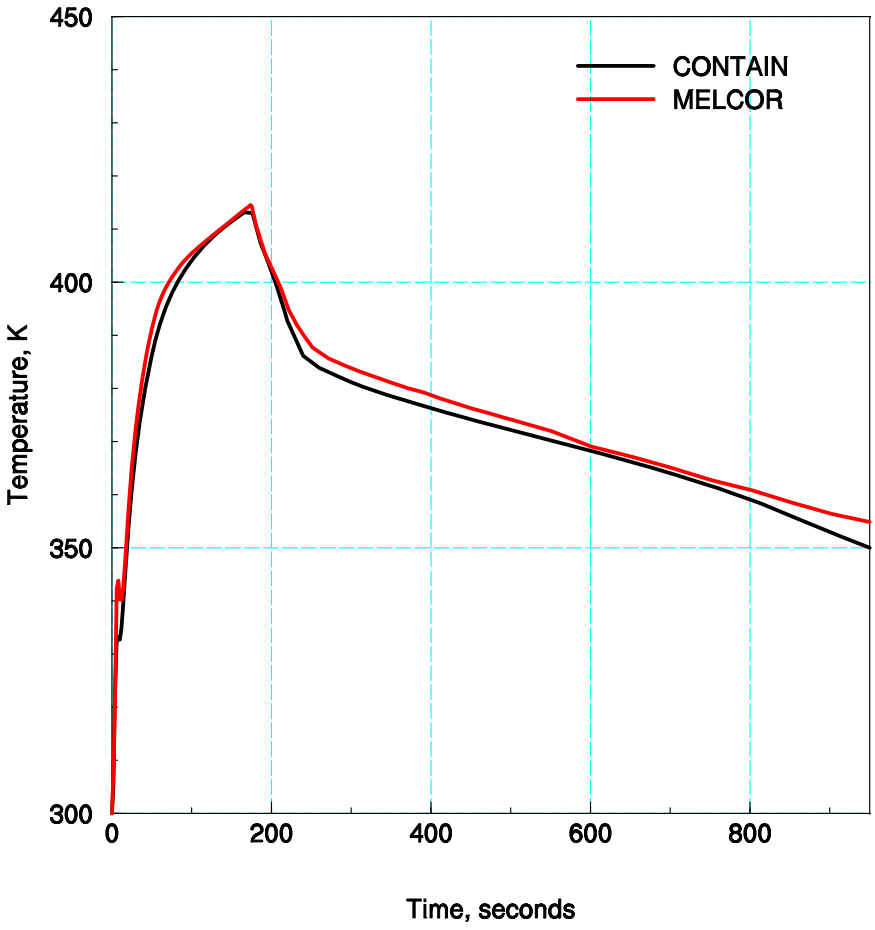

Figure 4-48 Comparison of MELCOR and CONTAIN average gas temperatures in operating region below spray nozzles (elevation 20.45 meters) for CVTR Test 4.

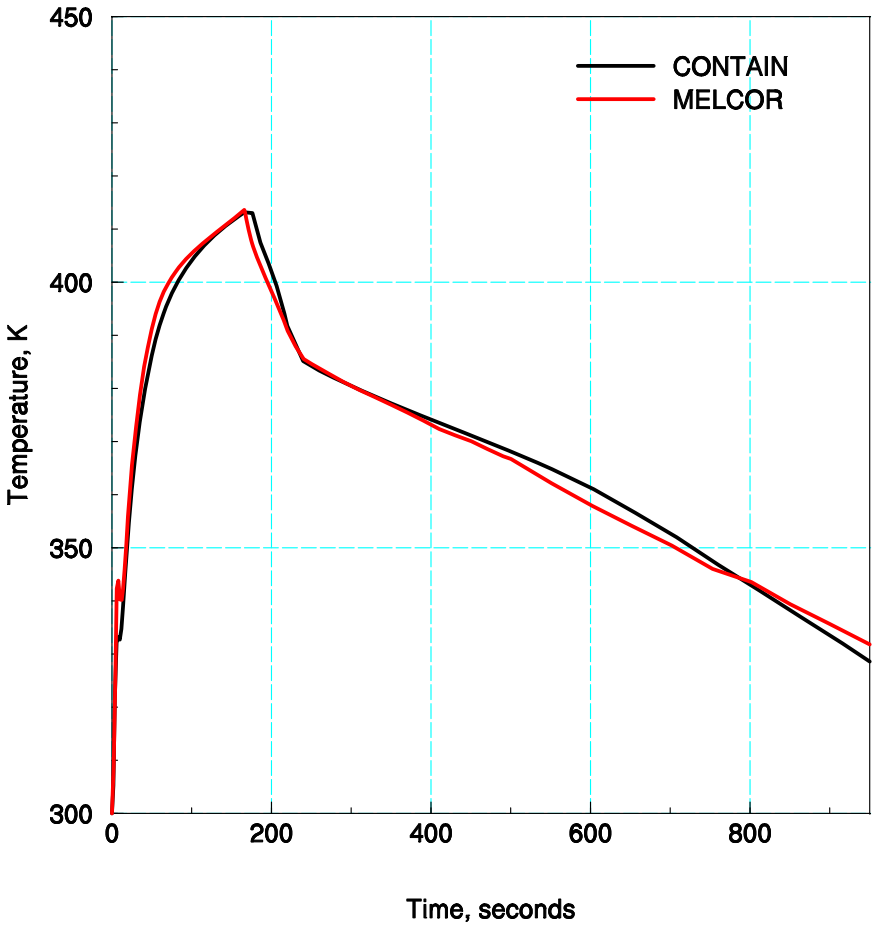

Figure 4-49 Comparison of MELCOR and CONTAIN average gas temperatures in operating region below spray nozzles (elevation 20.45 meters) for CVTR Test 5.

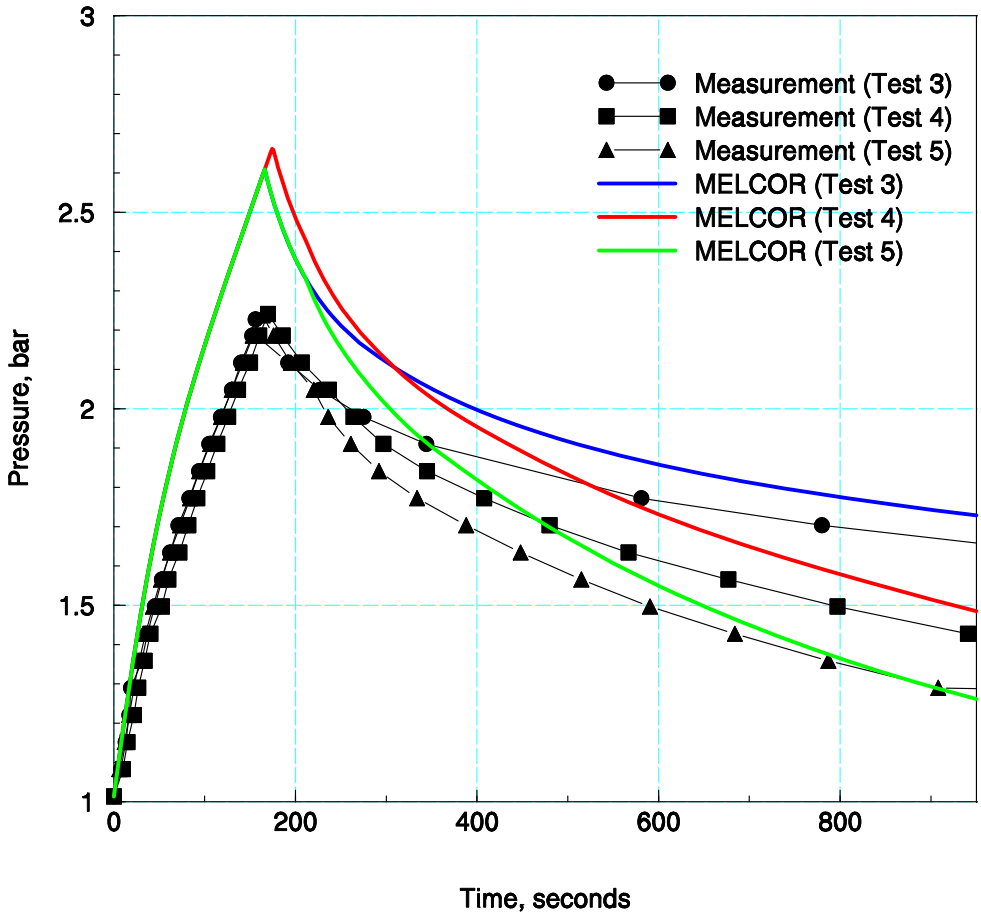

Figure 4-50 Comparison of measured and MELCOR calculated pressures for CVTR tests.

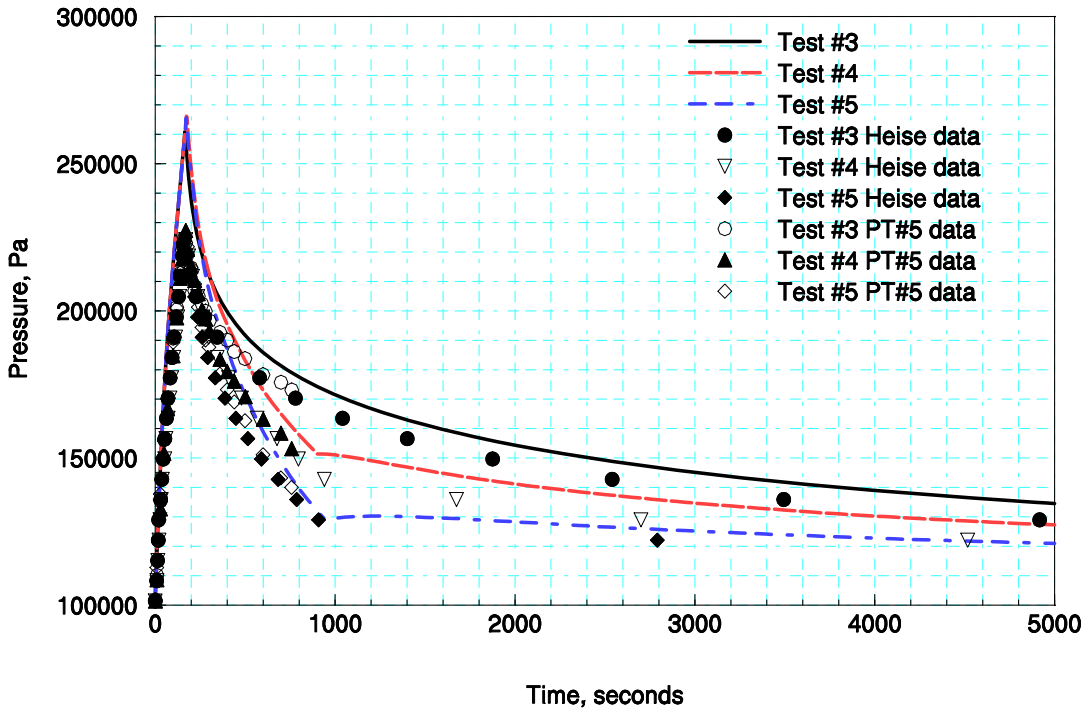

Figure 4-51 Comparison of measured and MELCOR calculated pressures for CVTR tests, showing the leveling of pressure when sprays are turned off.

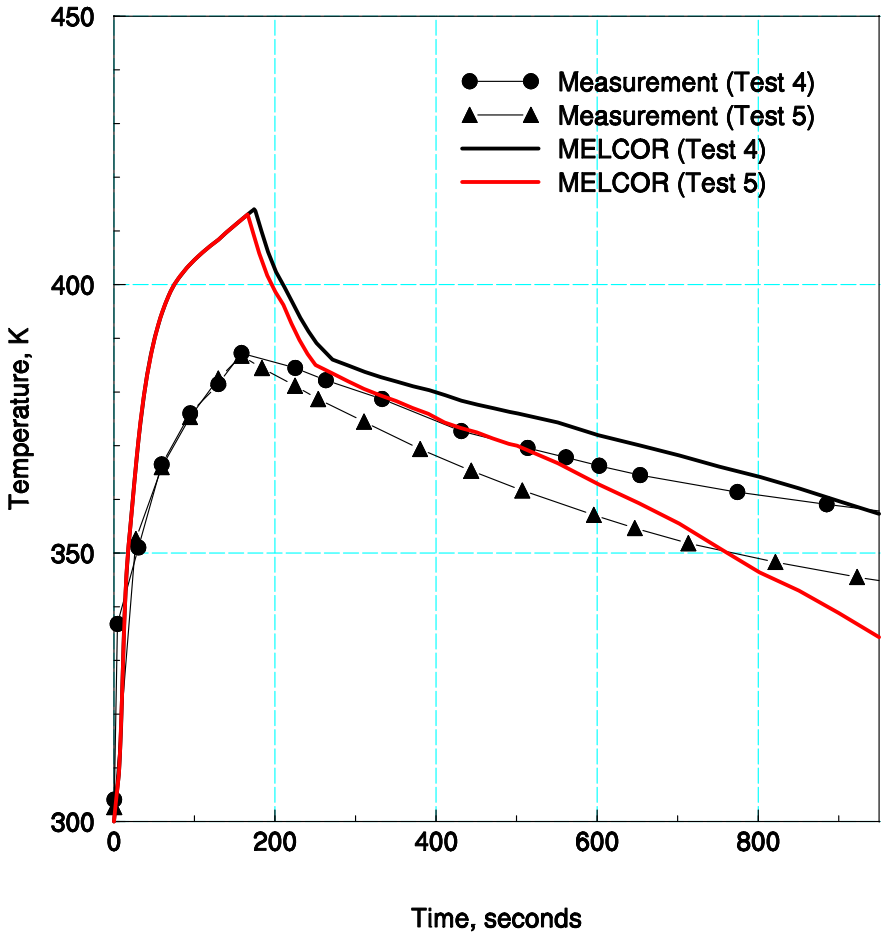

Figure 4-52 Comparison of measured and MELCOR calculated dome gas temperatures for CVTR spray tests.

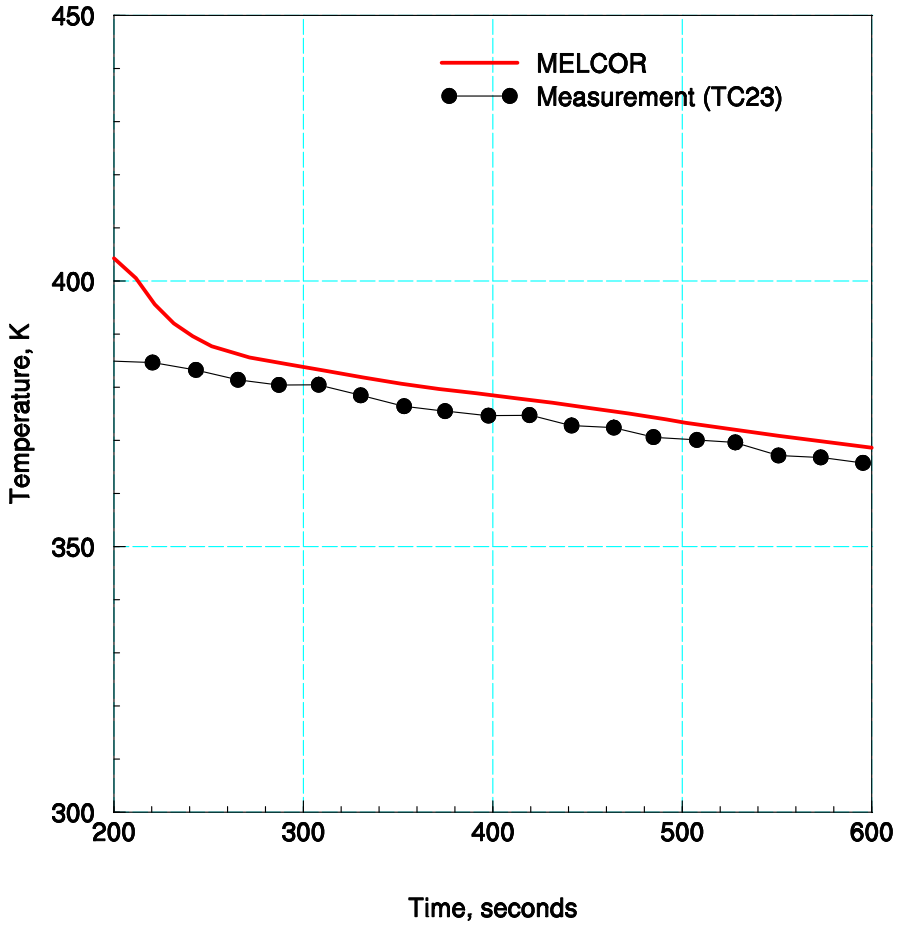

Figure 4-53 Comparison of measured and MELCOR calculated gas temperatures in operating region below the spray nozzles (average of calculated temperature in cells #11 and #13) for CVTR Test 4.

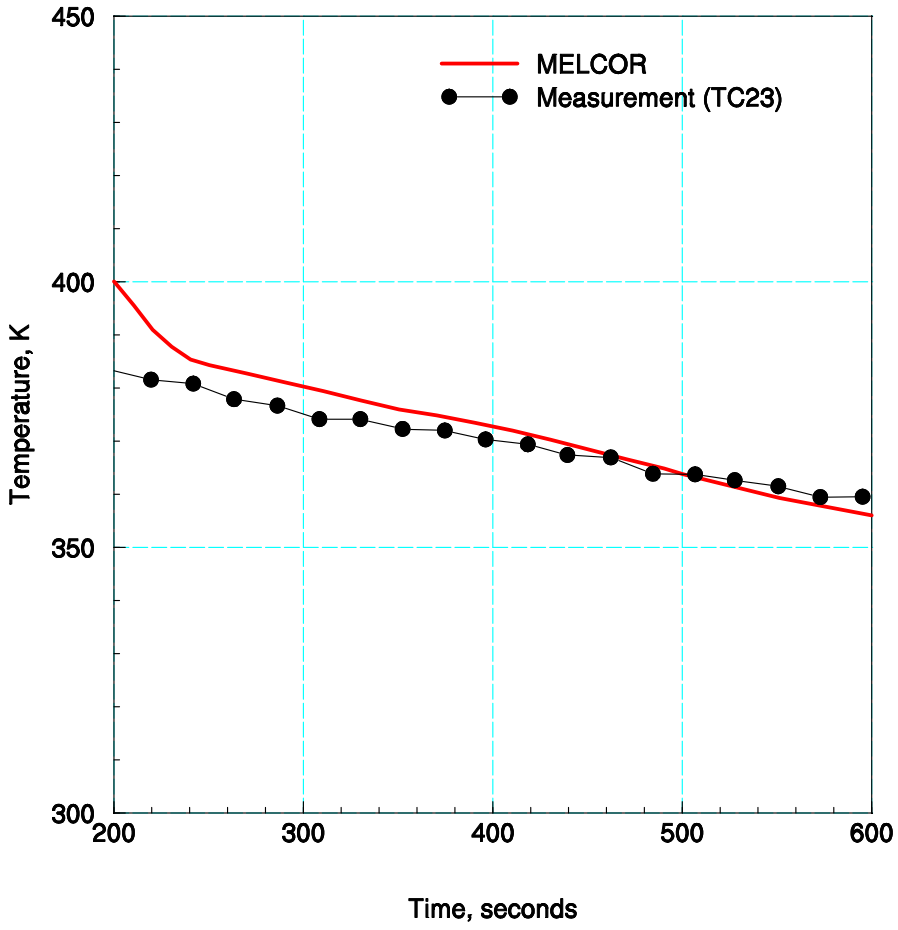

Figure 4-54 Comparison of measured and MELCOR calculated gas temperatures in operating region below the spray nozzles (average of calculated temperature in cells #11 and #13) for CVTR Test 5.

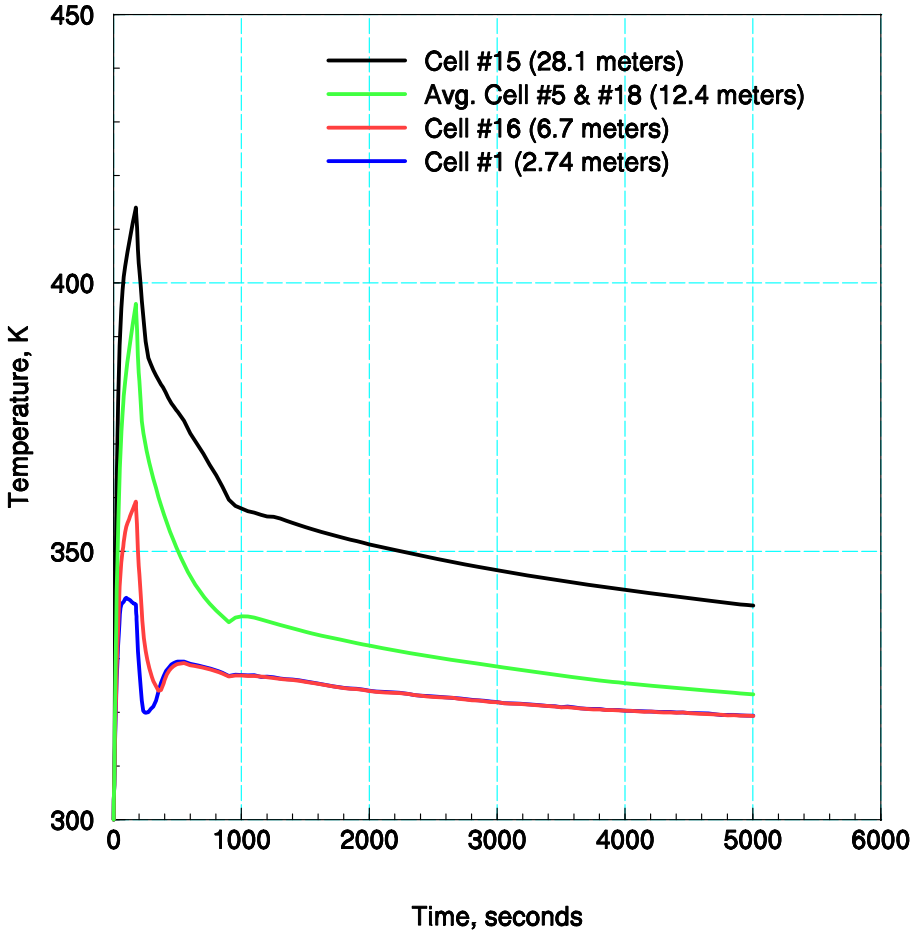

Figure 4-55 MELCOR calculated vertical gas temperature profile for CVTR Test 4.

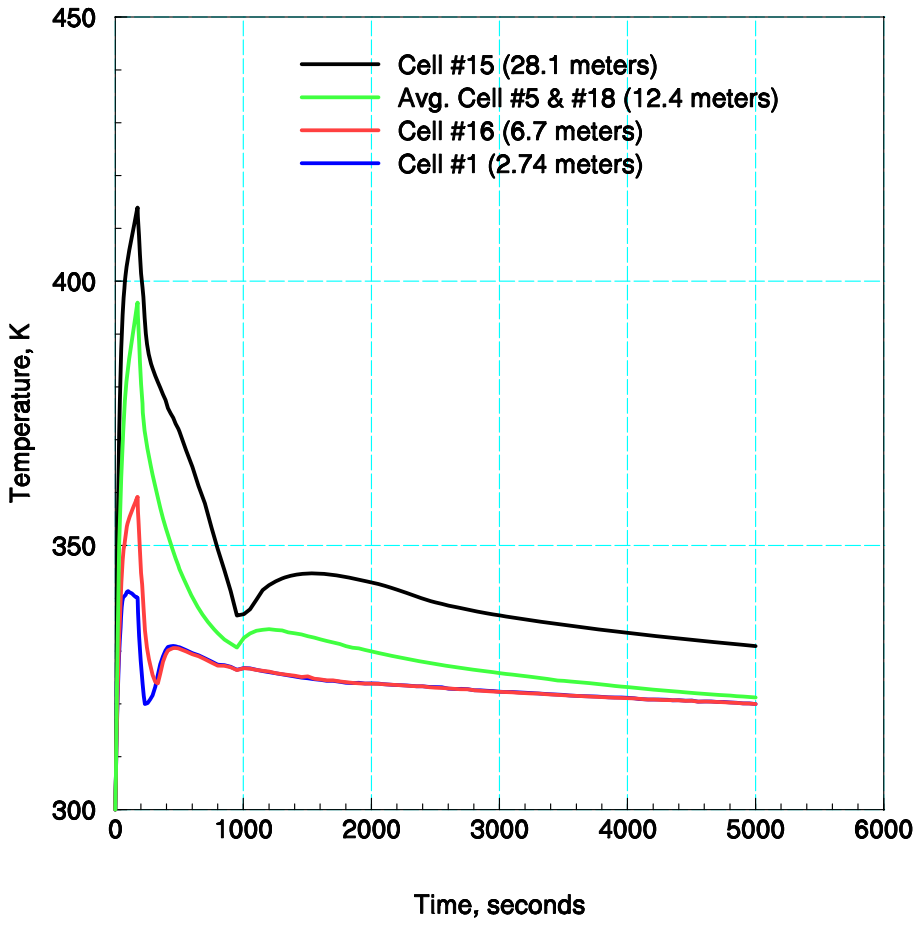

Figure 4-56 MELCOR calculated vertical gas temperature profile for CVTR Test 5.

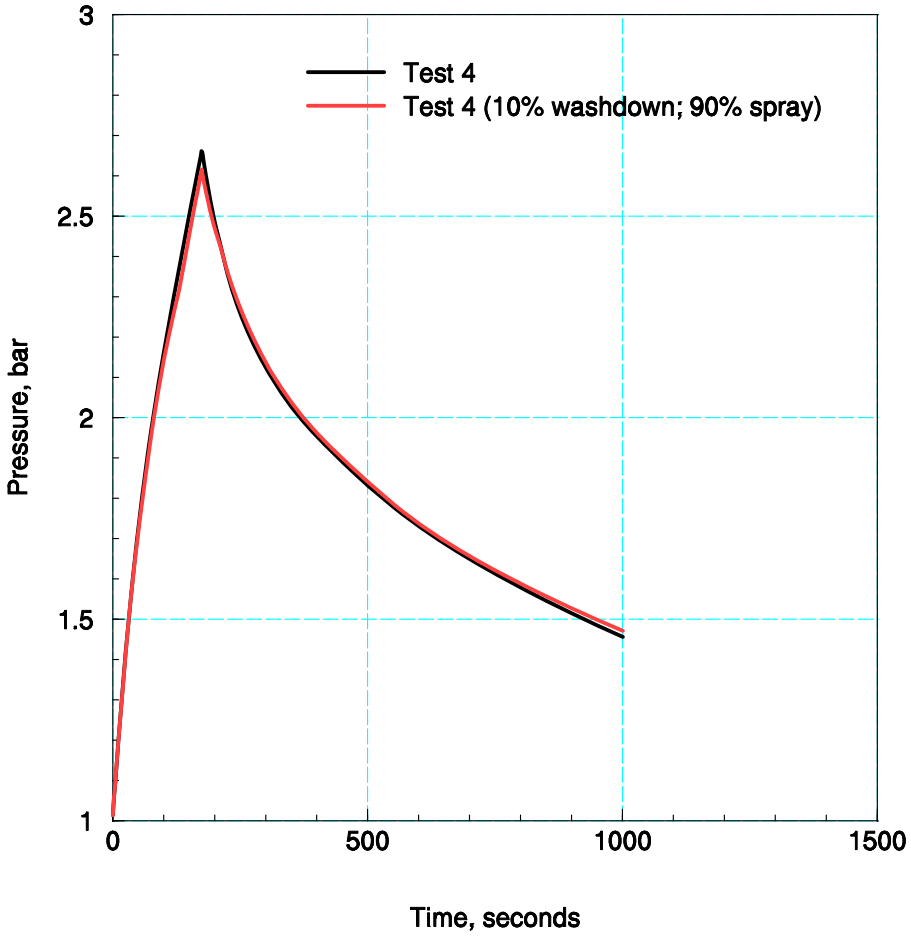

Figure 4-57 Comparison of MELCOR calculated pressures for CVTR Test 4 with and without (reference case) spray washdown of the containment wall in the operating region.

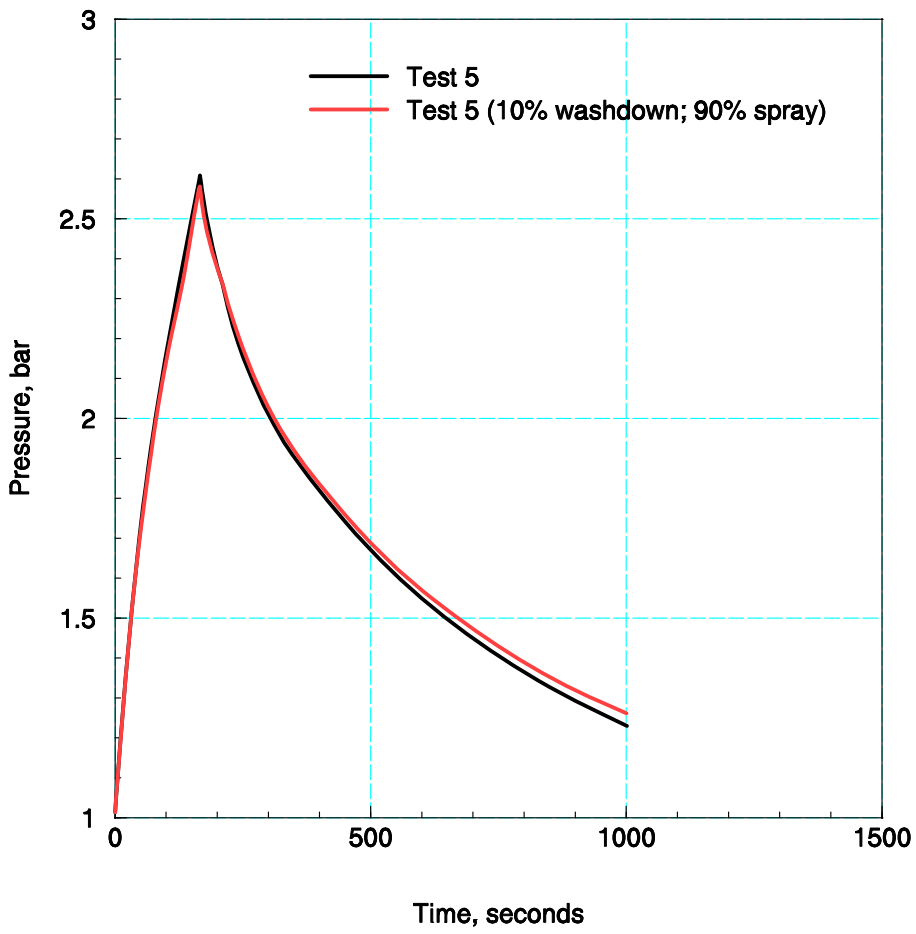

Figure 4-58 Comparison of MELCOR calculated pressures for CVTR Test 5 with and without (reference case) spray washdown of the containment wall in the operating region.

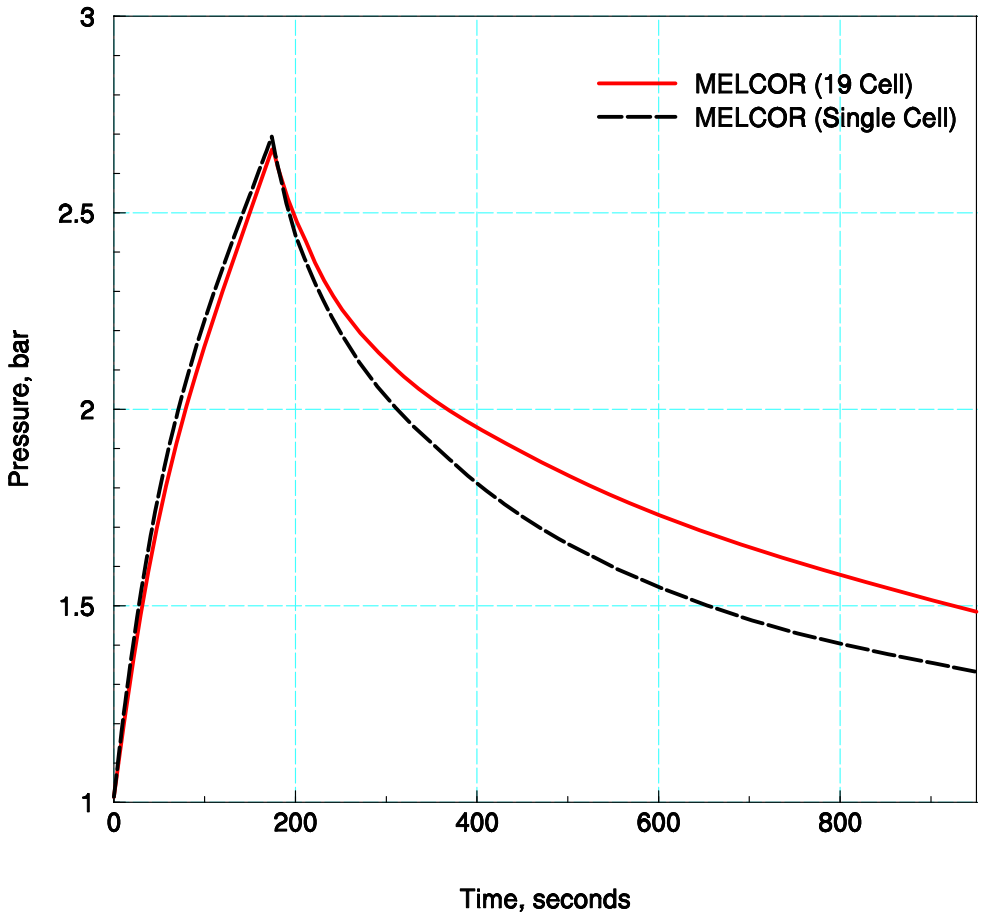

Figure 4-59 Pressure comparison between MELCOR single and multi-cell models for Test 4. (Sprays are activated at 210 seconds.)

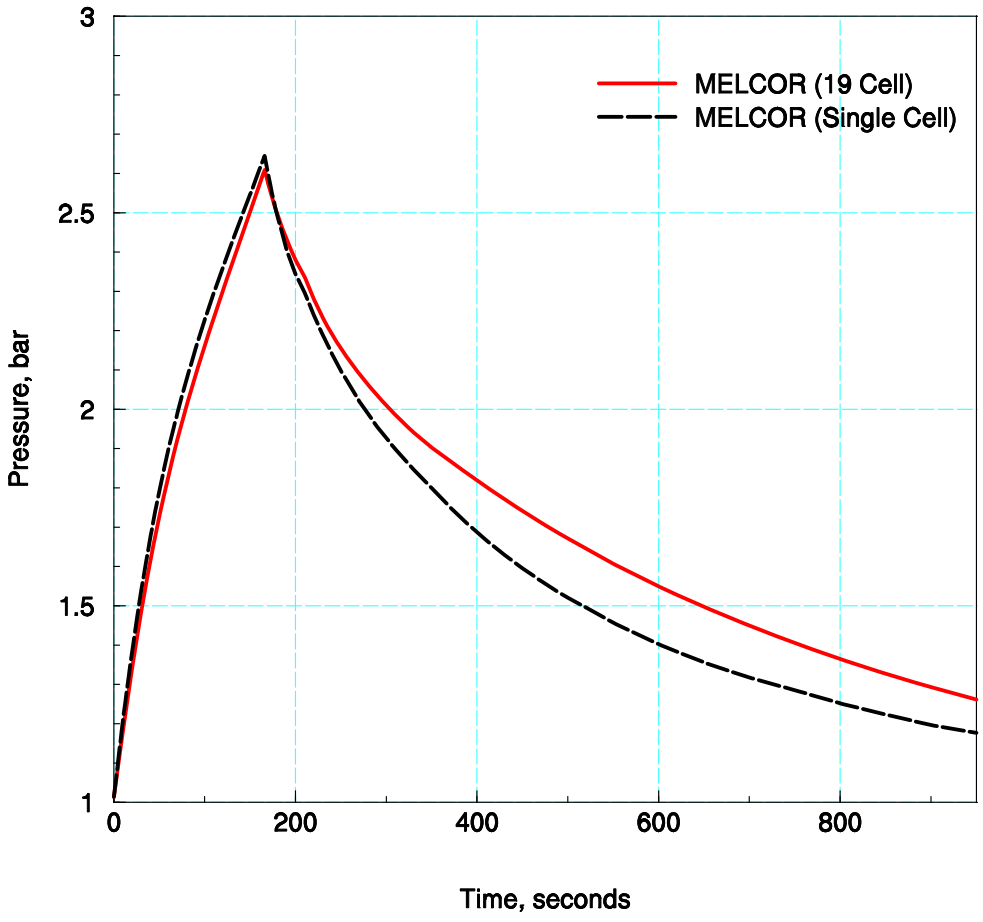

Figure 4-60 Pressure comparison between MELCOR single and multi-cell models for Test 5. (Sprays are activated at 210 seconds.)

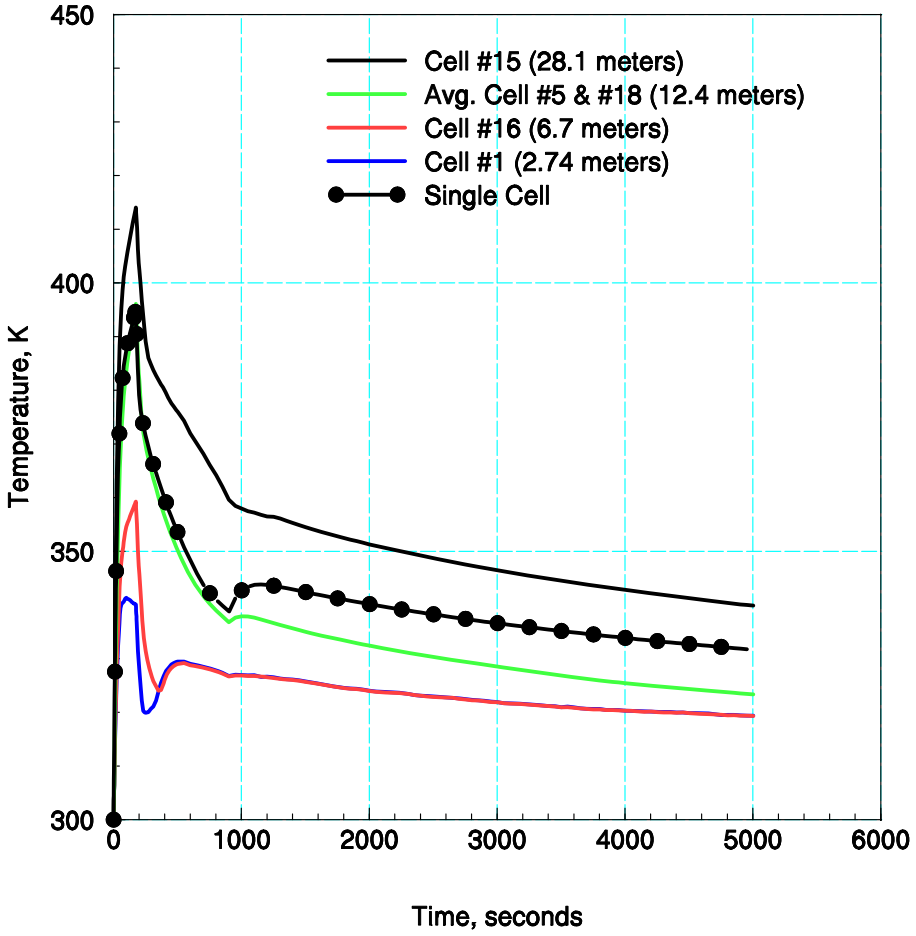

Figure 4-61 Long-term gas temperature comparisons between MELCOR single and multi-cell models for Test 4. (Sprays are activated at 210 seconds and deactivated at 900 seconds.)

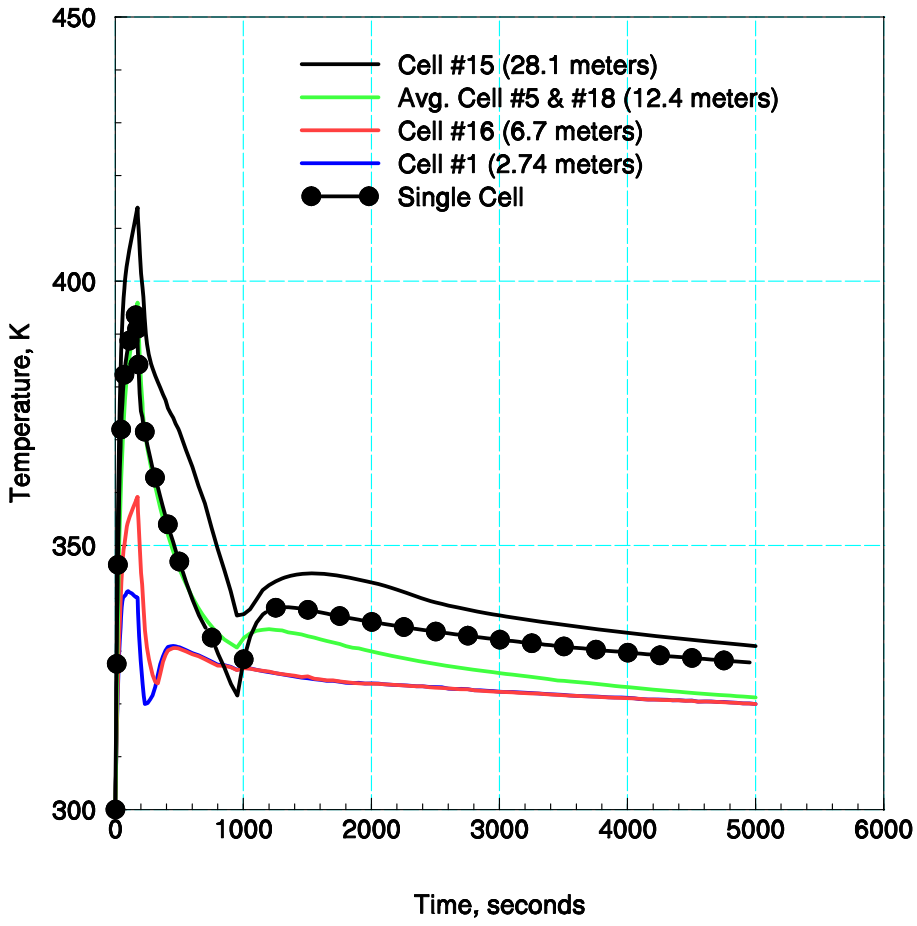

Figure 4-62 Long-term gas temperature comparisons between MELCOR single and multi-cell models for Test 5. (Sprays are activated at 210 seconds and deactivated at 952 seconds.)

5 Summary of Findings and Conclusions

In order to assess the adequacy of containment thermal-hydraulic modeling incorporated in the MELCOR code, a large scale containment test facility was analyzed. The CVTR experiments provided test data replicating a design basis simulation of a postulated main steam-line break inside a large dry PWR containment. A series of single cell and multi-cell calculations were performed to demonstrate the effect of code, user, and experimental uncertainties on predicted gas pressure and temperatures. The result of this effort is a conclusion that the MELCOR code is capable of providing reasonable predictions and is comparable to the CONTAIN code in this area. This study has also demonstrated the complexity associated with building an analytical simulation model of a containment experiment or postulated accident, with implicit demands on the user knowledge base. A few modeling short-comings were identified, but these either involved low ranked phenomena (e.g., condensate film flow), or were of a nature that conservative results were obtained (e.g., forced convection condensation).

5.1 Phenomena

Two of the more important phenomena investigated in the test series were condensation/ evaporation heat transfer and steam/gas transport. The MELCOR HMTA method used for atmosphere-to-structure energy transport has been found to be an accurate modeling approach for predicting trends and absolute rates of energy transfers, as demonstrated in the SETs and the CVTR assessments. Pressure suppression by internal water spraying as modeled by the MELCOR code shows that spray effectiveness is reliably calculated in both a single and multi-cell application. An auxiliary result of all these assessment efforts has been a compilation of user guidelines and remarks concerning the implications of the assessment to full-scale plant analysis.

5.2 Single Cell Calculations

It was shown that CVTR calculations made with the single cell model using the default option for the HMTA modeling (i.e., natural convective condensation) results in an over-prediction of maximum pressures during the blowdown period when steam continues to be injected into the facility. Within the bounds of calculation uncertainty, both in terms of facility and test specifications, the over predictions ranged from 0.3 to 0.7 bars (i.e., 24 to 50% gauge pressure error). As noted earlier, the amount of heat sinks (steel) and source rates were distorted for the CVTR facility free volume in such a way that atmospheric-to-structure energy transfer processes during a typical main steam line blowdown event are over emphasized. Therefore, the tendency of the code to over predict pressure (an indicator of atmospheric energy content) will be reduced somewhat for plant analyses. Additionally, there is a clear indication of compensating errors that are apparent when using the single cell model, where too little energy is extracted in the blowdown region (above the operating floor) and too much extracted in lower region of the facility, at a distance from the blowdown source. The cause of these compensating errors is mainly from a smearing of the steam distribution (air/steam mass ratio) throughout the facility as a result of using a single cell model. Because the CVTR facility and typical plant containments (PWR large dry) have similar free volume/heat sink distributions (~65–80% in the operating region), we can expect the CVTR facility and plant analyses to be predicted with similar energy transfer trends. The caution for users is that findings made in these code assessments with the

CVTR facility may not transfer directly to containment configurations substantially different or to scenarios where the location of the injection source is significantly skewed from that investigated here.

With respect to temperature predictions using the single cell model, all calculations (reference and sensitivity calculations) indicated superheating during the blowdown; whereas, the measurements appeared to be representative of an atmosphere that was saturated. Consequently, the gas temperature, even though "averaged," was calculated to be above the maximum temperature measured in the containment. The maximum saturation temperature calculated on the other hand was in much better agreement with the maximum temperature measured in the operating region, and could not be considered a conservative estimate of the maximum temperature measured in the facility.

During the depressurization period after the steam injection was terminated, the single cell model predicted a rate of pressure reduction that was higher than measured initially, but after a short period reproduced the slow depressurization trend measured. When compared to the local measured temperatures, the "average" calculated gas temperature was significantly over predicted below the operating floor, both during the blowdown and depressurization periods. However, above the operating floor, and after the blowdown, the gas temperatures was under predicted; and therefore, in this region and period, the single model is non-conservative.

For the code-to-code benchmark exercise, it was shown that during the blowdown period both the MELCOR and CONTAIN single cell calculations essentially agree for pressurization. A small difference in the gas temperature superheating was noted during the blowdown, but the saturation temperatures were predicted with similar magnitudes and trends. During the depressurization, the MELCOR code predicted a slightly faster rate of pressure decline that was attributed to differences in the amount of retained condensate on structures calculated between the codes. The difference in late time pressure and temperature calculations however was not considered significant. As a result it was determined that both codes produced similar pressure and temperature profiles for the CVTR test performed without spray activation.

5.3 Multi-Cell Calculations

The limitations of a single cell model for predicting local/regional atmospheric responses (air/steam mass ratios and gas temperatures) are obvious for conditions where large stratifications are anticipated. What is not so obvious is that a failure to predict stratification (single cell model) can still provide global or pressure trends with reasonable accuracy and maintain a conservative estimate of maximum pressure. All these features of the single cell model were demonstrated for the CVTR blowdown test. However, it was also shown that the single cell model significantly under predicted energy transfer in the operating region during the blowdown (via comparison of calculated and measured heat transfer coefficients on the containment wall), and consequently over predicted energy transfers in the lower containment. The CVTR multi-cell calculations showed that very good predictions of temperature stratifications (with the elevated injection) are obtained with both the MELCOR and CONTAIN codes. However, even with improvements in the calculated stratification, there still remained indicators of under prediction of energy transfers in the near region of the steam injection. In

this case, the under prediction points to a neglect of the forced convective condensation over a portion of the containment steel structures (containment wall and components) where the steam jet/plume contacted the structure surfaces. This hypothesis was confirmed through parametric forced convective condensation modeling in specific regions of interaction (heat plug #1 and #2 locations) based on visual (photo) observation, and supported by air current measurements made during the CVTR testing. The parametric analysis with forced convective modeling was incorporated into the CVTR multi-cell model and the resulting sensitivity calculation indicated improvement in local temperature predictions (i.e., superheating eliminated) and marginal improvement for the pressure prediction. The marginal improvement for pressure appeared to be due to the limited region where forced convection was implemented. For example, under prediction of energy transfer (by comparing measured to calculated structure surface temperatures) in the basement region indicated that turbulence enhanced energy transfer may extend to regions at some distance from the injection location.

The MELCOR multi-cell model was also used to simulate the CVTR atmosphere response to spray activation following termination of the steam injection. CVTR Tests 4 and 5, with increasing spray flow rates, were calculated for the entire test period (~1 hour). For each test, the measured pressure reduction trends were predicted with the code. These trends included the time when sprays were activated, and subsequently after the sprays were turned off. Significantly, the temperature measurements that showed a trend toward convergence of the containment vertical temperature profile with increasing spray flow rates were also predicted with the MELCOR code. Comparisons of pressure reductions calculated with MELCOR and CONTAIN (identical multi-cell model) showed good agreement, especially for Test 5, conducted at a higher spray flow rate.

In summary, the MELCOR simulation model is aided significantly by the modeling methodology in the code and the ability to include nodalizations that represent the actual geometric configuration of the containment. Most important in this regard is the demonstration that meaningful predictions of temperature stratification can be calculated for design basis MSLB postulated events. Consequently, the physically-based modeling method that is the foundation of the MELCOR code (e.g., the HMTA modeling method) allows for meaningful variation of physically identifiable parametric inputs (e.g., flow velocity along structure surfaces). The parametric application of the code can be an aid in evaluation of margins of safety or conservatism. In terms of the enhancement effects—that is, those that increase maximum containment loads—the default options were always found to result in the more conservative estimates, especially for maximum pressure.

Overall, the calculations performed for the CVTR tests (and SETs analyses) confirmed that the HMTA method of modeling heat and mass transfer for atmosphere-to-structure and atmosphere-to-spray droplets is a validated method for the conditions expected in containment atmospheres. This finding was made possible in part by rich user access to physically based parameter choices that are available in the code through input options.

5.4 User Guidelines and Implications for Plant Analyses

The reference calculations are presented as baseline examples to introduce discussions on modeling, while providing a reference for subsequent discussions involving sensitivity calculations. In most instances, the reference calculations are established using modeling choices that would typically be applied in containment analysis. From the perspective of a prototypical PWR large dry containment analysis, the distortion of geometric and source scaling in the tests generally support the viewpoint that MELCOR is a reliably conservative computational tool for predicting containment transient responses when applied by knowledgeable users. Many of the input models in the MELCOR code can be omitted when the accident analysis is limited to design basis type scenarios which are driven by containment thermal-hydraulics. Code input default options, with minor exceptions, were found appropriate for predicting the variety of heat and mass transfer conditions expected in domestic plant designs during postulated accidents. One of the more useful aids to new users of a code are a set of input decks that transition from the simple to the more complex simulations that represent actual plant containments along with postulated accident scenarios. For this reason, and for archival purposes, the input decks for all reference calculations (SETs and CVTR tests) are included as an appendix to this report. These decks may be consulted to acquire insights in determining the models and input that may be considered for performing plant containment analyses.

In general, containments should be analyzed using a multi-cell representation of the free volume when local versus global features are an important factor (such as for equipment qualification). Maximum pressure predictions, however, can often be calculated conservatively using a single cell representation of the containment; although, it was noted in this report that depressurization (i.e., the pressure relaxation period after the blowdown phase) may not be predicted conservatively with such a restrictive geometric model. The degree of non-conservatism observed for a single-cell model however may be reduced in cases where there is spray activation, since the sprays tend to reduce stratification. Note that the blowdown turbulence to the containment structures/components are usually not modeled since this additional complexity can only be addressed by parametric input (e.g., flow velocity specification).

Multi-cell models do not necessarily mean a large number of cells. Most gas and liquid water transport effects of importance to design basis assessments can be modeled with 15 to 20 cells - 3 to 6 cells in the open region above the operation deck is acceptable in most cases. The nodalization scheme used in the CVTR reference calculation is a good example of how a plant nodalization may be constructed. Open cylindrical regions (above operating floor) are typically modeled with stacked cylindrical volumes surrounded by an equivalently segmented annular volume. The horizontal flow areas (perpendicular to the vertical axis) between the cylinder and annulus segments are conveniently set to equal values, and segment lengths are input with similar dimension. Flows in open regions are relatively insensitive to loss coefficients due to the large flow areas generally modeled. Therefore, when loss coefficients are not provided, the form loss coefficients are set to 1.0 and frictional losses are effectively zeroed by inputting small segment lengths.

With respect to the HMTA input, specifically sensitivity coefficient [4110], the leading multiplier on the natural convective equation for Nusselt number (array location #1) should be changed from 0.1 to 0.14 to provide heat and mass transfer results that are consistent with the database for containment applications as demonstrated through various SETs analyses. Conservatism for most DBA containment type applications is typically addressed either by removing structures from the analysis or more often by a realization that the calculations for maximum loads neglect enhanced energy transfer from turbulence resulting from steam jet/plume interactions with surrounding structures (i.e., forced convective condensation).

Because the MELCOR code applies film tracking as the default option, care should be taken with regard to the specification of the axial length of rectangular structures, since the width of structure is the area divided by length. Special attention should be directed toward the accuracy of the amount of steel mass input to the calculation since peak containment loads during a DBA blowdown are sensitive to rapid energy transfers that occur between the atmosphere and steel structures (this includes concrete wall liner).

Note, for calculations where condensate drain-off from structures goes to an initially dry sump, the minimum (estimated) volume fraction of the pool below which equilibrium thermodynamics will be enforced is reduced by input from the default setting (1.0E-6) to 1.0E-10. The setting for this limit condition is via sensitivity coefficient 4411(5). Failure to satisfy the limit, that is, failure to have pool fractions above the set limit can, especially under superheated conditions, force evaporation of drain-off water and result in an artificial reduction for superheat. Therefore for plant analysis, the lower value is recommended.

It is recommended that sprays can be modeled with the default spray droplet size of 0.001 meter, unless the actual spray droplet average size or distribution is provided. The lack of observed superheating for DBA events when spray activation occurs after a blowdown period precludes a need to use smaller droplet sizes that reduce a tendency toward superheating. However, sensitivity calculations with smaller droplets size are warranted if significant superheating is predicted during the period of spray activation.

Sensitivity calculations should always be performed to complement reference or baseline code calculations. To gain insights for the most important areas for sensitivity calculations consult a PIRT-type study for the plant and scenario and/or perform a detailed energy partitioning study to determine the controlling parameters for energy transfers (e.g., structure types and locations) during the time periods of interest. Sensitivities may involve varying the amount of structure area or thickness within the uncertainty of the known specifications. Stratification may be affected by restricting flow path areas, and conservatisms resulting from neglect of forced flow turbulence may be assessed by including input for control volume velocities. For special concerns regarding phenomenological modeling adequacy, consult the database for separate effects test analyses for the dominant phenomenon under consideration. Finally, be cautious in extending specific conclusions regarding code adequacy from integral experiments to general plant applications where geometric scale and scenario variations are significant.

INTENTIONALLY BLANK

6 References

And98 Anderson, M. H., Herranz, L. E., and Corradini, M. L., "Experimental Analysis of Heat Transfer within the AP600 Containment Under Postulated Accident Conditions," Nuclear Engineering and Design, Vol. 185, pp. 153-172, 1998.

Car81 Carbajo, J. J., "Heat Transfer Coefficients Under LOCA Conditions in Containment Buildings," Nuclear Engineering Design, Vol 65, pp. 369-386, 1981.

Gau05a Gauntt, R. O., et al., "MELCOR Computer Code Manuals – Vol.1: Primer and User's Guide, Version 1.8.6 September 2005," NUREG/CR-6119, Vol. 1, Rev. 3, SAND 2005-5713, Sandia National Laboratories, Albuquerque, New Mexico, September 2005.

Gau05b Gauntt, R. O., et al., "MELCOR Computer Code Manuals – Vol.2: Reference Manuals, Version 1.8.6 September 2005," NUREG/CR-6119, Vol. 2, Rev. 3, SAND 2005-5713, Sandia National Laboratories, Albuquerque, New Mexico, September 2005.

Har79 Hargroves, D. W., et al., "CONTEMP-LT/028 – A Computer Program for Predicting Containment Pressure—Temperature Response to a Loss-of-Coolant Accident," NUREG/CR-0255, TREE-1279, R4, Idaho National Engineering Laboratory, Idaho Falls, Idaho, March 1979.

Her98 Herranz, L. E., Anderson, M. H., and Corradini, M. L., "A Diffusion Layer Model for Steam Condensation with the AP600 Containment," Nuclear Engineering and Design, Vol. 183, pp. 131-150, 1998.

Kar89 Karwat, H., "ISP23: Rupture of a Large-Diameter Pipe within the HDR-Containment," Vol. 1 and 2, CSNI Report No. 160, Committee on the Safety of Nuclear Installations – OECD Nuclear energy Agency, Paris, France, 1989.

Kar92 Karwat, H., "OECD-CSNI-ISP29, Distribution of Hydrogen within the HDR-Containment under Severe Accident Conditions – Final Comparison Report," Organization for Economic Cooperation and Development – Committee on the Safety of Nuclear Installations, August 1992.

Kat92 Kataoka, Y., et al., "Experiments on Convection Heat Transfer Along a Vertical Flat Plate Between Pools with Different Temperatures," Nuclear Technology, Vol. 99, pp. 386-396, September 1992.

Mur97 Murata, K.K., et al., "Code Manual for CONTAIN 2.0: A Computer Code for Nuclear Reactor Containment Analysis," NUREG/CR-6533, SAND97-1735, Sandia National Laboratories, Albuquerque, NM, December 1997.

Pet96 Peterson, P. F., "Theoretical Basis for the Uchida Correlation for Condensation in Reactor Containments," Nuclear Engineering and Design, Vol. 162, pp. 301-306, 1996.

Phe94 "Phebus PF FPT0 Preliminary Report, Part C – Degradation Phase," Phebus Report No. IP/94/211, Institut de Protection et de Surete Nucleaire, CEA, France, May 1994.

Sch70 Schmitt, R.C., Bingham, G.E., and Norberg, J.A., "Simulated Design Basis Accident Tests of the Carolinas Virginia Tube Reactor Containment - Final Report," IN-1403, UC-80, Idaho Nuclear Corporation, National Reactor Testing Station, Idaho Falls, Idaho, December 1970.

Sie81 Siegel, R. and Howell, J. R., Thermal Radiation Heat Transfer, 2nd Edition, McGraw-Hill Co., Inc., New York, NY, 1981.

Til02a Tills, J., Notafrancesco, A., and Murata, K., "An Assessment of CONTAIN 2.0: A Focus on Containment Thermal Hydraulics (Including Hydrogen Distributions)," SMSAB-02-02, July 2002, USNRC, Office of Nuclear Regulatory Research (ADAMS Accession Number ML022140438).

Til02b Tills, J., Notafrancesco, A., and Murata, K., "CONTAIN Code Qualification Report/User Guide for Auditing Design Basis PWR Calculations," SMSAB-02-03, August 2002, USNRC, Office of Nuclear Regulatory Research (ADAMS Accession Number ML022490381).

Til96 Tills, J., Griffth, R. O., Murata, K. K., and Stamps, D. W., "User Guidance on the CONTAIN Code for Advanced Light Water Reactors," SAND96-0947, Sandia National Laboratories, Albuquerque, New Mexico, April 1996. (Proprietary)

Wil96 Wilson, G.E. and Boyack, B.E., "The Role of the PIRT Process in Identifying Code Improvements and Executing Code Development," OECD Meeting, Annapolis, Maryland, November 5-8, 1996.

Appendix A. Containment Phenomena Identification

A-1 Introduction

The purpose of this appendix is to identify and describe various containment phenomena important for design basis accident (DBA) analysis, specifically during time periods dominated by high energy steam injections and/or pressure suppression with water sprays. Processes and phenomena described are general; that is, they apply to a variety of containment types (PWR, BWR, and ALWR). However, the relative importance of passive, pressure suppression features such as suppression pools and ice condensers are not treated here. Therefore, the phenomena listed in Table A-1 are more appropriately associated with PWR large dry containments, and so are useful for focusing on analysis of blowdown tests such as the CVTR containment tests, which closely replicates a design basis simulation of a postulated "intermediate" size MSLB. It is noted that the containment phenomena identification process proceeds without reference to codes or modeling capability, drawing on physical interpretation of processes that are judged to occur following the onset of postulated reactor accidents. Judgment, however, benefits from the review of calculations applied to separate (Appendices B through E) and integral tests (CVTR), and therefore calculations are not totally discounted in the identification process, especially when ranking of phenomena is a focus of the process. To provide a structure to the identification of important phenomena, phenomena are grouped by containment component and process – phenomena is discussed within this framework.

A-2 Components

A component is a generalized type of geometry and composition that encompasses a broad grouping of phenomena. A component is distinguished by a volume with a general type of physical composition and its boundaries (surfaces) across which the exchange of mass and energy occurs between volumes. The general composition classes within the containment are gases, liquids, and solids. Energy and mass exchanges may take place within a volume (as a source or sink or as exchanges between the constituents within a volume, e, (e.g., spray droplets), or at the surfaces between volumes.

There are three key components in a PWR dry containment: atmosphere, structure, and pool. All containment codes have models to represent these basic components, and most experimental and validation efforts investigate phenomena associated with these components. Usually, describing an atmosphere refers to a region inside the containment building where the constituents are predominantly steam and noncondensible gases (air); although, two-phase mixtures of suspended liquid (droplets) and gases may also be considered. Structures represent the physical boundaries of the atmosphere and affect the state of the atmosphere (e.g., temperature and pressure) as a result of both heat and mass transfers that occur at the surface of the structures. Surface exchanges are in turn governed by heat transfer into the structures (i.e., conduction limited). Pools are composed of liquids (i.e., water) and two-phase mixtures of liquid and gases (e.g., bubbles). For DBA analysis in a PWR dry containment, the pool component is generally not considered an important component since the volume of the pool during the early DBA period (seconds to minutes) is minimal. As a result, the pool component is not treated in this appendix. A description, therefore, of the two important components for DBA analysis is as follows:

- Atmosphere. The open volume or free flow volume for gases. It excludes an existing pool of water or a pool of water that may form during an accident.
- Structure. A solid material that communicates with the containment atmosphere through a surface. It may be an exterior wall, floor, or ceiling that forms the containment system boundary, an interior wall that divides the containment into subcompartments or otherwise forms a barrier to the flow of gases, or a structure that consumes interior space, such as pipes or other fixtures (equipment).

Communication between these components is through their surfaces. The surface of interest in this report is the interface between the containment atmosphere and structure. Surfaces include the boundary layers of air and water vapor that condenses on the solid structures, through which heat and mass transfer occur.

Note that the reactor coolant system (RCS) is not a component in a containment but typically forms a boundary condition for the containment code (e.g., CONTAIN, CONTEMPT, GOTHIC). However, in the case of the MELCOR code, the RCS may be included as a separate component where RCS phenomena are also modeled, and therefore provides a more unified treatment of DBA analysis. Such benefits of the MELCOR code are not covered here since the emphasis in this report is on the CVTR test program where steam injection is specified as a boundary condition for the containment.

A-3 Processes

Phenomena can be further classified by the main processes occurring within the containment. Five categories of processes are defined:

1. Pressurization/depressurization
2. Mixing
3. Transport
4. Heat transfer
5. Mass transfer

Pressurization is the process where the atmosphere pressure changes by means other than as a result of energy or mass exchange with structures. In this process the atmosphere boundaries are considered adiabatic. Rapid blowdowns into the containment are an example of a pressurization process (e.g., CVTR test for a postulated MSLB). Depressurization can occur during the expansion of gases when the containment boundary is breached. Such a condition may be the result of structural failure or a deliberate action referred to as containment venting. Additionally, depressurization can also take place as a result of some exchange taking place within the atmosphere, as in the case of energy and mass exchange with containment sprays.

Mixing is a process where separate fluids with distinguishable characteristics tend to come together to form a fluid with a single characteristic. Mixing is an intra-compartment process, whereas transport is an inter-compartment process. Mixing includes all phenomena that affect the mixing process occurring within a single open compartment or room. The characteristics can be temperature or constituent concentration. For example, when steam is injected into air, the incoming steam mixes and tends to proceed toward completion, with the final result being a

uniform steam/air mixture. In some cases the mixing process is incomplete for a substantial time period and during this time period the containment atmosphere is considered to be in an unmixed state. If mixing does not proceed to completion, but flow essentially stagnates, then a stratified condition is created. Mixing, in the region above the CVTR operating floor, proceeds fairly rapidly to completion during the blowdown. Therefore, this region trends towards a uniform mixture during the blowdown period.

Transport is a process where fluids move from one defined region to another (e.g., from the CVTR operating region to the lower containment). Transport usually refers to movement between compartments, such as convection loops that develop between a series of coupled compartments. Transport may occur between components within a compartment, for example, between structures and pools (condensate runoff). Transport may also occur for a single component, as in the case of the flow of condensate along a network of connected structures. The most commonly investigated processes within containment are those involving heat and mass transfer. These exchange processes take place both within and at the boundaries of components. For a solid component, the interior process is conduction. Sprays can exchange energy and mass with the atmosphere through evaporation or condensation or through sensible heat transfer; however, because sprays are considered part of the atmosphere, these exchanges are grouped under the pressurization-depressurization process. Condensation and evaporation also are important processes at the interface between the containment atmosphere and structures. Condensation and evaporation are categorized as a combination of mass and latent energy transfer processes. The exchange of energy without an accompanying exchange of mass, such as atmosphere to structure thermal radiation, is classified as a sensible energy transfer process. In most cases, these sensible energy transfers represent a small percentage of the total energy transfers that occur within containments during a DBA event.

A-4 Phenomena

In many physical processes, a number of phenomena can be involved. Therefore, dissection of a process, like mixing, will indicate an overlapping of various phenomena where boundaries are difficult to distinguish; however, each process can usually be identified, and in most situations observations of the process can reveal one or two phenomena that dominate. As previously noted, the phenomenon definition is a broad one that includes characteristics and events as well as phenomenological processes. Also, it should be realized that the chosen level of detail used in identifying phenomena associated with a process will often be a judgment based on our current ability to differentiate phenomena with the instrumentation commonly found in both integral- and separate-effects testing, and according to the details of the modeling. For example, the Dehbi, Kataoka, and Uchida condensation tests, referred to in Section 3 of this report, are separate-effects tests where natural or free convection condensation in the presence of air on a vertical surface is the phenomenon investigated. The details of the phenomena involve the diffusion of steam through an air/steam boundary layer adjacent to the vertical wall with flow or advection of condensate along the wall surface. Each phenomenon, diffusion through the boundary layer and conduction across the condensate film, is part of the general definition of free convective condensation. Assessment of the phenomenon is provided through a measure of total heat transfer into the wall, not the diffusion rate or conduction/advection associated with the condensate film.

Phenomena can be characterized by reference to safety equipment or a device if the phenomena are specific to that equipment and not otherwise described in a process group. For example, spray mass and energy exchange, and spray dynamics are phenomena specifically associated with an active safety system and are not considered in other basic phenomena descriptions. An example of cross-over of phenomena affecting more than one process would be spray dynamics causing a trending toward complete mixing, with a subsequent change in the bulk air/steam ratio that directly affects the heat and mass transfer process via steam diffusion through the boundary layer along a wall surface.

Table A-1 Important containment phenomena for design basis accident analysis during early rapid pressurization and de-pressurization periods (few minutes into event).

Component	Process	Phenomena
Atmosphere	Pressurization/de-pressurization	Multi-component gas compression/expansion Spray mass and energy exchange Atmospheric cooling by fan cooler*
	Mixing	Jet-plume gas interaction/entrainment (localized) Buoyancy/stratification (regional) Spray dynamics Fan dynamics
	Transport	Buoyancy Form and friction losses
Structure Interior	Heat transfer	1-D transient conduction
Structure Surface	Mass transfer	Free convection condensation/evaporation Forced convection condensation/evaporation

*Generally, not considered an important safety feature for pressure control during short-term blowdown periods, but may be more important for medium-term periods (i.e., post-blowdown); therefore, fan coolers are included here for completeness.

Appendix B. Dehbi Natural Convection Condensation Tests Analysis

Turbulent natural convection condensation in the presence of noncondensible gases is a fundamental process requiring accurate modeling in a containment analysis code. The Dehbi tests, while not complete in addressing all issues related to this process; do offer creditable data on saturated, steam/air natural convective condensation on vertical surfaces [1, 2]. Shown in Figure B-1 is the experimental configuration for the tests, showing the condensing vessel with a stagnant volume of steam/air in contact with a subcooled condensing tube. Dehbi measured local heat transfer rates to the tube due to condensation. The measured rates obtained for the small diameter cylinder were integral for average total heat transfer and corrected for tube curvature so that the reduced data could be applied as flat plate condensation data. Test results for the average heat transfer coefficient along the 3.5 meter condensing surface were fit according to the formula

$$\bar{h}_L = L^{\alpha}\left(\bar{T}_{\infty} - \bar{T}_w\right)^{\delta} F(X, p) \quad , \qquad \text{B.1}$$

where α and δ are determined experimentally, and F(X, p) is a function which depends on the air mass fraction, X and the pressure, p. Experimental data was obtained for pressures of 1.5, 3.0, and 4.5 atmospheres, wall subcooling ranging from 10 to 50 K, and air mass fractions ranging from 0.25 to 0.95. It was found that the data collapsed around a smooth curve with α = 0.05 and δ = -0.25. The function F(X, p) fits the data to air mass fraction at a specific pressure, as shown in Figure B-2. The Dehbi formula that correlates all data is given by

$$\bar{h}_L = \frac{L^{0.05}\left\{\left(3.7 + 28.7p\right) - \left(2438 + 458.3p\right)\log(X)\right\}}{\left(\bar{T}_{\infty} - \bar{T}_w\right)} \qquad \text{B.2}$$

The experimental uncertainty associated with the data is reported as ± 15%.

Shown in Figure B-3 is a comparison of the CONTAIN and MELCOR code calculations for the Dehbi test at a pressure of 1.5 atmosphere with a 30 K wall subcooling. The Dehbi correlation values are obtain using Equation B.2 for a range of air mass fractions with ± 15% uncertainty bars included. The CONTAIN results fall near the lower end of the -15% uncertainty bar. Shown also are results obtained for a CONTAIN standalone heat and mass transfer model computed within a MathCad worksheet. As indicated, results from both the code and worksheet are essentially identical. The worksheet model is important for investigating various nuances in condensation modeling, as will be discussed below.

Two MELCOR calculations are plotted in Figure B-3. The MELCOR (default) calculation is run with the default sensitivity coefficients for 1) the turbulent natural convection Nusselt number along a plate vertical plate, and 2) the heat transfer coefficient for the condensate film obtained

using the film tracking model. In the case of the Nusselt number correlation, both codes use a similar equation type[14],

$$Nu = ARa^{B} + C \qquad \text{B.3}$$

where

Nu = Nusselt number
Ra = Rayleigh number
A, B, C = sensitivity parameters

For the CONTAIN code the default parameters are set as follows,

A = 0.14
B = 1/3
C = 0.

The MELCOR defaults are identical, except that the leading coefficient A is set to 0.1. Our experience concerning the many discussions over the appropriate leading coefficient for Equation B.3 has revealed no shortage of opinions and no consensus. We note, for instance one of the older empirical correlations developed by McAdams has the coefficient set at 0.13. Appropriately, each code can be set through input to identical correlations depending on the whim of the user. Our choice however should be based on application and validation with the experiments conducted for conditions similar to the application. This importance of the Dehbi tests for containment analyses should be apparent in this regard.

The small difference that remains between the MELCOR (with CONTAIN sensitivity set) and the CONTAIN code results is due to varying methods used to define locations for property evaluation in the Grashof number used in the calculation of the Rayleigh number, $Ra = Gr\,\mathrm{Pr}$. Shown in Figure B-4 is a sketch of the heat and mass transfer process during condensation. In the CONTAIN code, the Grashof number is defined as

$$Gr = \frac{g\left|\rho_g - \rho_{if}\right| L^3}{\rho_{BL}\nu_{BL}^{\ 2}}, \qquad \text{B.4}$$

where the densities are appropriately evaluated in the bulk, diffusion boundary layer and at the interface between the gas and liquid film. Note that the kinematic viscosity, ν, is also evaluated in the diffusion boundary layer. In contrast to this method, the MELCOR code defines the Grashof number in the following manner,

[14] The evaluation of Nu is important for determining condensation rates since the Nusselt number is used in the heat and mass transfer analogy to determine the Sherwood number for mass transfers.

$$Gr = \frac{g\left|\rho_g - \rho_w\right| L^3 \rho_g^2}{\rho_{BL}\mu_{BL}^2} \qquad \text{B.5}$$

We note two differences in the defining equations. First, in MELCOR the density of the steam/air mixture at the condensing surface, (i.e., the film interface is evaluated not at the interface temperature but at the wall surface temperature). The density difference evaluated by MELCOR is technically incorrect but does not result in a significant error for the calculation of this test. The second difference is more important, involving the definition of the kinematic viscosity. In MELCOR, the viscosity is defined[15] as

$$\nu^* = \frac{\rho_g}{\mu_{BL}}. \qquad \text{B.6}$$

Splitting the evaluation of the denominator and numerator of the kinematic viscosity in this manner, where the density is evaluated in the bulk and viscosity in the boundary layer, appears unique to the MELCOR code. When MELCOR's Grashof number is defined in a manner similar to CONTAIN, the resulting calculation of the heat transfer coefficient is essentially identical to the CONTAIN code results, as shown in Figure B.3. In summary, the main difference between the MELCOR (CONTAIN sensitivity set) and CONTAIN code results is due to the differences in the evaluation of the kinematic viscosity. This difference can not be eliminated by input but can only be addressed through a code modification.

Shown in Figures B-5 and B-6 are comparisons of the CONTAIN and MELCOR results for the condensation tests at 3.0 and 4.5 atmospheres, respectively. In general, the codes produce similar results, except for the difference as noted above.

References

1) Dehbi B. B., et al, "The performance study of the tube water wall PCCL and an experimental correlation for steam condensation in the presence of air under natural convection," 2nd International Conference on Containment Design and Operation, Volume 2, Canadian Nuclear Society, Toronto, Canada, October 14-17, 1990.

2) Dehbi, B. B., et al, "A theoretical modeling of the effects of noncondensible gases on steam condensation under turbulent natural convection," AICE Symposium – Heat Transfer, Volume 87, Minneapolis, 1991.

[15] See source code listing in deck "hstn"

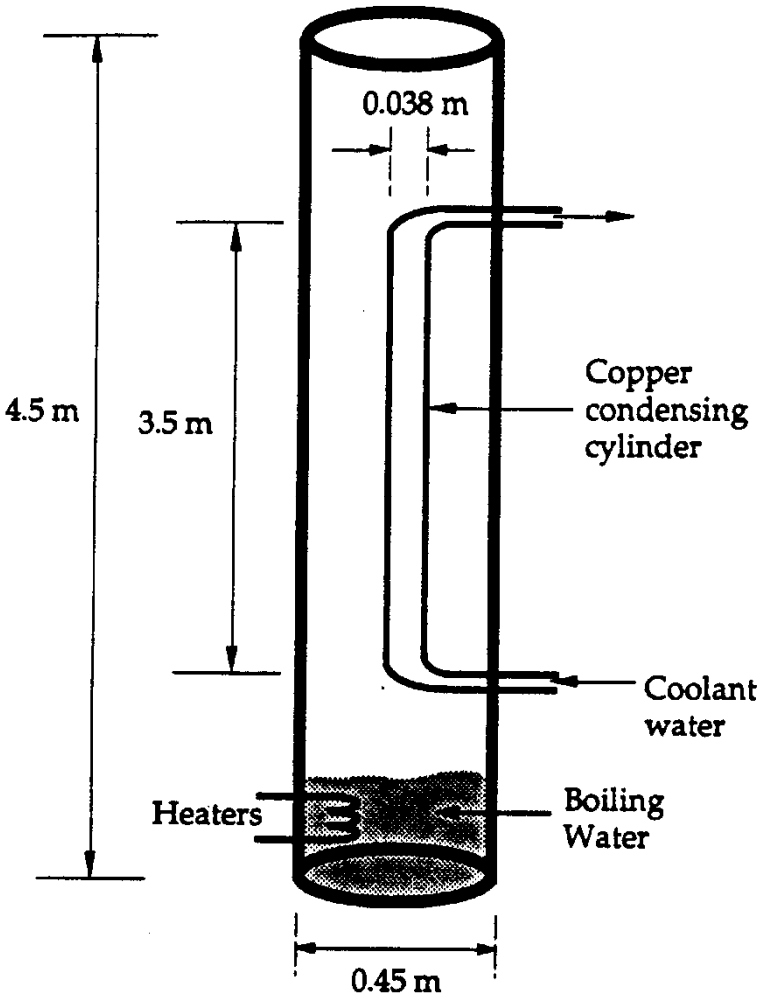

Figure B-1 Dehbi experimental facility [1].

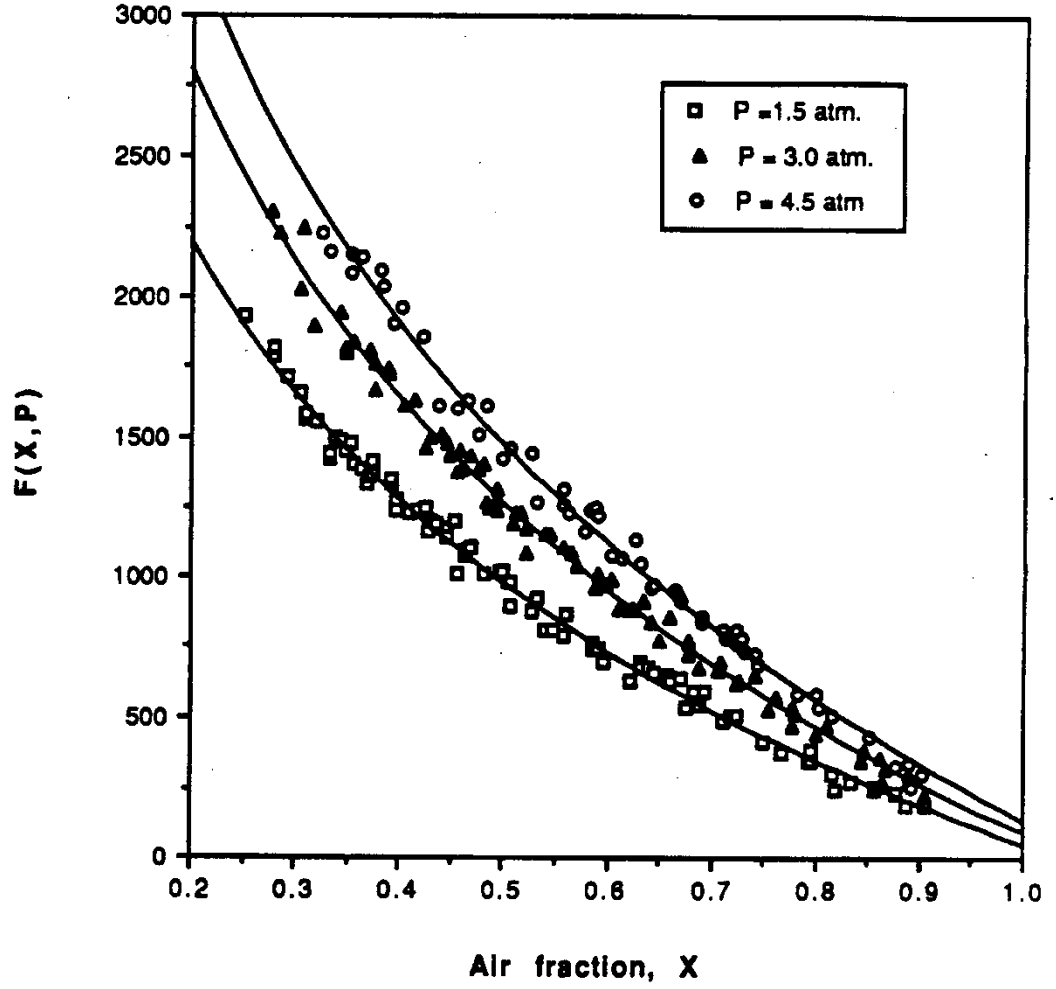

Figure B-2 Dehbi experimental correlation for natural convective condensation data [1].

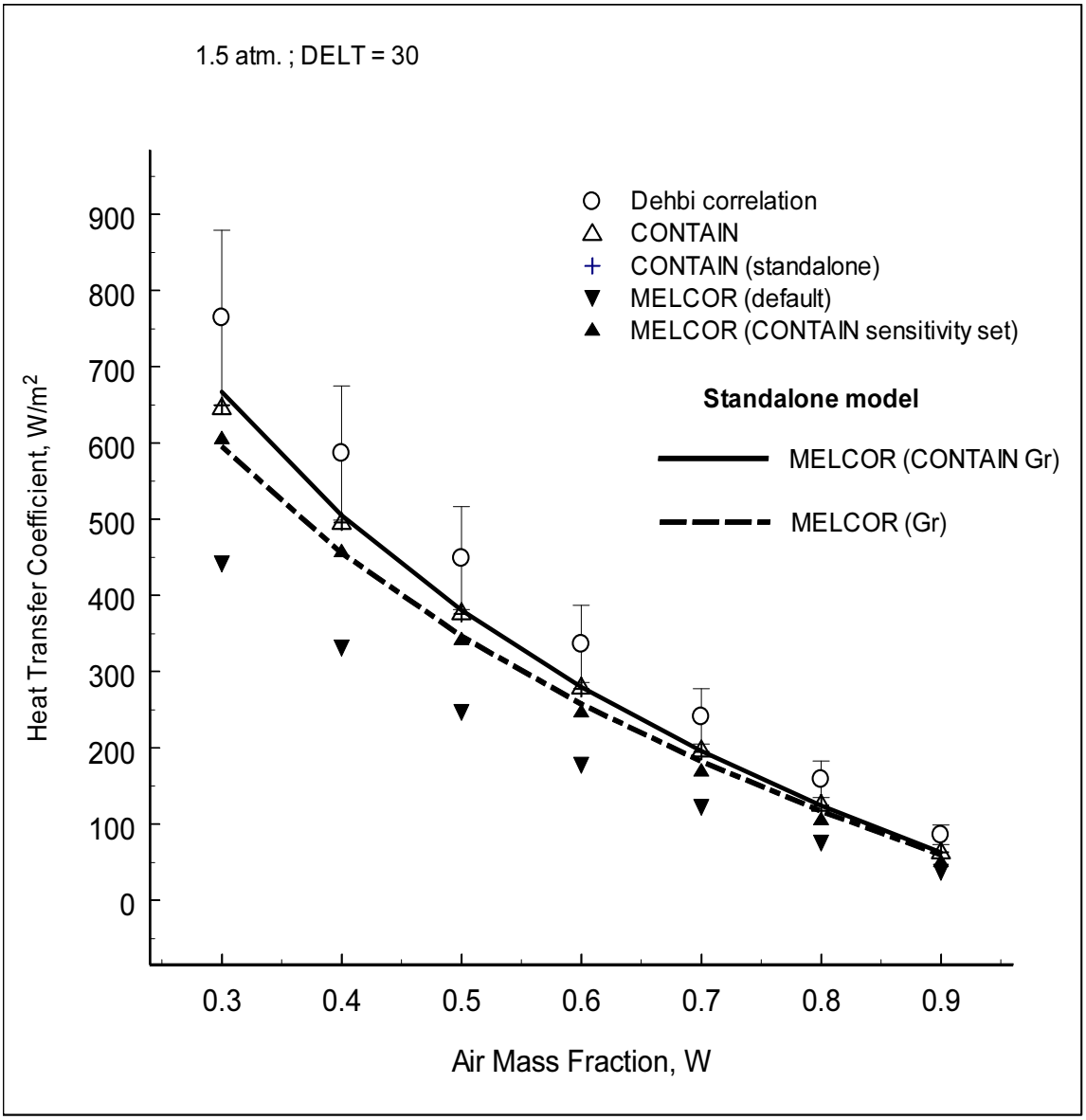

Figure B-3 Comparison of MELCOR and CONTAIN code calculations with Dehbi test results for natural convection condensation at a saturation pressure of 1.5 atmospheres.

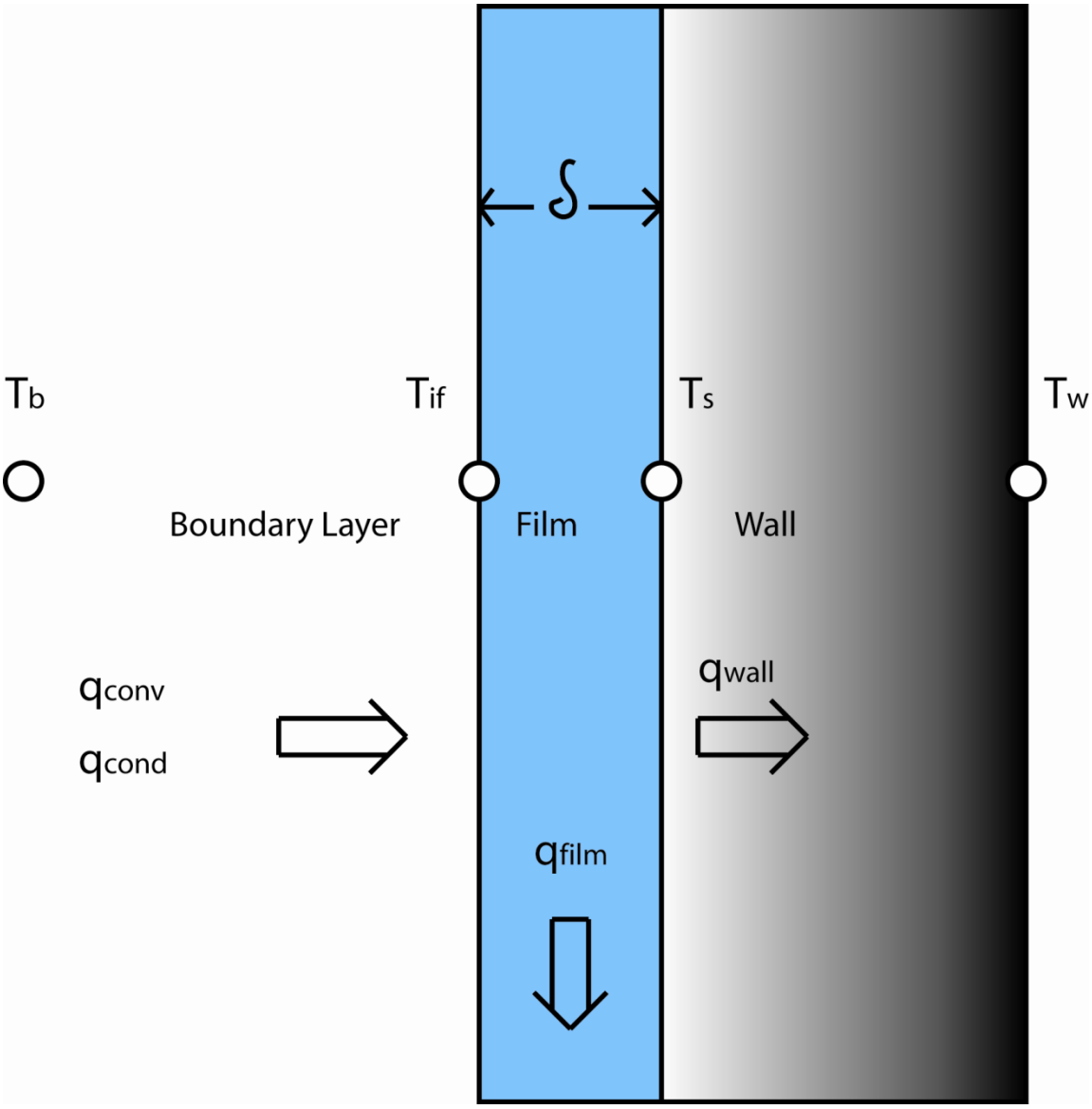

Figure B-4 Sketch of heat and mass transfer along a vertical wall showing nomenclature.

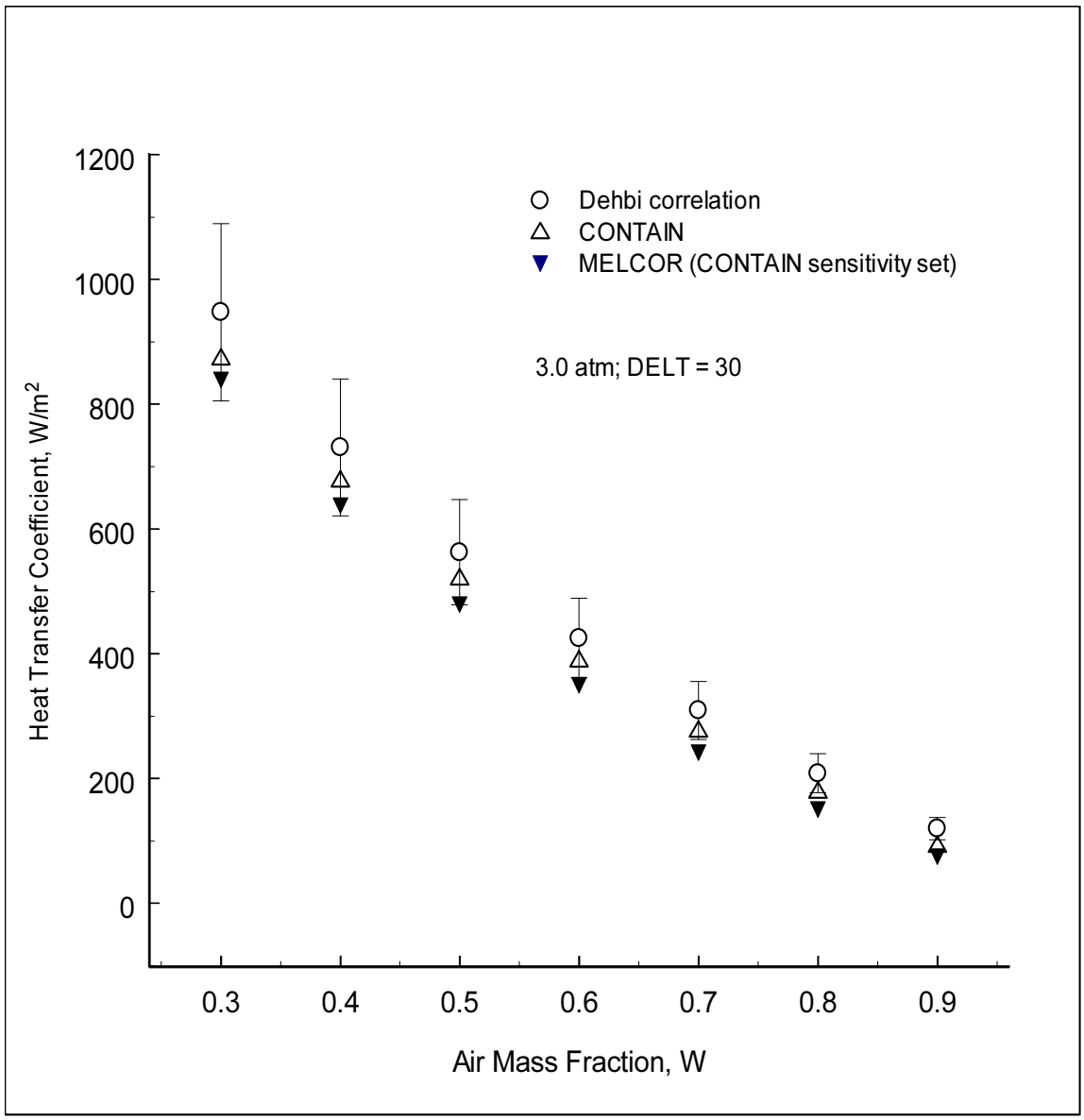

Figure B-5 Comparison of MELCOR and CONTAIN code calculations with Dehbi test results for natural convection condensation at a saturation pressure of 3.0 atmospheres.

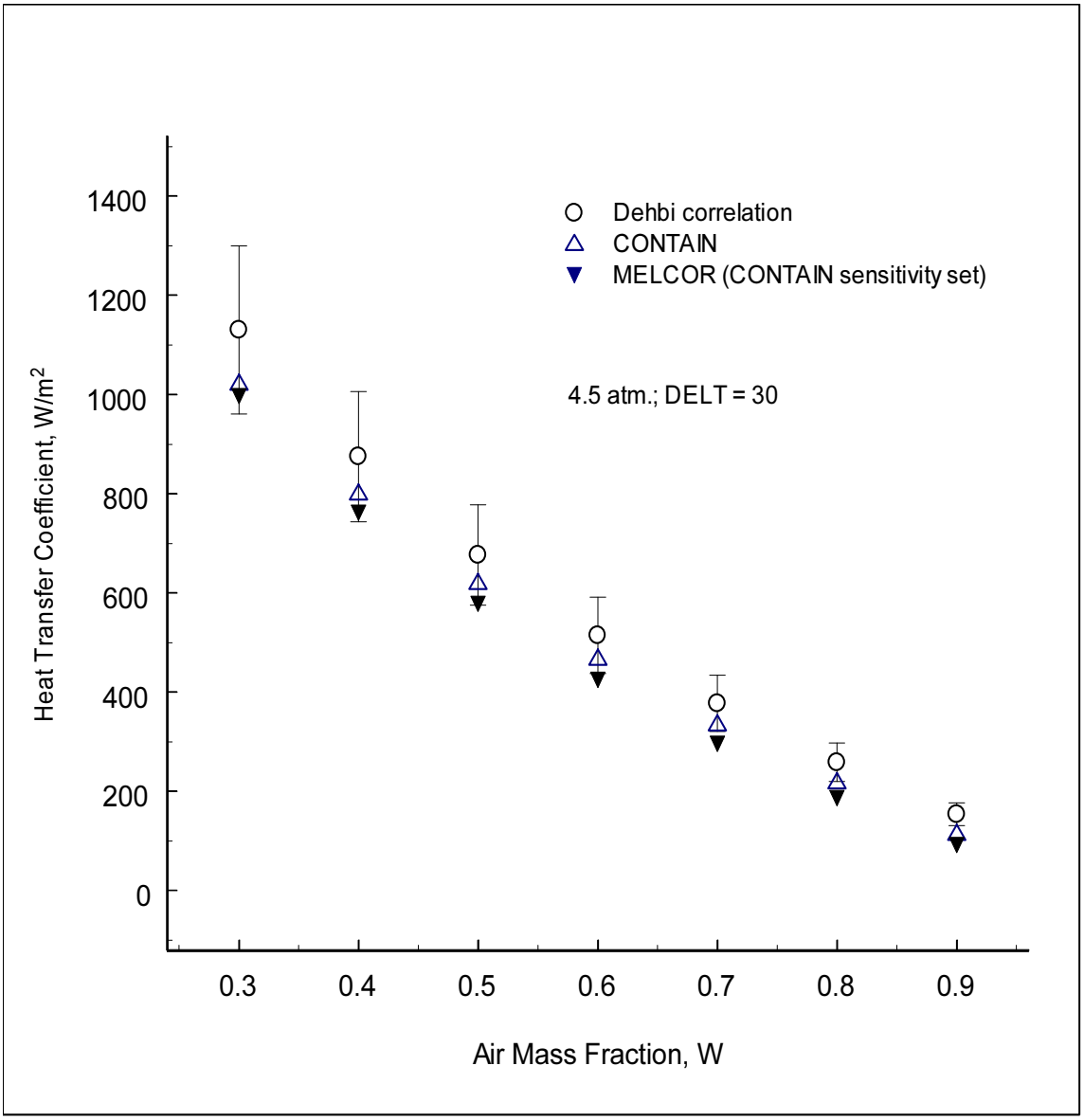

Figure B-6 Comparison of MELCOR and CONTAIN code calculations with Dehbi test results for natural convection condensation at a saturation pressure of 4.5 atmospheres.

INTENTIONALLY BLANK

Appendix C. Wisconsin Flat Plate Condensation Tests Analysis

The Wisconsin flat plate condensation tests are described in Huh93. These tests examine the effects of surface orientation on the condensation of steam in the presence of air. An air-steam mixture is directed into a rectangular flow-channel over a condensing surface that has a painted surface finish of high thermal conductivity and good wetting characteristics. The mixture flow is concurrent with the condensate flow. A series of tests were conducted for various surface orientations that varied from 0 to 90 degrees (vertical wall), air-steam mass fractions of 0 to 0.87, and mixture velocities of 1 to 3 m/s. Surface condensation was found to be a weak function of orientation; therefore, only the vertical test orientation is reported here, (i.e., the flow direction is downward).

Local heat transfer coefficients are determined from measured bulk atmosphere, surface temperature data and heat flux measurements taken along the length of the condensing plate. Average heat transfer coefficients are calculated using the measured total energy transfer to the entire plate via an energy balance on the plate coolant fluid. The coolant fluid is used to maintain a constant plate temperature throughout a test sequence. All the measurements are taken at steady state.

The test section is made of 1905 mm long polycarbonate-plates that are sandwiched to form a 152 mm square duct. The first 838 mm of the test section functions as an entrance length for the condensing mixture. This length is calculated to be sufficiently long so that the free stream turbulence level of the gas stream is dampened. The total length of the apparatus is such that the boundary layers of the opposite walls do not interact significantly; therefore, the test duct is a simulation of a flat plate condensing experiment. Condensation takes place on the cooled plate which is 1066 mm in length. The tests are conducted at 1 bar total pressure.

The MELCOR code was used to calculate the heat transfer coefficient for six tests that included air to steam ratios of 0.29 to 3.5, bulk to surface temperature differentials of 30 to 60 K, and flow velocities of 1 to 3 m/s. The results of these comparisons are shown in Table C-1.

At issue for this assessment were: 1) the accuracy of the heat and mass transfer analogy method under controlled condensing conditions (natural to forced convective regimes); 2) usage of the default CONTAIN mixed convective algorithm; and 3) adequacy of the film theory correction factor included in the CONTAIN model for adjustments during high mass transfer rates. The results of the comparison show that the MELCOR default implementation for both flow regime (laminar or turbulent) and mixed convection can result in significant under predictions for the total heat transfer coefficient (essentially the condensation heat transfer coefficient). Adjustment of sensitivity coefficients that control the equations that identify flow regime and mixed convection can be used to recover an implementation that is similar to the CONTAIN code. Adjustment of sensitivity coefficients is observed in this test analysis to improve the agreement of the MELCOR heat and mass transfer results both with the CONTAIN code and data. Some remaining differences between the code-to-code comparisons are believed to be the result of how boundary layer transport and dimensionless numbers are evaluated in each code.

References

Huhtiniemi, I.K. and Corradini, M.L., "Condensation in the presence of noncondensible gases," Nuclear Engineering Design, 141, pp. 429-446, 1993.

Table C-1 Comparison of CONTAIN/MELCOR and Experimental average heat transfer coefficients for the Wisconsin flat plate condensation tests.

Case #	T_{bulk},°C	T_w,°C	m_{air}/m_{steam}	V, m/s	h_{calc}	h_{exp}	$h_{exp(max,min)}$
1	70	30	3.5	1	**103.8** * (54.5) ** [82] ***	111.1	122.2 99.99
2	70	30	3.5	3	**210.7** (87) [108] {168} ****	213.9	235.3 192.5
3	80	30	1.78	1	**165.4** (94) [132]	163.9	180.3 147.5
4	80	30	1.78	3	**296.9** (99) [152] {240}	305.6	336.2 275.0
5	90	30	0.68	1	**292.1** (170) [237]	255.5	281.1 229.95
6	95	45	0.29	1	**501.5** (311) [431]	546.	600.6 491.4

* CONTAIN
** MELCOR (default sensitivity coefficients for HS package)
*** MELCOR (CONTAIN film heat transfer coefficient; CONTAIN natural and forced convection correlations for laminar and turbulent flow)
**** MELCOR (CONTAIN film heat transfer coefficient; CONTAIN natural and forced laminar and turbulent convection correlations, CONTAIN mixed flow convective correlation)

Appendix D. Phebus Test FPT0 Analysis

The Phebus Fission Product program includes a series of in-vessel and ex-vessel experimental efforts performed by the Institut de Protection et de Surete Nucleaire (IPSN) with contributions from the European Community Commission, Japan, Korea and the USA, at the Research Center of Cadarache (France) [Phe93]. In this appendix, only the thermal hydraulic behavior of the steam/gas mixture in the containment vessel (ex-vessel) during the Phebus FPT0 test is considered. Initial conditions and transient results for this test are recorded in Reference [Phe94]. The test has a variable steam and hydrogen injection into a steel vessel (10 m^3) with temperature controlled surfaces, Figure D-1. Condensation is allowed to occur only on three vertical condenser cylinders that extends from the top of the vessel. The upper portion of the condenser is held at a low temperature to enable atmospheric condensation while other surfaces (vessel walls, dry condenser, etc.) are kept at an elevated temperature in order to inhibit condensation. Condensation drains from the upper cylinder walls into an inner region of the lower, dry condenser region (held at a temperature above the saturation temperature). The collected condensate mass is measured at frequent intervals during the experiment. From these measurements, the rate of condensation on the condensing, wet cylinders are determined.

Steam is injected in the core mockup vessel upstream from the containment vessel at injection rates that vary from 0.0005 to 0.003 kg/s. During the steam/clad interaction period, hydrogen is generated in the core mockup region and the steam rate to the containment drops as a result of the steam/clad reaction, Figure D-2. The injection location to the containment vessel is at a low elevation which favors a well-mixed volume. Independent field code calculations have been performed for the program [Phe94a]. These calculations, along with measured gas temperatures in the vessel, have verified that the vessel atmosphere is uniformly mixed during the test, and that the flow velocity along the condenser surfaces is small, well below 1 m/s. As a result of these investigations, it is apparent that this test is useful as a separate effects test for free convective condensation phenomena.

Since the vessel walls are heated above the saturation temperature corresponding to the partial pressure of steam in the vessel, heat transfer to the vessel (and dry condenser walls) is only by sensible heat transfer (convection and radiation) which is significantly less than the atmosphere energy transfer to the condenser (wet) that occurs as a result of latent heat transfer during condensation. As a consequence of the relatively high wall temperatures of the vessel and dry condenser portions, the bulk or gas temperature is superheated throughout the test which is verified by humidity measurements taken inside the vessel.

The test was simulated with the CONTAIN code [Til02] using a single cell to represent the vessel atmosphere. Measured condenser (as a function of time) and vessel wall temperatures were specified in the simulation. Film flow modeling was used to predict the condensate film thickness on the condenser tubes, and the default free convective heat transfer equation for vertical walls was used to predict the Nusselt number *Nu* at the condenser surface:

$$Nu = 0.14 Ra^{0.33} \qquad \text{D.1}$$

where *Ra* is the Rayleigh number that satisfies $Ra > 10^7$ for turbulent conditions along the wall. The MELCOR code (version 1.8.6 YN) applied to the Phebus FPT0 test is reported in this appendix, and compared to the CONTAIN predictions and recorded Phebus test measurements (e.g., vessel gas pressure and temperatures, and the condensation rate on the condenser tubes). MELCOR input for Phebus FPT0 corresponds to the CONTAIN input described in Reference [Til02] (i.e., single cell model with initial and boundary conditions, free convective condensation -- film tracking -- with thermal radiation between atmosphere and structures).

Shown Figure D-3 is the comparison of previous CONTAIN reference comparisons to measured vessel pressures. The comparisons show good agreement between the calculations and data for the entire transient period. Plotted in Figure D-4 are the vessel pressure comparisons between two MELCOR calculations and the CONTAIN results for the Phebus FPT0 test. In the MELCOR calculation labeled "MELCOR (Sen. Coef.)," the leading multiplying coefficient in Equation D.1 is changed (sensitivity coefficient 4110(1)) from the default value 0.1 to 0.14. For the calculation labeled "MELCOR (w/o Sen. Coef.)," the leading multiplying coefficient for Equation D.1 is left as the default value, 0.1. As indicated by a comparison of the results in Figure D-4, the MELCOR and CONTAIN results are essentially identical providing the same equation is used to model convective heat transfer, and by analogy condensation on the wet portion of the condenser tubes.

Comparisons of the CONTAIN calculated and measured condenser condensation rates for the test are shown in Figure D-5. As with the pressure comparisons, there is good agreement shown between the calculation and measurements. A similar plot, comparing the MELCOR calculations with CONTAIN, is presented in Figure D-6. The MELCOR calculation with Equation D.1 modeled is shown to reproduce the CONTAIN results, and also the good agreement with Phebus measured condensation rates.

Figures D-7 and D-8, show similar comparisons between CONTAIN and test results, and code (MELCOR and CONTAIN) calculations for both gas and saturation temperatures, respectively. The superheating in the vessel ranges from ~10 to 25 K throughout the transient. These superheating amounts and timing are shown to be well predicted by both codes.

References

Phe93 "Phebus FP Programme – Final Report on the 4th Period," Phebus Report No. IP/93/195, Institut de Protection et de Surete Nucleaire, CEA, France, June 1993.

Phe94 "Phebus PF FPT0 Preliminary Report, Part C – Degradation Phase," Phebus Report No. IP/94/211, Institut de Protection et de Surete Nucleaire, CEA, France, May 1994.

Phe94a "Phebus-FP Information Meeting – Proceeding," Phebus Report No. IP/94/224, Institut de Protection et de Surete Nucleaire, CEA, France, November 1994.

Til02 J. Tills, A. Notafrancesco, and K. Murata, "An Assessment of CONTAIN 2.0: A Focus on Containment Thermal Hydraulics (Including Hydrogen Distributions)," SMSAB-02-02, USNRC, Office of Nuclear Regulatory Research, July, 2002.

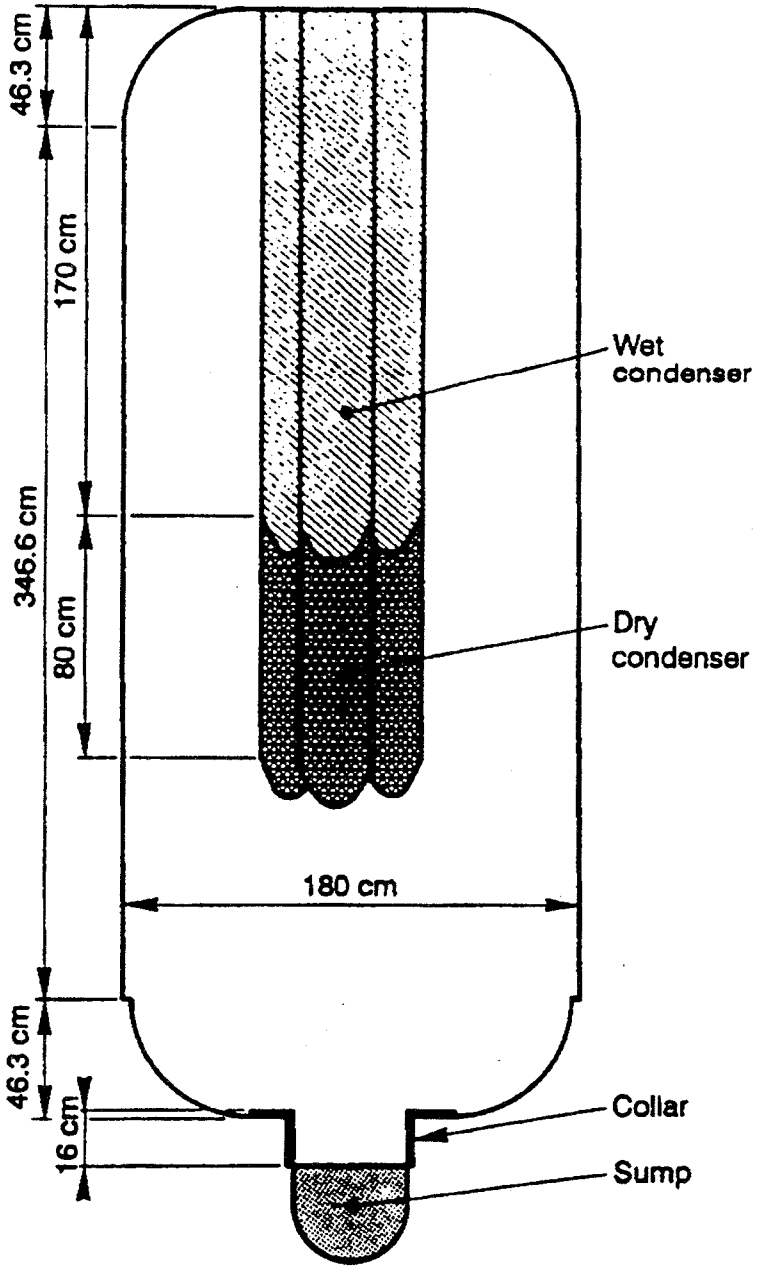

Figure D-1 Phebus containment vessel [Phe94].

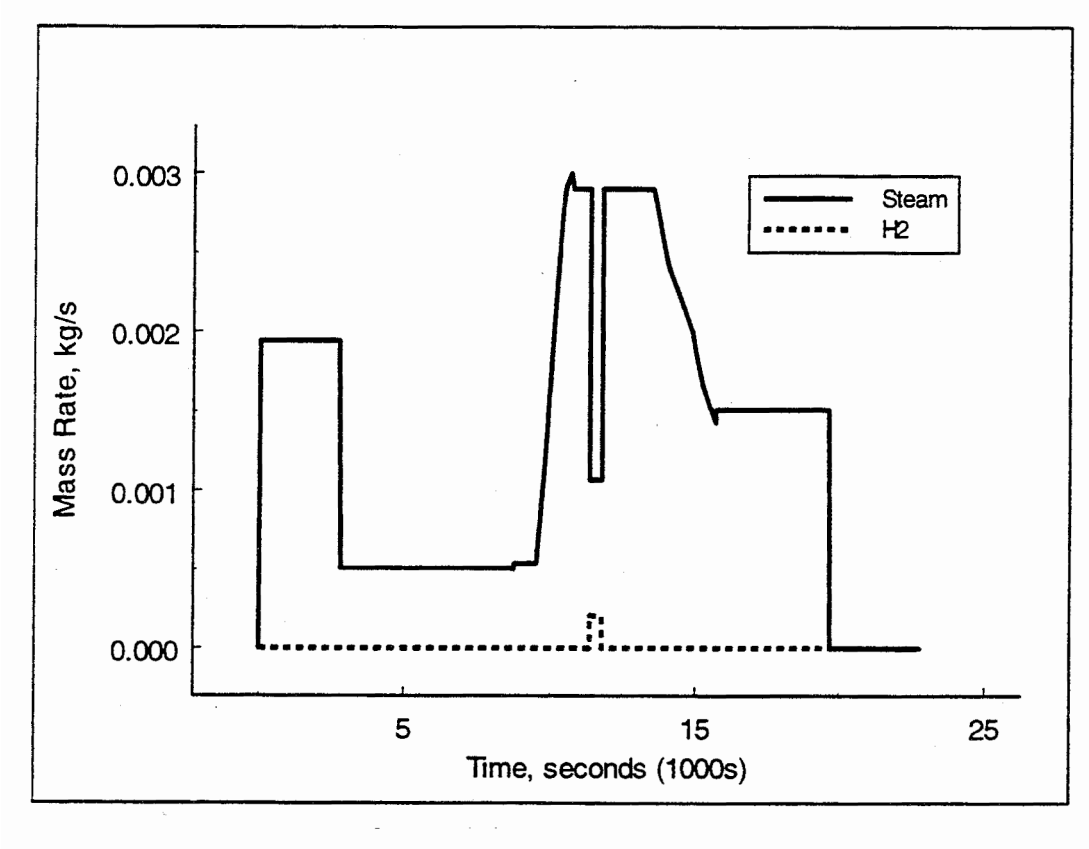

Figure D-2 Containment vessel injection rates for steam and hydrogen during the Phebus FPT0 test.

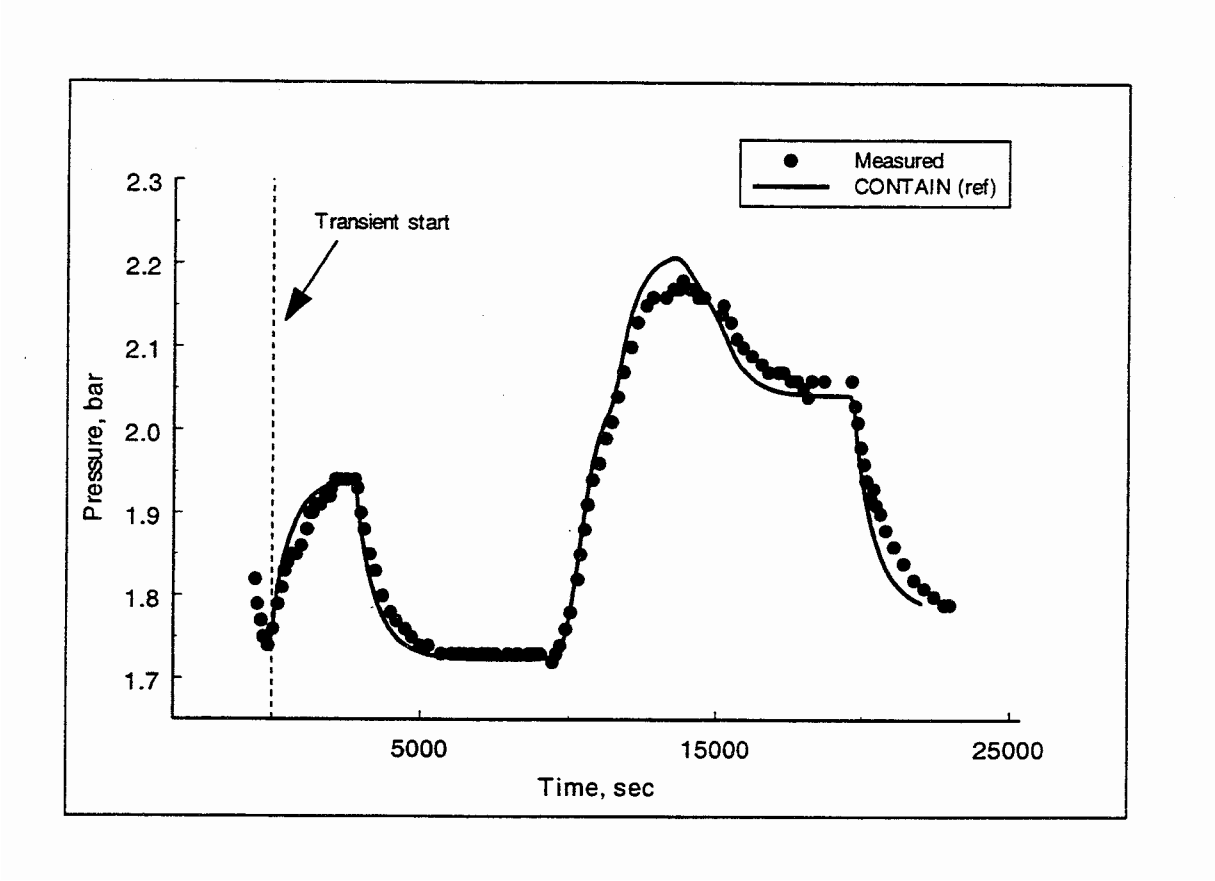

Figure D-3 Comparison of CONTAIN calculated and measured vessel pressure for Phebus FPT0 test [Til02].

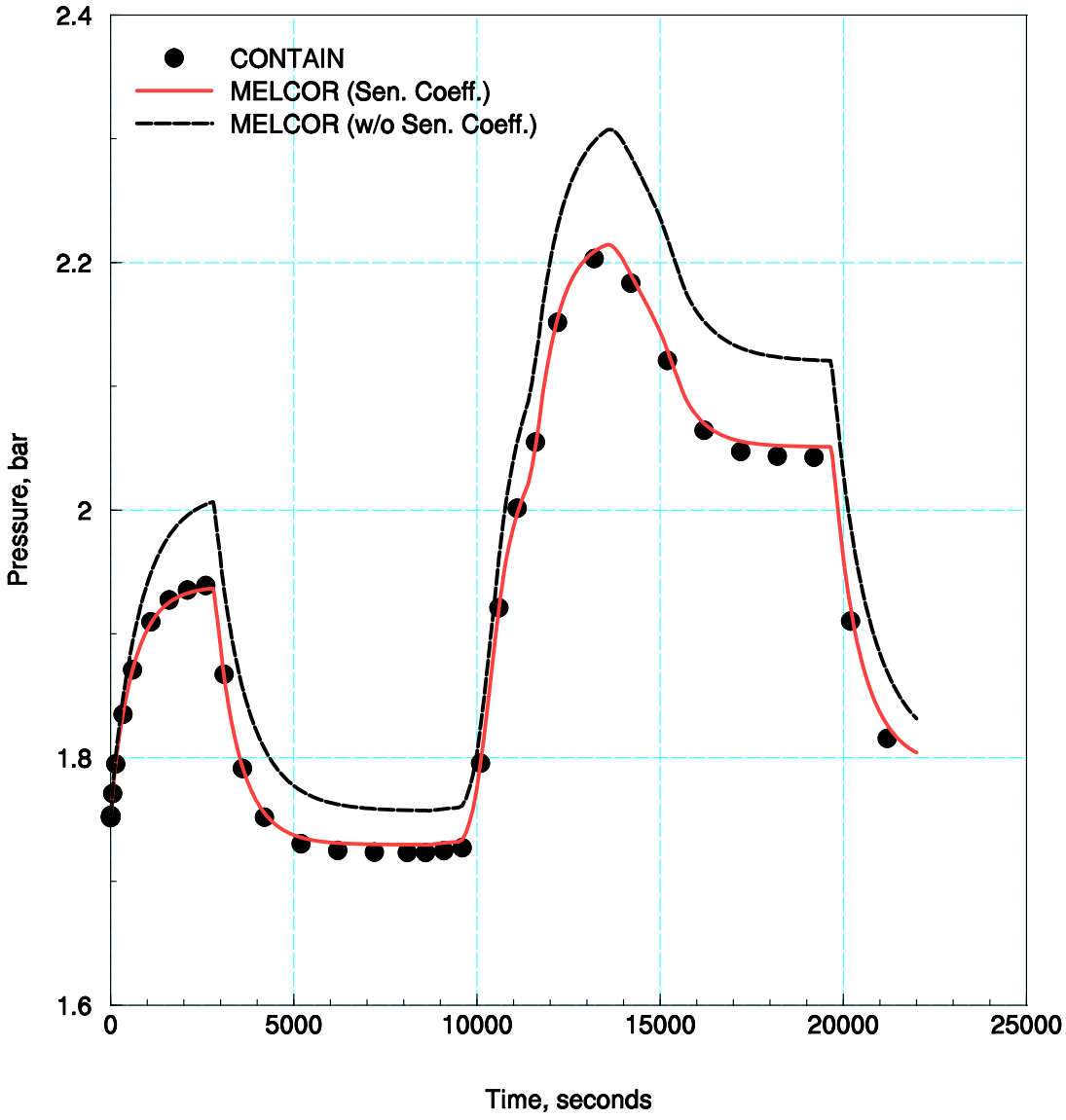

Figure D-4 Comparison of CONTAIN and MELCOR calculated vessel pressure for Phebus FPT0 test.

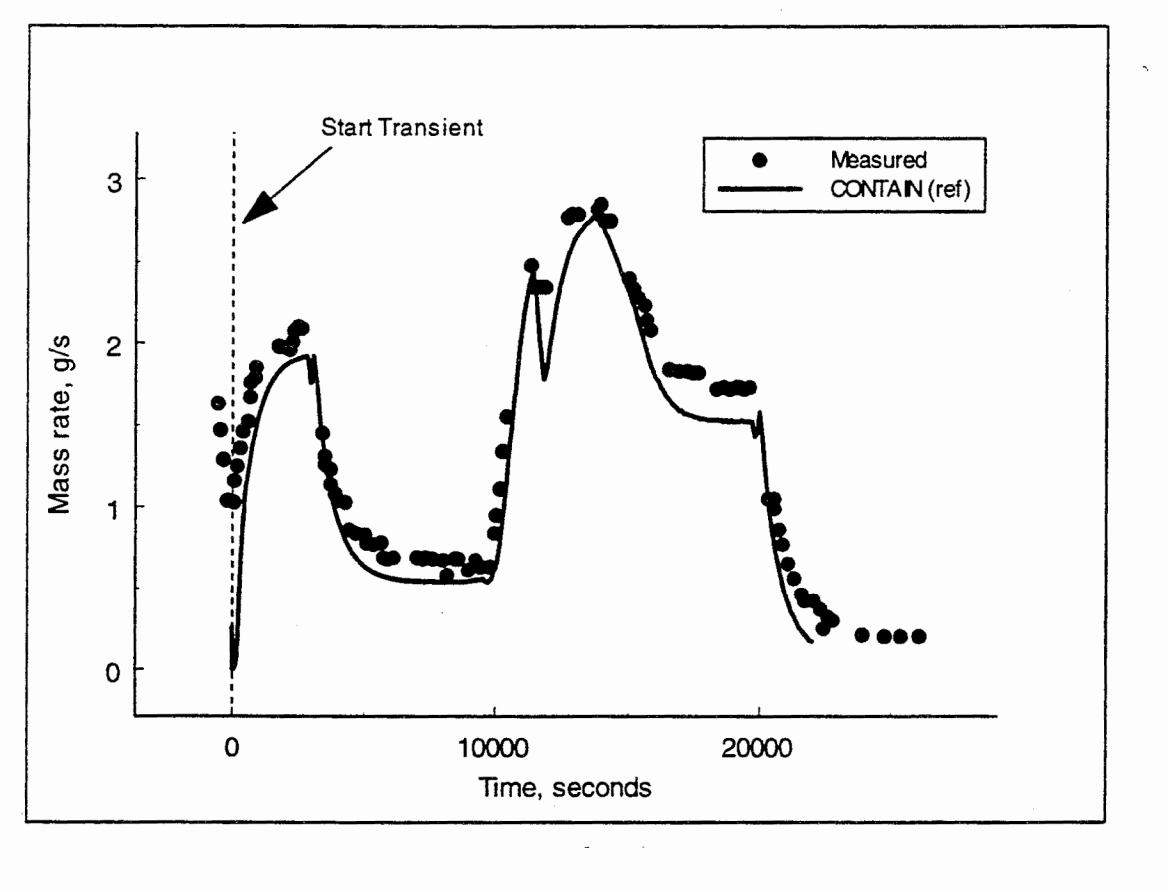

Figure D-5 Comparison between CONTAIN calculated and measured condensation rates for the Phebus FPT0 test [Til02].

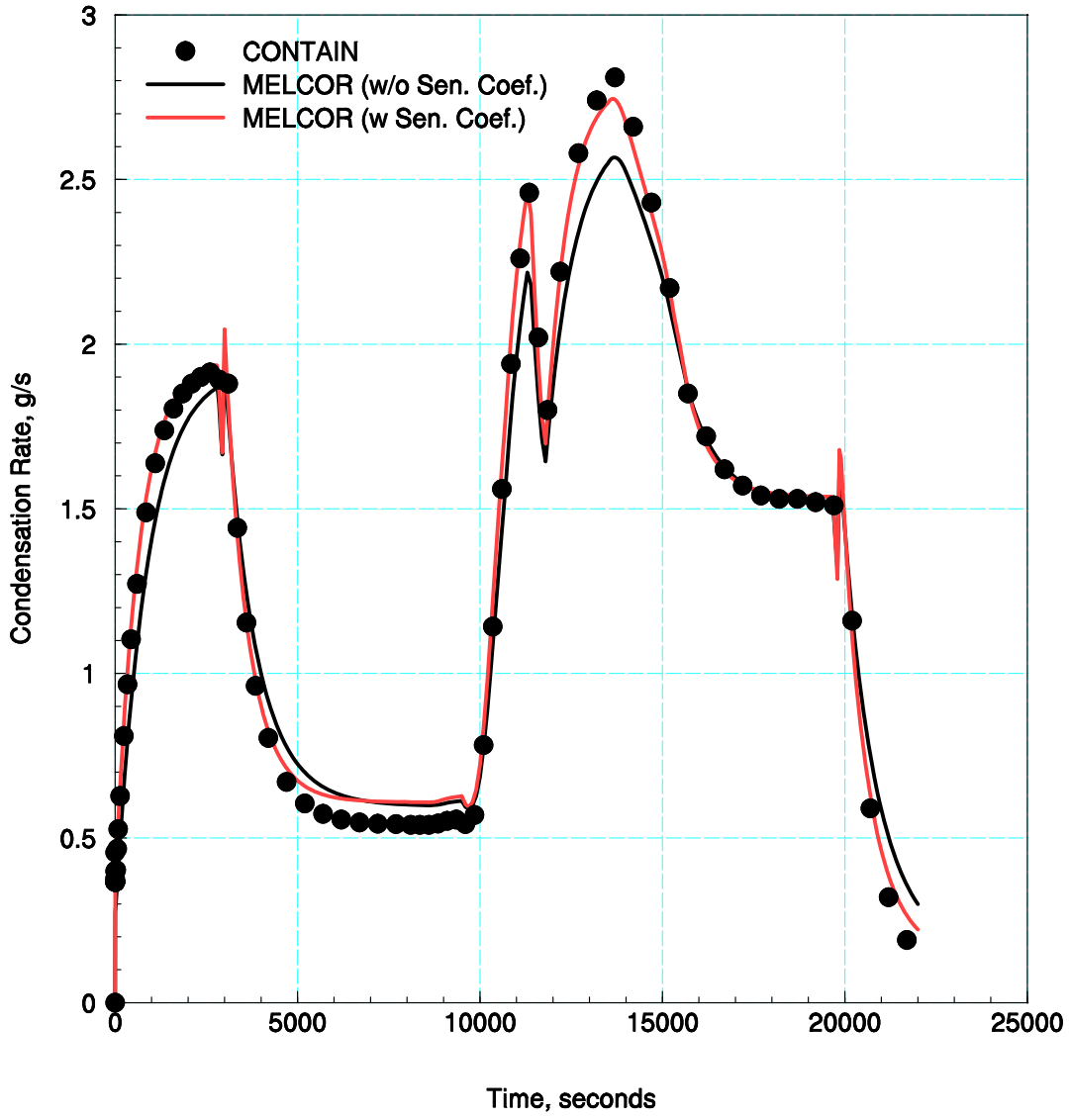

Figure D-6 Comparison of CONTAIN and MELCOR calculated condensation rates for Phebus FPT0 test.

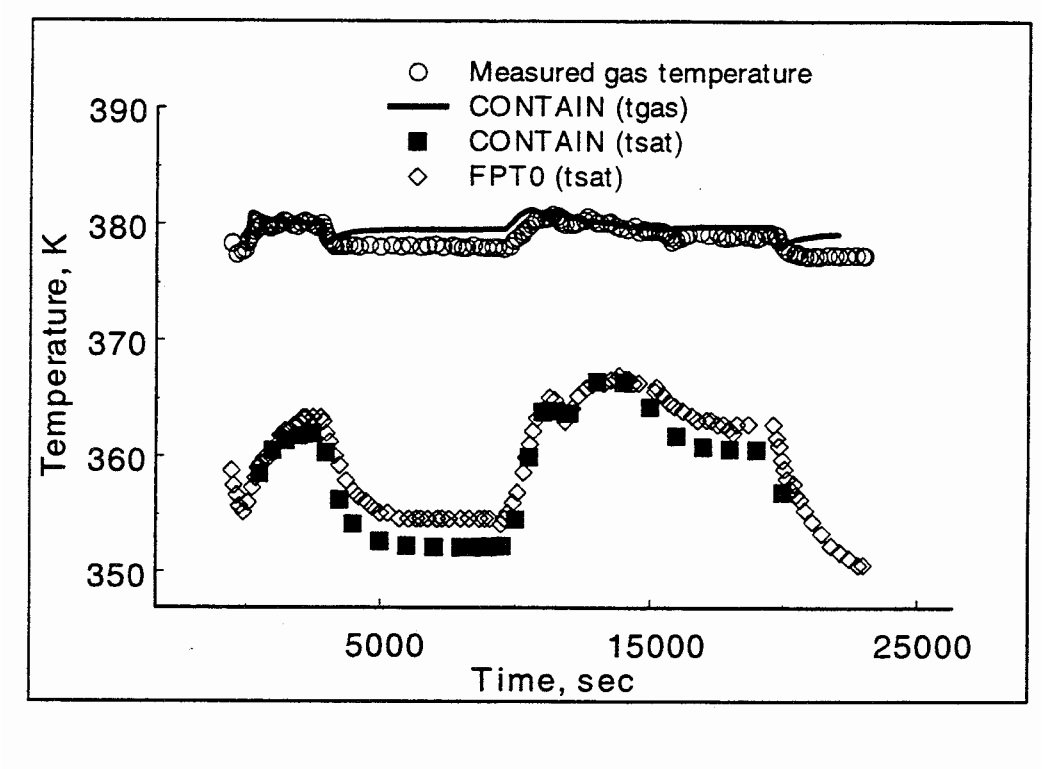

Figure D-7 Comparison of CONTAIN calculated and measured saturation and superheated gas temperatures for Phebus FPT0 test [Til02].

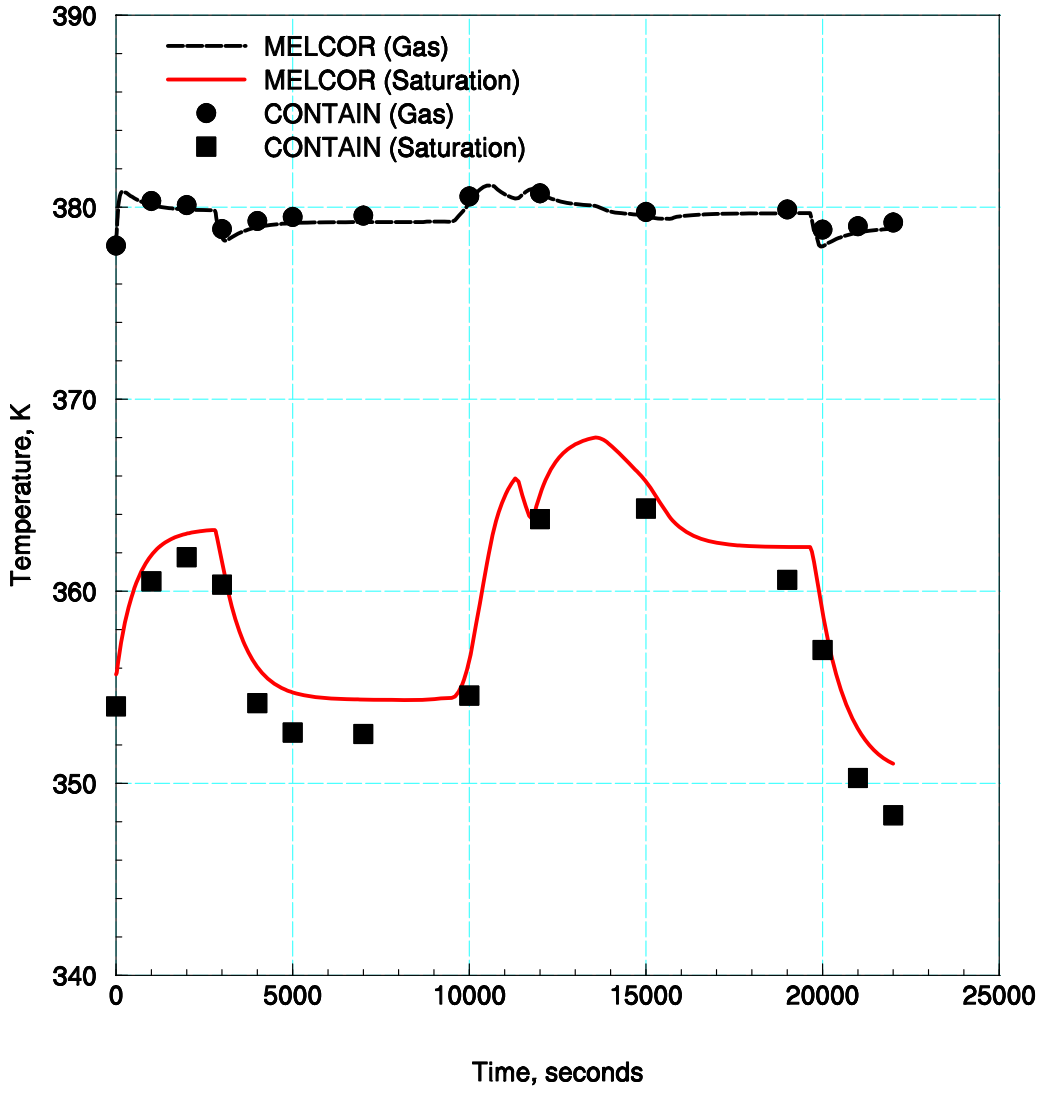

Figure D-8 Comparison of CONTAIN [Til02] and MELCOR (Sen. Coef.) calculated gas and saturation temperatures for Phebus FPT0 test.

Appendix E. JAERI Spray Tests Analysis

E-1 Introduction

A series of pressure suppression spray tests were conducted in Japan during the late 1970s in a 700 m^3 steel vessel (20 m high, 7 m in diameter) [1]. Two tests from that series are calculated in this appendix, PHS-1 and PHS-6. Spray water at 313 K is injected into the vessel containing a saturated air/steam mixture at 3.5 bar. The initial condition for the spray tests is obtained by first injecting steam into the vessel that is initially at 1 bar pressure. Vessel pressure is increased to slightly greater than 3.5 bar and then the steam is turned off and the pressure is allowed to relax to 3.5 bars before sprays are initiated. The vessel steel walls are insulated on the outside and pre-heated by the steam to an approximate saturation temperature of the air/steam mixture prior to the spray period. Because the vessel wall is "hot" at the beginning of the test (~395 K), no condensation occurs on the walls. The tests are therefore essentially separate effects tests for pressure reduction by sprays.

Shown in Figure E-1 is a sketch of the configuration used for the single nozzle PHS-6 test and the six nozzle PHS-1 test that has a lower nozzle elevation. A review of a typical spray nozzle droplet distribution with height indicates that for the single nozzle test spray droplets will not contact the vertical wall of the vessel; therefore, pressure suppression is assumed to involve the interaction of 100% spray water with the atmosphere. On the other hand, for the six nozzle test at least a portion of the injected spray water can be assumed to contact the vertical wall of the vessel, and therefore will vaporize, causing some degrading of the pressure reduction rate. Both tests provide an interesting range of possible spray conditions when performing design basis accident analysis studies.

For the MELCOR calculations, two vessel nodalization models are used, a single and a 16 cell model. The 16 cell model is shown in Figures E-2 and E-3 for the PHS-6 and PHS-1 test configurations, respectively. Listings of the input decks for both models used for each test are included in Appendix F of this report. The multi-cell model includes input for vessel wall segments that are linked using the film tracking modeling described in the MELCOR heat structure package of the MELCOR User Guide [2]. Spray carry over for the stacked volumes below the spray nozzle elevation is calculated in the code, and the spray junction (fall through links) input is described in the spray package also found in the MELCOR User Guide.

E-2 PHS-6 (single nozzle test)

Shown in Figure E-4 is the comparison of the measured and calculated pressure decline due to spray from a single nozzle (spray rate = 0.959E-03 m^3/s). The agreement is very good for the case modeled without spray contact with the vessel wall; therefore, the calculation represents confirmation of the spray-atmosphere energy exchange modeled in the MELCOR code. The case labeled "10% washdown; 90% spray" shows the pressure is over predicted when 10% of the spray water (liquid) is directly put onto the vessel wall, with the remaining 90% of spray water source injected into the atmosphere. The vaporization of the spray water on the hot vessel wall increases the vessel steam partial pressure, and consequently, the total vessel pressure. The over prediction of pressure in the case of washdown tends to confirm the initial assumption from spray distribution studies that the test with a single spray nozzle does not put spray droplets directly on the vessel wall. In Figure E-5, the comparison between measured and calculated gas

temperature is shown. Gas temperature measurements were made at various elevations (7.5 to 19.5 meters) and, for the PHS-6 test, revealed that the vessel atmosphere was uniformly mixed during the spray period. The slight increase in calculated gas temperature at about 1500 seconds reflects a transition in temperature from a saturated to a superheated condition. This condition is affected by the relative amount of latent to sensible heat transfer from atmosphere to spray droplet. In the calculation shown in Figure E-5, the initial spray droplet size is set to the default 0.001 meter diameter. Specifying a smaller size spray droplet (0.0002 meter) changes the latent to sensible heat transfer such that the amount of superheating is reduced while the pressure change is essentially unaffected. This result is shown in Figure E-6 for gas temperature comparison and in Figure E-7 for the pressure comparison run with the default and the smaller spray droplet size. In any case, superheating is not a significant concern for most containment loads studies. This is because the amount of energy available for transfer due to superheating is small in comparison to the energy associated with latent heat (condensation); and, consequently, small amounts of superheating are attended by only minor pressure variations. Figures E-8 and E-9 show the pressure and gas temperature comparisons for the multi-cell model. The results are essentially identical to the single cell model, and therefore confirm the model treatment of spray droplets falling through stacked volumes.

E-3 PHS-1 (multiple nozzle test)

Test PHS-1 differs from the previous test in that six nozzles are used, and the height of the injection is lowered from 18 to 15 meters above the floor. The higher spray rate (5.754E-03 m^3/s) requires that sump water be drained to avoid pressure effects from gas displacement. The single and multi-cell models include a sump flow path input that limits the sump to a maximum depth of 0.1 meter. Shown in Figure E-10 is the comparison of the measured and calculated pressure decline calculated with the single cell model. The various calculated cases show the pressure sensitivity to spray water/vessel wall contact. The case labeled “90% spray” shows the pressure decline for a 10% reduction in the spray rate without any spray water/vessel wall contact. The calculations indicate that a small amount of spray contact with the hot vessel wall significantly reduces the rate of pressure decline. A washdown amount of 10% initial spray rate gives a very good estimate for the actual pressure reduction. Plotted in Figure E-11 is the single cell model gas temperature compared to the measured gas temperatures. The single cell model calculation used the default spray droplet size; and, with the higher spray rate and the washdown effect, no significant superheating is predicted. As indicated by the gas temperature measurements, most of the vessel is uniformly mixed, even in the region just above the spray nozzle elevation.

The pressure comparison for the multi-cell model is shown in Figure E-12. The improvement in pressure between measurement and prediction is again obvious using a 10% washdown of the vessel wall and a 90% spray rate reduction for the direct droplet to atmosphere interaction. Plotted in Figure E-13 are the comparisons of the vertically measured and calculated gas temperatures for test PHS-1. The agreement between the temperature measurements and calculations at various elevations is good. This is especially true for the region just above the spray nozzle elevation where mixing is indicated by the measurements, and also calculated using the multi-cell model.

References

1. Kitani, S., "Containment spray experiments for pressure suppression," presentation at 1st International Conference on Liquid Atomization and Spray Systems, Tokyo, Japan, August 27-31, 1978.

2. Gauntt, R.O., et al., "MELCOR Computer Code Manuals: Vol. 1 Primer and User's Guide, Version 1.8.6 September 2005," NUREG/CR-6119, Vol. 1, Rev 3, SAND 2005-5713, Sandia National Laboratories, Albuquerque, New Mexico, September 2005.

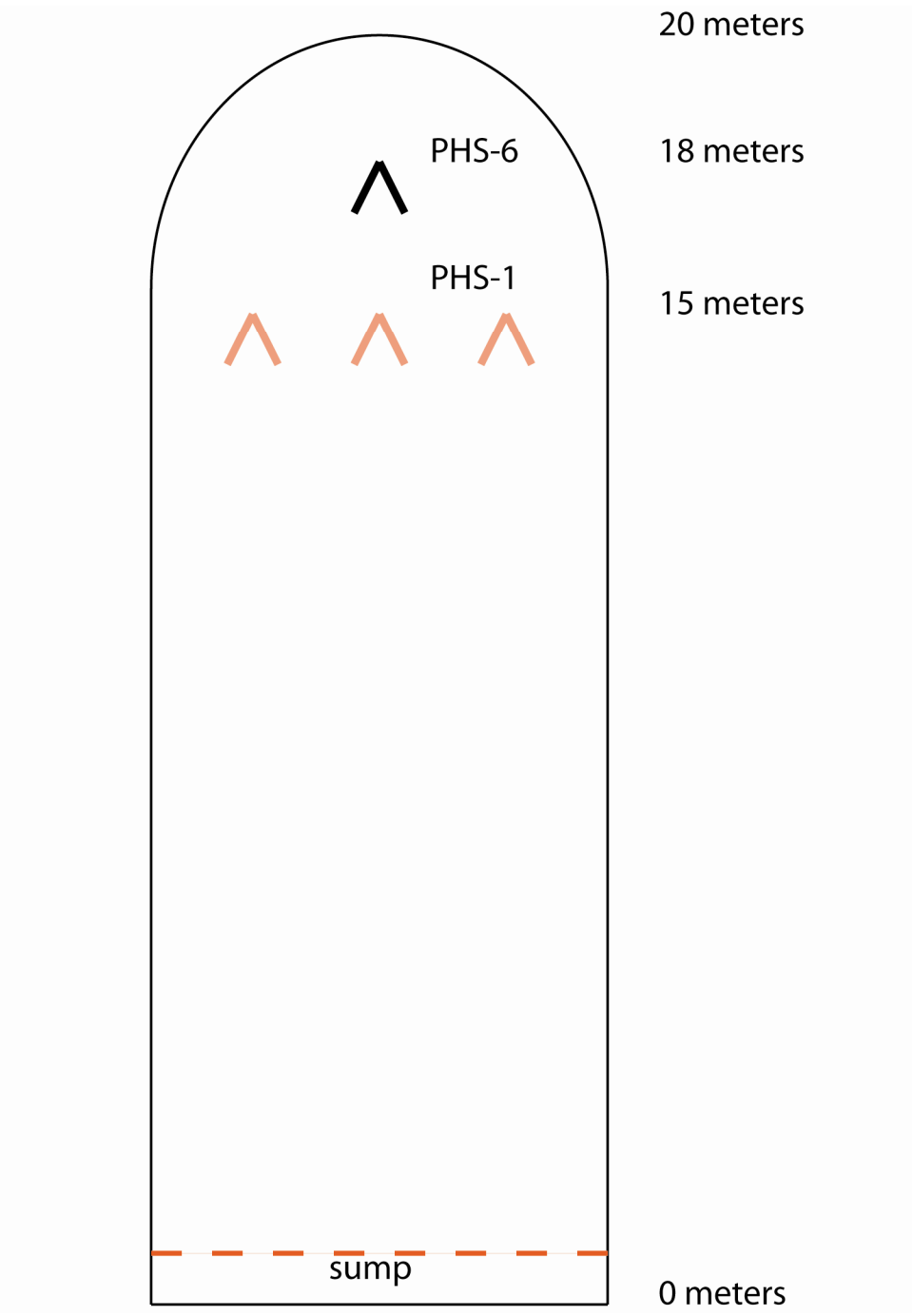

Figure E-1 JAERI spray vessel and test configuration for the single nozzle (PHS-6) and multiple nozzle (PHS-1) tests.

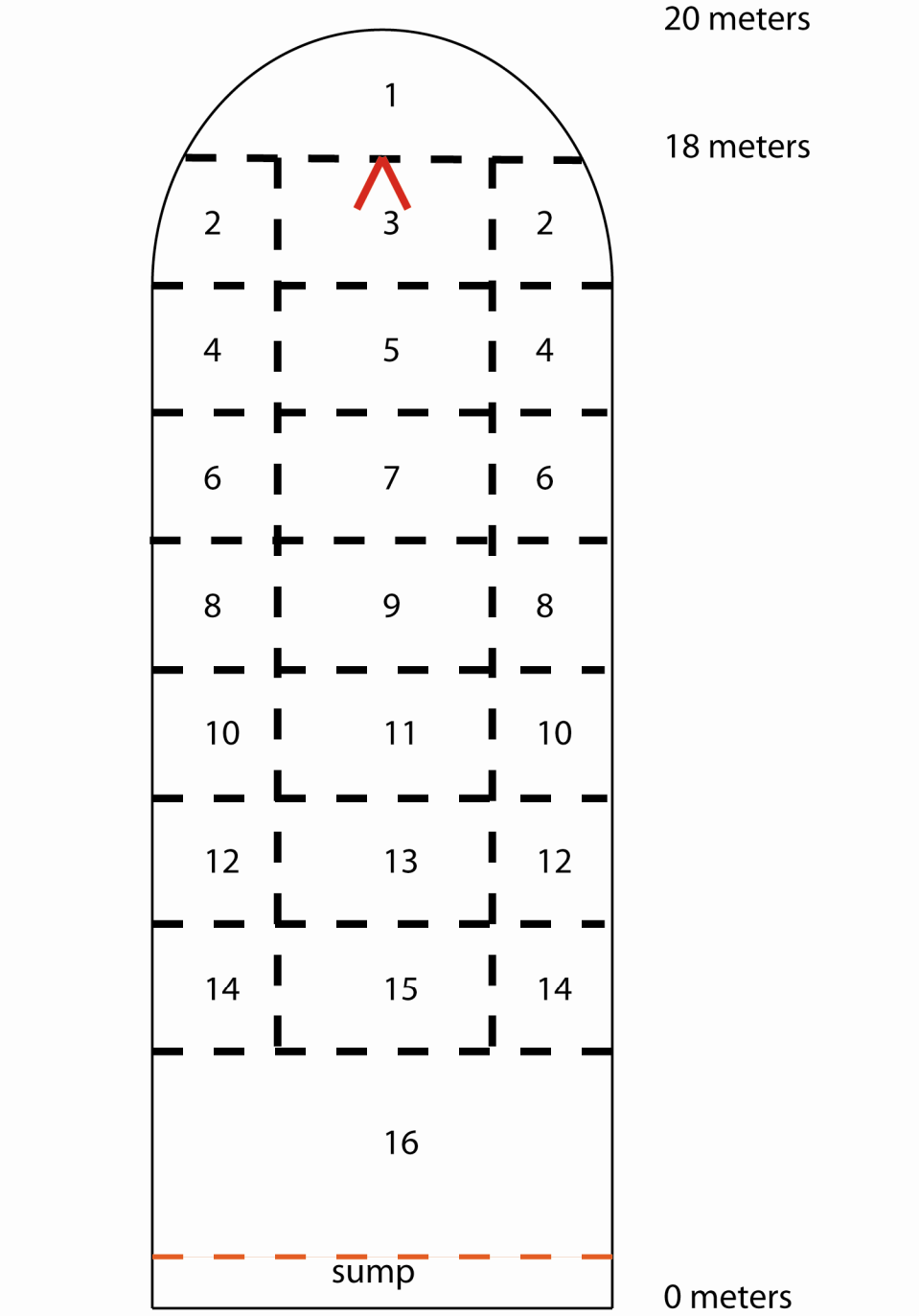

Figure E-2 MELCOR multi-cell model of the JAERI spray vessel, shown for spray nozzle test PHS-6 (single nozzle).

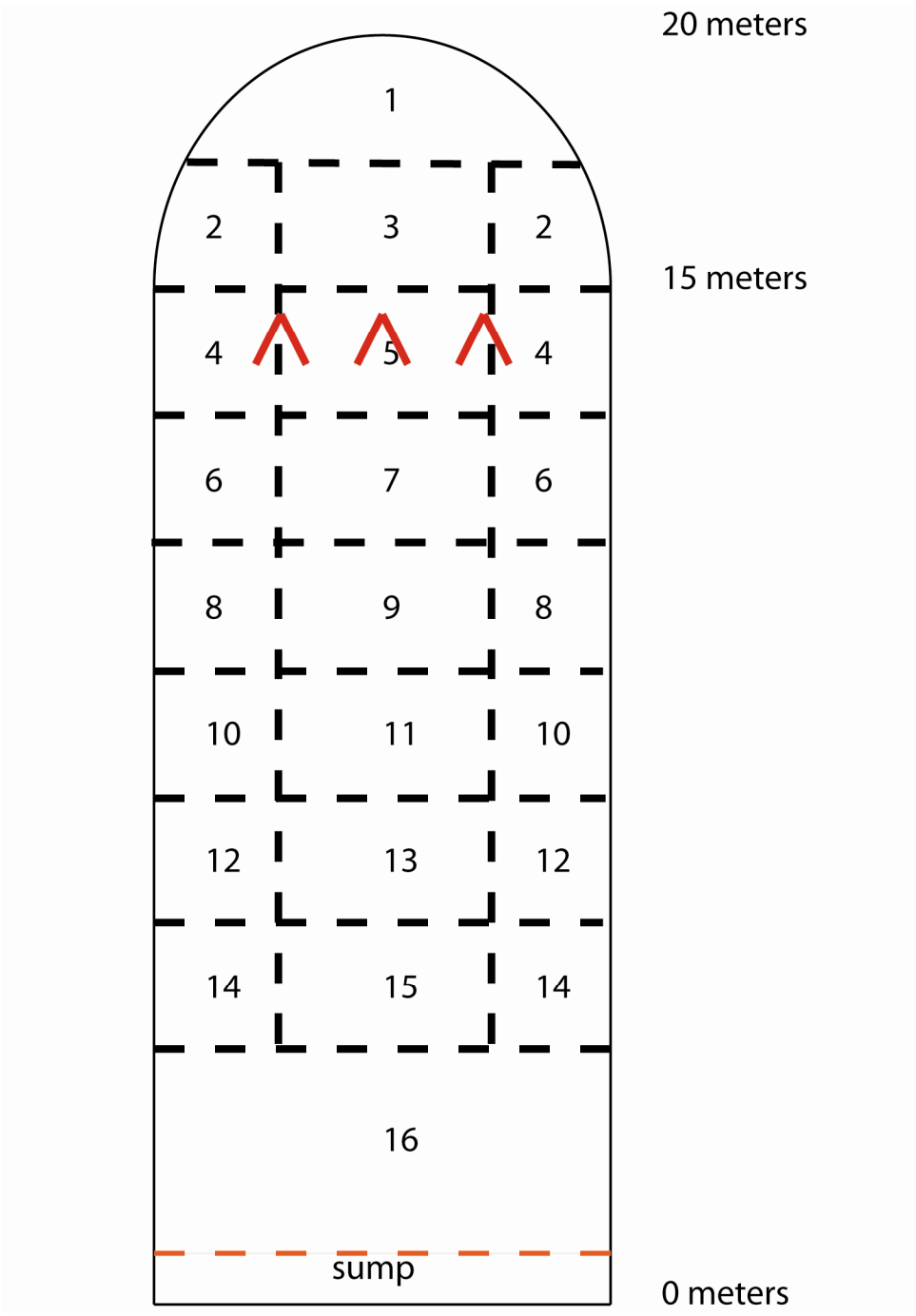

Figure E-3 MELCOR multi-cell model of the JAERI spray vessel, shown for spray nozzle test PHS-1 (multiple nozzles).

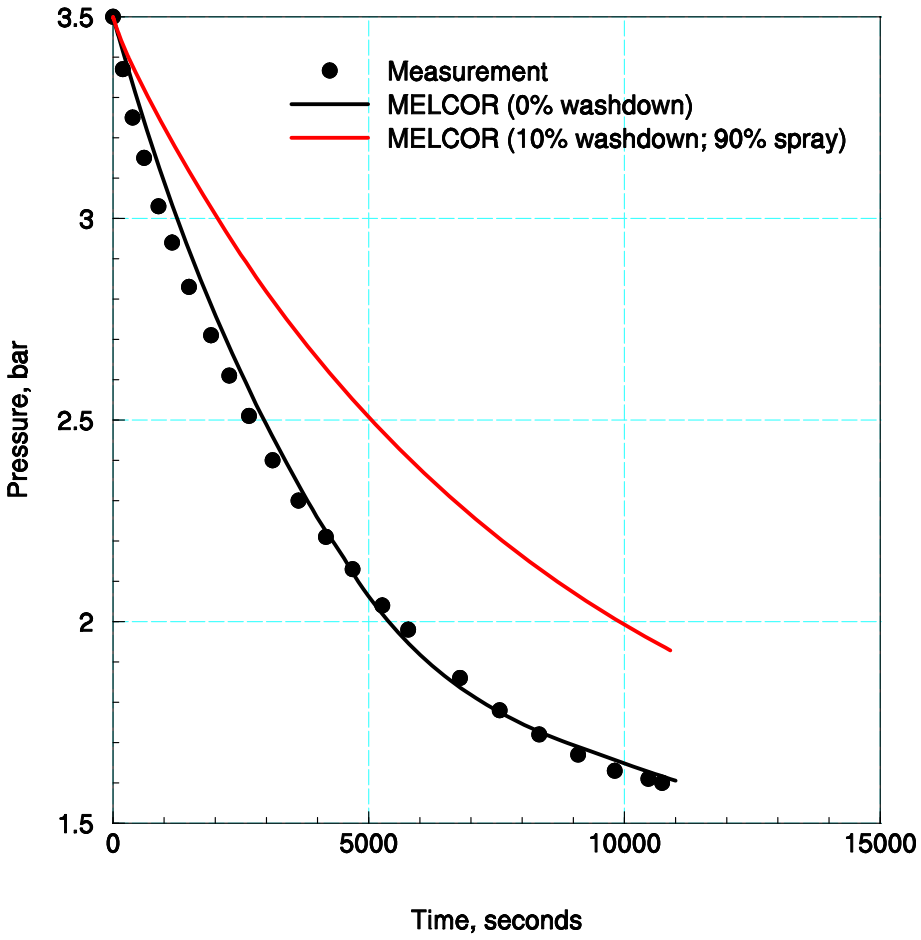

Figure E-4 Comparison of measured and MELCOR calculated (single cell) vessel pressure for JAERI PHS-6 spray test.

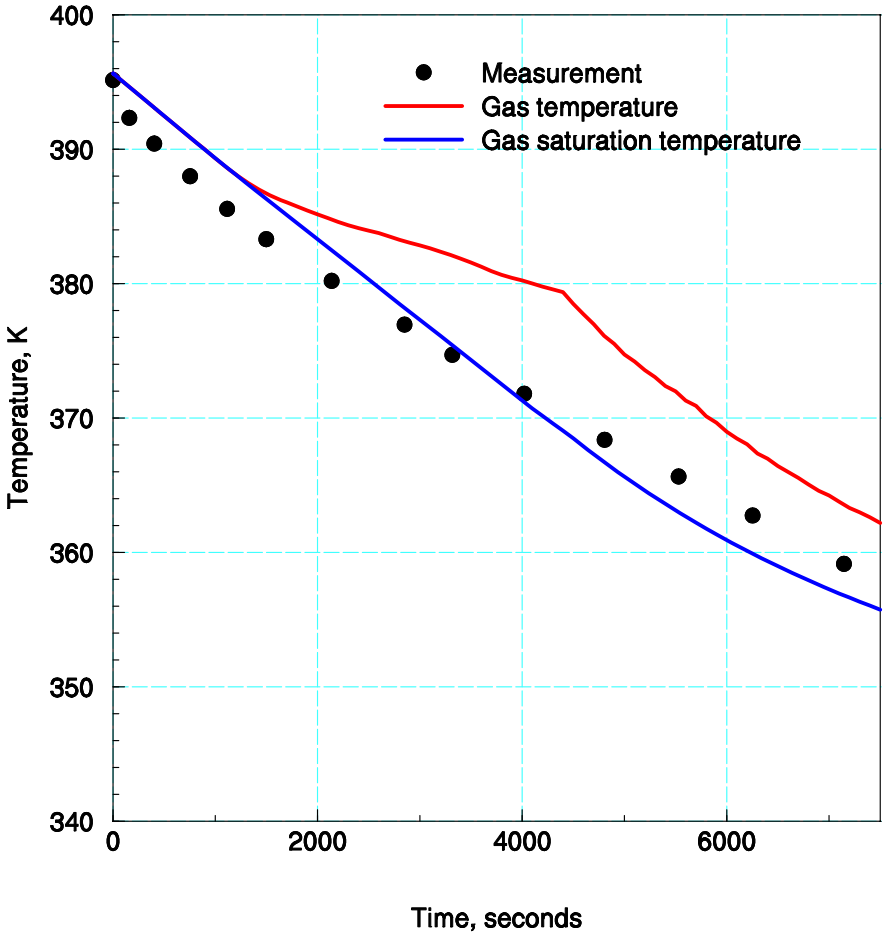

Figure E-5 Comparison of JAERI PHS-6 measured gas (below spray nozzle) and calculated gas and saturation temperature for the single cell model (without washdown).

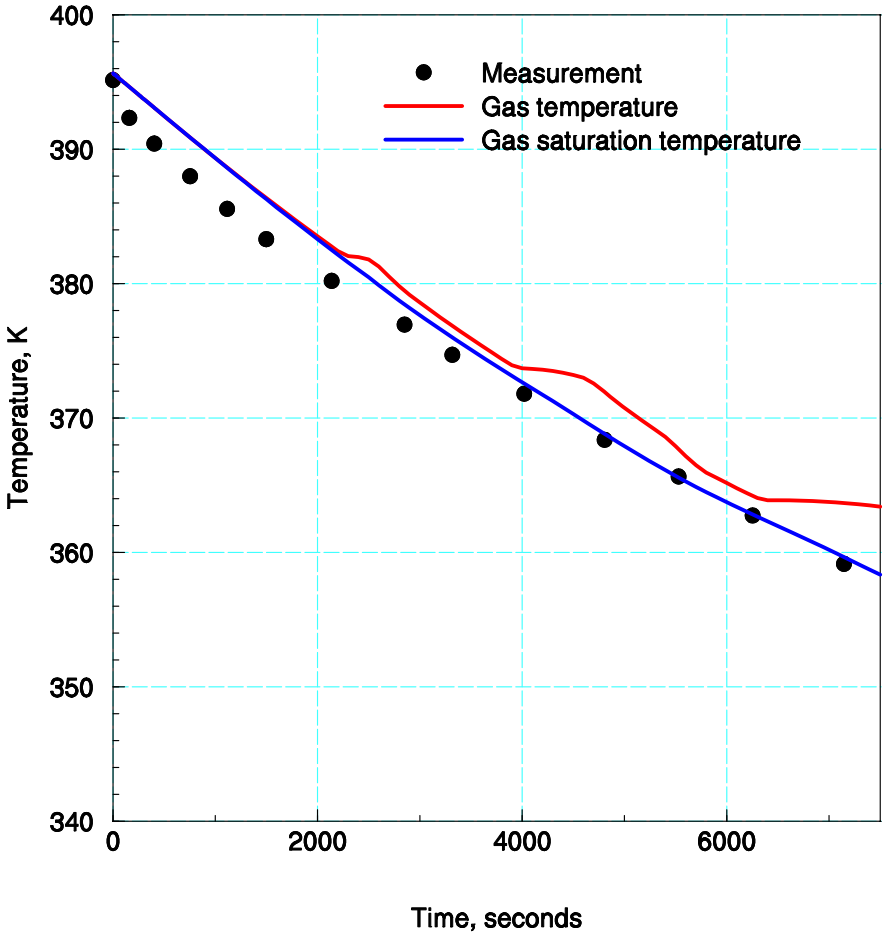

Figure E-6 Comparison of JAERI PHS-6 measured and calculated gas and saturated temperatures for the single cell model (no washdown) with the spray droplet diameter reduced to 0.0002 meters from the default 0.001 meters.

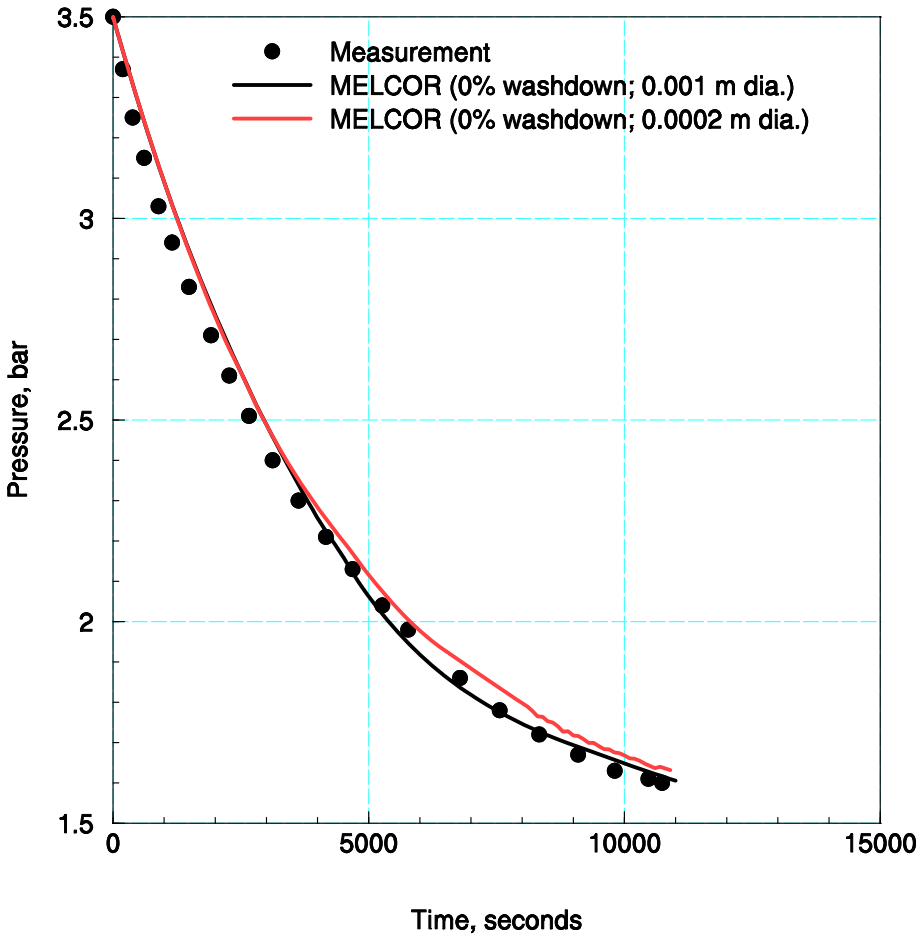

Figure E-7 Comparison of measured and calculated pressure with default (0.001 meter diameter spray droplet) and a small droplet size for JAERI PHS-6 spray test.

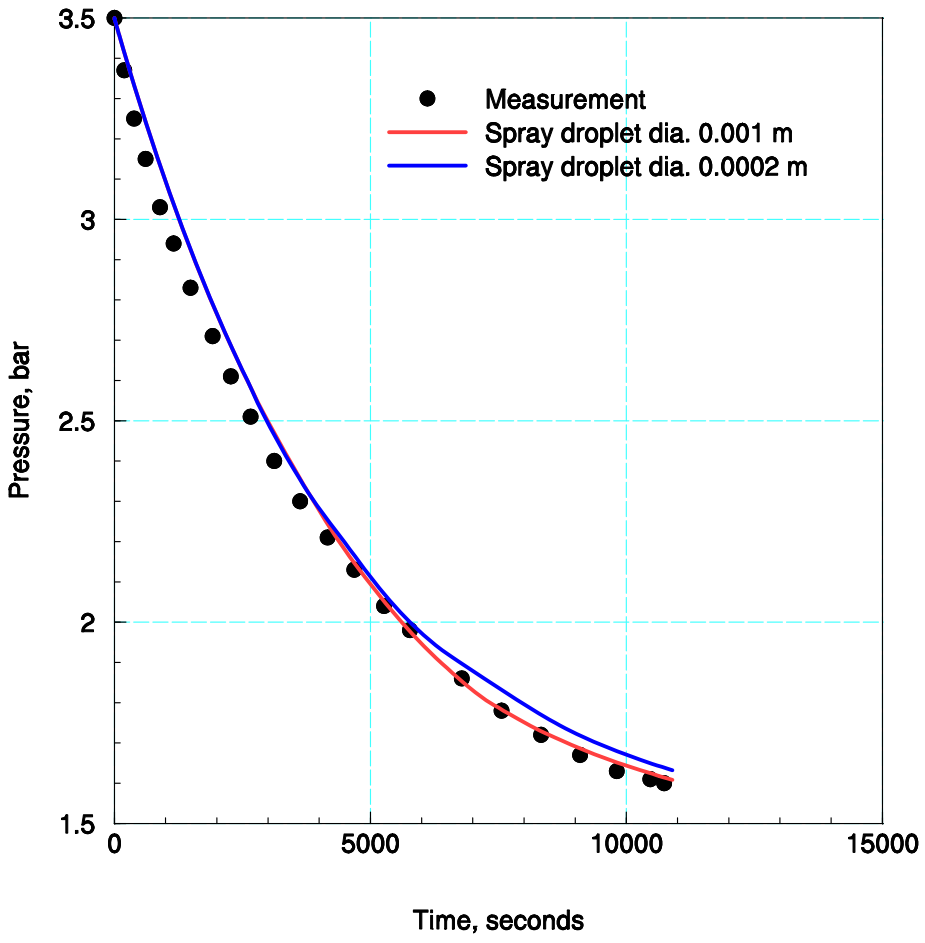

Figure E-8 Comparison of measured and calculated pressure using the multi-cell model for JAERI PHS-6 spray test.

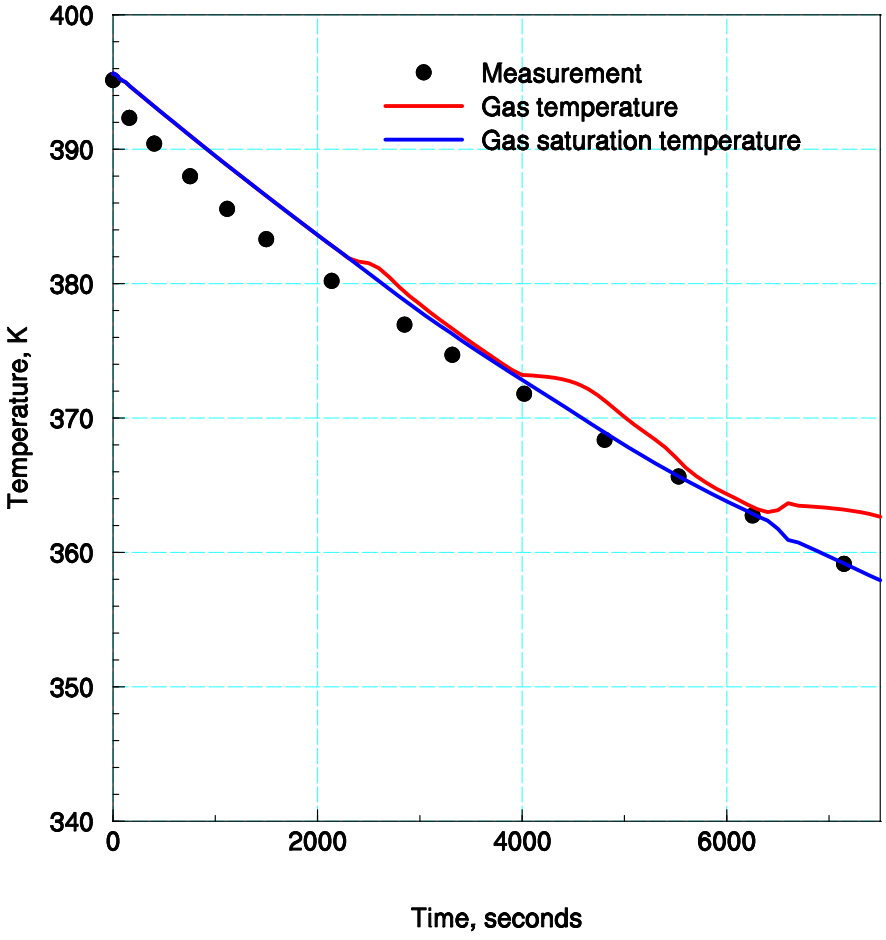

Figure E-9 Comparison of JAERI PHS-6 measured and calculated gas and saturated temperatures for the multi-cell model and a spray droplet diameter of 0.0002 meters.

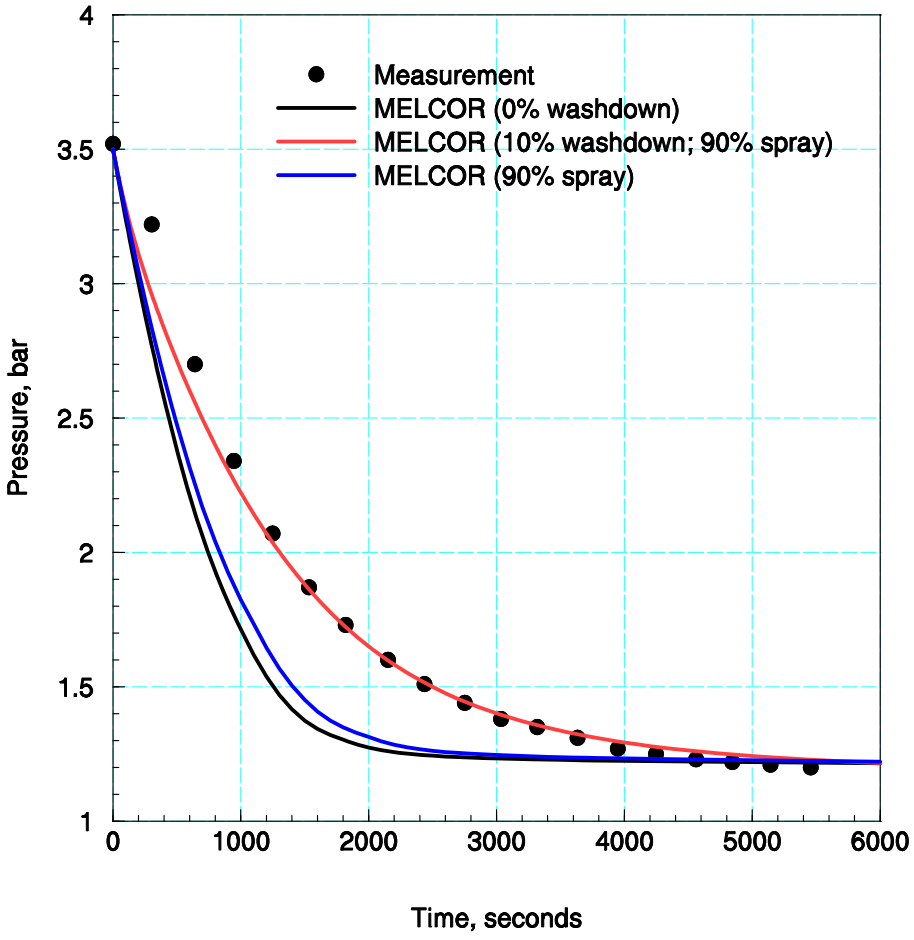

Figure E-10 Comparison of JAERI PHS-1 measured and calculated pressure using the single cell model with default spray droplet diameter (0.001 meter).

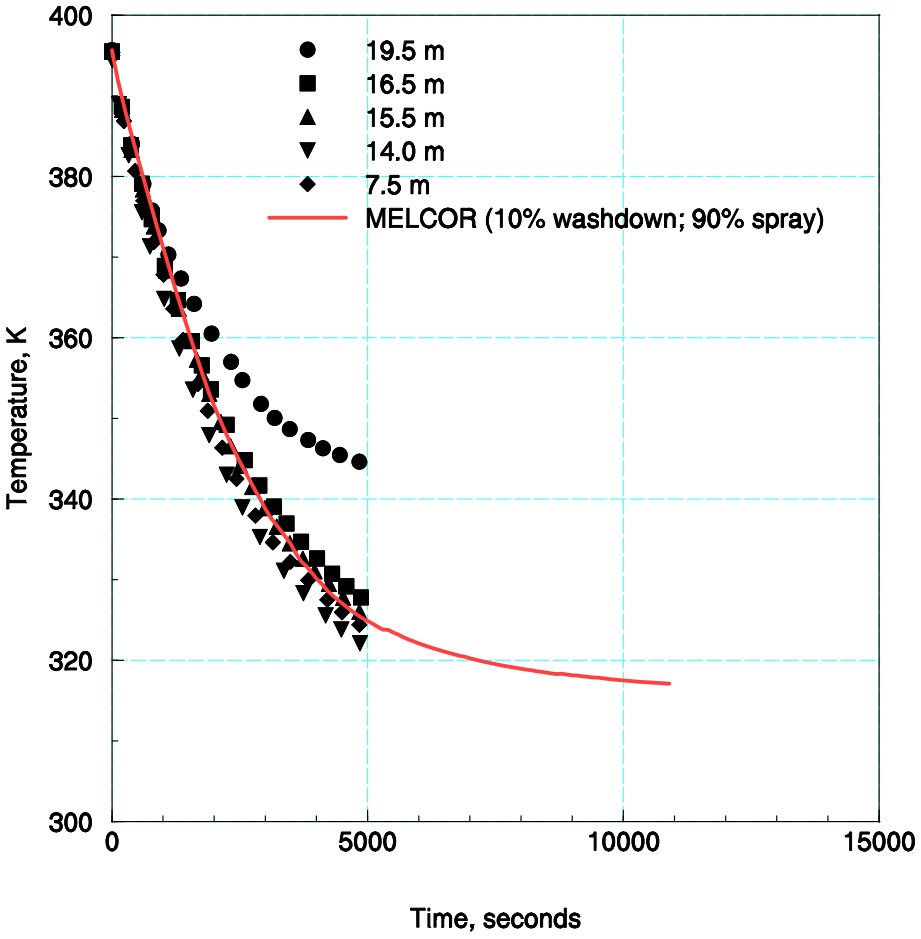

Figure E-11 Comparison of JAERI PHS-1 measured and calculated gas temperature for the single cell model using the default spray droplet diameter (0.001 meter).

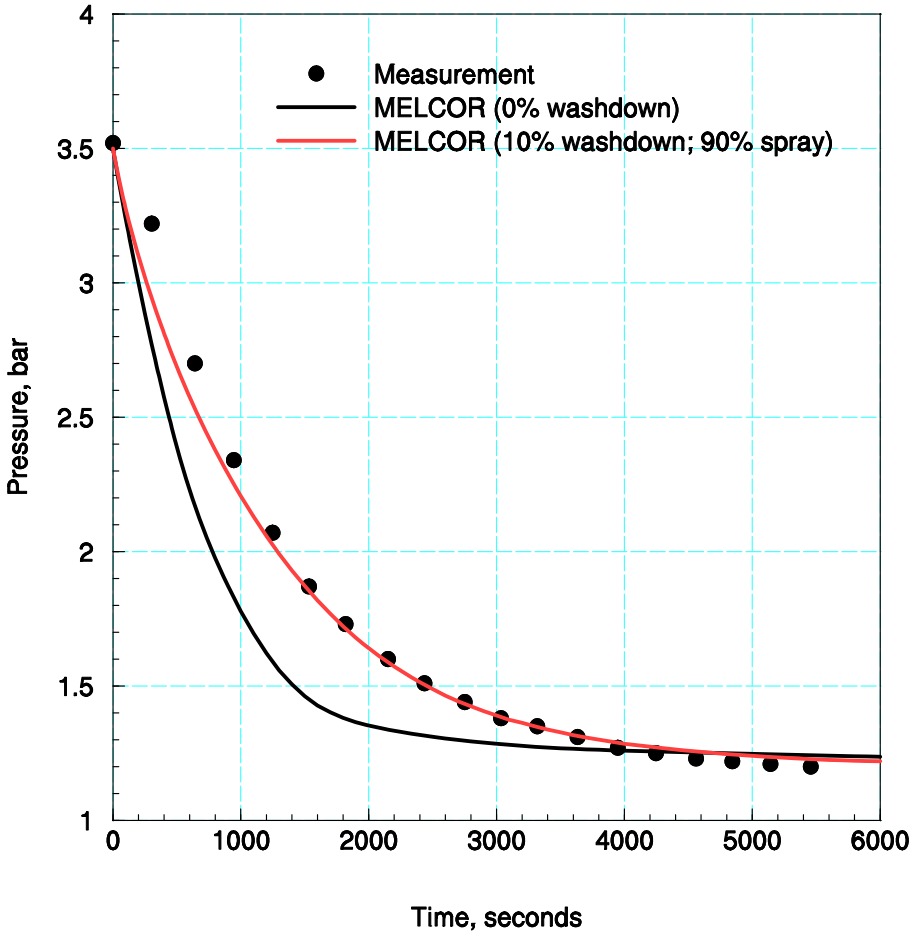

Figure E-12 Comparison of JAERI PHS-1 measured and calculated pressure for the multi-cell model using a default spray droplet diameter (0.001 meter).

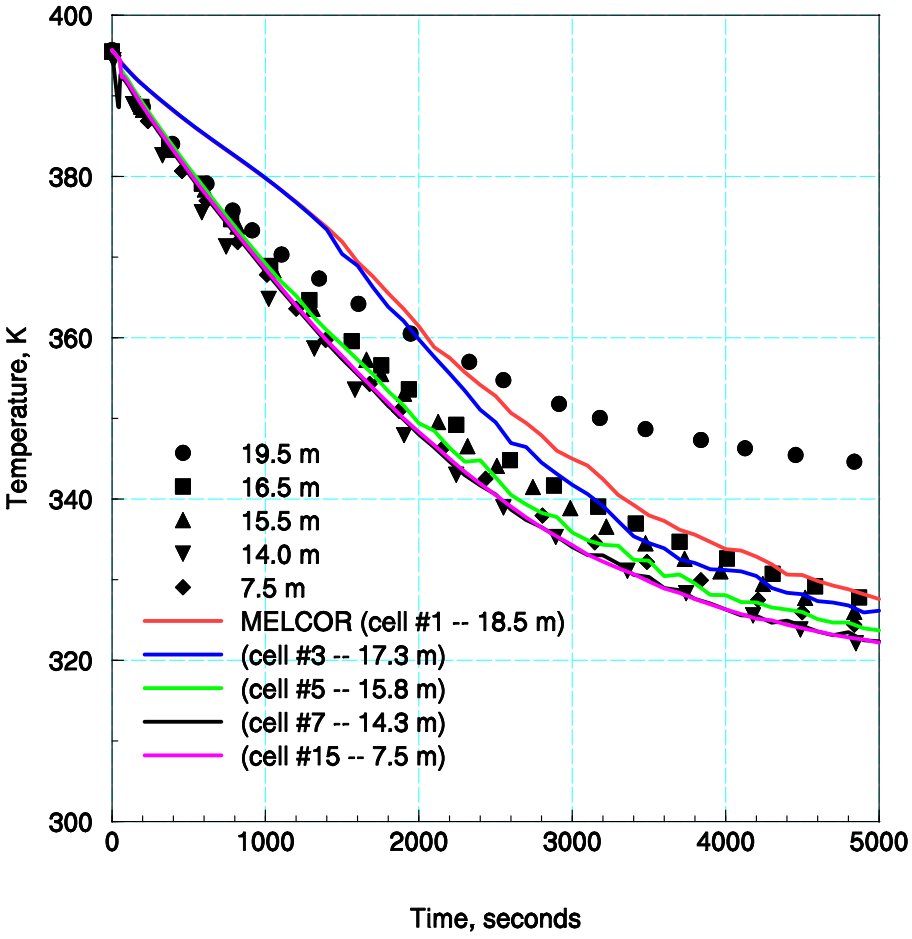

Figure E-13 Comparison of JAERI PHS-1 measured and calculated gas temperatures for multi-cell model using the default spray droplet diameter (0.001 meter).

Appendix F. Listings of MELCOR Input Files for SETs Analyses for Appendices B–E

Dehbi Test (1.5 atm.): EXEC Input –

```
*************************************************
*                                               *
*    Dehbi Calculation                          *
*    Using the film tracking input              *
*                                               *
*************************************************
*eor*   melgen
title   'Dehbi Test_1'
*
restartf        Case1.rst
outputf         Case1.out
diagf           Case1_g.dia
*
dttime 0.1
*
*
***********************************
* Active                          *
***********************************
*
r*i*f .\cont.txt
r*i*f .\mp.txt
r*i*f .\hs.txt
*
.  * terminate
*eor*   melcor
title   'Dehbi Test_1'
*
restartf        Case1.rst
outputf         Case1.out
diagf           Case1_g.dia
plotf           Case1.ptf
messagef        Case1.mes
*
crtout
*
cpulim  2000.0
cpuleft 30.0
*
restart 0
dttime  0.01
*
* tend  19998.0
tend 1000.0
*
*       time    dtmax   dtmin   dtedit  dtplot  dtrest
time1   0.0     0.1     0.001   10.0    5.0     50.0
time2   1000.    0.1     0.001   10.0     5.0    50.0
*
*
*
.  * terminate
```

Cont.txt:

```
*****************************************************************
***
***  containment volume model
***
***   containment cell          description
***         1                   Wair=0.3
***         2                   Wair=0.4
***         3                   Wair=0.5
***         4                   Wair=0.6
***         5                   Wair=0.7
***         6                   Wair=0.8
***         7                   Wair=0.9
***
*****************************************************************
***
*********************************
* CVH INPUT                     *
*********************************
*
*********************************
* Wair=0.3                      *
*********************************
*
*
*
cv00100  mix1        2  2  1     * Non-Equ Thermo, Vert flow, ctmt
cv001a0  3
cv001a1  pvol       1.5e5
cv001a2  tatm       378.061
cv001a3  mlfr.4     0.21
cv001a4  mlfr.5     0.79
* cv001a6  ph2o       0.0
cv001b1  0.0        0.0
cv001b2  10.0     1.0e10
*
*********************************
* Wair=0.4                     *
*********************************
*
cv00200  mix2  2  2  1     * Non-Equ Thermo, Vert flow, ctmt
cv002a0  3
cv002a1  pvol    1.5e5
cv002a2  tatm    374.896
cv002a3  mlfr.4  0.21
cv002a4  mlfr.5  0.79
cv002b1  0.0    0.0
cv002b2  10.0   1.0e10
*
*********************************
*  Wair=0.5                    *
*********************************
*
cv00300  mix3    2   2    1       * Non-Equ Thermo, Vert flow, ctmt
cv003a0  3
cv003a1  pvol    1.5e5
cv003a2  tatm    371.064
cv003a3  mlfr.4  0.21
cv003a4  mlfr.5  0.79
cv003b1  0.0     0.0
cv003b2  10.0    1.0e10
```

```
*
*********************************
*  Wair=0.6                     *
*********************************
*
cv00400  mix4    2   2    1       * Non-Equ Thermo, Vert flow, ctmt
cv004a0  3
cv004a1  pvol    1.5e5
cv004a2  tatm    366.276
cv004a3  mlfr.4  0.21
cv004a4  mlfr.5  0.79
cv004b1  0.0     0.0
cv004b2  10.0    1.0e10
*
*********************************
*  Wair=0.7                     *
*********************************
*
cv00500  mix5    2   2    1       * Non-Equ Thermo, Vert flow, ctmt
cv005a0  3
cv005a1  pvol    1.5e5
cv005a2  tatm    360.009
cv005a3  mlfr.4  0.21
cv005a4  mlfr.5  0.79
cv005b1  0.0    0.0
cv005b2  10.0   1.0e10
*
*********************************
*  Wair=0.8                     *
*********************************
* Cell number         =    6
* Cell bottom         =   2.631 m
* Cell top            =   2.981 m
* Cell height         =   0.35 m
* Cell volume         =   0.307628 m3
*
cv00600  mix6    2   2    1       * Non-Equ Thermo, Vert flow, ctmt
cv006a0  3
cv006a1  pvol    1.5e5
cv006a2  tatm    351.141
cv006a3  mlfr.4  0.21
cv006a4  mlfr.5  0.79
cv006b1  0.0   0.0
cv006b2  10.0  1.0e10
*
*********************************
*  Wair=0.9                     *
*********************************
*
cv00700  mix7    2   2    1       * Non-Equ Thermo, Vert flow, ctmt
cv007a0  3
cv007a1  pvol    1.5e5
cv007a2  tatm    336.21
cv007a3  mlfr.4  0.21
cv007a4  mlfr.5  0.79
cv007b1  0.0     0.0
cv007b2  10.0    1.0e10
*
.           * terminator
```

Hs.txt:

```
*****************************************************
***                                                 *
*** Heat Structure Input                            *
***                                                 *
*****************************************************
*
*****************************************************
* External data file write                          *
* Wall surface temperature                          *
*****************************************************
edf00100 tsur_data 7  write
edf00101 'tsur_data.txt'
edf00102 '1P,8e14.5'
edf00110 0. 5.0
edf001aa hs-temp.0010101
edf001bb hs-temp.0010201
edf001cc hs-temp.0010301
edf001dd hs-temp.0010401
edf001ee hs-temp.0010501
edf001ff hs-temp.0010601
edf001gg hs-temp.0010701
*
**************
* v1         *
**************
hs00101000   5   1  -1
hs00101001  v1
hs00101002  1.0  1.
hs00101100  -1  1  0.0
hs00101102  0.001  2
hs00101103  0.002  3
hs00101104  0.004  4
hs00101105  0.008  5
hs00101200  -1
hs00101201  cu   1
hs00101202  cu   2
hs00101203  cu   3
hs00101204  cu   4
hs00101300  -1
hs00101400   1   1  ext   0.5   0.5
hs00101500  0.41783 3.5 3.5
hs00101600  8010
hs00101800  -1
hs00101801  348.061  5
*
**************
* v2         *
**************
hs00102000   5   1  -1
hs00102001  v2
hs00102002  1.0  1.
hs00102100  -1  1  0.0
hs00102102  0.001  2
hs00102103  0.002  3
hs00102104  0.004  4
hs00102105  0.008  5
hs00102200  -1
hs00102201  cu   1
hs00102202  cu   2
hs00102203  cu   3
```

```
hs00102204  cu   4
hs00102300  -1
hs00102400   1   2  ext   0.5   0.5
hs00102500  0.41783 3.5 3.5
hs00102600  8020
hs00102800  -1
hs00102801  344.896  5
*
**************
* v3         *
**************
hs00103000   5   1  -1
hs00103001  v3
hs00103002  1.0  1.
hs00103100  -1  1  0.0
hs00103102  0.001  2
hs00103103  0.002  3
hs00103104  0.004  4
hs00103105  0.008  5
hs00103200  -1
hs00103201  cu   1
hs00103202  cu   2
hs00103203  cu   3
hs00103204  cu   4
hs00103300  -1
hs00103400   1   3  ext   0.5   0.5
hs00103500  0.41783 3.5 3.5
hs00103600  8030
hs00103800  -1
hs00103801  341.064  5
*
**************
* v4         *
**************
hs00104000   5   1  -1
hs00104001  v4
hs00104002  1.0  1.
hs00104100  -1  1  0.0
hs00104102  0.001  2
hs00104103  0.002  3
hs00104104  0.004  4
hs00104105  0.008  5
hs00104200  -1
hs00104201  cu   1
hs00104202  cu   2
hs00104203  cu   3
hs00104204  cu   4
hs00104300  -1
hs00104400   1   4  ext   0.5   0.5
hs00104500  0.41783 3.5 3.5
hs00104600  8040
hs00104800  -1
hs00104801  336.276  5
*
**************
* v5         *
**************
hs00105000   5   1  -1
hs00105001  v5
hs00105002  1.0  1.
hs00105100  -1  1  0.0
hs00105102  0.001  2
hs00105103  0.002  3
```

```
hs00105104  0.004  4
hs00105105  0.008  5
hs00105200  -1
hs00105201  cu   1
hs00105202  cu   2
hs00105203  cu   3
hs00105204  cu   4
hs00105300  -1
hs00105400   1   5  ext   0.5   0.5
hs00105500  0.41783 3.5 3.5
hs00105600  8050
hs00105800  -1
hs00105801  330.009  5
*
**************
* v6         *
**************
hs00106000   5   1  -1
hs00106001  v6
hs00106002  1.0  1.
hs00106100  -1  1  0.0
hs00106102  0.001  2
hs00106103  0.002  3
hs00106104  0.004  4
hs00106105  0.008  5
hs00106200  -1
hs00106201  cu   1
hs00106202  cu   2
hs00106203  cu   3
hs00106204  cu   4
hs00106300  -1
hs00106400   1   6  ext   0.5   0.5
hs00106500  0.41783 3.5 3.5
hs00106600  8060
hs00106800  -1
hs00106801  321.141  5
*
**************
* v7         *
**************
hs00107000   5   1  -1
hs00107001  v7
hs00107002  1.0  1.
hs00107100  -1  1  0.0
hs00107102  0.001  2
hs00107103  0.002  3
hs00107104  0.004  4
hs00107105  0.008  5
hs00107200  -1
hs00107201  cu   1
hs00107202  cu   2
hs00107203  cu   3
hs00107204  cu   4
hs00107300  -1
hs00107400   1   7  ext   0.5   0.5
hs00107500  0.41783 3.5 3.5
hs00107600  8070
hs00107800  -1
hs00107801  306.31  5
********************************
***                            *
*** Film Tracking input        *
***                            *
```

```
*******************************
hsft10000  1
hsft10100  101 0 0.0 0 0.0 0 0 0 0 0
hsft20000  1
hsft20100  102 0 0.0 0 0.0 0 0 0 0 0
hsft30000  1
hsft30100  103 0 0.0 0 0.0 0 0 0 0 0
hsft40000  1
hsft40100  104 0 0.0 0 0.0 0 0 0 0 0
hsft50000  1
hsft50100  105 0 0.0 0 0.0 0 0 0 0 0
hsft60000  1
hsft60100  106 0 0.0 0 0.0 0 0 0 0 0
hsft70000  1
hsft70100  107 0 0.0 0 0.0 0 0 0 0 0
*
* CF to specify rgt bc T=348.061
*************************************
cf01000 HS_RGT_SIDE_1 equals 1 0.0 348.061
*                                  constant value
cf01010  1.0 0.0 time
*************************************
* CF to specify rgt bc T=344.896
cf02000 HS_RGT_SIDE_2 equals 1 0.0 344.896
*                                  constant value
cf02010 1.0 0.0 time
*************************************
* CF to specify rgt bc T=341.064
cf03000 HS_RGT_SIDE_3 equals 1 0.0 341.064
*                                  constant value
cf03010 1.0 0.0 time
*************************************
* CF to specify rgt bc T=336.276
cf04000 HS_RGT_SIDE_4 equals 1 0.0 336.276
*                                  constant value
cf04010 1.0 0.0 time
*************************************
* CF to specify rgt bc T=330.009
cf05000 HS_RGT_SIDE_5 equals 1 0.0 330.009
*                                  constant value
cf05010 1.0 0.0 time
*************************************
* CF to specify rgt bc T=321.141
cf06000 HS_RGT_SIDE_6 equals 1 0.0 321.141
*                                  constant value
cf06010 1.0 0.0 time
*************************************
* CF to specify rgt bc T=306.31
cf07000 HS_RGT_SIDE_7 equals 1 0.0 306.31
*                                  constant value
cf07010 1.0 0.0 time
*************************************
*
.        * Terminator
```

Mp.txt:

```
*****************************************************
***
***   Non-Condensible gases
*****************************************************
***
```

```
***   Gas     Material Number
***
NCG000  O2        4
NCG001  N2        5
***
*****************************************************
***
***         Material Properties
*****************************************************
***         Property             Units
***         temperature           K
***         density               kg/m**3
***         heat capacity         J/kg-K
***         thermal conductivity  W/m-K
*****************************************************
* ---------------------------------------------------
***        Material 1 is CU
* ---------------------------------------------------
MPMAT00100   cu
***
***        Property     tab func
***
MPMAT00101   rho          1
MPMAT00102   cps          2
MPMAT00103   thc          3
***
***         density of cu
***
TF00100    'rho cu'  2  1.00  0.0
***
***        temperature     rho
***
TF00112      293.15       8933.
TF00113     3000.0        8933.
***
***         heat capacity of cu
***
TF00200     'cps cu'   2  1.00  0.0
***
***        temperature     cps
***
TF00212       293.15       385.
TF00213      3000.0        385.
***
***        thermal conductivity of cu
***
TF00300     'thc cu'    2    1.0  0.0
***
***         temperature     thc
***
TF00312       293.15        401.
TF00313      3000.0         401.
*
.
```

Wisconsin Flat Plate Condensation Tests: EXEC Input --

```
*************************************************
*                                               *
*    MELGEN INPUT                               *
*    Wisconsin Plate Calculation                *
*    MELCOR Default Setting                     *
*    Case 1 --- 1m/s                            *
```

```
*                                                  *
**************************************************
*eor*    melgen
*
title   'Case1'
*
restartf        Case1.rst
outputf         Case1.out
diagf           Case1_g.dia
*
tstart 0.0
dttime 0.1
*
*
*
*
***********************************
* Active                          *
***********************************
*
r*i*f .\cont.txt
r*i*f .\mp.txt
r*i*f .\hs.txt
r*i*f .\fl.txt
*
.  *terminate
*eor*    melcor
************************************************************
*            MELCOR Input                                  *
*            Wisconsin Plate Calculation                   *
************************************************************
*
title   'Case1'
*
restartf        Case1.rst
outputf         Case1.out
diagf           Case1_g.dia
plotf           Case1.ptf
messagef        Case1.mes
*
crtout
*
cpulim  2000.0
cpuleft 30.0
*
restart 0
* tstart 0.0
dttime  0.01
*
tend 500.0
* tend 2000.0
*
*       time    dtmax   dtmin   dtedit  dtplot  dtrest
time1     0.0   0.1     0.001   5.0     1.0      5.0
time2     500.   0.1     0.001   1.0     1.0      10.0
*
*
*
. *terminate
```

Cont.txt:

```
*********************************
* CVH INPUT                     *
*********************************
*
*************************************
* Wisconsin Test Analysis           *
*************************************
*
*
cv00100  Up_plen        2  2  1     * Non-Equ Thermo, Vert flow, ctmt
cv001a0  3
cv001a1  pvol       1.0e5
cv001a2  tatm       343.15
cv001a3  mlfr.4     0.21
cv001a4  mlfr.5     0.79
* cv001a6  ph2o       0.0
* cv001a5  rhum    0.0
cv001a6  mass.1     1.0e-10
cv001b1  12.0        0.0
cv001b2  22.0        1.0e5
*
*                                                                                cv00200
Chamber        2  2  1     * Non-Equ Thermo, Vert flow, ctmt        cv00200  Chamber
2  2  1     * Non-Equ Thermo, Vert flow, ctmt        cv002a0  3
cv002a1  pvol       1.0e5
cv002a2  tatm       343.15
cv002a3  mlfr.4     0.21
cv002a4  mlfr.5     0.79
* cv002a6  ph2o       0.0
* cv002a5  rhum    0.0
cv002a6  mass.1     1.0e-10
cv002b1  10.0        0.0
cv002b2  12.0        2.0
cv00203  1.0
*
cv00300  Lo_Plen        2  2  1     * Non-Equ Thermo, Vert flow, ctmt
cv003a0  3
cv003a1  pvol       1.0e5
cv003a2  tatm       343.15
cv003a3  mlfr.4     0.21
cv003a4  mlfr.5     0.79
* cv003a6  ph2o       0.0
* cv003a5  rhum    0.0
cv003a6  mass.1     1.0e-10
cv003b1  0.0       0.0
cv003b2  10.0      1.0e5
*
.                                    * terminator
```

Fl.txt:

```
*************************************************
* FL input                                      *
*************************************************
*
*************************************************
* Up_Plen to Chamber                            *
*************************************************
*                  Volumes    Junc Elev
*                 FM    TO   FM    TO
```

```
fl00100 c#1-c#2    1     2   12.0  12.0
*
fl00101   1.0   0.03   1.0  * A, L, Frac Open
fl00102   0    0   0    0
fl00103   1.0   1.0   0.7   0.7       * k(forward), k(reverse), CDCHKF,CDCHKR
fl001s1   1.0   0.001   0.402
fl001t1 2   900           * control func. for velocity
*
*****************************************************
* Chamber to Lo_Plen                                 *
*****************************************************
*                  Volumes    Junc Elev
*                 FM    TO   FM    TO
fl00200 c#2-c#3    2     3   10.0  10.0
*
fl00201   1.0   0.03   1.0  * A, L, Frac Open
fl00202   0    0   0    0
fl00203   1.0     1.0  0.7   0.7       * k(forward), k(reverse), CDCHKF,CDCHKR
fl002s1   1.0   0.001   0.46
*
cf90000 'injection'  equals  1  1.0  0.0
cf90010   0.0   1.0  time
.              * terminator
```

Hs.txt:

```
*****************************************************
***                                                *
*** Heat Structure Input                           *
***                                                *
*****************************************************
* SC00000 4253 2328. 5 * Upper Re for Laminar
* SC00001 4253 2329. 6 * Lower Re for Turbulent
* SC00002 4253 -100. 7 * ef1
* SC00003 4253 8.6957 8 * C
* SC00004 4253 -0.6 9   * ef2
* SC00005 4253 0.0 10   * ef3
* SC00006 4253 1.0 11   * ef4
* SC00007 4110 0.14 1   * Cturb
*
*****************************************************
* External data file write                          *
* Wall surface temperature                          *
*****************************************************
edf00100 tsur_data 1  write
edf00101 'tsur_data.txt'
edf00102 '1P,2e14.5'
edf00110 0. 5.0
edf001aa hs-temp.0010101
*
**************
* v1         *
**************
hs00101000   5   1  -1
hs00101001  v1
hs00101002  10.0  1.
hs00101100  -1  1  0.0
hs00101102  0.001  2
hs00101103  0.002  3
hs00101104  0.004  4
hs00101105  0.008  5
hs00101200  -1
```

```
hs00101201  cu   1
hs00101202  cu   2
hs00101203  cu   3
hs00101204  cu   4
hs00101300  -1
hs00101400   1   2  ext   0.5   0.5
hs00101500  0.162032 1.066  1.066
hs00101600  8010
hs00101800  -1
hs00101801  303.15  5
*
**********************************
* v2 (drain down structure        *
**********************************
hs00102000   5   1  -1
hs00102001  v2
hs00102002  1.0  1.
hs00102100  -1  1  0.0
hs00102102  0.001  2
hs00102103  0.002  3
hs00102104  0.004  4
hs00102105  0.008  5
hs00102200  -1
hs00102201  cu   1
hs00102202  cu   2
hs00102203  cu   3
hs00102204  cu   4
hs00102300  -1
hs00102400   1   3  ext   0.5   0.5
hs00102500  1.0 1.0 1.0
hs00102600  0
hs00102800  -1
hs00102801  303.15  5
*
*******************************
***                           *
*** Film Tracking input       *
***                           *
*******************************
hsft10000  2
hsft10100  101 1 0.0 0 0.0 0 0 0 0 0
hsft10101  102 1.0 0.0
hsft10200  102 0 0.0 0 0.0 0 0 0 0 0
*
* CF to specify rgt bc T=303.15
****************************************
cf01000 HS_RGT_SIDE_1 equals 1 0.0 303.15
*                               constant value
cf01010  1.0 0.0 time
****************************************
****************************************
*
.        * terminator
```

Mp.txt:

```
*****************************************************
***
***   Non-Condensible gases
*****************************************************
***
***   Gas     Material Number
```

```
***
NCG000  O2       4
NCG001  N2       5
***
*****************************************************
***
***         Material Properties
*****************************************************
***         Property             Units
***         temperature           K
***         density               kg/m**3
***         heat capacity         J/kg-K
***         thermal conductivity  W/m-K
*****************************************************
* -------------------------------------------------
***        Material 1 is CU
* -------------------------------------------------
MPMAT00100   cu
***
***        Property     tab func
***
MPMAT00101   rho          1
MPMAT00102   cps          2
MPMAT00103   thc          3
***
***         density of cu
***
TF00100    'rho cu'  2  1.00  0.0
***
***        temperature     rho
***
TF00112      293.15       8933.
TF00113     3000.0        8933.
***
***         heat capacity of cu
***
TF00200     'cps cu'   2  1.00  0.0
***
***        temperature     cps
***
TF00212       293.15       385.
TF00213      3000.0        385.
***
***        thermal conductivity of cu
***
TF00300     'thc cu'    2    1.0  0.0
***
***         temperature     thc
***
TF00312       293.15        401.
TF00313      3000.0         401.
*
.    *terminate
```

Phebus Test FPT0: EXEC Input --

```
************************************************
*                                              *
*    Phebus Calculation                        *
*    Using the film tracking input             *
*                                              *
************************************************
```

```
*eor*   melgen
title   'Phebus'
*
restartf        Case1.rst
outputf         Case1.out
diagf           Case1_g.dia
*
dttime 0.1
*
************************************                              *
************************************                              * Active
*
************************************
*
r*i*f .\cont.txt
r*i*f .\mp.txt
r*i*f .\hs.txt
r*i*f .\fl.txt
*
.  * terminate
*eor*   melcor
title   'Phebus'
*
restartf        Case1.rst
outputf         Case1.out
diagf           Case1_g.dia
plotf           Case1.ptf
messagef        Case1.mes
*
crtout
*
cpulim  2000.0
cpuleft 30.0
*
restart 0
dttime  0.01
*
* tend  19998.0
tend 22000.0
*tend 2000.
*
*       time    dtmax   dtmin   dtedit  dtplot  dtrest
time1   0.0     0.1     0.001    10.0    5.0     50.0
time2   100.    0.1     0.001    20.0    20.     100.0
time3   500.    0.5     0.001    50.0    20.0    100.0
time4   4000.   0.5     0.001    100.    50.0    500.0
time5   8000.   0.5     0.001    100.    100.    500.0
time6   12000.  0.5     0.001    200.0   50.0    1000.
time7   22000.  0.5     0.001    100.    100.0   1000.
*
*
.  * terminate
```

Cont.txt:

```
*******************************************
***
*** Phebus containment
***
CV10000  'Containment'   2   2   1
CV10001  2    0
CV100A0  3
```

```
CV100A1  PVOL  1.75313e5
CV100A2  RHUM  0.43483
CV100A3  TATM  378.086
CV100A4  TPOL  363.15
CV100A5  ZPOL  0.369
CV100A6  MLFR.4   0.04993  * Oxygen
CV100A7  MLFR.5   0.95007  * Nitrogen
CV100B1  0.0    0.0
CV100B2  0.53037  0.144099
CV100B3  4.44307  10.10071
CV100C1  MASS.3   200   2
CV100C2  AE       210   2
CV100C3  MASS.6   300   2
CV100C4  TE       310   8
***
TF20000  'steam_rate'  38  1.0  0.0
*           time          mass rate
TF20011  0.00000E+00    1.10000E-06
TF20012  3.80000E+01    1.94000E-03
TF20013  2.79100E+03    1.94000E-03
TF20014  2.85100E+03    5.10000E-04
TF20015  8.62100E+03    5.10000E-04
TF20016  8.73800E+03    5.00000E-04
TF20017  8.76800E+03    5.40000E-04
TF20018  9.52900E+03    5.40000E-04
TF20019  9.88835E+03    1.21000E-03
TF20020  1.00530E+04    1.85000E-03
TF20021  1.03000E+04    2.51000E-03
TF20022  1.04220E+04    2.79000E-03
TF20023  1.05130E+04    2.91000E-03
TF20024  1.06900E+04    3.00000E-03
TF20025  1.07760E+04    2.90000E-03
TF20026  1.13620E+04    2.90000E-03
TF20027  1.13630E+04    1.07000E-03
TF20028  1.17830E+04    1.07000E-03
TF20029  1.17840E+04    2.90000E-03
TF20030  1.35290E+04    2.90000E-03
TF20031  1.36730E+04    2.76000E-03
TF20032  1.39600E+04    2.49000E-03
TF20033  1.40470E+04    2.42000E-03
TF20034  1.44820E+04    2.20000E-03
TF20035  1.48880E+04    2.00000E-03
TF20036  1.50030E+04    1.88000E-03
TF20037  1.51750E+04    1.73000E-03
TF20038  1.52330E+04    1.67000E-03
TF20039  1.54940E+04    1.53000E-03
TF20040  1.55520E+04    1.51000E-03
TF20041  1.56970E+04    1.43000E-03
TF20042  1.57270E+04    1.51000E-03
TF20043  1.59620E+04    1.51000E-03
TF20044  1.76310E+04    1.51000E-03
TF20045  1.86560E+04    1.51000E-03
TF20046  1.96520E+04    1.51000E-03
TF20047  1.97100E+04    4.12000E-07
TF20048  2.27850E+04    1.16000E-07
***
TF21000  'steam_energy'  38   1.0   0.0
*          time           energy
TF21011  0.00000E+00    3.02144E+00
TF21012  3.80000E+01    5.32871E+03
TF21013  2.79100E+03    5.32871E+03
TF21014  2.85100E+03    1.40085E+03
TF21015  8.62100E+03    1.40085E+03
```

```
TF21016  8.73800E+03    1.37338E+03
TF21017  8.76800E+03    1.48325E+03
TF21018  9.52900E+03    1.48325E+03
TF21019  9.88835E+03    3.32358E+03
TF21020  1.00530E+04    5.08151E+03
TF21021  1.03000E+04    6.89437E+03
TF21022  1.04220E+04    7.66346E+03
TF21023  1.05130E+04    7.99307E+03
TF21024  1.06900E+04    8.24028E+03
TF21025  1.07760E+04    7.96560E+03
TF21026  1.13620E+04    7.96560E+03
TF21027  1.13630E+04    2.93903E+03
TF21028  1.17830E+04    2.93903E+03
TF21029  1.17840E+04    7.96560E+03
TF21030  1.35290E+04    7.96560E+03
TF21031  1.36730E+04    7.58106E+03
TF21032  1.39600E+04    6.83943E+03
TF21033  1.40470E+04    6.64716E+03
TF21034  1.44820E+04    6.04287E+03
TF21035  1.48880E+04    5.49352E+03
TF21036  1.50030E+04    5.16391E+03
TF21037  1.51750E+04    4.75189E+03
TF21038  1.52330E+04    4.58709E+03
TF21039  1.54940E+04    4.20254E+03
TF21040  1.55520E+04    4.14761E+03
TF21041  1.56970E+04    3.92787E+03
TF21042  1.57270E+04    4.14761E+03
TF21043  1.59620E+04    4.14761E+03
TF21044  1.76310E+04    4.14761E+03
TF21045  1.86560E+04    4.14761E+03
TF21046  1.96520E+04    4.14761E+03
TF21047  1.97100E+04    1.13167E+00
TF21048  2.27850E+04    3.18624E-01
***
TF30000  'H2_mass'   6   1.0   0.0
*         time    mass rate
TF30011   0.0     0.0
TF30012   11362.  0.0
TF30013   11363.  2.1e-4
TF30014   11783.  2.1e-4
TF30015   11784.  0.0
TF30016   1.0e5   0.0
***
TF31000  'H2_temp'   6   1.0   0.0
*         time    mass rate
TF31011   0.0     423.15
TF31012   11362.  423.15
TF31013   11363.  423.15
TF31014   11783.  423.15
TF31015   11784.  423.15
TF31016   1.0e5   423.15
***
************************************
***
***  Environment
***
CV11000   'Environment'   2   2   1
CV11001  2    0
CV110A0  3
CV110A1  PVOL  1.0e5
CV110A2  TATM  300.0
CV110A5  MLFR.4   0.04993  * Oxygen
CV110A6  MLFR.5   0.95007  * Nitrogen
```

```
CV110B1  -1.0    0.0
CV110B2  20.0    1.0e6
***
*
.  * terminate
```

Fl.txt:

```
****************************************
***
*** flow to maintain sump level
***
****************************************
fl10000 c#100-c#110   100  110  0.0   0.0
fl10001  0.01  1.0   1.0
fl10002  0
fl10003  1.5   1.5
fl100s1  0.01  1.0e-6  0.2
fl100t1  2   900
*
cf90000  'drain' add  2  0.1  0.0
cf90010  9.0   0.0  cfvalu.900
cf90011  1.0   0.0  cfvalu.910
*
cf91000  'rate'  tab-fun  1  1.0  0.0
cf91003   920
cf91010   1.0   0.0  cvh-cliqlev.100
*
tf92000   'level-set'  4  1.0  0.0
tf92011   0.0   0.0
tf92012   0.37  0.0
tf92013   0.40  0.1
tf92014   0.42  0.4
*
. * terminate
```

Hs.txt:

```
****************************************
***
***  Heat Structure Input for Phebus
***
****************************************
*
****************************************
* vessel
****************************************
hs00101000  5   1  -1
hs00101001  vessel
hs00101002  0.0   1.
hs00101100  -1    1  0.0
hs00101102   0.001  2
hs00101103   0.002  3
hs00101104   0.004  4
hs00101105   0.008  5
hs00101200   -1
hs00101201   cu   1
hs00101202   cu   2
hs00101203   cu   3
hs00101204   cu   4
hs00101300   -1
hs00101400   1  100  ext  0.5  0.5
```

```
hs00101401   0.85 gray-gas-a 1.236
hs00101500   25.16   3.9    3.9
hs00101600   2240 110  ext  0.5  0.5
hs00101800   -1
hs00101801   383.15  5
*
hs00102000  5   1   -1
hs00102001  wet
hs00102002  2.9    1.
hs00102100  -1   1    0.0
hs00102102   0.001  2
hs00102103   0.002  3
hs00102104   0.004  4
hs00102105   0.008  5
hs00102200   -1
hs00102201   cu   1
hs00102202   cu   2
hs00102203   cu   3
hs00102204   cu   4
hs00102300   -1
hs00102400   1  100  ext  0.5  0.5
hs00102401   0.85 gray-gas-a 1.236
hs00102500   2.324   1.5   1.5
hs00102600   2250 110  ext  0.5  0.5
hs00102800   -1
hs00102801   352.15  5
*
hs00103000  5   1   -1
hs00103001  dry
hs00103002  2.1    1.
hs00103100  -1   1    0.0
hs00103102   0.001  2
hs00103103   0.002  3
hs00103104   0.004  4
hs00103105   0.008  5
hs00103200   -1
hs00103201   cu   1
hs00103202   cu   2
hs00103203   cu   3
hs00103204   cu   4
hs00103300   -1
hs00103400   1  100  ext  0.5  0.5
hs00103401   0.85 gray-gas-a 1.236
hs00103500   1.062   0.8   0.8
hs00103600   2260 110  ext  0.5  0.5
hs00103800   -1
hs00103801   393.15  5
*
hs00104000  5   1   -1
hs00104001  collar
hs00104002  0.37    1.
hs00104100  -1   1    0.0
hs00104102   0.001  2
hs00104103   0.002  3
hs00104104   0.004  4
hs00104105   0.008  5
hs00104200   -1
hs00104201   cu   1
hs00104202   cu   2
hs00104203   cu   3
hs00104204   cu   4
hs00104300   -1
hs00104400   1  100  ext  0.5  0.5
```

```
hs00104401   0.85 gray-gas-a 1.236
hs00104500   0.303   0.16   0.16
hs00104600   2270 110  ext  0.5  0.5
hs00104800   -1
hs00104801   366.15  5
*
hs00105000  5   1   -1
hs00105001  swall
hs00105002  0.0    1.
hs00105100  -1   1    0.0
hs00105102   0.001  2
hs00105103   0.002  3
hs00105104   0.004  4
hs00105105   0.008  5
hs00105200   -1
hs00105201   cu   1
hs00105202   cu   2
hs00105203   cu   3
hs00105204   cu   4
hs00105300   -1
hs00105400   1  100  ext  0.5  0.5
hs00105401   0.85 gray-gas-a 1.236
hs00105500   0.84   0.37   0.37
hs00105600   2280 110  ext  0.5  0.5
hs00105800   -1
hs00105801   363.15  5
*
hs00106000  5   1   -1
hs00106001  sflr
hs00106002  0.    -1.0e-7
hs00106100  -1   1    0.0
hs00106102   0.001  2
hs00106103   0.002  3
hs00106104   0.004  4
hs00106105   0.008  5
hs00106200   -1
hs00106201   cu   1
hs00106202   cu   2
hs00106203   cu   3
hs00106204   cu   4
hs00106300   -1
hs00106400   1  100  ext  0.5  0.5
hs00106500   0.3895   0.7   0.7
hs00106600   2280 110  ext  0.5  0.5
hs00106800   -1
hs00106801   363.15  5
***
***
TF24000  'vessel_T'  2  1.0  0.0
*          time         Temp
TF24011  0.00000E+00    383.15
TF24012  1.0e5          383.15
*
TF25000  'wet_T'  10  1.0  0.0
*          time          Temp
TF25011  0.00000E+00    353.15
TF25012  2941.          353.15
TF25013  3001.          350.15
TF25014  9529.          350.15
TF25015  10690.         354.15
TF25016  13529.         354.15
TF25017  15494.         353.15
TF25018  19802.         353.15
```

```
TF25019  19860.         349.15
TF25020  22785.         349.15
*
TF26000  'dry_T'  2  1.0  0.0
*           time         Temp
TF26011  0.00000E+00    393.15
TF26012  1.0e5          393.15
*
TF27000  'collar_T'  2  1.0  0.0
*           time         Temp
TF27011  0.00000E+00    366.15
TF27012  1.0e5          366.15
*
TF28000  'swall_T'  2  1.0  0.0
*           time         Temp
TF28011  0.00000E+00    363.15
TF28012  1.0e5          363.15
*
.   * terminate
```

Mp.txt:

```
*****************************************************
***
***   Non-Condensible gases
*****************************************************
***
***   Gas     Material Number
***
NCG000  O2       4
NCG001  N2       5
NCG002  H2       6
***
*****************************************************
***
***         Material Properties
*****************************************************
***         Property             Units
***         temperature           K
***         density               kg/m**3
***         heat capacity         J/kg-K
***         thermal conductivity  W/m-K
*****************************************************
* -------------------------------------------------
***        Material 1 is CU
* -------------------------------------------------
MPMAT00100   cu
***
***        Property     tab func
***
MPMAT00101   rho          1
MPMAT00102   cps          2
MPMAT00103   thc          3
***
***         density of cu
***
TF00100    'rho cu'  2  1.00  0.0
***
***        temperature     rho
***
TF00112      293.15       8933.
TF00113     3000.0        8933.
```

```
***
***         heat capacity of cu
***
TF00200     'cps cu'   2  1.00  0.0
***
***        temperature     cps
***
TF00212       293.15       385.
TF00213      3000.0        385.
***
***        thermal conductivity of cu
***
TF00300     'thc cu'    2    1.0  0.0
***
***         temperature     thc
***
TF00312       293.15        401.
TF00313      3000.0         401.
*
.       *terminate
```

JAERI Spray Test (PHS-1): EXEC Input --

```
** JAERI Test PHS_1
********************************************************************************
********************************************************************************
*eor*      melgen
**********************
**********************
***                  ***
***  MELGEN INPUT  ***
***                  ***
**********************
TITLE     'JAERI'
***JOBID      JAERI
CRTOUT
OUTPUTF   'JAERI.out'
RESTARTF  'JAERI.rst'
DIAGF     'JAERI.gdia'
TSTART     0.
DTTIME    .1
***
EDF11100 special-data   8  write
EDF11101 'th.txt'
EDF11102  13E12.5
EDF11110  0.0  0.5
EDF11111  10.  1.0
EDF11112  20.  5.0
EDF11113  100. 10.0
EDF11114  500.0 100.0
EDF11115  1000.  100.0
EDF11116  12000.  100.0
EDF111AA CVH-P.009
EDF111AB CVH-TVAP.009
EDF111AC CVH-TSAT(A).009
EDF111AD CVH-TSAT(P).009
EDF111AE CVH-TLIQ.016
EDF111AF CVH-CLIQLEV.016
EDF111AG CVH-MASS.1.016
EDF111AH HS-FILM-MASS-L.00110
*********************************************************
* Containment Sprays                                    *
```

```
************************************************************
*** Source in cell#2
*          Name       Vol   Elev     CF#
SPRSR0100  spray1     6     15.0    310
*            T,K        Flow
SPRSR0101   313.15     0.002877
*
SPRSR0102   0.001      1.
***
*** Source in cell#3
*          Name       Vol   Elev     CF#
SPRSR0200  spray1     7     15.0    310
*            T,K        Flow
SPRSR0201   313.15     0.002877
*
SPRSR0202   0.001      1.
**
* Time to activate sprays
CF31000   SPRAY_Time   L-GT  2   1.   0.
CF31001   .FALSE.
CF31010   1.   0.   TIME
CF31011   0.   0.  TIME
CF31005   LATCH
*
***
* Carry over of spray droplets
***       From    To    Fraction
*SPRJUN01   3      5      1.0
*SPRJUN02   5      7      1.0
SPRJUN03   7      9      1.0
SPRJUN04   9     11      1.0
SPRJUN05   11    13      1.0
SPRJUN06   13    15      1.0
SPRJUN07   15    16      1.0
*SPRJUN08   2      4      1.0
*SPRJUN09   4      6      1.0
SPRJUN10   6      8      1.0
SPRJUN11   8      10     1.0
SPRJUN12   10     12     1.0
SPRJUN13   12     14     1.0
SPRJUN14   14     16     1.0
***
SPRSUMP0   16
SPRSUMP1   16
************************************************************
*** Sensitivity Study
************************************************************
* Turbulent convection coefficient
sc41100  4110  0.14  1
sc42510  4251  0.00005 2
************************************************************
***
r*i*f   mp.txt
r*i*f   cont.txt
r*i*f   hs.txt
r*i*f   fl.txt
************************************************************
.  * terminate
*eor* melcor
************************
***  MELCOR INPUT    ***
************************
TITLE     'JAERI'
```

```
***JOBID      ref
*
OUTPUTF   'JAERI.out'
PLOTF     'JAERI.ptf'
RESTARTF  'JAERI.rst'
MESSAGEF  'JAERI.mes'
DIAGF     'JAERI.dia'
*
CRTOUT
***CYMESF    10 10
*
RESTART  -1
tend  11000.
***EXACTTIME1         100.
CPULIM             2.0e6
CPULEFT            100.0
*cvhtrace 3
*
************************************
*** Invoke desired sequences
************************************
***
***
************************************************************
*
*          TIME    DTMAX     DTMIN     DTEDIT    DTPLOT    DTREST
*
TIME1       0.0     0.1      1.0e-8      0.5       0.5     10.0
TIME2       10.     0.2      1.0E-8      1.0       1.0     20.0
TIME3       20.     0.5      1.0E-8      5.0       5.0     50.0
TIME4      100.     1.0      1.0E-8      10.0      10.0     50.0
TIME5      500.     1.0      1.0E-8      100.0      100.0    200.0
TIME6     1000.     1.0      1.0E-6      100.0      100.0    500.0
TIME7    11000.     1.0      1.0E-6     100.0      100.0    100.0
************************************************************
***** END OF MELCOR INPUT ***********************************
************************************************************
.  * terminate
```

Cont.txt:

```
***
cv00100  'cell1'  2   2   4
cv00101   2   0
cv001A0   3
cv001A1   PVOL 3.5e5
cv001A2   RHUM  1.0
cv001A3   TATM  395.65
cv001A4   MLFR.4 0.21   * Oxygen
cv001A5   MLFR.5 0.79   * Nitrogen
cv001B1   18.0     0.0
cv001B2   19.0    34.851
***
cv00200  'cell2'  2   2   4
cv00201   2   0
cv002A0   3
cv002A1   PVOL 3.5e5
cv002A2   RHUM  1.0
cv002A3   TATM  395.65
cv002A4   MLFR.4 0.21   * Oxygen
cv002A5   MLFR.5 0.79   * Nitrogen
cv002B1   16.56   0.0
```

```
cv002B2   18.0    23.64
***
cv00300  'cell3'  2   2   4
cv00301   2   0
cv003A0   3
cv003A1   PVOL 3.5e5
cv003A2   RHUM  1.0
cv003A3   TATM  395.65
cv003A4   MLFR.4 0.21   * Oxygen
cv003A5   MLFR.5 0.79   * Nitrogen
cv003B1   16.56     0.0
cv003B2   18.0     26.767
***
cv00400  'cell4'  2   2   4
cv00401   2   0
cv004A0   3
cv004A1   PVOL 3.5e5
cv004A2   RHUM  1.0
cv004A3   TATM  395.65
cv004A4   MLFR.4 0.21   * Oxygen
cv004A5   MLFR.5 0.79   * Nitrogen
cv004B1   15.0     0.0
cv004B2   16.56    28.998
***
cv00500  'cell5'  2   2   4
cv00501   2   0
cv005A0   3
cv005A1   PVOL 3.5e5
cv005A2   RHUM  1.0
cv005A3   TATM  395.65
cv005A4   MLFR.4 0.21   * Oxygen
cv005A5   MLFR.5 0.79   * Nitrogen
cv005B1   15.0     0.0
cv005B2   16.56     28.998
***
cv00600  'cell6'  2   2   4
cv00601   2   0
cv006A0   3
cv006A1   PVOL 3.5e5
cv006A2   RHUM  1.0
cv006A3   TATM  395.65
cv006A4   MLFR.4 0.21   * Oxygen
cv006A5   MLFR.5 0.79   * Nitrogen
cv006B1   13.5     0.0
cv006B2   15.0     27.882
***
cv00700  'cell7'  2   2   4
cv00701   2   0
cv007A0   3
cv007A1   PVOL 3.5e5
cv007A2   RHUM  1.0
cv007A3   TATM  395.65
cv007A4   MLFR.4 0.21   * Oxygen
cv007A5   MLFR.5 0.79   * Nitrogen
cv007B1   13.5     0.0
cv007B2   15.0     27.882
***
cv00800  'cell8'  2   2   4
cv00801   2   0
cv008A0   3
cv008A1   PVOL 3.5e5
cv008A2   RHUM  1.0
cv008A3   TATM  395.65
```

```
cv008A4   MLFR.4 0.21   * Oxygen
cv008A5   MLFR.5 0.79   * Nitrogen
cv008B1   12.0     0.0
cv008B2   13.5     27.882
***
cv00900  'cell9'  2   2   4
cv00901   2   0
cv009A0   3
cv009A1   PVOL 3.5e5
cv009A2   RHUM  1.0
cv009A3   TATM  395.65
cv009A4   MLFR.4 0.21   * Oxygen
cv009A5   MLFR.5 0.79   * Nitrogen
cv009B1   12.0     0.0
cv009B2   13.5     27.882
***
cv01000  'cell10'  2   2   4
cv01001   2   0
cv010A0   3
cv010A1   PVOL 3.5e5
cv010A2   RHUM  1.0
cv010A3   TATM  395.65
cv010A4   MLFR.4 0.21   * Oxygen
cv010A5   MLFR.5 0.79   * Nitrogen
cv010B1   10.0     0.0
cv010B2   12.0     37.176
***
cv01100  'cell11'  2   2   4
cv01101   2   0
cv011A0   3
cv011A1   PVOL 3.5e5
cv011A2   RHUM  1.0
cv011A3   TATM  395.65
cv011A4   MLFR.4 0.21   * Oxygen
cv011A5   MLFR.5 0.79   * Nitrogen
cv011B1   10.0     0.0
cv011B2   12.0     37.176
***
cv01200  'cell12'  2   2   4
cv01201   2   0
cv012A0   3
cv012A1   PVOL 3.5e5
cv012A2   RHUM  1.0
cv012A3   TATM  395.65
cv012A4   MLFR.4 0.21   * Oxygen
cv012A5   MLFR.5 0.79   * Nitrogen
cv012B1   8.50     0.0
cv012B2   10.0     27.882
***
cv01300  'cell13'  2   2   4
cv01301   2   0
cv013A0   3
cv013A1   PVOL 3.5e5
cv013A2   RHUM  1.0
cv013A3   TATM  395.65
cv013A4   MLFR.4 0.21   * Oxygen
cv013A5   MLFR.5 0.79   * Nitrogen
cv013B1   8.50     0.0
cv013B2   10.0     27.882
***
cv01400  'cell14'  2   2   4
cv01401   2   0
cv014A0   3
```

```
cv014A1   PVOL 3.5e5
cv014A2   RHUM  1.0
cv014A3   TATM  395.65
cv014A4   MLFR.4 0.21   * Oxygen
cv014A5   MLFR.5 0.79   * Nitrogen
cv014B1   6.50     0.0
cv014B2   8.50     37.176
***
cv01500  'cell15'  2   2   4
cv01501   2   0
cv015A0   3
cv015A1   PVOL 3.5e5
cv015A2   RHUM  1.0
cv015A3   TATM  395.65
cv015A4   MLFR.4 0.21   * Oxygen
cv015A5   MLFR.5 0.79   * Nitrogen
cv015B1   6.50     0.0
cv015B2   8.50     37.176
***
cv01600  'cell16'  2   2   4
cv01601   2   0
cv016A0   3
cv016A1   PVOL 3.5e5
cv016A2   RHUM  1.0
cv016A3   TATM  395.65
cv016A4   MLFR.4 0.21   * Oxygen
cv016A5   MLFR.5 0.79   * Nitrogen
cv016B1   0.00     0.0
cv016B2   6.50     241.646
***
*** Environment
cv01700  'Environ'  2  2  1
cv01701  2   0
cv017A0  3
cv017A1  pvol  1.0e5
cv017A2  tatm  300.
cv017A5  mlfr.4  0.21   * Oxygen
cv017A6  mlfr.5  0.79   * Nitrogen
cv017B1  -1.0    0.0
cv017B2  20.0    1.0e6
*
. *terminate
```

Fl.txt:

```
***
* vertical pathways
***
fl10000 'c#1-c#2'  1   2  18.0  18.0
*         FLARA    FLLEN   FLOPO    FLHGTF   FLHGTT
fl10001  12.074    1.0     1.0       0.05     0.05
fl10002   0     0     1      1
fl10003   1.0    1.0
fl100S1   12.074   1.0e-6   1.0    1.0e-6
***
fl10100 'c#1-c#3'  1   3  18.0  18.0
*         FLARA    FLLEN   FLOPO    FLHGTF   FLHGTT
fl10101  18.588    1.0     1.0       0.05     0.05
fl10102   0     0     1      1
fl10103   1.0    1.0
fl101S1  18.588   1.0e-6   1.0    1.0e-6
***
```

```
fl10200 'c#3-c#5'  3   5  16.56  16.56
*         FLARA    FLLEN   FLOPO    FLHGTF   FLHGTT
fl10201  18.588    1.0     1.0       0.05     0.05
fl10202   0     0     1      1
fl10203   1.0    1.0
fl102S1  18.588   1.0e-6   1.0    1.0e-6
***
fl10300 'c#5-c#7'  5   7  15.0  15.0
*         FLARA    FLLEN   FLOPO    FLHGTF   FLHGTT
fl10301  18.588    1.0     1.0       0.05     0.05
fl10302   0     0     1      1
fl10303   1.0    1.0
fl103S1  18.588   1.0e-6   1.0    1.0e-6
***
fl10400 'c#7-c#9'  7   9  13.5  13.5
*         FLARA    FLLEN   FLOPO    FLHGTF   FLHGTT
fl10401  18.588    1.0     1.0       0.05     0.05
fl10402   0     0     1      1
fl10403   1.0    1.0
fl104S1  18.588   1.0e-6   1.0    1.0e-6
***
fl10500 'c#9-c#11'  9   11  12.0  12.0
*         FLARA    FLLEN   FLOPO    FLHGTF   FLHGTT
fl10501  18.588    1.0     1.0       0.05     0.05
fl10502   0     0     1      1
fl10503   1.0    1.0
fl105S1  18.588   1.0e-6   1.0    1.0e-6
***
fl10600 'c#11-c#13'  11   13  10.0  10.0
*         FLARA    FLLEN   FLOPO    FLHGTF   FLHGTT
fl10601  18.588    1.0     1.0       0.05     0.05
fl10602   0     0     1      1
fl10603   1.0    1.0
fl106S1  18.588   1.0e-6   1.0    1.0e-6
***
fl10700 'c#13-c#15'  13   15  8.5  8.5
*         FLARA    FLLEN   FLOPO    FLHGTF   FLHGTT
fl10701  18.588    1.0     1.0       0.05     0.05
fl10702   0     0     1      1
fl10703   1.0    1.0
fl107S1  18.588   1.0e-6   1.0    1.0e-6
***
fl10800 'c#15-c#16'  15   16  6.5  6.5
*         FLARA    FLLEN   FLOPO    FLHGTF   FLHGTT
fl10801  18.588    1.0     1.0       0.05     0.05
fl10802   0     0     1      1
fl10803   1.0    1.0
fl108S1  18.588   1.0e-6   1.0    1.0e-6
***
fl10900 'c#2-c#4'  2   4  16.56  16.56
*         FLARA    FLLEN   FLOPO    FLHGTF   FLHGTT
fl10901  18.588    1.0     1.0       0.05     0.05
fl10902   0     0     1      1
fl10903   1.0    1.0
fl109S1  18.588   1.0e-6   1.0    1.0e-6
***
fl11000 'c#4-c#6'  4   6  15.0   15.0
*         FLARA    FLLEN   FLOPO    FLHGTF   FLHGTT
fl11001  18.588    1.0     1.0       0.05     0.05
fl11002   0     0     1      1
fl11003   1.0    1.0
fl110S1  18.588   1.0e-6   1.0    1.0e-6
***
```

```
fl11100 'c#6-c#8'  6   8  13.5   13.5
*         FLARA    FLLEN   FLOPO    FLHGTF   FLHGTT
fl11101  18.588    1.0     1.0       0.05     0.05
fl11102   0     0     1      1
fl11103   1.0    1.0
fl1115S1  18.588   1.0e-6   1.0    1.0e-6
***
fl11200 'c#8-c#10'  8   10  12.0   12.0
*         FLARA    FLLEN   FLOPO    FLHGTF   FLHGTT
fl11201  18.588    1.0     1.0       0.05     0.05
fl11202   0     0     1      1
fl11203   1.0    1.0
fl1125S1  18.588   1.0e-6   1.0    1.0e-6
***
fl11300 'c#10-c#12'  10   12  10.0   10.0
*         FLARA    FLLEN   FLOPO    FLHGTF   FLHGTT
fl11301  18.588    1.0     1.0       0.05     0.05
fl11302   0     0     1      1
fl11303   1.0    1.0
fl1135S1  18.588   1.0e-6   1.0    1.0e-6
***
fl11400 'c#12-c#14'  12   14  8.5   8.5
*         FLARA    FLLEN   FLOPO    FLHGTF   FLHGTT
fl11401  18.588    1.0     1.0       0.05     0.05
fl11402   0     0     1      1
fl11403   1.0    1.0
fl1145S1  18.588   1.0e-6   1.0    1.0e-6
***
fl11500 'c#14-c#16'  14   16  6.5   6.5
*         FLARA    FLLEN   FLOPO    FLHGTF   FLHGTT
fl11501  18.588    1.0     1.0       0.05     0.05
fl11502   0     0     1      1
fl11503   1.0    1.0
fl1155S1  18.588   1.0e-6   1.0    1.0e-6
***
* horizontal pathways
***
fl11600 'c#2-c#3'  2   3  17.28   17.28
*         FLARA    FLLEN   FLOPO    FLHGTF   FLHGTT
fl11601  22.008    1.0     1.0       0.72     0.72
fl11602   3     0     1      1
fl11603   1.0    1.0
fl1165S1  22.008   1.0e-6   1.0    1.0e-6
***
fl11700 'c#4-c#5'  4   5  15.78   15.78
*         FLARA    FLLEN   FLOPO    FLHGTF   FLHGTT
fl11701  23.842    1.0     1.0       0.78     0.78
fl11702   3     0     1      1
fl11703   1.0    1.0
fl1175S1  23.842   1.0e-6   1.0    1.0e-6
***
fl11800 'c#6-c#7'  6   7  14.25   14.25
*         FLARA    FLLEN   FLOPO    FLHGTF   FLHGTT
fl11801  22.925    1.0     1.0       0.75     0.75
fl11802   3     0     1      1
fl11803   1.0    1.0
fl1185S1  22.925   1.0e-6   1.0    1.0e-6
***
fl11900 'c#8-c#9'  8   9  12.75   12.75
*         FLARA    FLLEN   FLOPO    FLHGTF   FLHGTT
fl11901  22.925    1.0     1.0       0.75     0.75
fl11902   3     0     1      1
fl11903   1.0    1.0
```

```
fl119S1  22.925   1.0e-6   1.0    1.0e-6
***
fl12000 'c#10-c#11'  10   11  11.0   11.0
*         FLARA    FLLEN   FLOPO    FLHGTF   FLHGTT
fl12001  30.567    1.0     1.0       1.0     1.0
fl12002   3     0     1      1
fl12003   1.0    1.0
fl120S1  30.567   1.0e-6   1.0    1.0e-6
***
fl12100 'c#12-c#13'  12   13  9.25   9.25
*         FLARA    FLLEN   FLOPO    FLHGTF   FLHGTT
fl12101  22.925    1.0     1.0       0.75     0.75
fl12102   3     0     1      1
fl12103   1.0    1.0
fl121S1  22.925   1.0e-6   1.0    1.0e-6
***
fl12200 'c#14-c#15'  14   15  7.5  7.5
*         FLARA    FLLEN   FLOPO    FLHGTF   FLHGTT
fl12201  30.567    1.0     1.0       1.0     1.0
fl12202   3     0     1      1
fl12203   1.0    1.0
fl122S1  30.567   1.0e-6   1.0    1.0e-6
***
****************************************
***
*** flow to maintain sump level
***
****************************************
fl12300 c#16-c#17   16  17  0.0   0.0
fl12301  0.01  1.0   1.0
fl12302  0
fl12303  1.5   1.5
fl123s1  0.01  1.0e-6  0.2
fl123t1  2   900
*
cf90000  'drain' add  2  0.1  0.0
cf90010  9.0   0.0  cfvalu.900
cf90011  1.0   0.0  cfvalu.910
*
cf91000  'rate'  tab-fun  1  1.0  0.0
cf91003   920
cf91010   1.0   0.0  cvh-cliqlev.016
*
tf92000   'level-set'  4  1.0  0.0
tf92011   0.0   0.0
tf92012   0.1  0.0
tf92013   0.11  0.1
tf92014   0.12  0.6
*
.  * terminate
```

Hs.txt:

```
* vessel vertical wall in cell #2
hs00110000   14   1   -1
hs00110001   wall2
hs00110002   16.56  1.
hs00110100   -1   1   0.0
hs00110102  0.001     2
hs00110103  0.002     3
hs00110104  0.004     4
hs00110105  0.006     5
```

```
hs00110106  0.01      6
hs00110107  0.015     7
hs00110108  0.02      8
hs00110109  0.025     9
hs00110110  0.027     10
hs00110111  0.037     11
hs00110112  0.057     12
hs00110113  0.067     13
hs00110114  0.077     14
hs00110200  -1
hs00110201  ss     1
hs00110202  ss     2
hs00110203  cs        3
hs00110204  cs        4
hs00110205  cs        5
hs00110206  cs        6
hs00110207  cs        7
hs00110208  cs        8
hs00110209  cs        9
hs00110210  insul     10
hs00110211  insul     11
hs00110212  insul     12
hs00110213  insul     13
hs00110300  -1
hs00110400  1  002  ext  0.5 0.5
* hs00110401  0.9  gray-gas-a  3.0
hs00110500  31.124  18.85  1.44
hs00110600  0
hs00110800  -1
hs00110801  395.65  14
***
* vessel vertical wall in cell #4
hs00111000   14   1   -1
hs00111001   wall4
hs00111002   15.0  1.
hs00111100   -1   1   0.0
hs00111102  0.001     2
hs00111103  0.002     3
hs00111104  0.004     4
hs00111105  0.006     5
hs00111106  0.01      6
hs00111107  0.015     7
hs00111108  0.02      8
hs00111109  0.025     9
hs00111110  0.027     10
hs00111111  0.037     11
hs00111112  0.057     12
hs00111113  0.067     13
hs00111114  0.077     14
hs00111200  -1
hs00111201  ss     1
hs00111202  ss     2
hs00111203  cs        3
hs00111204  cs        4
hs00111205  cs        5
hs00111206  cs        6
hs00111207  cs        7
hs00111208  cs        8
hs00111209  cs        9
hs00111210  insul     10
hs00111211  insul     11
hs00111212  insul     12
hs00111213  insul     13
```

```
hs00111300  -1
hs00111400  1  004  ext  0.5 0.5
* hs00111401  0.9  gray-gas-a  3.0
hs00111500  33.718  18.85  1.56
hs00111600  0
hs00111800  -1
hs00111801  395.65  14
*
***
* vessel vertical wall in cell #6
hs00112000   14   1   -1
hs00112001   wall6
hs00112002   13.5  1.
hs00112100   -1   1   0.0
hs00112102  0.001     2
hs00112103  0.002     3
hs00112104  0.004     4
hs00112105  0.006     5
hs00112106  0.01      6
hs00112107  0.015     7
hs00112108  0.02      8
hs00112109  0.025     9
hs00112110  0.027     10
hs00112111  0.037     11
hs00112112  0.057     12
hs00112113  0.067     13
hs00112114  0.077     14
hs00112200  -1
hs00112201  ss     1
hs00112202  ss     2
hs00112203  cs        3
hs00112204  cs        4
hs00112205  cs        5
hs00112206  cs        6
hs00112207  cs        7
hs00112208  cs        8
hs00112209  cs        9
hs00112210  insul     10
hs00112211  insul     11
hs00112212  insul     12
hs00112213  insul     13
hs00112300  -1
hs00112400  1  006  ext  0.5 0.5
* hs00112401  0.9  gray-gas-a  3.0
hs00112500  32.421  18.85  1.5
hs00112600  0
hs00112800  -1
hs00112801  395.65  14
***
* vessel vertical wall in cell #8
hs00113000   14   1   -1
hs00113001   wall8
hs00113002   12.0  1.
hs00113100   -1   1   0.0
hs00113102  0.001     2
hs00113103  0.002     3
hs00113104  0.004     4
hs00113105  0.006     5
hs00113106  0.01      6
hs00113107  0.015     7
hs00113108  0.02      8
hs00113109  0.025     9
hs00113110  0.027     10
```

```
hs00113111  0.037     11
hs00113112  0.057     12
hs00113113  0.067     13
hs00113114  0.077     14
hs00113200  -1
hs00113201  ss     1
hs00113202  ss     2
hs00113203  cs        3
hs00113204  cs        4
hs00113205  cs        5
hs00113206  cs        6
hs00113207  cs        7
hs00113208  cs        8
hs00113209  cs        9
hs00113210  insul     10
hs00113211  insul     11
hs00113212  insul     12
hs00113213  insul     13
hs00113300  -1
hs00113400  1  008  ext  0.5 0.5
* hs00113401  0.9  gray-gas-a  3.0
hs00113500  32.421  18.85  1.5
hs00113600  0
hs00113800  -1
hs00113801  395.65  14
***
* vessel vertical wall in cell #10
hs00114000   14   1   -1
hs00114001   wall10
hs00114002   10.0  1.
hs00114100   -1   1   0.0
hs00114102  0.001     2
hs00114103  0.002     3
hs00114104  0.004     4
hs00114105  0.006     5
hs00114106  0.01      6
hs00114107  0.015     7
hs00114108  0.02      8
hs00114109  0.025     9
hs00114110  0.027     10
hs00114111  0.037     11
hs00114112  0.057     12
hs00114113  0.067     13
hs00114114  0.077     14
hs00114200  -1
hs00114201  ss     1
hs00114202  ss     2
hs00114203  cs        3
hs00114204  cs        4
hs00114205  cs        5
hs00114206  cs        6
hs00114207  cs        7
hs00114208  cs        8
hs00114209  cs        9
hs00114210  insul     10
hs00114211  insul     11
hs00114212  insul     12
hs00114213  insul     13
hs00114300  -1
hs00114400  1  010  ext  0.5 0.5
* hs00114401  0.9  gray-gas-a  3.0
hs00114500  43.228  18.85  2.0
hs00114600  0
```

```
hs00114800  -1
hs00114801  395.65  14
***
* vessel vertical wall in cell #12
hs00115000   14   1   -1
hs00115001   wall12
hs00115002   8.5  1.
hs00115100   -1   1   0.0
hs00115102  0.001     2
hs00115103  0.002     3
hs00115104  0.004     4
hs00115105  0.006     5
hs00115106  0.01      6
hs00115107  0.015     7
hs00115108  0.02      8
hs00115109  0.025     9
hs00115110  0.027     10
hs00115111  0.037     11
hs00115112  0.057     12
hs00115113  0.067     13
hs00115114  0.077     14
hs00115200  -1
hs00115201  ss     1
hs00115202  ss     2
hs00115203  cs        3
hs00115204  cs        4
hs00115205  cs        5
hs00115206  cs        6
hs00115207  cs        7
hs00115208  cs        8
hs00115209  cs        9
hs00115210  insul     10
hs00115211  insul     11
hs00115212  insul     12
hs00115213  insul     13
hs00115300  -1
hs00115400  1  012  ext  0.5 0.5
* hs00115401  0.9  gray-gas-a  3.0
hs00115500  32.421  18.85  1.5
hs00115600  0
hs00115800  -1
hs00115801  395.65  14
***
* vessel vertical wall in cell #14
hs00116000   14   1   -1
hs00116001   wall14
hs00116002   6.5  1.
hs00116100   -1   1   0.0
hs00116102  0.001     2
hs00116103  0.002     3
hs00116104  0.004     4
hs00116105  0.006     5
hs00116106  0.01      6
hs00116107  0.015     7
hs00116108  0.02      8
hs00116109  0.025     9
hs00116110  0.027     10
hs00116111  0.037     11
hs00116112  0.057     12
hs00116113  0.067     13
hs00116114  0.077     14
hs00116200  -1
hs00116201  ss     1
```

```
hs00116202  ss     2
hs00116203  cs        3
hs00116204  cs        4
hs00116205  cs        5
hs00116206  cs        6
hs00116207  cs        7
hs00116208  cs        8
hs00116209  cs        9
hs00116210  insul     10
hs00116211  insul     11
hs00116212  insul     12
hs00116213  insul     13
hs00116300  -1
hs00116400  1  014  ext  0.5 0.5
* hs00116401  0.9  gray-gas-a  3.0
hs00116500  43.228  18.85  2.
hs00116600  0
hs00116800  -1
hs00116801  395.65  14
***
* vessel vertical wall in cell #16
hs00117000   14   1   -1
hs00117001   wall16
hs00117002   0.  1.
hs00117100   -1   1   0.0
hs00117102  0.001     2
hs00117103  0.002     3
hs00117104  0.004     4
hs00117105  0.006     5
hs00117106  0.01      6
hs00117107  0.015     7
hs00117108  0.02      8
hs00117109  0.025     9
hs00117110  0.027     10
hs00117111  0.037     11
hs00117112  0.057     12
hs00117113  0.067     13
hs00117114  0.077     14
hs00117200  -1
hs00117201  ss     1
hs00117202  ss     2
hs00117203  cs        3
hs00117204  cs        4
hs00117205  cs        5
hs00117206  cs        6
hs00117207  cs        7
hs00117208  cs        8
hs00117209  cs        9
hs00117210  insul     10
hs00117211  insul     11
hs00117212  insul     12
hs00117213  insul     13
hs00117300  -1
hs00117400  1  016  ext  0.5 0.5
* hs00117401  0.9  gray-gas-a  3.0
hs00117500  140.492  18.85  6.5
hs00117600  0
hs00117800  -1
hs00117801  395.65  14
***
* vessel roof
hs00118000   14   1   -1
hs00118001   top
```

```
hs00118002   19.0  0.
hs00118100   -1   1   0.0
hs00118102  0.001     2
hs00118103  0.002     3
hs00118104  0.004     4
hs00118105  0.006     5
hs00118106  0.01      6
hs00118107  0.015     7
hs00118108  0.02      8
hs00118109  0.025     9
hs00118110  0.027     10
hs00118111  0.037     11
hs00118112  0.057     12
hs00118113  0.067     13
hs00118114  0.077     14
hs00118200  -1
hs00118201  ss     1
hs00118202  ss     2
hs00118203  cs        3
hs00118204  cs        4
hs00118205  cs        5
hs00118206  cs        6
hs00118207  cs        7
hs00118208  cs        8
hs00118209  cs        9
hs00118210  insul     10
hs00118211  insul     11
hs00118212  insul     12
hs00118213  insul     13
hs00118300  -1
hs00118400  1  001  ext  0.5 0.5
* hs00118401  0.9  gray-gas-a  3.0
hs00118500  43.228  7.0  0.077
hs00118600  0
hs00118800  -1
hs00118801  395.65  14
************************************************
* vessel floor
hs00119000   14   1   -1
hs00119001   floor
hs00119002   0.0  -1.0e-7
hs00119100   -1   1   0.0
hs00119102  0.001     2
hs00119103  0.002     3
hs00119104  0.004     4
hs00119105  0.006     5
hs00119106  0.01      6
hs00119107  0.015     7
hs00119108  0.02      8
hs00119109  0.025     9
hs00119110  0.027     10
hs00119111  0.037     11
hs00119112  0.057     12
hs00119113  0.067     13
hs00119114  0.077     14
hs00119200  -1
hs00119201  ss     1
hs00119202  ss     2
hs00119203  cs        3
hs00119204  cs        4
hs00119205  cs        5
hs00119206  cs        6
hs00119207  cs        7
```

```
hs00119208  cs        8
hs00119209  cs        9
hs00119210  insul     10
hs00119211  insul     11
hs00119212  insul     12
hs00119213  insul     13
hs00119300  -1
hs00119400  1  016  ext  0.5 0.5
* hs00119401  0.9  gray-gas-a  3.0
hs00119500  37.176  7.0  0.077
hs00119600  0
hs00119800  -1
hs00119801  395.65  14
*
* Film tracking for vertical wall
hsft10000   8
*         idstrc numdrn frainl ntpl frainr ntpr imsrcl iesrcl imsrcr iesrcr
hsft10100  111     1      0.0   0    0.0     0    0      0      0       0
hsft10101  112    1.0   0.0
hsft10200  112     1      0.0   0    0.0     0    0      0      0       0
hsft10201  113    1.0   0.0
hsft10300  113     1      0.0   0    0.0     0    0      0      0       0
hsft10301  114    1.0   0.0
hsft10400  114     1      0.0   0    0.0     0    0      0      0       0
hsft10401  115    1.0   0.0
hsft10500  115     1      0.0   0    0.0     0    0      0      0       0
hsft10501  116    1.0   0.0
hsft10600  116     1      0.0   0    0.0     0    0      0      0       0
hsft10601  117    1.0   0.0
hsft10700  117     1      0.0   0    0.0     0    0      0      0       0
hsft10701  118    1.0   0.0
hsft10800  118     0      0.0   0    0.0     0    0      0      0       0
. *terminate
```

Mp.txt:

```
************************************************************
***
***             NON-CONDENSIBLES GAS PACKAGE
***
************************************************************
***
***      GAS  MATEERIAL NUMBER
NCG001   o2   4                                  * oxygen
NCG002   n2   5                                  * nitrogen
***
************************************************************
***
************************************************************
***
************************************************************
***
***             MATERIAL PROPERTIES PACKAGE
***
***
***               Property              Units
***
***               temperature           K
***             density               kg/m*3
***             heat capacity         J/kg-K
***             thermal conductivity  W/m-K
***
```

```
************************************************************
***
***             MATERIAL 1 IS INSULATION
***             ========================
***
MPMAT00100      INSUL
MPMAT00101      RHO       13
MPMAT00102      CPS       14
MPMAT00103      THC       15
TF01300         'RHO INSUL'   2   1.00   0.0
TF01312         273.15    220.
TF01313         5000.0    220.
TF01400         'CPS INSUL'   2   1.00   0.0
TF01412         273.15    1000.
TF01413         5000.0    1000.
TF01500         'THC INSUL'   2   1.00   0.0
TF01512         273.15    0.0488
TF01513         5000.0    0.0488
***
************************************************************
MPMAT00200  'CS'
MPMAT00201   RHO     16
MPMAT00202   CPS     17
MPMAT00203   THC     18
TF01600       'RHO CS'   2   1.0   0.0
TF01612      273.15    7860.
TF01613      1000.     7860.
TF01700       'CPS CS'  2    1.0   0.0
TF01712       273.15   460.7
TF01713      1000.     460.7
TF01800       'THC CS'  2    1.0   0.0
TF01812       273.15   43.3
TF01813      1000.     43.3
MPMAT00300  'SS'
MPMAT00301   RHO  19
MPMAT00302   CPS  20
MPMAT00303   THC  21
TF01900      'RHO SS'  2   1.0  0.0
TF01912      273.15  9030.
TF01913     1000.    9030.
TF02000      'CPS SS'  2   1.0  0.0
TF02012      273.15    460.
TF02013      1000.     460.
TF02100      'THC SS'  2    1.0   0.0
TF02112      273.15   16.2
TF02113     1000.     16.2
. * terminate
```

INTENTIONALLY BLANK

Appendix G. Listings of MELCOR Input Files for CVTR Reference Cases: Single Cell Model (Test 3) Multi-Cell Models (Tests 3, 4 and 5)

Single Cell Model (Test 3): EXEC Input --

```
** CVTR Test #3A *********************************
************************************************
*eor*      melgen
**********************
**********************
***                ***
***  MELGEN INPUT  ***
***                ***
**********************
TITLE     'CVTR'
***JOBID      CVTR
CRTOUT
OUTPUTF   'CVTR.out'
RESTARTF  'CVTR.rst'
DIAGF     'CVTR.gdia'
TSTART     0.
DTTIME    .1
***
EDF11100 special-data   5  write
EDF11101 'th.txt'
EDF11102  13E12.5
EDF11110  0.0  2.0
EDF11111  20.  5.0
EDF11112  80. 10.0
EDF11113  160. 1.0
EDF11114  180.0 10.0
EDF11115  250.  20.0
EDF11116  500.  50.0
EDF11117 1000.  50.0
EDF111AA CVH-P.100
EDF111AB CVH-TVAP.100
EDF111AC CVH-TSAT(A).100
EDF111AD CVH-TSAT(P).100
EDF111AE CFVALU.1
************************************************************
*** Sensitivity Study
************************************************************
* Turbulent convection coefficient
sc41100  4110  0.14  1
sc42510  4251  0.00005 2
sc44110  4411  1.0e-10 5        * negate equilibrium calc.
************************************************************
***
r*i*f   mp.txt
r*i*f   cont.txt
r*i*f   hs.txt
************************************************************
.  * terminate
*eor* melcor
************************
***  MELCOR INPUT    ***
************************
```

```
TITLE     'CVTR'
***JOBID      ref
*
OUTPUTF   'CVTR.out'
PLOTF     'CVTR.ptf'
RESTARTF  'CVTR.rst'
MESSAGEF  'CVTR.mes'
DIAGF     'CVTR.dia'
*
CRTOUT
***CYMESF    10 10
*
RESTART  -1
tend  1.0e3
***EXACTTIME1         100.
CPULIM             2.0e6
CPULEFT            100.0
*cvhtrace 3
*
************************************
*** Invoke desired sequences
************************************
***
***
************************************************************
*
*          TIME    DTMAX     DTMIN     DTEDIT    DTPLOT    DTREST
*
TIME1       0.0     1.0      1.0e-8      2.0       2.0     20.0
TIME2      20.0     1.0      1.0E-8      10.0      5.0     20.0
TIME3      80.0     2.0      1.0E-8      50.0      10.0    50.0
TIME4     160.0     2.0      1.0E-8      50.0      1.0     20.0
TIME5     180.0     2.0      1.0E-8      20.0      10.0     20.0
TIME6     250.0     2.0      1.0E-6      50.0      20.0     50.0
TIME7     500.0     5.0      1.0E-6     100.0      50.0     100.0
TIME8    1000.0     5.0      1.0E-6     100.0      50.0     100.0
************************************************************
***** END OF MELCOR INPUT ***********************************
************************************************************
.  * terminate
```

Cont.txt:

```
************************************************
***
*** Operating region
***
CV10000  'Containment'  2   2   4
CV10001   2   0
CV100A0   3
CV100A1   PVOL 1.013565e5
CV100A2   RHUM  0.49418
CV100A3   TATM  300.
CV100A4   MLFR.4 0.2095   * Oxygen
CV100A5   MLFR.5 0.7905   * Nitrogen
CV100B1   0.0  0.0
CV100B2   26.0 6425.66
CV100C1   MASS.3  200  2
CV100C2   AE      210  2
***
TF20000 'steam_rate' 4  1.0  0.0
TF20011  0.0      45.139
TF20012  166.392  45.139
```

```
TF20013  166.428  0.0
TF20014  3600.0   0.0
***
TF21000 'steam_Enth' 4  1.0  0.0
TF21011  0.0      1.25468364e8
TF21012  166.392  1.25468364e8
TF21013  166.428  0.0
TF21014  3600.0   0.0
***
.  * terminate
```

Hs.txt:

```
 ************************************************
***                                              *
***  Heat Structure Input for CVTR Single Cell   *
***                                              *
************************************************
*
************************************************
* ht struc 1-o, bnl cyl shell in operating region *
************************************************
hs00101000   11   1   -1
hs00101001   cylsho
hs00101002   0.0   1.
hs00101100   -1   1   0.0
hs00101102  0.0022    2
hs00101103  0.00635   3
hs00101104  0.01135   4
hs00101105  0.014     5
hs00101106  0.01855   6
hs00101107  0.02815   7
hs00101108  0.04735   8
hs00101109  0.06655   9
hs00101110  0.14      10
hs00101111  0.2       11
hs00101200  -1
hs00101201  cvtrstel  1
hs00101202  cvtrstel  2
hs00101203  cvtrconc  3
hs00101204  cvtrconc  4
hs00101205  cvtrconc  5
hs00101206  cvtrconc  6
hs00101207  cvtrconc  7
hs00101208  cvtrconc  8
hs00101209  cvtrconc  9
hs00101210  cvtrconc  10
hs00101300  -1
hs00101400  1  100  ext  0.5 0.5
hs00101401  0.9  gray-gas-a  3.0
hs00101500  1437.  11.  20.
hs00101600  0
hs00101800  -1
hs00101801  300.  11
*
****************************************
* heat plug                            *
****************************************
hs00102000   11   1   -1
hs00102001   plug
hs00102002   0.0   1.
hs00102100   -1   1   0.0
```

```
hs00102102  0.0022    2
hs00102103  0.00635   3
hs00102104  0.01135   4
hs00102105  0.014     5
hs00102106  0.01855   6
hs00102107  0.02815   7
hs00102108  0.04735   8
hs00102109  0.06655   9
hs00102110  0.14      10
hs00102111  0.2       11
hs00102200  -1
hs00102201  cvtrstel  1
hs00102202  cvtrstel  2
hs00102203  cvtrconc  3
hs00102204  cvtrconc  4
hs00102205  cvtrconc  5
hs00102206  cvtrconc  6
hs00102207  cvtrconc  7
hs00102208  cvtrconc  8
hs00102209  cvtrconc  9
hs00102210  cvtrconc  10
hs00102300  -1
hs00102400  1  100  ext  0.5 0.5
hs00102401  0.9  gray-gas-a  3.0
hs00102500  0.1  11.  0.1
hs00102600  0
hs00102800  -1
hs00102801  300.  11
*
****************************************
* ht struc 2-o, dome                   *
****************************************
hs00103000   10   1   -1
hs00103001   dome
hs00103002   25.8  0.
hs00103100   -1   1   0.0
hs00103102  0.00408   2
hs00103103  0.0127    3
hs00103104  0.01724   4
hs00103105  0.02214   5
hs00103106  0.03193   6
hs00103107  0.05152   7
hs00103108  0.09068   8
hs00103109  0.14      9
hs00103110  0.2       10
hs00103200  -1
hs00103201  cvtrstel  1
hs00103202  cvtrstel  2
hs00103203  cvtrconc  3
hs00103204  cvtrconc  4
hs00103205  cvtrconc  5
hs00103206  cvtrconc  6
hs00103207  cvtrconc  7
hs00103208  cvtrconc  8
hs00103209  cvtrconc  9
hs00103300  -1
hs00103400  1  100  ext  0.5 0.5
hs00103401  0.9  gray-gas-a  3.0
hs00103500  499.  3.  0.2
hs00103600  0
hs00103800  -1
hs00103801  300.  10
*
```

```
************************************************
* ht struc 4-o, operating floor in op region top *
************************************************
hs00104000   7   1   -1
hs00104001   opflrflr
hs00104002   10.  -1.0e-7
hs00104100   -1   1   0.0
hs00104102  0.004     2
hs00104103  0.012     3
hs00104104  0.028     4
hs00104105  0.06      5
hs00104106  0.124     6
hs00104107  0.188     7
hs00104200  -1
hs00104201  cvtrconc  1
hs00104202  cvtrconc  2
hs00104203  cvtrconc  3
hs00104204  cvtrconc  4
hs00104205  cvtrconc  5
hs00104206  cvtrconc  6
hs00104300  -1
hs00104400  1  100  ext  0. 1.0
hs00104401  0.9  gray-gas-a  3.0
hs00104500  230.  1.  0.188
hs00104600  0
hs00104800  -1
hs00104801  300.  7
*
************************************************
* ht struc 11-o, steam gen shield assumed to be  *
* in operating region as walls                   *
************************************************
hs00105000   7   1   -1
hs00105001   stmgensw
hs00105002   10.  1.
hs00105100   -1   1   0.0
hs00105102  0.004     2
hs00105103  0.012     3
hs00105104  0.028     4
hs00105105  0.06      5
hs00105106  0.124     6
hs00105107  0.188     7
hs00105200  -1
hs00105201  cvtrconc  1
hs00105202  cvtrconc  2
hs00105203  cvtrconc  3
hs00105204  cvtrconc  4
hs00105205  cvtrconc  5
hs00105206  cvtrconc  6
hs00105300  -1
hs00105400  1  100  ext  0.5 0.5
hs00105401  0.9  gray-gas-a  3.0
hs00105500  37.16  5.  0.188
hs00105600  0
hs00105800  -1
hs00105801  300.  7
*
*********************************************
* ht struc 14-o, pressurizer discharge tank   *
*********************************************
hs00106000   3   1   -1
hs00106001   prdctow
hs00106002   10.  1.
```

```
hs00106100   -1   1   0.0
hs00106102  0.00212   2
hs00106103  0.006355  3
hs00106200  -1
hs00106201  cvtrstel  1
hs00106202  cvtrstel  2
hs00106300  -1
hs00106400  1  100  ext  0.5 0.5
hs00106401  0.9  gray-gas-a  3.0
hs00106500  42.18  5.  5.
hs00106600  0
hs00106800  -1
hs00106801  300.  3
*
************************************************
* ht struc 15-o, steam generator               *
************************************************
hs00107000   4   1   -1
hs00107001   stgenow
hs00107002   10.  1.
hs00107100   -1   1   0.0
hs00107102  0.007     2
hs00107103  0.021     3
hs00107104  0.0381    4
hs00107200  -1
hs00107201  cvtrstel  1
hs00107202  cvtrstel  2
hs00107203  cvtrstel  3
hs00107300  -1
hs00107400  1  100  ext  0.5 0.5
hs00107401  0.9  gray-gas-a  3.0
hs00107500  95.32  5.  5.
hs00107600  0
hs00107800  -1
hs00107801  300.  4
*
************************************************
* ht struc 19-o, fuel handling apparatus       *
************************************************
hs00108000   3   1   -1
hs00108001   fuhdlaow
hs00108002   10.  1.
hs00108100   -1   1   0.0
hs00108102  0.003978  2
hs00108103  0.01193   3
hs00108200  -1
hs00108201  cvtrstel  1
hs00108202  cvtrstel  2
hs00108300  -1
hs00108400  1  100  ext  0.5 0.5
hs00108401  0.9  gray-gas-a  3.0
hs00108500  92.90  5.  5.
hs00108600  0
hs00108800  -1
hs00108801  300.   3
*
************************************************
* ht struc 20-o, all of "i" beams              *
************************************************
hs01108000   3   1   -1
hs01108001   ibeamow
hs01108002   10.  1.
hs01108100   -1   1   0.0
```

```
hs01108102  0.006857  2
hs01108103  0.02057   3
hs01108200  -1
hs01108201  cvtrstel  1
hs01108202  cvtrstel  2
hs01108300  -1
hs01108400  1  100  ext  0.5 0.5
hs01108401  0.9  gray-gas-a  3.0
hs01108500  418.  5.  5.
hs01108600  0
hs01108800  -1
hs01108801  300.  3
*
*******************************************
* ht strucms-o, bnl addt'l steel            *
*******************************************
hs00109000   3   1   -1
hs00109001   miscstow
hs00109002   10.  1.
hs00109100   -1   1   0.0
hs00109102  0.001588  2
hs00109103  0.004763  3
hs00109200  -1
hs00109201  cvtrstel  1
hs00109202  cvtrstel  2
hs00109300  -1
hs00109400  1  100  ext  0.5 0.5
hs00109401  0.9  gray-gas-a  3.0
hs00109500  2383.33  5.  5.
hs00109600  0
hs00109800  -1
hs00109801  300.  3
*
***********************************************
* ht struc 5-b, header cavity, assumed to be in *
* basement as walls                           *
***********************************************
hs00110000   7   1   -1
hs00110001   hdrcav
hs00110002   10.  1.
hs00110100   -1   1   0.0
hs00110102  0.004     2
hs00110103  0.012     3
hs00110104  0.028     4
hs00110105  0.06      5
hs00110106  0.124     6
hs00110107  0.188     7
hs00110200  -1
hs00110201  cvtrconc  1
hs00110202  cvtrconc  2
hs00110203  cvtrconc  3
hs00110204  cvtrconc  4
hs00110205  cvtrconc  5
hs00110206  cvtrconc  6
hs00110300  -1
hs00110400  1  100  ext  0.5 0.5
hs00110401  0.9  gray-gas-a  3.0
hs00110500  121.24  5.  0.188
hs00110600  0
hs00110800  -1
hs00110801  300.  7
*
*****************************************************
```

```
* ht struc 6-i, reactor compartment assumed to be walls  *
*********************************************************
hs00111000   7   1   -1
hs00111001   reacompw
hs00111002   10.  1.
hs00111100   -1   1   0.0
hs00111102  0.004     2
hs00111103  0.012     3
hs00111104  0.028     4
hs00111105  0.06      5
hs00111106  0.124     6
hs00111107  0.188     7
hs00111200  -1
hs00111201  cvtrconc  1
hs00111202  cvtrconc  2
hs00111203  cvtrconc  3
hs00111204  cvtrconc  4
hs00111205  cvtrconc  5
hs00111206  cvtrconc  6
hs00111300  -1
hs00111400  1  100  ext  0.5 0.5
hs00111401  0.9  gray-gas-a  3.0
hs00111500  154.22  5.  0.188
hs00111600  0
hs00111800  -1
hs00111801  300.  7
*
*****************************************************
* ht struc 7-i, fuel canal assumed to be walls      *
*****************************************************
hs00112000   7   1   -1
hs00112001   fucanalw
hs00112002   10.  1.
hs00112100   -1   1   0.0
hs00112102  0.004     2
hs00112103  0.012     3
hs00112104  0.028     4
hs00112105  0.06      5
hs00112106  0.124     6
hs00112107  0.188     7
hs00112200  -1
hs00112201  cvtrconc  1
hs00112202  cvtrconc  2
hs00112203  cvtrconc  3
hs00112204  cvtrconc  4
hs00112205  cvtrconc  5
hs00112206  cvtrconc  6
hs00112300  -1
hs00112400  1  100  ext  0.5 0.5
hs00112401  0.9  gray-gas-a  3.0
hs00112500  148.64  5.  0.188
hs00112600  0
hs00112800  -1
hs00112801  300.   7
*
*************************************************
* ht struc 8-b, fuel canal support assumed to be *
* in basement as walls                           *
*************************************************
hs00113000   7   1   -1
hs00113001   fucansup
hs00113002   10.  1.
hs00113100   -1   1   0.0
```

```
hs00113102  0.004     2
hs00113103  0.012     3
hs00113104  0.028     4
hs00113105  0.06      5
hs00113106  0.124     6
hs00113107  0.188     7
hs00113200  -1
hs00113201  cvtrconc  1
hs00113202  cvtrconc  2
hs00113203  cvtrconc  3
hs00113204  cvtrconc  4
hs00113205  cvtrconc  5
hs00113206  cvtrconc  6
hs00113300  -1
hs00113400  1  100  ext  0.5 0.5
hs00113401  0.9  gray-gas-a  3.0
hs00113500  26.01  5.  0.188
hs00113600  0
hs00113800  -1
hs00113801  300.  7
*
*********************************************
* ht struc 9-i, floor of reactor cavity top   *
*********************************************
hs00114000   7   1   -1
hs00114001   rcvflrin
hs00114002   10.  -1.0e-7
hs00114100   -1   1   0.0
hs00114102  0.004     2
hs00114103  0.012     3
hs00114104  0.028     4
hs00114105  0.06      5
hs00114106  0.124     6
hs00114107  0.188     7
hs00114200  -1
hs00114201  cvtrconc  1
hs00114202  cvtrconc  2
hs00114203  cvtrconc  3
hs00114204  cvtrconc  4
hs00114205  cvtrconc  5
hs00114206  cvtrconc  6
hs00114300  -1
hs00114400  1  100  ext  0.5 0.5
hs00114401  0.9  gray-gas-a  3.0
hs00114500  13.3  1.  0.188
hs00114600  0
hs00114800  -1
hs00114801  300.    7
*
***********************************************
* ht struc 10-b, cvtr concrete supports assumed  *
* to be in basement as walls                     *
***********************************************
hs00115000   7   1   -1
hs00115001   concsupw
hs00115002   10.  1.
hs00115100   -1   1   0.0
hs00115102  0.004     2
hs00115103  0.012     3
hs00115104  0.028     4
hs00115105  0.06      5
hs00115106  0.124     6
hs00115107  0.188     7
```

```
hs00115200  -1
hs00115201  cvtrconc  1
hs00115202  cvtrconc  2
hs00115203  cvtrconc  3
hs00115204  cvtrconc  4
hs00115205  cvtrconc  5
hs00115206  cvtrconc  6
hs00115300  -1
hs00115400  1  100  ext  0.5 0.5
hs00115401  0.9  gray-gas-a  3.0
hs00115500  89.19  5.  5.
hs00115600  0
hs00115800  -1
hs00115801  300.   7
*
************************************************
* ht struc 12-b, moderator overflow tank       *
************************************************
hs00116000   3   1   -1
hs00116001   mdovftbw
hs00116002   10.  1.
hs00116100   -1   1   0.0
hs00116102  0.003175  2
hs00116103  0.009525  3
hs00116200  -1
hs00116201  cvtrstel  1
hs00116202  cvtrstel  2
hs00116300  -1
hs00116400  1  100  ext  0.5 0.5
hs00116401  0.9  gray-gas-a  3.0
hs00116500  103.  5.  5.
hs00116600  0
hs00116800  -1
hs00116801  300.   3
*
************************************************
* ht struc 13-i, pressurizer                   *
************************************************
hs00117000   5   1   -1
hs00117001   press
hs00117002   10.  1.
hs00117100   -1   1   0.0
hs00117102  0.007     2
hs00117103  0.021     3
hs00117104  0.0391    4
hs00117105  0.0572    5
hs00117200  -1
hs00117201  cvtrstel  1
hs00117202  cvtrstel  2
hs00117203  cvtrstel  3
hs00117204  cvtrstel  4
hs00117300  -1
hs00117400  1  100  ext  0.5 0.5
hs00117401  0.9  gray-gas-a  3.0
hs00117500  32.7  5.  5.
hs00117600  0
hs00117800  -1
hs00117801  300.   5
*
*******************************************
* ht struc 16-b, moderator coolers        *
*******************************************
hs00118000   3   1   -1
```

```
hs00118001   modcobw
hs00118002   10.  1.
hs00118100   -1   1   0.0
hs00118102  0.001058  2
hs00118103  0.003175  3
hs00118200  -1
hs00118201  cvtrstel  1
hs00118202  cvtrstel  2
hs00118300  -1
hs00118400  1  100  ext  0.5 0.5
hs00118401  0.9  gray-gas-a  3.0
hs00118500  52.03  5.  5.
hs00118600  0
hs00118800  -1
hs00118801  300.   3
*
*****************************************
* ht struc 17-i, shutdown coolers           *
*****************************************
hs00119000   3   1   -1
hs00119001   shdcoiw
hs00119002   10.  1.
hs00119100   -1   1   0.0
hs00119102  0.000508  2
hs00119103  0.001524  3
hs00119200  -1
hs00119201  cvtrstel  1
hs00119202  cvtrstel  2
hs00119300  -1
hs00119400  1  100  ext  0.5 0.5
hs00119401  0.9  gray-gas-a  3.0
hs00119500  12.26  5.  5.
hs00119600  0
hs00119800  -1
hs00119801  300.   3
*
*****************************************
* ht struc 18-b, pumps-primary & injection *
*****************************************
hs00120000   3   1   -1
hs00120001   pmpsbw
hs00120002   10.  1.
hs00120100   -1   1   0.0
hs00120102  0.004233  2
hs00120103  0.0127    3
hs00120200  -1
hs00120201  cvtrstel  1
hs00120202  cvtrstel  2
hs00120300  -1
hs00120400  1  100  ext  0.5 0.5
hs00120401  0.9  gray-gas-a  3.0
hs00120500  46.45  5.  5.
hs00120600  0
hs00120800  -1
hs00120801  300.    3
*
*****************************************
* basement floor                          *
*****************************************
hs00121000   7   1   -1
hs00121001   baseflr
hs00121002   0.  -1.0e-7
hs00121100   -1   1   0.0
```

```
hs00121102  0.004     2
hs00121103  0.012     3
hs00121104  0.028     4
hs00121105  0.06      5
hs00121106  0.124     6
hs00121107  0.188     7
hs00121200  -1
hs00121201  cconc  1
hs00121202  cconc  2
hs00121203  cconc  3
hs00121204  cconc  4
hs00121205  cconc  5
hs00121206  cconc  6
hs00121300  -1
hs00121400  1  100  ext  0. 1.0
hs00121401  0.9  gray-gas-a  3.0
hs00121500  245.26  5.  0.188
hs00121600  0
hs00121800  -1
hs00121801  295.   7
*
CF00100   tsurf equals 1  1.0
CF00110   1.0  0.0 hs-temp.0010101
.  * terminate
```

Mp.txt:

```
*************************************************************
***
***             NON-CONDENSIBLES GAS PACKAGE
***
*************************************************************
***
***      GAS  MATEERIAL NUMBER
NCG001   o2   4                                  * oxygen
NCG002   n2   5                                  * nitrogen
***
*************************************************************
***
*************************************************************
***
*************************************************************
***
***             MATERIAL PROPERTIES PACKAGE
***
***
***               Property              Units
***
***               temperature           K
***             density               kg/m*3
***             heat capacity         J/kg-K
***             thermal conductivity  W/m-K
***
*************************************************************
*************************************************************
*************************************************************
*************************************************************
***
***             MATERIAL 1 IS CONCRETE
***             ======================
***
MPMAT00100      CVTRCONC
MPMAT00101      RHO       13
```

```
MPMAT00102      CPS       14
MPMAT00103      THC       15
TF01300         'RHO CONCRETE'   2   1.00   0.0
TF01312         273.15    1.
TF01313         5000.0    1.
TF01400         'CPS CONCRETE'   2   1.00   0.0
TF01412         273.15    2.025e6
TF01413         5000.0    2.025e6
TF01500         'THC CONCRETE'   2   1.00   0.0
TF01512         273.15    1.385
TF01513         5000.0    1.385
***
************************************************************
***
***             MATERIAL 2 IS CARBON STEEL
***             ==========================
***
MPMAT00200      'CVTRSTEL'
MPMAT00201       RHO          16
MPMAT00202       CPS          17
MPMAT00203       THC          18
TF01600         'RHO CARBON STEEL'   2   1.00   0.0
TF01612          273.15       1.0
TF01613          5000.0       1.0
TF01700         'CPS CARBON STEEL'   2   1.00   0.0
TF01712          273.15       3.689e6
TF01713          5000.0       3.689e6
TF01800         'THC CARBON STEEL'   2   1.00   0.0
TF01812          273.15       45.18
TF01813          5000.0       45.18
***
************************************************************
************************************************************
***
***             MATERIAL 3 IS Gap Gas
***             =====================================
***
MPMAT00300      'GAS'
MPMAT00301       RHO          19
MPMAT00302       CPS          20
MPMAT00303       THC          21
TF01900         'RHO GAS'   2   1.00   0.0
TF01912          273.15       1.0
TF01913          5000.0       1.0
TF02000         'CPS GAS'   2   1.00   0.0
TF02012          273.15       1.0e3
TF02013          5000.0       1.0e3
TF02100         'THC GAS'   2   1.00   0.0
TF02111          273.15       0.03
TF02112          5000.0       0.03
***
***
***             MATERIAL 4 IS CONTAIN CONC
***             ======================
***
MPMAT00400      CCONC
MPMAT00401      RHO       22
MPMAT00402      CPS       23
MPMAT00403      THC       24
TF02200         'RHO CONC'   2   1.00   0.0
TF02212         273.15    2400.
TF02213         5000.0    2400.
TF02300         'CPS CONC'   2   1.00   0.0
```

```
TF02312         273.15    1000.
TF02313         5000.0    1000.
TF02400         'THC CONC'   2   1.00   0.0
TF02412         273.15    2.6
TF02413         5000.0    2.6
***
.  * terminate
```

Multi-Cell Model (Test 3): EXEC Input

```
** CVTR Test #3A ***************************************
************************************************************
*eor*      melgen
**********************
**********************
***                  ***
***  MELGEN INPUT  ***
***                  ***
**********************
TITLE     'CVTR'
***JOBID      CVTR
CRTOUT
OUTPUTF   'CVTR.out'
RESTARTF  'CVTR.rst'
DIAGF     'CVTR.gdia'
TSTART     0.
DTTIME    .1
***
************************************************************
*** Sensitivity Study
************************************************************
* Turbulent convection coefficient
sc41100  4110  0.14  1
sc42510  4251  0.00005 2
sc44110  4411  1.0e-10 5
************************************************************
***
r*i*f   mp.txt
r*i*f   cont.txt
r*i*f   fl.txt
r*i*f   hs_multi.txt
************************************************************
.  * terminate
*eor* melcor
************************
***  MELCOR INPUT    ***
************************
TITLE     'CVTR'
***JOBID      ref
*
OUTPUTF   'CVTR.out'
PLOTF     'CVTR.ptf'
RESTARTF  'CVTR.rst'
MESSAGEF  'CVTR.mes'
DIAGF     'CVTR.dia'
*
CRTOUT
***CYMESF    10 10
*
RESTART  -1
tend  1.0e3
***EXACTTIME1         100.
CPULIM             2.0e6
```

```
CPULEFT            100.0
*cvhtrace 3
*
************************************
*** Invoke desired sequences
************************************
***
***
************************************************************
*
*          TIME    DTMAX     DTMIN     DTEDIT    DTPLOT    DTREST
*
TIME1       0.0     1.0      1.0e-8      2.0       2.0     20.0
TIME2      20.0     1.0      1.0E-8      10.0      5.0     20.0
TIME3      80.0     2.0      1.0E-8      50.0      10.0    50.0
TIME4     160.0     2.0      1.0E-8      50.0      1.0     20.0
TIME5     180.0     2.0      1.0E-8      20.0      10.0     20.0
TIME6     250.0     2.0      1.0E-6      50.0      20.0     50.0
TIME7     500.0     5.0      1.0E-6     100.0      50.0     100.0
TIME8    1000.0     5.0      1.0E-6     100.0      50.0     100.0
************************************************************
***** END OF MELCOR INPUT ************************************
************************************************************
.  * terminate
```

Cont.txt:

```
***
cv00100  'C B reg'  2   2   4
cv00101   2   0
cv001A0   3
cv001A1   PVOL 1.013565e5
cv001A2   RHUM  0.49418
cv001A3   TATM  300.
cv001A4   MLFR.4 0.2095   * Oxygen
cv001A5   MLFR.5 0.7905   * Nitrogen
cv001B1   0.0  0.0
cv001B2   2.0  245.
cv001B3   5.5  443.012
***
cv00200  'A B reg'  2   2   4
cv00201   2   0
cv002A0   3
cv002A1   PVOL 1.013565e5
cv002A2   RHUM  0.49418
cv002A3   TATM  300.
cv002A4   MLFR.4 0.2095   * Oxygen
cv002A5   MLFR.5 0.7905   * Nitrogen
cv002B1   0.0  0.0
cv002B2   2.0  245.
cv002B3   5.5  443.012
***
cv00300  'C L I reg'  2   2   4
cv00301   2   0
cv003A0   3
cv003A1   PVOL 1.013565e5
cv003A2   RHUM  0.49418
cv003A3   TATM  300.
cv003A4   MLFR.4 0.2095   * Oxygen
cv003A5   MLFR.5 0.7905   * Nitrogen
cv003B1   7.9  0.0
cv003B2   10.4 307.6625
***
cv00400  'A L I reg'  2   2   4
cv00401   2   0
```

```
cv004A0   3
cv004A1   PVOL 1.013565e5
cv004A2   RHUM  0.49418
cv004A3   TATM  300.
cv004A4   MLFR.4 0.2095   * Oxygen
cv004A5   MLFR.5 0.7905   * Nitrogen
cv004B1   7.9  0.0
cv004B2   10.4 307.6625
***
cv00500  'C H I reg'  2   2   4
cv00501   2   0
cv005A0   3
cv005A1   PVOL 1.013565e5
cv005A2   RHUM  0.49418
cv005A3   TATM  300.
cv005A4   MLFR.4 0.2095   * Oxygen
cv005A5   MLFR.5 0.7905   * Nitrogen
cv005B1   12.8  0.0
cv005B2   15.2  307.6625
***
cv00600  'A H I reg'  2   2   4
cv00601   2   0
cv006A0   3
cv006A1   PVOL 1.013565e5
cv006A2   RHUM  0.49418
cv006A3   TATM  300.
cv006A4   MLFR.4 0.2095   * Oxygen
cv006A5   MLFR.5 0.7905   * Nitrogen
cv006B1   12.8  0.0
cv006B2   15.2  307.6625
***
cv00700  'C B O reg'  2   2   4
cv00701   2   0
cv007A0   3
cv007A1   PVOL 1.013565e5
cv007A2   RHUM  0.49418
cv007A3   TATM  300.
cv007A4   MLFR.4 0.2095   * Oxygen
cv007A5   MLFR.5 0.7905   * Nitrogen
cv007B1   15.2  0.0
cv007B2   16.8  197.802
***
cv00800  'A B O reg'  2   2   4
cv00801   2   0
cv008A0   3
cv008A1   PVOL 1.013565e5
cv008A2   RHUM  0.49418
cv008A3   TATM  300.
cv008A4   MLFR.4 0.2095   * Oxygen
cv008A5   MLFR.5 0.7905   * Nitrogen
cv008B1   15.2  0.0
cv008B2   16.8  197.802
cv008C1   MASS.3 200 2
cv008C2   AE     210 2
***
cv00900  'C M L O reg'  2   2   4
cv00901   2   0
cv009A0   3
cv009A1   PVOL 1.013565e5
cv009A2   RHUM  0.49418
cv009A3   TATM  300.
cv009A4   MLFR.4 0.2095   * Oxygen
cv009A5   MLFR.5 0.7905   * Nitrogen
```

```
cv009B1   16.8  0.0
cv009B2   18.6  197.802
***
cv01000  'A M L O reg'  2   2   4
cv01001   2   0
cv010A0   3
cv010A1   PVOL 1.013565e5
cv010A2   RHUM  0.49418
cv010A3   TATM  300.
cv010A4   MLFR.4 0.2095   * Oxygen
cv010A5   MLFR.5 0.7905   * Nitrogen
cv010B1   16.8  0.0
cv010B2   18.6  197.802
cv010C1   MASS.3 200 2
cv010C2   AE     210 2
***
cv01100  'C M H O reg'  2   2   4
cv01101   2   0
cv011A0   3
cv011A1   PVOL 1.013565e5
cv011A2   RHUM  0.49418
cv011A3   TATM  300.
cv011A4   MLFR.4 0.2095   * Oxygen
cv011A5   MLFR.5 0.7905   * Nitrogen
cv011B1   18.6  0.0
cv011B2   22.3  395.604
***
cv01200  'A M H O reg'  2   2   4
cv01201   2   0
cv012A0   3
cv012A1   PVOL 1.013565e5
cv012A2   RHUM  0.49418
cv012A3   TATM  300.
cv012A4   MLFR.4 0.2095   * Oxygen
cv012A5   MLFR.5 0.7905   * Nitrogen
cv012B1   18.6  0.0
cv012B2   22.3  395.604
***
cv01300  'C T O reg'  2   2   4
cv01301   2   0
cv013A0   3
cv013A1   PVOL 1.013565e5
cv013A2   RHUM  0.49418
cv013A3   TATM  300.
cv013A4   MLFR.4 0.2095   * Oxygen
cv013A5   MLFR.5 0.7905   * Nitrogen
cv013B1   22.3  0.0
cv013B2   25.9  448.89
***
cv01400  'A T O reg'  2   2   4
cv01401   2   0
cv014A0   3
cv014A1   PVOL 1.013565e5
cv014A2   RHUM  0.49418
cv014A3   TATM  300.
cv014A4   MLFR.4 0.2095   * Oxygen
cv014A5   MLFR.5 0.7905   * Nitrogen
cv014B1   22.3  0.0
cv014B2   25.9  448.89
***
cv01500  'D reg'  2   2   4
cv01501   2   0
cv015A0   3
```

```
cv015A1   PVOL 1.013565e5
cv015A2   RHUM  0.49418
cv015A3   TATM  300.
cv015A4   MLFR.4 0.2095   * Oxygen
cv015A5   MLFR.5 0.7905   * Nitrogen
cv015B1   25.9  0.0
cv015B2   34.8  1484.16
***
cv01600  'A H I reg'  2   2   4
cv01601   2   0
cv016A0   3
cv016A1   PVOL 1.013565e5
cv016A2   RHUM  0.49418
cv016A3   TATM  300.
cv016A4   MLFR.4 0.2095   * Oxygen
cv016A5   MLFR.5 0.7905   * Nitrogen
cv016B1   5.5   0.0
cv016B2   7.9   307.6625
***
cv01700  'C L I reg'  2   2   4
cv01701   2   0
cv017A0   3
cv017A1   PVOL 1.013565e5
cv017A2   RHUM  0.49418
cv017A3   TATM  300.
cv017A4   MLFR.4 0.2095   * Oxygen
cv017A5   MLFR.5 0.7905   * Nitrogen
cv017B1   5.5   0.0
cv017B2   7.9   307.6625
***
cv01800  'C H I reg'  2   2   4
cv01801   2   0
cv018A0   3
cv018A1   PVOL 1.013565e5
cv018A2   RHUM  0.49418
cv018A3   TATM  300.
cv018A4   MLFR.4 0.2095   * Oxygen
cv018A5   MLFR.5 0.7905   * Nitrogen
cv018B1   10.4   0.0
cv018B2   12.8   307.6625
***
cv01900  'A H I reg'  2   2   4
cv01901   2   0
cv019A0   3
cv019A1   PVOL 1.013565e5
cv019A2   RHUM  0.49418
cv019A3   TATM  300.
cv019A4   MLFR.4 0.2095   * Oxygen
cv019A5   MLFR.5 0.7905   * Nitrogen
cv019B1   10.4   0.0
cv019B2   12.8   307.6625
***
TF20000 'steam_rate' 4  1.0  0.0
TF20011  0.0      22.5695
TF20012  166.392  22.5695
TF20013  166.428  0.0
TF20014  3600.0   0.0
***
TF21000 'steam_Enth' 4  1.0  0.0
TF21011  0.0      0.62734182e8
TF21012  166.392  0.62734182e8
TF21013  166.428  0.0
TF21014  3600.0   0.0
```

```
***
.   * terminate
```

Fl.txt:

```
*********************************************************
* Internal flow paths in multi-volume CVTR Containment  *
*********************************************************
FL00100  '1 TO 16' 1  16 5.5  5.5
FL00101  156.88  7.62  1.0  0.1  0.1
FL00102  0     0
FL00103  1.0   1.0
FL001S1  156.88  1.0E-6  100.
***
FL00200  '2 TO 17' 2  17 5.5  5.5
FL00201  156.88  7.62  1.0  0.1  0.1
FL00202  0     0
FL00203  1.0   1.0
FL002S1  156.88  1.0E-6  100.
***
FL00300  '3 TO 18' 3  18 10.4  10.4
FL00301  156.88  8.53  1.0  0.1  0.1
FL00302  0     0
FL00303  1.0   1.0
FL003S1  156.88  1.0E-6  100.
***
FL00400  '3 TO 16' 3  16 7.9  7.9
FL00401  156.88  8.53  1.0  0.1  0.1
FL00402  0     0
FL00403  1.0   1.0
FL004S1  156.88  1.0E-6  100.
***
FL00500  '5 TO 18' 5  18 12.8  12.8
FL00501  156.88  8.53  1.0  0.1  0.1
FL00502  0     0
FL00503  1.0   1.0
FL005S1  156.88  1.0E-6  100.
***
FL00600  '4 TO 19' 4  19 10.4  10.4
FL00601  156.88  8.53  1.0  0.1  0.1
FL00602  0     0
FL00603  1.0   1.0
FL006S1  156.88  1.0E-6  100.
***
FL00700  '4 TO 17' 4  17 7.9  7.9
FL00701  156.88  8.53  1.0  0.1  0.1
FL00702  0     0
FL00703  1.0   1.0
FL007S1  156.88  1.0E-6  100.
***
FL00800  '6 TO 19' 6  19 12.8  12.8
FL00801  156.88  8.53  1.0  0.1  0.1
FL00802  0     0
FL00803  1.0   1.0
FL008S1  156.88  1.0E-6  100.
***
FL00900  '5 TO 7' 5  7 15.2  15.2
FL00901  5.0  0.5  1.0  0.1  0.1
FL00902  0     0
FL00903  1.0   1.0
FL009S1  5.0  1.0E-6  100.
***
FL01000  '6 TO 8' 6  8 15.2  15.2
FL01001  30.  6.0  1.0  0.1  0.1
FL01002  0     0
```

```
FL01003  1.0   1.0
FL010S1  30.  1.0E-6  100.
***
FL01100  '7 TO 8' 7  8 16.  16.
FL01101  71.8  5.84  1.0  1.6  1.6
FL01102  3   0
FL01103  1.0   1.0
FL011S1  71.8  1.0E-6  100.
***
FL01200  '7 TO 9' 7  9 16.8  16.8
FL01201  156.88  5.83  1.0  0.1  0.1
FL01202  0   0
FL01203  1.0   1.0
FL012S1  156.88  1.0E-6  100.
***
FL01300  '8 TO 10' 8  10 16.8  16.8
FL01301  156.88  5.83  1.0  0.1  0.1
FL01302  0   0
FL01303  1.0   1.0
FL013S1  156.88  1.0E-6  100.
***
FL01400  '9 TO 10' 9  10 17.7  17.7
FL01401  71.8  5.84  1.0  1.8  1.8
FL01402  3   0
FL01403  1.0   1.0
FL014S1  71.8  1.0E-6  100.
***
FL01500  '9 TO 11' 9  11 18.6  18.6
FL01501  156.88  5.83  1.0  0.1  0.1
FL01502  0   0
FL01503  1.0   1.0
FL015S1  156.88  1.0E-6  100.
***
FL01600  '10 TO 12' 10  12 18.6  18.6
FL01601  156.88  5.83  1.0  0.1  0.1
FL01602  0   0
FL01603  1.0   1.0
FL016S1  156.88  1.0E-6  100.
***
FL01700  '11 TO 12' 11  12 20.45  20.45
FL01701  143.64  7.33  1.0  3.7  3.7
FL01702  3   0
FL01703  1.0   1.0
FL017S1  143.64  1.0E-6  100.
***
FL01800  '11 TO 13' 11  13 22.3  22.3
FL01801  156.88  7.33  1.0  0.1  0.1
FL01802  0   0
FL01803  1.0   1.0
FL018S1  156.88  1.0E-6  100.
***
FL01900  '12 TO 14' 12  14 22.3  22.3
FL01901  156.88  7.33  1.0  0.1  0.1
FL01902  0   0
FL01903  1.0   1.0
FL019S1  156.88  1.0E-6  100.
***
FL02000  '13 TO 15' 13  15 25.9  25.9
FL02001  156.88  7.65  1.0  0.1  0.1
FL02002  0   0
FL02003  1.0   1.0
FL020S1  156.88  1.0E-6  100.
***
```

```
FL02100  '14 TO 15' 14  15 25.9  25.9
FL02101  156.88  7.69  1.0  0.1  0.1
FL02102  0   0
FL02103  1.0   1.0
FL021S1  156.88  1.0E-6  100.
***
FL02200  '1 TO 2' 1  2 4.125  4.125
FL02201  107.73  7.61  1.0  1.375  1.375
FL02202  3   0
FL02203  1.0   1.0
FL022S1  107.73  1.0E-6  100.
***
FL02300  '1 TO 2' 1  2 1.375  1.375
FL02301  107.73  7.61  1.0  1.375  1.375
FL02302  3   0
FL02303  1.0   1.0
FL023S1  107.73  1.0E-6  100.
***
FL02400  '3 TO 4' 3  4 9.775  9.775
FL02401  48.38  8.6  1.0  0.625  0.625
FL02402  3   0
FL02403  1.0   1.0
FL024S1  48.38  1.0E-6  100.
***
FL02500  '3 TO 4' 3  4 8.525  8.525
FL02501  48.38  8.6  1.0  0.625  0.625
FL02502  3   0
FL02503  1.0   1.0
FL025S1  48.38  1.0E-6  100.
***
FL02600  '5 TO 6' 5  6 14.6  14.6
FL02601  48.38  8.6  1.0  0.6  0.6
FL02602  3   0
FL02603  1.0   1.0
FL026S1  48.38  1.0E-6  100.
***
FL02700  '5 TO 6' 5  6 13.4  13.4
FL02701  48.38  8.6  1.0  0.6  0.6
FL02702  3   0
FL02703  1.0   1.0
FL027S1  48.38  1.0E-6  100.
***
FL02800  '16 TO 17' 16  17 7.3  7.3
FL02801  48.38  8.6  1.0  0.6  0.6
FL02802  3   0
FL02803  1.0   1.0
FL028S1  48.38  1.0E-6  100.
***
FL02900  '16 TO 17' 16  17 6.1  6.1
FL02901  48.38  8.6  1.0  0.6  0.6
FL02902  3   0
FL02903  1.0   1.0
FL029S1  48.38  1.0E-6  100.
***
FL03000  '18 TO 19' 18  19 12.2 12.2
FL03001  48.38  8.6  1.0  0.6  0.6
FL03002  3   0
FL03003  1.0   1.0
FL030S1  48.38  1.0E-6  100.
***
FL03100  '18 TO 19' 18  19 11. 11.
FL03101  48.38  8.6  1.0  0.6  0.6
FL03102  3   0
```

```
FL03103  1.0   1.0
FL031S1  48.38  1.0E-6  100.
***
.   * terminate
```

Hs_multi.txt:

```
************************************************
* Central basement                             *
************************************************
*
************************************************
* ht struc 5-b, header cavity, assumed to be in *
* basement as walls                            *
************************************************
hs00110000   7   1   -1
hs00110001   hdrcav_1
hs00110002   0.  1.
hs00110100   -1   1   0.0
hs00110102  0.004     2
hs00110103  0.012     3
hs00110104  0.028     4
hs00110105  0.06      5
hs00110106  0.124     6
hs00110107  0.188     7
hs00110200  -1
hs00110201  cvtrconc  1
hs00110202  cvtrconc  2
hs00110203  cvtrconc  3
hs00110204  cvtrconc  4
hs00110205  cvtrconc  5
hs00110206  cvtrconc  6
hs00110300  -1
hs00110400  1  001  ext  0.5 0.5
hs00110401  0.9  gray-gas-a  3.0
hs00110500  121.24  5.48  5.48
hs00110600  0
hs00110800  -1
hs00110801  300.  7
*
************************************************
* ht struc 8-b, fuel canal support assumed to be *
* in basement as walls                         *
************************************************
hs00113000   7   1   -1
hs00113001   fucansup_1
hs00113002   0.  1.
hs00113100   -1   1   0.0
hs00113102  0.004     2
hs00113103  0.012     3
hs00113104  0.028     4
hs00113105  0.06      5
hs00113106  0.124     6
hs00113107  0.188     7
hs00113200  -1
hs00113201  cvtrconc  1
hs00113202  cvtrconc  2
hs00113203  cvtrconc  3
hs00113204  cvtrconc  4
hs00113205  cvtrconc  5
hs00113206  cvtrconc  6
hs00113300  -1
hs00113400  1  001  ext  0.5 0.5
hs00113401  0.9  gray-gas-a  3.0
hs00113500  13.005  5.48  5.48
```

```
hs00113600  0
hs00113800  -1
hs00113801  300.  7
*
************************************************
* ht struc 10-b, cvtr concrete supports assumed  *
* to be in basement as walls                     *
************************************************
hs00115000   7   1   -1
hs00115001   concsupw_1
hs00115002   0.  1.
hs00115100   -1   1   0.0
hs00115102  0.004     2
hs00115103  0.012     3
hs00115104  0.028     4
hs00115105  0.06      5
hs00115106  0.124     6
hs00115107  0.188     7
hs00115200  -1
hs00115201  cvtrconc  1
hs00115202  cvtrconc  2
hs00115203  cvtrconc  3
hs00115204  cvtrconc  4
hs00115205  cvtrconc  5
hs00115206  cvtrconc  6
hs00115300  -1
hs00115400  1  001  ext  0.5 0.5
hs00115401  0.9  gray-gas-a  3.0
hs00115500  44.593  5.48  5.48
hs00115600  0
hs00115800  -1
hs00115801  300.   7
*
************************************************
* ht struc 12-b, moderator overflow tank         *
************************************************
hs00116000   3   1   -1
hs00116001   mdovftbw_1
hs00116002   0.  1.
hs00116100   -1   1   0.0
hs00116102  0.003175  2
hs00116103  0.009525  3
hs00116200  -1
hs00116201  cvtrstel  1
hs00116202  cvtrstel  2
hs00116300  -1
hs00116400  1  001  ext  0.5 0.5
hs00116401  0.9  gray-gas-a  3.0
hs00116500  51.5  5.48  5.48
hs00116600  0
hs00116800  -1
hs00116801  300.   3
*
*********************************************
* ht struc 16-b, moderator coolers           *
*********************************************
hs00118000   3   1   -1
hs00118001   modcobw_1
hs00118002   0.  1.
hs00118100   -1   1   0.0
hs00118102  0.001058  2
hs00118103  0.003175  3
hs00118200  -1
```

```
hs00118201  cvtrstel  1
hs00118202  cvtrstel  2
hs00118300  -1
hs00118400  1  001  ext  0.5 0.5
hs00118401  0.9  gray-gas-a  3.0
hs00118500  26.015  5.48  5.48
hs00118600  0
hs00118800  -1
hs00118801  300.   3
*
*****************************************
* ht struc 18-b, pumps-primary & injection *
*****************************************
hs00120000   3   1   -1
hs00120001   pmpsbw_1
hs00120002   0.  1.
hs00120100   -1   1   0.0
hs00120102  0.004233  2
hs00120103  0.0127    3
hs00120200  -1
hs00120201  cvtrstel  1
hs00120202  cvtrstel  2
hs00120300  -1
hs00120400  1  001  ext  0.5 0.5
hs00120401  0.9  gray-gas-a  3.0
hs00120500  23.225  5.48  5.48
hs00120600  0
hs00120800  -1
hs00120801  300.    3
*
*********************************************
* ht strucms-o, bnl addt'l steel             *
*********************************************
hs00109000   3   1   -1
hs00109001   miscstow_1
hs00109002   3.0  1.
hs00109100   -1   1   0.0
hs00109102  0.001588  2
hs00109103  0.004763  3
hs00109200  -1
hs00109201  cvtrstel  1
hs00109202  cvtrstel  2
hs00109300  -1
hs00109400  1  001  ext  0.5 0.5
hs00109401  0.9  gray-gas-a  3.0
hs00109500  438.94  2.48  2.48
hs00109600  0
hs00109800  -1
hs00109801  300.  3
*
*****************************************
* basement floor                         *
*****************************************
hs00121000   7   1   -1
hs00121001   baseflr_1
hs00121002   0.  -1.0e-7
hs00121100   -1   1   0.0
hs00121102  0.004     2
hs00121103  0.012     3
hs00121104  0.028     4
hs00121105  0.06      5
hs00121106  0.124     6
hs00121107  0.188     7
```

```
hs00121200  -1
hs00121201  cconc  1
hs00121202  cconc  2
hs00121203  cconc  3
hs00121204  cconc  4
hs00121205  cconc  5
hs00121206  cconc  6
hs00121300  -1
hs00121400  1  001  ext  0. 1.0
hs00121401  0.9  gray-gas-a  3.0
hs00121500  122.63  5.  0.188
hs00121600  0
hs00121800  -1
hs00121801  295.   7
*
****************************************
* Annulus basement region              *
****************************************
************************************************
* ht struc 1-b, bnl cyl shell in operating region *
************************************************
hs00201000   11   1   -1
hs00201001   cylsho_2
hs00201002   0.0   1.
hs00201100   -1   1   0.0
hs00201102  0.0022    2
hs00201103  0.00635   3
hs00201104  0.01135   4
hs00201105  0.014     5
hs00201106  0.01855   6
hs00201107  0.02815   7
hs00201108  0.04735   8
hs00201109  0.06655   9
hs00201110  0.14      10
hs00201111  0.2       11
hs00201200  -1
hs00201201  cvtrstel  1
hs00201202  cvtrstel  2
hs00201203  cvtrconc  3
hs00201204  cvtrconc  4
hs00201205  cvtrconc  5
hs00201206  cvtrconc  6
hs00201207  cvtrconc  7
hs00201208  cvtrconc  8
hs00201209  cvtrconc  9
hs00201210  cvtrconc  10
hs00201300  -1
hs00201400  1  002  ext  0.5 0.5
hs00201401  0.9  gray-gas-a  3.0
hs00201500  304.  5.48  5.48
hs00201600  0
hs00201800  -1
hs00201801  300.  11
*
************************************************
* ht struc 5-b, header cavity, assumed to be in *
* basement as walls                             *
************************************************
*hs00210000   7   1   -1
*hs00210001   hdrcav_2
*hs00210002   0.  1.
*hs00210100   -1   1   0.0
*hs00210102  0.004     2
```

```
*hs00210103  0.012     3
*hs00210104  0.028     4
*hs00210105  0.06      5
*hs00210106  0.124     6
*hs00210107  0.188     7
*hs00210200  -1
*hs00210201  cvtrconc  1
*hs00210202  cvtrconc  2
*hs00210203  cvtrconc  3
*hs00210204  cvtrconc  4
*hs00210205  cvtrconc  5
*hs00210206  cvtrconc  6
*hs00210300  -1
*hs00210400  1  002  ext  0.5 0.5
*hs00210500  121.24  5.48  5.48
*hs00210600  0
*hs00210800  -1
*hs00210801  300.  7
*
************************************************
* ht struc 8-b, fuel canal support assumed to be *
* in basement as walls                           *
************************************************
hs00213000   7   1   -1
hs00213001   fucansup_2
hs00213002   0.  1.
hs00213100   -1   1   0.0
hs00213102  0.004     2
hs00213103  0.012     3
hs00213104  0.028     4
hs00213105  0.06      5
hs00213106  0.124     6
hs00213107  0.188     7
hs00213200  -1
hs00213201  cvtrconc  1
hs00213202  cvtrconc  2
hs00213203  cvtrconc  3
hs00213204  cvtrconc  4
hs00213205  cvtrconc  5
hs00213206  cvtrconc  6
hs00213300  -1
hs00213400  1  002  ext  0.5 0.5
hs00213401  0.9  gray-gas-a  3.0
hs00213500  13.005  5.48  5.48
hs00213600  0
hs00213800  -1
hs00213801  300.  7
*
************************************************
* ht struc 10-b, cvtr concrete supports assumed  *
* to be in basement as walls                     *
************************************************
hs00215000   7   1   -1
hs00215001   concsupw1
hs00215002   0.  1.
hs00215100   -1   1   0.0
hs00215102  0.004     2
hs00215103  0.012     3
hs00215104  0.028     4
hs00215105  0.06      5
hs00215106  0.124     6
hs00215107  0.188     7
hs00215200  -1
```

```
hs00215201  cvtrconc  1
hs00215202  cvtrconc  2
hs00215203  cvtrconc  3
hs00215204  cvtrconc  4
hs00215205  cvtrconc  5
hs00215206  cvtrconc  6
hs00215300  -1
hs00215400  1  002  ext  0.5 0.5
hs00215401  0.9  gray-gas-a  3.0
hs00215500  44.593  5.48  5.48
hs00215600  0
hs00215800  -1
hs00215801  300.   7
*
************************************************
* ht struc 12-b, moderator overflow tank       *
************************************************
hs00216000   3   1   -1
hs00216001   mdovftbw_2
hs00216002   0.  1.
hs00216100   -1   1   0.0
hs00216102  0.003175  2
hs00216103  0.009525  3
hs00216200  -1
hs00216201  cvtrstel  1
hs00216202  cvtrstel  2
hs00216300  -1
hs00216400  1  002  ext  0.5 0.5
hs00216401  0.9  gray-gas-a  3.0
hs00216500  51.5  5.48  5.48
hs00216600  0
hs00216800  -1
hs00216801  300.   3
*
*******************************************
* ht struc 16-b, moderator coolers        *
*******************************************
hs00218000   3   1   -1
hs00218001   modcobw_2
hs00218002   0.  1.
hs00218100   -1   1   0.0
hs00218102  0.001058  2
hs00218103  0.003175  3
hs00218200  -1
hs00218201  cvtrstel  1
hs00218202  cvtrstel  2
hs00218300  -1
hs00218400  1  002  ext  0.5 0.5
hs00218401  0.9  gray-gas-a  3.0
hs00218500  26.015  5.48  5.48
hs00218600  0
hs00218800  -1
hs00218801  300.   3
*
*******************************************
* ht struc 18-b, pumps-primary & injection *
*******************************************
hs00220000   3   1   -1
hs00220001   pmpsbw_2
hs00220002   0.  1.
hs00220100   -1   1   0.0
hs00220102  0.004233  2
hs00220103  0.0127    3
```

```
hs00220200  -1
hs00220201  cvtrstel  1
hs00220202  cvtrstel  2
hs00220300  -1
hs00220400  1  002  ext  0.5 0.5
hs00220401  0.9  gray-gas-a  3.0
hs00220500  23.225  5.48  5.48
hs00220600  0
hs00220800  -1
hs00220801  300.    3
*
*******************************************
* ht strucms-o, bnl addt'l steel            *
*******************************************
hs00209000   3   1   -1
hs00209001   miscstow_2
hs00209002   3.0  1.
hs00209100   -1   1   0.0
hs00209102  0.001588  2
hs00209103  0.004763  3
hs00209200  -1
hs00209201  cvtrstel  1
hs00209202  cvtrstel  2
hs00209300  -1
hs00209400  1  002  ext  0.5 0.5
hs00209401  0.9  gray-gas-a  3.0
hs00209500  438.94  2.48  2.48
hs00209600  0
hs00209800  -1
hs00209801  300.  3
*
*****************************************
* basement floor                         *
*****************************************
hs00221000   7   1   -1
hs00221001   baseflr_2
hs00221002   0.  -1.0e-7
hs00221100   -1   1   0.0
hs00221102  0.004     2
hs00221103  0.012     3
hs00221104  0.028     4
hs00221105  0.06      5
hs00221106  0.124     6
hs00221107  0.188     7
hs00221200  -1
hs00221201  cconc  1
hs00221202  cconc  2
hs00221203  cconc  3
hs00221204  cconc  4
hs00221205  cconc  5
hs00221206  cconc  6
hs00221300  -1
hs00221400  1  001  ext  0. 1.0
hs00221401  0.9  gray-gas-a  3.0
hs00221500  122.63  5.  0.188
hs00221600  0
hs00221800  -1
hs00221801  295.   7
*
*****************************************
* Central low intermediate               *
*****************************************
*********************************************************
```

```
* ht struc 6-i, reactor compartment assumed to be walls  *
*********************************************************
hs00311000   7   1   -1
hs00311001   reacompw_3
hs00311002   7.9  1.
hs00311100   -1   1   0.0
hs00311102  0.004     2
hs00311103  0.012     3
hs00311104  0.028     4
hs00311105  0.06      5
hs00311106  0.124     6
hs00311107  0.188     7
hs00311200  -1
hs00311201  cvtrconc  1
hs00311202  cvtrconc  2
hs00311203  cvtrconc  3
hs00311204  cvtrconc  4
hs00311205  cvtrconc  5
hs00311206  cvtrconc  6
hs00311300  -1
hs00311400  1  003 ext  0.5 0.5
hs00311401  0.9  gray-gas-a  3.0
hs00311500  38.555  2.5  2.5
hs00311600  0
hs00311800  -1
hs00311801  300.  7
*
*****************************************************
* ht struc 7-i, fuel canal assumed to be walls      *
*****************************************************
hs00312000   7   1   -1
hs00312001   fucanalw_3
hs00312002   7.9  1.
hs00312100   -1   1   0.0
hs00312102  0.004     2
hs00312103  0.012     3
hs00312104  0.028     4
hs00312105  0.06      5
hs00312106  0.124     6
hs00312107  0.188     7
hs00312200  -1
hs00312201  cvtrconc  1
hs00312202  cvtrconc  2
hs00312203  cvtrconc  3
hs00312204  cvtrconc  4
hs00312205  cvtrconc  5
hs00312206  cvtrconc  6
hs00312300  -1
hs00312400  1  003 ext  0.5 0.5
hs00312401  0.9  gray-gas-a  3.0
hs00312500  37.16  2.5  2.5
hs00312600  0
hs00312800  -1
hs00312801  300.   7
*
*********************************************
* ht struc 9-i, floor of reactor cavity top   *
*********************************************
hs00314000   7   1   -1
hs00314001   rcvflrin_3
hs00314002   7.9  -1.0e-7
hs00314100   -1   1   0.0
hs00314102  0.004     2
```

```
hs00314103  0.012     3
hs00314104  0.028     4
hs00314105  0.06      5
hs00314106  0.124     6
hs00314107  0.188     7
hs00314200  -1
hs00314201  cvtrconc  1
hs00314202  cvtrconc  2
hs00314203  cvtrconc  3
hs00314204  cvtrconc  4
hs00314205  cvtrconc  5
hs00314206  cvtrconc  6
hs00314300  -1
hs00314400  1  003 ext  0.5 0.5
hs00314401  0.9  gray-gas-a  3.0
hs00314500  6.65  1.  0.188
hs00314600  0
hs00314800  -1
hs00314801  300.    7
*
*********************************************
* ht struc 9-b, roof of reactor cavity top   *
*********************************************
*hs000315000   7   1   -1
*hs000315001   rcvflrin_3
*hs000315002   10.4  0.
*hs000315100   -1   1   0.0
*hs000315102  0.004     2
*hs000315103  0.012     3
*hs000315104  0.028     4
*hs000315105  0.06      5
*hs000315106  0.124     6
*hs000315107  0.188     7
*hs000315200  -1
*hs000315201  cvtrconc  1
*hs000315202  cvtrconc  2
*hs000315203  cvtrconc  3
*hs000315204  cvtrconc  4
*hs000315205  cvtrconc  5
*hs000315206  cvtrconc  6
*hs000315300  -1
*hs000315400  1  003 ext 0.5  0.5
*hs000315500  6.65  1.  0.188
*hs000315600  0
*hs000315800  -1
*hs000315801  300.    7
*
*********************************************
* ht struc 13-i, pressurizer                 *
*********************************************
hs00317000   5   1   -1
hs00317001   press_3
hs00317002   7.9  1.
hs00317100   -1   1   0.0
hs00317102  0.007     2
hs00317103  0.021     3
hs00317104  0.0391    4
hs00317105  0.0572    5
hs00317200  -1
hs00317201  cvtrstel  1
hs00317202  cvtrstel  2
hs00317203  cvtrstel  3
hs00317204  cvtrstel  4
```

```
hs00317300  -1
hs00317400  1  003  ext  0.5 0.5
hs00317401  0.9  gray-gas-a  3.0
hs00317500  8.175  2.5  2.5
hs00317600  0
hs00317800  -1
hs00317801  300.   5
*
*******************************************
* ht struc 17-i, shutdown coolers           *
*******************************************
hs00319000   3   1   -1
hs00319001   shdcoiw_3
hs00319002   7.9  1.
hs00319100   -1   1   0.0
hs00319102  0.000508  2
hs00319103  0.001524  3
hs00319200  -1
hs00319201  cvtrstel  1
hs00319202  cvtrstel  2
hs00319300  -1
hs00319400  1  003 ext  0.5 0.5
hs00319401  0.9  gray-gas-a  3.0
hs00319500  6.13  2.5  2.5
hs00319600  0
hs00319800  -1
hs00319801  300.   3
*
*******************************************
* ht strucms-o, bnl addt'l steel            *
*******************************************
hs00309000   3   1   -1
hs00309001   miscstow_3
hs00309002   7.9  1.
hs00309100   -1   1   0.0
hs00309102  0.001588  2
hs00309103  0.004763  3
hs00309200  -1
hs00309201  cvtrstel  1
hs00309202  cvtrstel  2
hs00309300  -1
hs00309400  1  003 ext  0.5 0.5
hs00309401  0.9  gray-gas-a  3.0
hs00309500  219.46  2.5  2.5
hs00309600  0
hs00309800  -1
hs00309801  300.  3
*
*******************************************
* Annulus low intermediate                  *
*******************************************
*********************************************************
* ht struc 1-i, bnl cyl shell in basement region x 0.64 *
*********************************************************
hs00401000   11   1   -1
hs00401001   cylsho_4
hs00401002   7.9   1.
hs00401100   -1   1   0.0
hs00401102  0.0022    2
hs00401103  0.00635   3
hs00401104  0.01135   4
hs00401105  0.014     5
hs00401106  0.01855   6
```

```
hs00401107  0.02815   7
hs00401108  0.04735   8
hs00401109  0.06655   9
hs00401110  0.14      10
hs00401111  0.2       11
hs00401200  -1
hs00401201  cvtrstel  1
hs00401202  cvtrstel  2
hs00401203  cvtrconc  3
hs00401204  cvtrconc  4
hs00401205  cvtrconc  5
hs00401206  cvtrconc  6
hs00401207  cvtrconc  7
hs00401208  cvtrconc  8
hs00401209  cvtrconc  9
hs00401210  cvtrconc  10
hs00401300  -1
hs00401400  1  004 ext  0.5 0.5
hs00401401  0.9  gray-gas-a  3.0
hs00401500  135.25  11.  2.5
hs00401600  0
hs00401800  -1
hs00401801  300.  11
*
*******************************************
* ht strucms-o, bnl addt'l steel            *
*******************************************
hs00409000   3   1   -1
hs00409001   miscstow_4
hs00409002   7.9  1.
hs00409100   -1   1   0.0
hs00409102  0.001588  2
hs00409103  0.004763  3
hs00409200  -1
hs00409201  cvtrstel  1
hs00409202  cvtrstel  2
hs00409300  -1
hs00409400  1  004 ext  0.5 0.5
hs00409401  0.9  gray-gas-a  3.0
hs00409500  219.46  2.5  2.5
hs00409600  0
hs00409800  -1
hs00409801  300.  3
*
*******************************************
* Central high intermediate                *
*******************************************
*************************************************
* ht struc 4-i, roof of operation floor         *
*************************************************
hs00504000   7   1   -1
hs00504001   roof_5
hs00504002   15.2  0.
hs00504100   -1   1   0.0
hs00504102  0.004     2
hs00504103  0.012     3
hs00504104  0.028     4
hs00504105  0.06      5
hs00504106  0.124     6
hs00504107  0.188     7
hs00504200  -1
hs00504201  cvtrconc  1
hs00504202  cvtrconc  2
```

```
hs00504203  cvtrconc  3
hs00504204  cvtrconc  4
hs00504205  cvtrconc  5
hs00504206  cvtrconc  6
hs00504300  -1
hs00504400  1  005 ext  0. 1.0
hs00504401  0.9  gray-gas-a  3.0
hs00504500  115.  1.  0.188
hs00504600  0
hs00504800  -1
hs00504801  300.  7
*
*********************************************************
* ht struc 6-i, reactor compartment assumed to be walls  *
*********************************************************
hs00511000   7   1   -1
hs00511001   reacompw_5
hs00511002   12.8  1.
hs00511100   -1   1   0.0
hs00511102  0.004     2
hs00511103  0.012     3
hs00511104  0.028     4
hs00511105  0.06      5
hs00511106  0.124     6
hs00511107  0.188     7
hs00511200  -1
hs00511201  cvtrconc  1
hs00511202  cvtrconc  2
hs00511203  cvtrconc  3
hs00511204  cvtrconc  4
hs00511205  cvtrconc  5
hs00511206  cvtrconc  6
hs00511300  -1
hs00511400  1  005 ext  0.5 0.5
hs00511401  0.9  gray-gas-a  3.0
hs00511500  38.555  2.4  2.4
hs00511600  0
hs00511800  -1
hs00511801  300.  7
*
*****************************************************
* ht struc 7-i, fuel canal assumed to be walls      *
*****************************************************
hs00512000   7   1   -1
hs00512001   fucanalw_5
hs00512002   12.8  1.
hs00512100   -1   1   0.0
hs00512102  0.004     2
hs00512103  0.012     3
hs00512104  0.028     4
hs00512105  0.06      5
hs00512106  0.124     6
hs00512107  0.188     7
hs00512200  -1
hs00512201  cvtrconc  1
hs00512202  cvtrconc  2
hs00512203  cvtrconc  3
hs00512204  cvtrconc  4
hs00512205  cvtrconc  5
hs00512206  cvtrconc  6
hs00512300  -1
hs00512400  1  005 ext  0.5 0.5
hs00512401  0.9  gray-gas-a  3.0
```

```
hs00512500  37.16  2.4  2.4
hs00512600  0
hs00512800  -1
hs00512801  300.   7
*
************************************************
* ht struc 13-i, pressurizer                   *
************************************************
hs00517000   5   1   -1
hs00517001   press_5
hs00517002   12.8  1.
hs00517100   -1   1   0.0
hs00517102  0.007     2
hs00517103  0.021     3
hs00517104  0.0391    4
hs00517105  0.0572    5
hs00517200  -1
hs00517201  cvtrstel  1
hs00517202  cvtrstel  2
hs00517203  cvtrstel  3
hs00517204  cvtrstel  4
hs00517300  -1
hs00517400  1  005 ext  0.5 0.5
hs00517401  0.9  gray-gas-a  3.0
hs00517500  8.175  2.4  2.4
hs00517600  0
hs00517800  -1
hs00517801  300.   5
*
*********************************************
* ht strucms-o, bnl addt'l steel            *
*********************************************
hs00509000   3   1   -1
hs00509001   miscstow_5
hs00509002   12.8  1.
hs00509100   -1   1   0.0
hs00509102  0.001588  2
hs00509103  0.004763  3
hs00509200  -1
hs00509201  cvtrstel  1
hs00509202  cvtrstel  2
hs00509300  -1
hs00509400  1  005  ext  0.5 0.5
hs00509401  0.9  gray-gas-a  3.0
hs00509500  125.4  2.4  2.4
hs00509600  0
hs00509800  -1
hs00509801  300.  3
*
*********************************************
* Annulus high intermediate                 *
*********************************************
**************************************************
* ht struc 1-i, bnl cyl shell in operating region *
**************************************************
hs00601000   11   1   -1
hs00601001   cylsho_6
hs00601002   12.8   1.
hs00601100   -1   1   0.0
hs00601102  0.0022    2
hs00601103  0.00635   3
hs00601104  0.01135   4
hs00601105  0.014     5
```

```
hs00601106  0.01855   6
hs00601107  0.02815   7
hs00601108  0.04735   8
hs00601109  0.06655   9
hs00601110  0.14      10
hs00601111  0.2       11
hs00601200  -1
hs00601201  cvtrstel  1
hs00601202  cvtrstel  2
hs00601203  cvtrconc  3
hs00601204  cvtrconc  4
hs00601205  cvtrconc  5
hs00601206  cvtrconc  6
hs00601207  cvtrconc  7
hs00601208  cvtrconc  8
hs00601209  cvtrconc  9
hs00601210  cvtrconc  10
hs00601300  -1
hs00601400  1  006 ext  0.5 0.5
hs00601401  0.9  gray-gas-a  3.0
hs00601500  135.25 11.  2.4
hs00601600  0
hs00601800  -1
hs00601801  300.  11
*
************************************************
* ht struc 4-i, roof of operation floor          *
************************************************
hs00604000   7   1   -1
hs00604001   roof_6
hs00604002   15.2  0.
hs00604100   -1   1   0.0
hs00604102  0.004     2
hs00604103  0.012     3
hs00604104  0.028     4
hs00604105  0.06      5
hs00604106  0.124     6
hs00604107  0.188     7
hs00604200  -1
hs00604201  cvtrconc  1
hs00604202  cvtrconc  2
hs00604203  cvtrconc  3
hs00604204  cvtrconc  4
hs00604205  cvtrconc  5
hs00604206  cvtrconc  6
hs00604300  -1
hs00604400  1  006 ext  0. 1.0
hs00604401  0.9  gray-gas-a  3.0
hs00604500  115.  1.  0.188
hs00604600  0
hs00604800  -1
hs00604801  300.  7
*
*********************************************
* ht strucms-o, bnl addt'l steel             *
*********************************************
hs00609000   3   1   -1
hs00609001   miscstow_6
hs00609002   12.8  1.
hs00609100   -1   1   0.0
hs00609102  0.001588  2
hs00609103  0.004763  3
hs00609200  -1
```

```
hs00609201  cvtrstel  1
hs00609202  cvtrstel  2
hs00609300  -1
hs00609400  1  006 ext  0.5 0.5
hs00609401  0.9  gray-gas-a  3.0
hs00609500  125.4  2.4  2.4
hs00609600  0
hs00609800  -1
hs00609801  300.  3
*
**************************************
* Central bottom operating           *
**************************************
************************************************
* ht struc 4-o, operating floor in op region top *
************************************************
hs00704000   7   1   -1
hs00704001   opflrflr_7
hs00704002   15.2  -1.0e-7
hs00704100   -1   1   0.0
hs00704102  0.004     2
hs00704103  0.012     3
hs00704104  0.028     4
hs00704105  0.06      5
hs00704106  0.124     6
hs00704107  0.188     7
hs00704200  -1
hs00704201  cvtrconc  1
hs00704202  cvtrconc  2
hs00704203  cvtrconc  3
hs00704204  cvtrconc  4
hs00704205  cvtrconc  5
hs00704206  cvtrconc  6
hs00704300  -1
hs00704400  1  007 ext  0. 1.0
hs00704401  0.9  gray-gas-a  3.0
hs00704500  115.  1.  0.188
hs00704600  0
hs00704800  -1
hs00704801  300.  7
*
*******************************************
* ht strucms-o, bnl addt'l steel           *
*******************************************
hs00709000   3   1   -1
hs00709001   miscstow_7
hs00709002   15.2  1.
hs00709100   -1   1   0.0
hs00709102  0.001588  2
hs00709103  0.004763  3
hs00709200  -1
hs00709201  cvtrstel  1
hs00709202  cvtrstel  2
hs00709300  -1
hs00709400  1  007 ext  0.5 0.5
hs00709401  0.9  gray-gas-a  3.0
hs00709500  62.68  1.6  1.6
hs00709600  0
hs00709800  -1
hs00709801  300.  3
*
**************************************
* Annulus bottom operating           *
```

```
****************************************
************************************************
* ht struc 1-o, bnl cyl shell in operating region *
************************************************
hs00801000   11   1   -1
hs00801001   cylsho_8
hs00801002   15.2   1.
hs00801100   -1   1   0.0
hs00801102  0.0022    2
hs00801103  0.00635   3
hs00801104  0.01135   4
hs00801105  0.014     5
hs00801106  0.01855   6
hs00801107  0.02815   7
hs00801108  0.04735   8
hs00801109  0.06655   9
hs00801110  0.14      10
hs00801111  0.2       11
hs00801200  -1
hs00801201  cvtrstel  1
hs00801202  cvtrstel  2
hs00801203  cvtrconc  3
hs00801204  cvtrconc  4
hs00801205  cvtrconc  5
hs00801206  cvtrconc  6
hs00801207  cvtrconc  7
hs00801208  cvtrconc  8
hs00801209  cvtrconc  9
hs00801210  cvtrconc  10
hs00801300  -1
hs00801400  1  008 ext  0.5 0.5
hs00801401  0.9  gray-gas-a  3.0
hs00801500  98.686  11.  1.6
hs00801600  0
hs00801800  -1
hs00801801  300.  11
*
************************************************
* ht struc 4-o, operating floor in op region top *
************************************************
hs00804000   7   1   -1
hs00804001   opflrflr_8
hs00804002   15.2  -1.0e-7
hs00804100   -1   1   0.0
hs00804102  0.004     2
hs00804103  0.012     3
hs00804104  0.028     4
hs00804105  0.06      5
hs00804106  0.124     6
hs00804107  0.188     7
hs00804200  -1
hs00804201  cvtrconc  1
hs00804202  cvtrconc  2
hs00804203  cvtrconc  3
hs00804204  cvtrconc  4
hs00804205  cvtrconc  5
hs00804206  cvtrconc  6
hs00804300  -1
hs00804400  1  008 ext  0. 1.0
hs00804401  0.9  gray-gas-a  3.0
hs00804500  115.  1.  0.188
hs00804600  0
hs00804800  -1
```

```
hs00804801  300.  7
*
************************************************
* ht struc 11-o, steam gen shield assumed to be  *
* in operating region as walls                   *
************************************************
hs00805000   7   1   -1
hs00805001   stmgensw_8
hs00805002   15.2  1.
hs00805100   -1   1   0.0
hs00805102  0.004     2
hs00805103  0.012     3
hs00805104  0.028     4
hs00805105  0.06      5
hs00805106  0.124     6
hs00805107  0.188     7
hs00805200  -1
hs00805201  cvtrconc  1
hs00805202  cvtrconc  2
hs00805203  cvtrconc  3
hs00805204  cvtrconc  4
hs00805205  cvtrconc  5
hs00805206  cvtrconc  6
hs00805300  -1
hs00805400  1  008 ext  0.5 0.5
hs00805401  0.9  gray-gas-a  3.0
hs00805500  12.38  5.  1.6
hs00805600  0
hs00805800  -1
hs00805801  300.  7
*
*********************************************
* ht struc 14-o, pressurizer discharge tank   *
*********************************************
hs00806000   3   1   -1
hs00806001   prdctow_8
hs00806002   15.2  1.
hs00806100   -1   1   0.0
hs00806102  0.00212   2
hs00806103  0.006355  3
hs00806200  -1
hs00806201  cvtrstel  1
hs00806202  cvtrstel  2
hs00806300  -1
hs00806400  1  008 ext  0.5 0.5
hs00806401  0.9  gray-gas-a  3.0
hs00806500  10.545  5.  1.6
hs00806600  0
hs00806800  -1
hs00806801  300.  3
*
*********************************************
* ht struc 15-o, steam generator              *
*********************************************
hs00807000   4   1   -1
hs00807001   stgenow_8
hs00807002   15.2  1.
hs00807100   -1   1   0.0
hs00807102  0.007     2
hs00807103  0.021     3
hs00807104  0.0381    4
hs00807200  -1
hs00807201  cvtrstel  1
```

```
hs00807202  cvtrstel  2
hs00807203  cvtrstel  3
hs00807300  -1
hs00807400  1  008 ext  0.5 0.5
hs00807401  0.9  gray-gas-a  3.0
hs00807500  23.83  5.  1.6
hs00807600  0
hs00807800  -1
hs00807801  300.  4
*
*********************************************
* ht struc 20-o, all of "i" beams             *
*********************************************
hs00808000   3   1   -1
hs00808001   ibeamow_8
hs00808002   15.2  1.
hs00808100   -1   1   0.0
hs00808102  0.006857  2
hs00808103  0.02057   3
hs00808200  -1
hs00808201  cvtrstel  1
hs00808202  cvtrstel  2
hs00808300  -1
hs00808400  1  008 ext  0.5 0.5
hs00808401  0.9  gray-gas-a  3.0
hs00808500  30.98  5.  1.6
hs00808600  0
hs00808800  -1
hs00808801  300.  3
*
*********************************************
* ht strucms-o, bnl addt'l steel             *
*********************************************
hs00809000   3   1   -1
hs00809001   miscstow_8
hs00809002   15.2  1.
hs00809100   -1   1   0.0
hs00809102  0.001588  2
hs00809103  0.004763  3
hs00809200  -1
hs00809201  cvtrstel  1
hs00809202  cvtrstel  2
hs00809300  -1
hs00809400  1  008 ext  0.5 0.5
hs00809401  0.9  gray-gas-a  3.0
hs00809500  62.68  5.  1.6
hs00809600  0
hs00809800  -1
hs00809801  300.  3
*
*********************************************
* Central mid low operating                  *
*********************************************
*********************************************
* ht struc 19-o, fuel handling apparatus      *
*********************************************
hs00908000   3   1   -1
hs00908001   fuhdlaow_9
hs00908002   16.8  1.
hs00908100   -1   1   0.0
hs00908102  0.003978  2
hs00908103  0.01193   3
hs00908200  -1
```

```
hs00908201  cvtrstel  1
hs00908202  cvtrstel  2
hs00908300  -1
hs00908400  1  009 ext  0.5 0.5
hs00908401  0.9  gray-gas-a  3.0
hs00908500  46.45  1.8 1.8
hs00908600  0
hs00908800  -1
hs00908801  300.   3
*
*******************************************
* ht strucms-o, bnl addt'l steel            *
*******************************************
hs00909000   3   1   -1
hs00909001   miscstow_9
hs00909002   16.8  1.
hs00909100   -1   1   0.0
hs00909102  0.001588  2
hs00909103  0.004763  3
hs00909200  -1
hs00909201  cvtrstel  1
hs00909202  cvtrstel  2
hs00909300  -1
hs00909400  1  009 ext  0.5 0.5
hs00909401  0.9  gray-gas-a  3.0
hs00909500  62.68  1.8  1.8
hs00909600  0
hs00909800  -1
hs00909801  300.  3
*
*******************************************
* Annulus mid low operating                 *
*******************************************
*************************************************
* ht struc 1-o, bnl cyl shell in operating region *
*************************************************
hs01001000   11   1   -1
hs01001001   cylsho_10
hs01001002   16.8   1.
hs01001100   -1   1   0.0
hs01001102  0.0022    2
hs01001103  0.00635   3
hs01001104  0.01135   4
hs01001105  0.014     5
hs01001106  0.01855   6
hs01001107  0.02815   7
hs01001108  0.04735   8
hs01001109  0.06655   9
hs01001110  0.14      10
hs01001111  0.2       11
hs01001200  -1
hs01001201  cvtrstel  1
hs01001202  cvtrstel  2
hs01001203  cvtrconc  3
hs01001204  cvtrconc  4
hs01001205  cvtrconc  5
hs01001206  cvtrconc  6
hs01001207  cvtrconc  7
hs01001208  cvtrconc  8
hs01001209  cvtrconc  9
hs01001210  cvtrconc  10
hs01001300  -1
hs01001400  1  010  ext  0.5 0.5
```

```
hs01001401  0.9  gray-gas-a  3.0
hs01001500  98.686  11.  1.8
hs01001600  0
hs01001800  -1
hs01001801  300.  11
*
************************************************
* ht struc 11-o, steam gen shield assumed to be  *
* in operating region as walls                   *
************************************************
hs01005000   7   1   -1
hs01005001   stmgensw_10
hs01005002   16.8  1.
hs01005100   -1   1   0.0
hs01005102  0.004     2
hs01005103  0.012     3
hs01005104  0.028     4
hs01005105  0.06      5
hs01005106  0.124     6
hs01005107  0.188     7
hs01005200  -1
hs01005201  cvtrconc  1
hs01005202  cvtrconc  2
hs01005203  cvtrconc  3
hs01005204  cvtrconc  4
hs01005205  cvtrconc  5
hs01005206  cvtrconc  6
hs01005300  -1
hs01005400  1  010  ext  0.5 0.5
hs01005401  0.9  gray-gas-a  3.0
hs01005500  12.39  5.  1.8
hs01005600  0
hs01005800  -1
hs01005801  300.  7
*
*********************************************
* ht struc 14-o, pressurizer discharge tank   *
*********************************************
hs01006000   3   1   -1
hs01006001   prdctow_10
hs01006002   16.8  1.
hs01006100   -1   1   0.0
hs01006102  0.00212   2
hs01006103  0.006355  3
hs01006200  -1
hs01006201  cvtrstel  1
hs01006202  cvtrstel  2
hs01006300  -1
hs01006400  1  010  ext  0.5 0.5
hs01006401  0.9  gray-gas-a  3.0
hs01006500  10.545  5.  1.8
hs01006600  0
hs01006800  -1
hs01006801  300.  3
*
*********************************************
* ht struc 15-o, steam generator              *
*********************************************
hs01007000   4   1   -1
hs01007001   stgenow_10
hs01007002   16.8  1.
hs01007100   -1   1   0.0
hs01007102  0.007     2
```

```
hs01007103  0.021     3
hs01007104  0.0381    4
hs01007200  -1
hs01007201  cvtrstel  1
hs01007202  cvtrstel  2
hs01007203  cvtrstel  3
hs01007300  -1
hs01007400  1  010  ext  0.5 0.5
hs01007401  0.9  gray-gas-a  3.0
hs01007500  23.83  5.  1.8
hs01007600  0
hs01007800  -1
hs01007801  300.  4
*
************************************************
* ht struc 19-o, fuel handling apparatus        *
************************************************
hs01008000   3   1   -1
hs01008001   fuhdlaow_10
hs01008002   16.8  1.
hs01008100   -1   1   0.0
hs01008102  0.003978  2
hs01008103  0.01193   3
hs01008200  -1
hs01008201  cvtrstel  1
hs01008202  cvtrstel  2
hs01008300  -1
hs01008400  1  010  ext  0.5 0.5
hs01008401  0.9  gray-gas-a  3.0
hs01008500  46.45  5.  1.8
hs01008600  0
hs01008800  -1
hs01008801  300.   3
*
************************************************
* ht struc 20-o, all of "i" beams               *
************************************************
hs01040000   3   1   -1
hs01040001   ibeamow_10
hs01040002   16.8  1.
hs01040100   -1   1   0.0
hs01040102  0.006857  2
hs01040103  0.02057   3
hs01040200  -1
hs01040201  cvtrstel  1
hs01040202  cvtrstel  2
hs01040300  -1
hs01040400  1  010  ext  0.5 0.5
hs01040401  0.9  gray-gas-a  3.0
hs01040500  30.98  5. 1.8
hs01040600  0
hs01040800  -1
hs01040801  300.  3
*
*********************************************
* ht strucms-o, bnl addt'l steel             *
*********************************************
hs01009000   3   1   -1
hs01009001   miscstow_10
hs01009002   16.8  1.
hs01009100   -1   1   0.0
hs01009102  0.001588  2
hs01009103  0.004763  3
```

```
hs01009200  -1
hs01009201  cvtrstel  1
hs01009202  cvtrstel  2
hs01009300  -1
hs01009400  1  010  ext  0.5 0.5
hs01009401  0.9  gray-gas-a  3.0
hs01009500  62.7  5.  1.8
hs01009600  0
hs01009800  -1
hs01009801  300.  3
*
************************************************
* Central mid high operating                   *
************************************************
*********************************************
* ht strucms-o, bnl addt'l steel             *
*********************************************
hs01109000   3   1   -1
hs01109001   miscstow_11
hs01109002   18.6  1.
hs01109100   -1   1   0.0
hs01109102  0.001588  2
hs01109103  0.004763  3
hs01109200  -1
hs01109201  cvtrstel  1
hs01109202  cvtrstel  2
hs01109300  -1
hs01109400  1  011  ext  0.5 0.5
hs01109401  0.9  gray-gas-a  3.0
hs01109500  0.1  5.  3.7
hs01109600  0
hs01109800  -1
hs01109801  300.  3
*
*********************************************
* Annulus mid high operating                 *
*********************************************
************************************************
* ht struc 1-o, bnl cyl shell in operating region *
************************************************
hs01201000   11   1   -1
hs01201001   cylsho_12
hs01201002   18.6   1.
hs01201100   -1   1   0.0
hs01201102  0.0022    2
hs01201103  0.00635   3
hs01201104  0.01135   4
hs01201105  0.014     5
hs01201106  0.01855   6
hs01201107  0.02815   7
hs01201108  0.04735   8
hs01201109  0.06655   9
hs01201110  0.14      10
hs01201111  0.2       11
hs01201200  -1
hs01201201  cvtrstel  1
hs01201202  cvtrstel  2
hs01201203  cvtrconc  3
hs01201204  cvtrconc  4
hs01201205  cvtrconc  5
hs01201206  cvtrconc  6
hs01201207  cvtrconc  7
hs01201208  cvtrconc  8
```

```
hs01201209  cvtrconc  9
hs01201210  cvtrconc  10
hs01201300  -1
hs01201400  1  012  ext  0.5 0.5
hs01201401  0.9  gray-gas-a  3.0
hs01201500  197.136  11.  3.7
hs01201600  0
hs01201800  -1
hs01201801  300.  11
*
************************************************
* ht struc 11-o, steam gen shield assumed to be  *
* in operating region as walls                   *
************************************************
hs01205000   7   1   -1
hs01205001   stmgensw_12
hs01205002   18.6  1.
hs01205100   -1   1   0.0
hs01205102  0.004     2
hs01205103  0.012     3
hs01205104  0.028     4
hs01205105  0.06      5
hs01205106  0.124     6
hs01205107  0.188     7
hs01205200  -1
hs01205201  cvtrconc  1
hs01205202  cvtrconc  2
hs01205203  cvtrconc  3
hs01205204  cvtrconc  4
hs01205205  cvtrconc  5
hs01205206  cvtrconc  6
hs01205300  -1
hs01205400  1  012  ext  0.5 0.5
hs01205401  0.9  gray-gas-a  3.0
hs01205500  12.38  5.  3.7
hs01205600  0
hs01205800  -1
hs01205801  300.  7
*
*********************************************
* ht struc 14-o, pressurizer discharge tank   *
*********************************************
hs01206000   3   1   -1
hs01206001   prdctow_12
hs01206002   18.6  1.
hs01206100   -1   1   0.0
hs01206102  0.00212   2
hs01206103  0.006355  3
hs01206200  -1
hs01206201  cvtrstel  1
hs01206202  cvtrstel  2
hs01206300  -1
hs01206400  1  012  ext  0.5 0.5
hs01206401  0.9  gray-gas-a  3.0
hs01206500  21.09  5.  3.7
hs01206600  0
hs01206800  -1
hs01206801  300.  3
*
*********************************************
* ht struc 15-o, steam generator              *
*********************************************
hs01207000   4   1   -1
```

```
hs01207001   stgenow_12
hs01207002   18.6  1.
hs01207100   -1   1   0.0
hs01207102  0.007     2
hs01207103  0.021     3
hs01207104  0.0381    4
hs01207200  -1
hs01207201  cvtrstel  1
hs01207202  cvtrstel  2
hs01207203  cvtrstel  3
hs01207300  -1
hs01207400  1  012  ext  0.5 0.5
hs01207401  0.9  gray-gas-a  3.0
hs01207500  47.66  5.  3.7
hs01207600  0
hs01207800  -1
hs01207801  300.  4
*
*********************************************
* ht struc 20-o, all of "i" beams             *
*********************************************
hs01208000   3   1   -1
hs01208001   ibeamow_12
hs01208002   18.6  1.
hs01208100   -1   1   0.0
hs01208102  0.006857  2
hs01208103  0.02057   3
hs01208200  -1
hs01208201  cvtrstel  1
hs01208202  cvtrstel  2
hs01208300  -1
hs01208400  1  012  ext  0.5 0.5
hs01208401  0.9  gray-gas-a  3.0
hs01208500  30.98  5.  3.7
hs01208600  0
hs01208800  -1
hs01208801  300.  3
*
*******************************************
* ht strucms-o, bnl addt'l steel            *
*******************************************
hs01209000   3   1   -1
hs01209001   miscstow_12
hs01209002   18.6  1.
hs01209100   -1   1   0.0
hs01209102  0.001588  2
hs01209103  0.004763  3
hs01209200  -1
hs01209201  cvtrstel  1
hs01209202  cvtrstel  2
hs01209300  -1
hs01209400  1  012  ext  0.5 0.5
hs01209401  0.9  gray-gas-a  3.0
hs01209500  0.1  5.  3.7
hs01209600  0
hs01209800  -1
hs01209801  300.  3
*
*********************************************
* Central top operating                      *
*********************************************
*
*
```

```
*********************************************
* Annulus top operating                     *
*********************************************
************************************************
* ht struc 1-o, bnl cyl shell in operating region *
************************************************
hs01401000   11   1   -1
hs01401001   cylsho_14
hs01401002   22.3   1.
hs01401100   -1   1   0.0
hs01401102  0.0022    2
hs01401103  0.00635   3
hs01401104  0.01135   4
hs01401105  0.014     5
hs01401106  0.01855   6
hs01401107  0.02815   7
hs01401108  0.04735   8
hs01401109  0.06655   9
hs01401110  0.14      10
hs01401111  0.2       11
hs01401200  -1
hs01401201  cvtrstel  1
hs01401202  cvtrstel  2
hs01401203  cvtrconc  3
hs01401204  cvtrconc  4
hs01401205  cvtrconc  5
hs01401206  cvtrconc  6
hs01401207  cvtrconc  7
hs01401208  cvtrconc  8
hs01401209  cvtrconc  9
hs01401210  cvtrconc  10
hs01401300  -1
hs01401400  1  014  ext  0.5 0.5
hs01401401  0.9  gray-gas-a  3.0
hs01401500  196.136  11.  3.6
hs01401600  0
hs01401800  -1
hs01401801  300.  11
*
************************************************
* Dome operating                               *
************************************************
****************************************
* ht struc 2-o, dome                   *
****************************************
hs01503000   10   1   -1
hs01503001   dome
hs01503002   34.8  0.
hs01503100   -1   1   0.0
hs01503102  0.00408   2
hs01503103  0.0127    3
hs01503104  0.01724   4
hs01503105  0.02214   5
hs01503106  0.03193   6
hs01503107  0.05152   7
hs01503108  0.09068   8
hs01503109  0.14      9
hs01503110  0.2       10
hs01503200  -1
hs01503201  cvtrstel  1
hs01503202  cvtrstel  2
hs01503203  cvtrconc  3
hs01503204  cvtrconc  4
```

```
hs01503205  cvtrconc  5
hs01503206  cvtrconc  6
hs01503207  cvtrconc  7
hs01503208  cvtrconc  8
hs01503209  cvtrconc  9
hs01503300  -1
hs01503400  1  015  ext  0.5 0.5
hs01503401  0.9  gray-gas-a  3.0
hs01503500  499.  3.  8.9
hs01503600  0
hs01503800  -1
hs01503801  300.  10
*
*******************************************************
* Central low intermediate                             *
*******************************************************
************************************************************
* ht struc 6-i, reactor compartment assumed to be walls  *
************************************************************
hs01611000   7   1   -1
hs01611001   reacompw_16
hs01611002   5.5  1.
hs01611100   -1   1   0.0
hs01611102  0.004     2
hs01611103  0.012     3
hs01611104  0.028     4
hs01611105  0.06      5
hs01611106  0.124     6
hs01611107  0.188     7
hs01611200  -1
hs01611201  cvtrconc  1
hs01611202  cvtrconc  2
hs01611203  cvtrconc  3
hs01611204  cvtrconc  4
hs01611205  cvtrconc  5
hs01611206  cvtrconc  6
hs01611300  -1
hs01611400  1  016  ext  0.5 0.5
hs01611401  0.9  gray-gas-a  3.0
hs01611500  38.555  5.  2.4
hs01611600  0
hs01611800  -1
hs01611801  300.  7
*
*****************************************************
* ht struc 7-i, fuel canal assumed to be walls      *
*****************************************************
hs01612000   7   1   -1
hs01612001   fucanalw_16
hs01612002   5.5  1.
hs01612100   -1   1   0.0
hs01612102  0.004     2
hs01612103  0.012     3
hs01612104  0.028     4
hs01612105  0.06      5
hs01612106  0.124     6
hs01612107  0.188     7
hs01612200  -1
hs01612201  cvtrconc  1
hs01612202  cvtrconc  2
hs01612203  cvtrconc  3
hs01612204  cvtrconc  4
hs01612205  cvtrconc  5
```

```
hs01612206  cvtrconc  6
hs01612300  -1
hs01612400  1  016  ext  0.5 0.5
hs01612401  0.9  gray-gas-a  3.0
hs01612500  37.16  5.  2.4
hs01612600  0
hs01612800  -1
hs01612801  300.   7
*
*********************************************
* ht struc 9-i, floor of reactor cavity top   *
*********************************************
hs01613000   7   1   -1
hs01613001   rcvflrin_16
hs01613002   5.5  -1.0e-7
hs01613100   -1   1   0.0
hs01613102  0.004     2
hs01613103  0.012     3
hs01613104  0.028     4
hs01613105  0.06      5
hs01613106  0.124     6
hs01613107  0.188     7
hs01613200  -1
hs01613201  cvtrconc  1
hs01613202  cvtrconc  2
hs01613203  cvtrconc  3
hs01613204  cvtrconc  4
hs01613205  cvtrconc  5
hs01613206  cvtrconc  6
hs01613300  -1
hs01613400  1  016  ext  0.5 0.5
hs01613401  0.9  gray-gas-a  3.0
hs01613500  6.65  1.  0.188
hs01613600  0
hs01613800  -1
hs01613801  300.    7
*
*********************************************
* ht struc 9-b, roof of reactor cavity top   *
*********************************************
*hs001614000   7   1   -1
*hs001614001   rcvflrin_16
*hs001614002   7.9  0.
*hs001614100   -1   1   0.0
*hs001614102  0.004     2
*hs001614103  0.012     3
*hs001614104  0.028     4
*hs001614105  0.06      5
*hs001614106  0.124     6
*hs001614107  0.188     7
*hs001614200  -1
*hs001614201  cvtrconc  1
*hs001614202  cvtrconc  2
*hs001614203  cvtrconc  3
*hs001614204  cvtrconc  4
*hs001614205  cvtrconc  5
*hs001614206  cvtrconc  6
*hs001614300  -1
*hs001614400  1  016  ext 0.5  0.5
*hs001614500  6.65  1.  0.188
*hs001614600  0
*hs001614800  -1
*hs001614801  300.    7
```

```
*
************************************************
* ht struc 13-i, pressurizer                   *
************************************************
hs01617000   5   1   -1
hs01617001   press_16
hs01617002   5.5  1.
hs01617100   -1   1   0.0
hs01617102  0.007     2
hs01617103  0.021     3
hs01617104  0.0391    4
hs01617105  0.0572    5
hs01617200  -1
hs01617201  cvtrstel  1
hs01617202  cvtrstel  2
hs01617203  cvtrstel  3
hs01617204  cvtrstel  4
hs01617300  -1
hs01617400  1  016  ext  0.5 0.5
hs01617401  0.9  gray-gas-a  3.0
hs01617500  8.175  5.  2.4
hs01617600  0
hs01617800  -1
hs01617801  300.   5
*
*********************************************
* ht struc 17-i, shutdown coolers           *
*********************************************
hs01619000   3   1   -1
hs01619001   shdcoiw_16
hs01619002   5.5  1.
hs01619100   -1   1   0.0
hs01619102  0.000508  2
hs01619103  0.001524  3
hs01619200  -1
hs01619201  cvtrstel  1
hs01619202  cvtrstel  2
hs01619300  -1
hs01619400  1  016  ext  0.5 0.5
hs01619401  0.9  gray-gas-a  3.0
hs01619500  6.13  5.  2.4
hs01619600  0
hs01619800  -1
hs01619801  300.   3
*
*********************************************
* ht strucms-o, bnl addt'l steel            *
*********************************************
hs01609000   3   1   -1
hs01609001   miscstow_16
hs01609002   5.5  1.
hs01609100   -1   1   0.0
hs01609102  0.001588  2
hs01609103  0.004763  3
hs01609200  -1
hs01609201  cvtrstel  1
hs01609202  cvtrstel  2
hs01609300  -1
hs01609400  1  016  ext  0.5 0.5
hs01609401  0.9  gray-gas-a  3.0
hs01609500  219.46  5.  2.4
hs01609600  0
hs01609800  -1
```

```
hs01609801  300.  3
*
****************************************
* Annulus low intermediate             *
****************************************
************************************************
* ht struc 1-o, bnl cyl shell in operating region *
************************************************
hs01701000   11   1   -1
hs01701001   cylsho_17
hs01701002   5.5   1.
hs01701100   -1   1   0.0
hs01701102  0.0022    2
hs01701103  0.00635   3
hs01701104  0.01135   4
hs01701105  0.014     5
hs01701106  0.01855   6
hs01701107  0.02815   7
hs01701108  0.04735   8
hs01701109  0.06655   9
hs01701110  0.14      10
hs01701111  0.2       11
hs01701200  -1
hs01701201  cvtrstel  1
hs01701202  cvtrstel  2
hs01701203  cvtrconc  3
hs01701204  cvtrconc  4
hs01701205  cvtrconc  5
hs01701206  cvtrconc  6
hs01701207  cvtrconc  7
hs01701208  cvtrconc  8
hs01701209  cvtrconc  9
hs01701210  cvtrconc  10
hs01701300  -1
hs01701400  1  017  ext  0.5 0.5
hs01701401  0.9  gray-gas-a  3.0
hs01701500  135.25  11.  2.4
hs01701600  0
hs01701800  -1
hs01701801  300.  11
*
*********************************************
* ht strucms-o, bnl addt'l steel             *
*********************************************
hs01709000   3   1   -1
hs01709001   miscstow_17
hs01709002   5.5  1.
hs01709100   -1   1   0.0
hs01709102  0.001588  2
hs01709103  0.004763  3
hs01709200  -1
hs01709201  cvtrstel  1
hs01709202  cvtrstel  2
hs01709300  -1
hs01709400  1  017  ext  0.5 0.5
hs01709401  0.9  gray-gas-a  3.0
hs01709500  219.46  5.  2.4
hs01709600  0
hs01709800  -1
hs01709801  300.  3
*
****************************************
* Central high intermediate            *
```

```
*****************************************
*********************************************************
* ht struc 6-i, reactor compartment assumed to be walls  *
*********************************************************
hs01811000   7   1   -1
hs01811001   reacompw_18
hs01811002   10.4  1.
hs01811100   -1   1   0.0
hs01811102  0.004     2
hs01811103  0.012     3
hs01811104  0.028     4
hs01811105  0.06      5
hs01811106  0.124     6
hs01811107  0.188     7
hs01811200  -1
hs01811201  cvtrconc  1
hs01811202  cvtrconc  2
hs01811203  cvtrconc  3
hs01811204  cvtrconc  4
hs01811205  cvtrconc  5
hs01811206  cvtrconc  6
hs01811300  -1
hs01811400  1  018  ext  0.5 0.5
hs01811401  0.9  gray-gas-a  3.0
hs01811500  38.555  5.  2.4
hs01811600  0
hs01811800  -1
hs01811801  300.  7
*
*****************************************************
* ht struc 7-i, fuel canal assumed to be walls      *
*****************************************************
hs01812000   7   1   -1
hs01812001   fucanalw_18
hs01812002   10.4  1.
hs01812100   -1   1   0.0
hs01812102  0.004     2
hs01812103  0.012     3
hs01812104  0.028     4
hs01812105  0.06      5
hs01812106  0.124     6
hs01812107  0.188     7
hs01812200  -1
hs01812201  cvtrconc  1
hs01812202  cvtrconc  2
hs01812203  cvtrconc  3
hs01812204  cvtrconc  4
hs01812205  cvtrconc  5
hs01812206  cvtrconc  6
hs01812300  -1
hs01812400  1  018  ext  0.5 0.5
hs01812401  0.9  gray-gas-a  3.0
hs01812500  37.16  5.  2.4
hs01812600  0
hs01812800  -1
hs01812801  300.   7
*
*********************************************
* ht struc 13-i, pressurizer                *
*********************************************
hs01817000   5   1   -1
hs01817001   press_18
hs01817002   10.4  1.
```

```
hs01817100   -1   1   0.0
hs01817102  0.007     2
hs01817103  0.021     3
hs01817104  0.0391    4
hs01817105  0.0572    5
hs01817200  -1
hs01817201  cvtrstel  1
hs01817202  cvtrstel  2
hs01817203  cvtrstel  3
hs01817204  cvtrstel  4
hs01817300  -1
hs01817400  1  018  ext  0.5 0.5
hs01817401  0.9  gray-gas-a  3.0
hs01817500  8.175  5.  2.4
hs01817600  0
hs01817800  -1
hs01817801  300.   5
*
*********************************************
* ht strucms-o, bnl addt'l steel             *
*********************************************
hs01809000   3   1   -1
hs01809001   miscstow_18
hs01809002   10.4  1.
hs01809100   -1   1   0.0
hs01809102  0.001588  2
hs01809103  0.004763  3
hs01809200  -1
hs01809201  cvtrstel  1
hs01809202  cvtrstel  2
hs01809300  -1
hs01809400  1  018  ext  0.5 0.5
hs01809401  0.9  gray-gas-a  3.0
hs01809500  0.1  5.  2.4
hs01809600  0
hs01809800  -1
hs01809801  300.  3
*
*********************************************
* Annulus high intermediate                  *
*********************************************
*************************************************
* ht struc 1-o, bnl cyl shell in operating region *
*************************************************
hs01901000   11   1   -1
hs01901001   cylsho_19
hs01901002   10.4   1.
hs01901100   -1   1   0.0
hs01901102  0.0022    2
hs01901103  0.00635   3
hs01901104  0.01135   4
hs01901105  0.014     5
hs01901106  0.01855   6
hs01901107  0.02815   7
hs01901108  0.04735   8
hs01901109  0.06655   9
hs01901110  0.14      10
hs01901111  0.2       11
hs01901200  -1
hs01901201  cvtrstel  1
hs01901202  cvtrstel  2
hs01901203  cvtrconc  3
hs01901204  cvtrconc  4
```

```
hs01901205  cvtrconc  5
hs01901206  cvtrconc  6
hs01901207  cvtrconc  7
hs01901208  cvtrconc  8
hs01901209  cvtrconc  9
hs01901210  cvtrconc  10
hs01901300  -1
hs01901400  1  019  ext  0.5 0.5
hs01901401  0.9  gray-gas-a  3.0
hs01901500  135.25  11.  2.4
hs01901600  0
hs01901800  -1
hs01901801  300.  11
*
*******************************************
* ht strucms-o, bnl addt'l steel            *
*******************************************
hs01909000   3   1   -1
hs01909001   miscstow_19
hs01909002   10.4  1.
hs01909100   -1   1   0.0
hs01909102  0.001588  2
hs01909103  0.004763  3
hs01909200  -1
hs01909201  cvtrstel  1
hs01909202  cvtrstel  2
hs01909300  -1
hs01909400  1  019  ext  0.5 0.5
hs01909401  0.9  gray-gas-a  3.0
hs01909500  125.4  5.  2.4
hs01909600  0
hs01909800  -1
hs01909801  300.  3
*
.  * terminate
```

Mp.txt:

```
************************************************************
***
***             NON-CONDENSIBLES GAS PACKAGE
***
************************************************************
***
***      GAS  MATEERIAL NUMBER
NCG001   o2   4                                  * oxygen
NCG002   n2   5                                  * nitrogen
***
************************************************************
***
************************************************************
***
************************************************************
***
***             MATERIAL PROPERTIES PACKAGE
***
***
***               Property              Units
***
***               temperature           K
***             density               kg/m*3
***             heat capacity         J/kg-K
***             thermal conductivity  W/m-K
***
************************************************************
```

```
************************************************************
************************************************************
************************************************************
***
***             MATERIAL 1 IS CONCRETE
***             ======================
***
MPMAT00100      CVTRCONC
MPMAT00101      RHO       13
MPMAT00102      CPS       14
MPMAT00103      THC       15
TF01300         'RHO CONCRETE'   2   1.00   0.0
TF01312         273.15    1.
TF01313         5000.0    1.
TF01400         'CPS CONCRETE'   2   1.00   0.0
TF01412         273.15    2.025e6
TF01413         5000.0    2.025e6
TF01500         'THC CONCRETE'   2   1.00   0.0
TF01512         273.15    1.385
TF01513         5000.0    1.385
***
************************************************************
***
***             MATERIAL 2 IS CARBON STEEL
***             ==========================
***
MPMAT00200      'CVTRSTEL'
MPMAT00201       RHO          16
MPMAT00202       CPS          17
MPMAT00203       THC          18
TF01600         'RHO CARBON STEEL'   2   1.00   0.0
TF01612          273.15       1.0
TF01613          5000.0       1.0
TF01700         'CPS CARBON STEEL'   2   1.00   0.0
TF01712          273.15       3.689e6
TF01713          5000.0       3.689e6
TF01800         'THC CARBON STEEL'   2   1.00   0.0
TF01812          273.15       45.18
TF01813          5000.0       45.18
***
************************************************************
************************************************************
***
***             MATERIAL 3 IS Gap Gas
***             =====================================
***
MPMAT00300      'GAS'
MPMAT00301       RHO          19
MPMAT00302       CPS          20
MPMAT00303       THC          21
TF01900         'RHO GAS'   2   1.00   0.0
TF01912          273.15       1.0
TF01913          5000.0       1.0
TF02000         'CPS GAS'   2   1.00   0.0
TF02012          273.15       1.0e3
TF02013          5000.0       1.0e3
TF02100         'THC GAS'   2   1.00   0.0
TF02111          273.15       0.03
TF02112          5000.0       0.03
***
***
***             MATERIAL 4 IS CONTAIN CONC
***             ======================
```

```
***
MPMAT00400      CCONC
MPMAT00401      RHO       22
MPMAT00402      CPS       23
MPMAT00403      THC       24
TF02200         'RHO CONC'   2   1.00   0.0
TF02212         273.15    2400.
TF02213         5000.0    2400.
TF02300         'CPS CONC'   2   1.00   0.0
TF02312         273.15    1000.
TF02313         5000.0    1000.
TF02400         'THC CONC'   2   1.00   0.0
TF02412         273.15    2.6
TF02413         5000.0    2.6
***
.  * terminate
```

Multi-Cell Model (Test 4): EXEC Input

```
** CVTR Test #4A ***************************************
************************************************************
*eor*      melgen
**********************
**********************
***                ***
***  MELGEN INPUT  ***
***                ***
**********************
TITLE     'CVTR'
***JOBID      CVTR
CRTOUT
OUTPUTF   'CVTR.out'
RESTARTF  'CVTR.rst'
DIAGF     'CVTR.gdia'
TSTART     0.
DTTIME    .1
***
************************************************************
* Containment Sprays                                       *
************************************************************
*** Source in cell#13
*          Name       Vol   Elev     CF#
SPRSR0100  spray13     13    25.8    310
*            T,K        Flow
SPRSR0101   288.0     9.1485e-3
*
SPRSR0102   0.001      1.
*
*** Source in cell#14
*          Name       Vol   Elev     CF#
SPRSR0200  spray14     14    25.8    310
*            T,K        Flow
SPRSR0201   288.0     9.1485e-3
*
SPRSR0202   0.001      1.
**
* Time to activate sprays
CF31000   SPRAY_Time   L-GT  2   1.   0.
CF31001   .FALSE.
CF31010   1.   0.   TIME
CF31011   0.  210.  TIME
CF31005   LATCH
*
```

```
*  Carry over of droplets
*      From  To   Fraction
SPRJUN01  13   11   1.0
SPRJUN02  11    9   1.0
SPRJUN03   9    7   1.0
*
SPRJUN04  14    12  1.0
SPRJUN05  12    10  1.0
SPRJUN06  10     8  1.0
*
SPRSUMP0   1
SPRSUMP1   7    8
************************************************************
*** Sensitivity Study
************************************************************
* Turbulent convection coefficient
sc41100  4110  0.14  1
sc42510  4251  0.00005 2
sc44110  4411  1.0e-10 5          * negate equilibrium calc.
************************************************************
***
r*i*f   mp.txt
r*i*f   cont.txt
r*i*f   fl.txt
r*i*f   hs_multi.txt
************************************************************
.  * terminate
*eor* melcor
************************
***  MELCOR INPUT    ***
************************
TITLE     'CVTR'
***JOBID      ref
*
OUTPUTF   'CVTR.out'
PLOTF     'CVTR.ptf'
RESTARTF  'CVTR.rst'
MESSAGEF  'CVTR.mes'
DIAGF     'CVTR.dia'
*
CRTOUT
***CYMESF    10 10
*
RESTART  -1
tend  1.0e3
***EXACTTIME1         100.
CPULIM             2.0e6
CPULEFT            100.0
*cvhtrace 3
*
************************************
*** Invoke desired sequences
************************************
***
***
************************************************************
*
*          TIME    DTMAX     DTMIN     DTEDIT    DTPLOT    DTREST
*
TIME1       0.0     1.0      1.0e-8      2.0       2.0     20.0
TIME2      20.0     1.0      1.0E-8     10.0       5.0     20.0
TIME3      80.0     2.0      1.0E-8     50.0      10.0     50.0
TIME4     160.0     2.0      1.0E-8     50.0       1.0     20.0
```

```
TIME5     180.0    2.0     1.0E-8     20.0     10.0    20.0
TIME6     250.0    2.0     1.0E-6     50.0     20.0    50.0
TIME7     500.0    5.0     1.0E-6    100.0     50.0    100.0
TIME8    1000.0    5.0     1.0E-6    100.0     50.0    100.0
************************************************************
***** END OF MELCOR INPUT ***********************************
************************************************************
.  * terminate
```

Multi-Cell Model (Test 5): EXEC Input

```
** CVTR Test #5A ********************************************
************************************************************
*eor*      melgen
**********************
**********************
***                ***
***  MELGEN INPUT  ***
***                ***
**********************
TITLE     'CVTR'
***JOBID      CVTR
CRTOUT
OUTPUTF   'CVTR.out'
RESTARTF  'CVTR.rst'
DIAGF     'CVTR.gdia'
TSTART     0.
DTTIME    .1
***
************************************************************
* Containment Sprays                                       *
************************************************************
*** Source in cell#13
*          Name       Vol   Elev     CF#
SPRSR0100  spray13     13    25.8    310
*            T,K        Flow
SPRSR0101   288.0    1.5775e-2
*
SPRSR0102   0.001      1.
*
*** Source in cell#14
*          Name       Vol   Elev     CF#
SPRSR0200  spray14     14    25.8    310
*            T,K        Flow
SPRSR0201   288.0    1.5775e-2
*
SPRSR0202   0.001      1.
**
* Time to activate sprays
CF31000   SPRAY_Time   L-GT  2   1.   0.
CF31001   .FALSE.
CF31010   1.   0.   TIME
CF31011   0.  210.  TIME
CF31005   LATCH
*
*  Carry over of droplets
*      From  To   Fraction
SPRJUN01  13   11   1.0
SPRJUN02  11    9   1.0
SPRJUN03   9    7   1.0
*
SPRJUN04  14    12  1.0
SPRJUN05  12    10  1.0
SPRJUN06  10     8  1.0
```

```
*
SPRSUMP0   1
SPRSUMP1   7    8
************************************************************
*** Sensitivity Study
************************************************************
* Turbulent convection coefficient
sc41100  4110  0.14  1
sc42510  4251  0.00005 2
sc44110  4411  1.0e-10 5
************************************************************
***
r*i*f   mp.txt
r*i*f   cont.txt
r*i*f   fl.txt
r*i*f   hs_multi.txt
************************************************************
.  * terminate
*eor* melcor
************************
***  MELCOR INPUT    ***
************************
TITLE     'CVTR'
***JOBID      ref
*
OUTPUTF   'CVTR.out'
PLOTF     'CVTR.ptf'
RESTARTF  'CVTR.rst'
MESSAGEF  'CVTR.mes'
DIAGF     'CVTR.dia'
*
CRTOUT
***CYMESF    10 10
*
RESTART  -1
tend  1.0e3
***EXACTTIME1         100.
CPULIM             2.0e6
CPULEFT            100.0
*cvhtrace 3
*
************************************
*** Invoke desired sequences
************************************
***
***
************************************************************
*
*          TIME    DTMAX     DTMIN     DTEDIT    DTPLOT    DTREST
*
TIME1       0.0     1.0      1.0e-8      2.0       2.0     20.0
TIME2      20.0     1.0      1.0E-8      10.0      5.0     20.0
TIME3      80.0     2.0      1.0E-8      50.0      10.0    50.0
TIME4     160.0     2.0      1.0E-8      50.0      1.0     20.0
TIME5     180.0     2.0      1.0E-8      20.0      10.0     20.0
TIME6     250.0     2.0      1.0E-6      50.0      20.0     50.0
TIME7     500.0     5.0      1.0E-6     100.0      50.0     100.0
TIME8    1000.0     5.0      1.0E-6     100.0      50.0     100.0
************************************************************
***** END OF MELCOR INPUT ************************************
************************************************************
.  * terminate
```

DISTRIBUTION:

10 U.S. Nuclear Regulatory Commission
Attn: Allen Notafrancesco, Mail Stop T10-K8
Office of Nuclear Regulatory Research
Rockville, Maryland 20852-2738

1 Farouk Eltawila, MS10-E32 (electronic copy)
U.S. Nuclear Regulatory Commission
Office of Nuclear Regulatory Research
Division of Systems Analysis
Washington, DC 20555-0001

1 Hossein Emaili, MS 10 K8 (electronic copy)
U.S. Nuclear Regulatory Commission
Office of Nuclear Regulatory Research
Washington, DC 20555-0001

1 Richard Lee, MS T10-K8 (electronic copy)
U.S. Nuclear Regulatory Commission
Office of Nuclear Regulatory Research
Washington, DC 20555-0001

1 Michael Salay, MS T10-E10 (electronic copy)
U.S. Nuclear Regulatory Commission
Office of Nuclear Regulatory Research
Washington, DC 20555-0001

1 Allen Notafrancesco, MS T10-K8 (electronic copy)
U.S. Nuclear Regulatory Commission
Office of Nuclear Regulatory Research
Washington, DC 20555-0001

1 Jack Tills & Associates, Inc. (electronic copy)
Sandia Park, New Mexico 87047-0549

1 MS 0736 Dana A. Powers, 06770 (electronic copy)
1 MS 0736 Marianne Walck, 06800 (electronic copy)
1 MS 0748 Randall O. Gauntt, 06762 (electronic copy)
1 MS 0748 Larry L. Humphries, 06762 (electronic copy)
1 MS 0748 Donald A Kalinich, 06762 (electronic copy)
1 MS 0748 Pamela Longmire, 06762
1 MS 0748 Jeffrey D. Brewer, 06761 (electronic copy)

1 MS 0899 Technical Library, 9536 (electronic copy)